THÈSE PRÉSENTÉE À

L'UNIVERSITÉ DU QUÉBEC À CHICOUTIMI

COMME EXIGENCE PARTIELLE

DU DOCTORAT EN SCIENCES DE LA TERRE ET DE L'ATMOSPHÈRE

PAR

SAMUEL MORFIN

INFLUENCE DE LA MISE EN PLACE PERVASIVE DE MAGMA D'ANATEXIE SOUS FORME DE COMPLEXE D'INJECTION DANS LA CROÛTE CONTINENTALE

MAI 2014

RÉSUMÉ

La différenciation crustale, qui donne à la croûte continentale ses caractéristiques spécifiques, est un processus qui dépend notamment du transfert vers la surface de magmas d'anatexie formés à la base de la croûte. Une alternative au modèle de "dyking", dominant dans la littérature, est la migration pervasive des magmas d'anatexie. Ce mécanisme de transfert forme des complexes d'injections qui sont des zones de haut grade métamorphique dans lesquelles de grandes quantités de leucogranites sont injectées de façon pervasive. Les complexes d'injections sont avant tout décrits et définis comme des réseaux d'extraction et de transfert de magmas dans la littérature. Cependant, l'observation de ces terrains et les modélisations numériques laissent supposer qu'une partie non-négligeable de magmas est piégée dans ces réseaux.

L'hypothèse testée au cours de ce doctorat est que les complexes d'injections sont des zones d'accumulation de magmas. Il est aussi postulé que cette accumulation de magmas a une influence importante sur certains paramètres de la croûte continentale.

Pour tester ces hypothèses, une étude de terrain basée sur une cartographie régionale de la sous-province d'Opinaca a été effectuée. Les terrains de l'Opinaca sont surtout composés de roches métasédimentaires (90 % de métagreywackes et à 10 % de métapélites) qui contiennent une quantité variable de leucogranites présents sous forme de veines et de dykes.

L'analyse métamorphique des terrains métasédimentaires indique que le degré maximal de fusion partielle à l'échelle régionale est d'environ 15 %. En comparaison, grâce à la description d'un grand nombre d'affleurements, il est estimé que le contenu typique d'un affleurement en leucogranite est d'environ 65 %. Cette différence entre la quantité de leucogranites produits *in situ* (15 %) et la quantité de leucogranites observée (65 %), qui est plus grande que les erreurs pour chacune des estimations, indique que le complexe d'injection de l'Opinaca agit comme un réservoir de magmas d'anatexie.

L'accumulation de magmas se situe à des niveaux profonds de la croûte, plus profonds que les modèles classiques. Cela a des implications sur certains paramètres de la croûte. Notamment, les leucogranites sont enrichis en éléments producteurs de chaleur comparativement à leur source et aux métasédiments en général. L'accumulation de leucogranites dans le complexe d'injection de l'Opinaca se traduit alors par une augmentation de production de chaleur à des niveaux profonds (relativement à un scénario où les granites sont transportés dans la croûte supérieure).

L'analyse lithogéochimique, associée à la pétrographie, montre que les leucogranites accumulés dans le complexe d'injection de l'Opinaca sont presque tous issus d'un fractionnement précoce (interprété comme un fractionnement "en route" des leucogranites). L'analyse des leucogranites montre des évidences (géochimiques et pétrographiques) d'un fractionnement de feldspath potassique qui forme des cumulats et un liquide résiduel enrichi en plagioclase albitique et en quartz. De nombreux leucogranites montrent des évidences géochimiques (appauvrissement extrême en terres rares), pétrographiques

(présence de grenat) et texturales (grande proportion de pegmatites) qui indiquent que le complexe d'injection de l'Opinaca est composé majoritairement de granites évolués. L'accumulation de ceux-ci dans la croûte moyenne profonde a des implications pour la différenciation crustale, car cela remet en cause la vision classique du transfert et de l'évolution des leucogranites dans l'ensemble de la croûte. Une conséquence importante est la capacité des complexes d'injections à libérer des fluides à la fin de l'épisode métamorphique. Ceux-ci peuvent réhydrater des assemblages de haut grade et possiblement produire une fusion partielle secondaire par influx d'eau.

L'ensemble de l'étude a permis de mieux comprendre les mécanismes et l'impact de la mise en place pervasive de magmas d'anatexie dans la croûte continentale. Les conséquences de la mise en place d'un complexe d'injection, soulevées dans le cadre de cette recherche, sont importantes dans la compréhension globale de la croûte continentale et du processus de différenciation.

REMERCIEMENTS

Les chapitres qui suivent sont l'accomplissement d'un processus qui va au-delà de la rédaction d'articles ou de la présentation de résultats. Il représente aussi un cheminement personnel incroyable. Depuis mon arrivée au Québec seul et naïf en juin 2008 (pour finir perdu à la Baie-James trois jours plus tard), jusqu'aux conférences et à la publication d'articles, un long chemin a été parcouru. Ce chemin, à la fois professionnel et personnel n'as pas été parcouru seul, bien au contraire.

J'ai le plaisir de remercier mon directeur, le professeur Ed Sawyer, qui m'a tant appris, m'a poussé, a toujours été disponible et à l'écoute. Travailler à ses côtés et profiter de son expertise fut un plaisir et un privilège.

Mon co-directeur, Daniel Bandyayera, est une personne très importante, qui a été plus qu'un conseiller scientifique et un collègue, mais aussi le premier membre, et bien sûr le plus sage, de ma famille d'adoption au Québec.

Je tiens à remercier aussi l'ensemble du corps professoral, des professionnels et du personnel administratif du département des Sciences de la Terre. Particulièrement Mme Barnes, et l'équipe de la Chaire en métallogénie magmatique, pour le soutien, les discussions et les conseils.

Je suis aussi fier d'avoir rencontré et d'être devenu ami avec tant de mes collègues, les étudiants du REDiST. Parmi eux, je tiens particulièrement à remercier Dominique, Julien et Denis pour leur aide direct à mon projet. À tous mes amis, merci.

Cette thèse a eu pour bande sonore principale la musique de Springsteen, qui, à fond dans les oreilles, les yeux clos quelques minutes, permet de passer par dessus des moments durs.

Je remercie affectueusement ma compagne, Émilie, sans qui la fin du doctorat n'aurait pas été la même, pour son soutien, sa patience, ses conseils et sa confiance en moi. J'ai une pensée pour les moments difficiles, pour ma tante Joëlle, disparue durant mon doctorat. Je remercie aussi toute ma famille, dont j'ai toujours ressenti le soutien malgré la distance qui nous sépare.

Je suis heureux d'avoir rendu ma famille fière par mon accomplissement dans mes études et je dédie mon travail à mes parents, mes frères, mes grands-parents et le petit dernier, Élie.

TABLE DES MATIÈRES

CHAPITRE 1 - Introduction 1
1.1 Introduction 2
1.1.1 Importance de la différenciation crustale 2
1.1.2 L'influence du transfert de magma sur la différenciation crustale 3
1.1.3 Importance de la fusion partielle de la croûte et sa différenciation 4
1.1.4 Importance de la migration pervasive comme mécanisme de transfert des magmas d'anatexie 5
1.1.5 Les complexes d'injections: terrains formés par la migration pervasive de magmas d'anatexie 9
1.2 Problématique 9
1.3 Hypothèse 10
1.4 Objectifs 11
1.5 Zone d'étude 12
1.5.1 Contexte géologique - La Sous-province d'Opinaca dans la Province du Supérieur 12
1.5.2 Description de l'Opinaca 15
1.5.2.1 Description générale 15
1.5.2.2 Description structurale 16
1.5.3 Description des composantes du complexe d'injection 16
1.5.3.1 Unités métasédimentaires 17
1.5.3.2 Veines leucogranitiques 18
1.6 Méthodologie 19
1.6.1 Travail de terrain 19
1.6.2 Analyse pétrographique 20
1.6.3 Microsonde 20
1.6.4 Lithogéochimie 21
1.6.5 Isotopes d'oxygène 21
1.6.6 SHRIMP U/Pb 22
1.7 Format de la thèse 22
1.8 Références 26

CHAPITRE 2 - New geochronological constraints from SHRIMP U-Pb analysis in zircon from the Opinaca Subprovince, Superior Province, Quebec 32
2.1 Résumé 33
2.2 Abstract 34
2.3 Introduction 35
2.4 Geological context 36
2.4.1 The Opinaca Subprovince in the Superior Province 36
2.4.1.1 Part of a large scale series of metasedimentary basins 36

2.4.1.2 Opinaca Subprovince surroundings 39
2.4.2 Review of the Opinaca geochronology 42
2.5 SHRIMP methodology 45
2.6 Results 48
2.6.1 Sample MAN4C: granulite facies metapelite 46
2.6.1.1 Sample description 46
2.6.1.2 Zircon morphology 57
2.6.1.3 Results 61
2.6.2 Sample 6116A: granulite facies metapelite 64
2.6.2.1 Sample description 64
2.6.2.2 Zircon morphology 65
2.6.2.3 Results 65
2.6.3 Sample 6263A2: metagreywacke 66
2.6.3.1 Sample description 67
2.6.3.2 Zircon morphology 68
2.6.3.3 Results 68
2.6.4 Sample 6263A3: Opx-bearing metagreywacke 69
2.6.4.1 Sample description 69
2.6.4.2 Zircon morphology 69
2.6.4.3 Results 70
2.6.5 Sample 6263C1: injected leucogranite 71
2.6.5.1 Sample description 71
2.6.5.2 Zircon morphology 71
2.6.5.3 Results 72
2.7 Discussion 72
2.7.1 Transition from inherited zircon to those formed in the injection complex 72
2.7.2 Populations of inherited zircon 75
2.7.2.1 Provenance of the sediments 79
2.7.3 Timing of the injection complex 80
2.7.4 Significance of post-injection complex ages 81
2.7.5 Isotopic disturbance and Discordia intercepts 81
2.8 Conclusion 82
2.9 Acknowledgements 83
2.10 References 84

CHAPITRE 3 - Large volumes of anatectic melt retained in granulite facies migmatites: An injection complex in northern Quebec 90
3.1 Résumé 91
3.2 Abstract 93
3.3 Introduction 94
3.4 Opinaca Subprovince in the Superior Province 97
3.5 The Opinaca Subprovince 102

3.5.1 Structural characteristics 105
3.5.2 Migmatites 107
3.5.3 Thin leucocratic felsic veins in migmatites 110
3.5.4 Large leucocratic dykes and sills 114
3.6 U-Pb SHRIMP geochronology *115*
3.6.1 Results 120
3.7 Petrology of the migmatites *121*
3.7.1 Metagreywacke paleosome 121
3.7.2 Migmatites 126
3.7.3 Rehydration of high temperature mineral assemblages 128
3.7.4 Temperature and pressure during anatexis 129
3.8 Discussion *131*
3.8.1 Timing of granulite facies metamorphism and injection of leucogranite 131
3.8.2 Percentage of melt produced by local anatexis 132
3.8.3 Accumulation of felsic melt in the Opinaca Subprovince 134
3.8.4 Potential source of the felsic magma 138
3.8.5 Why an injection complex? 138
3.8.6 Why thin veins and dykes? 139
3.8.7 Some consequences of an injection complex in the deep middle crust 141
3.8.7.1 Transfer of heat producing elements into the injection complex 141
3.8.7.2 Latent heat of crystallization 146
3.8.7.3 Addition of H_2O 146
3.9 Conclusion *147*
3.10 Acknowledgments *148*
3.11 References *149*

CHAPITRE 4 - The geochemical signature of a felsic injection complex in the continental crust: Opinaca Subprovince, Quebec *161*
4.1 Résumé *162*
4.2 Abstract *164*
4.3 Introduction *166*
4.4 Geological context *168*
4.4.1 Regional geology 168
4.4.2 Geochronology 172
4.4.3 Local geology 174
4.4.3.1. Metamorphic conditions 177
4.5 The leucogranitic veins and dykes *182*
4.5.1 Macroscopic features 182
4.5.2 Petrology of the leucocratic veins 185
4.5.3 Microstructure of the leucogranite 187

4.6 Geochemistry of the leucogranites ___ *189*
4.6.1 Sampling and analytical methods ___ **189**
4.6.2 Major oxides ___ **197**
4.6.3 Trace elements ___ **200**
4.6.4 Oxygen isotopes ___ **207**
4.7 Discussion ___ *207*
4.7.1 Modelling major element compositions ___ **209**
4.7.1.1 Composition of the source material ___ 209
4.7.1.2 Composition of the initial melt ___ 210
4.7.1.3 Low TiO_2, FeO and MgO ___ 211
4.7.1.4 Evolution of leucogranites by fractional crystallisation ___ 213
4.7.1.5 Trace elements ___ 219
4.7.2 H_2O released in the host ___ **223**
4.7.2.1 $\delta^{18}O$ reequilibration ___ 223
4.7.2.2 H_2O available ___ 224
4.7.2.3 Importance of water fluxed partial melting ___ 226
4.7.2.4 Implications of water release ___ 227
4.8 Conclusion ___ *228*
4.9 Acknowledgments ___ *229*
4.10 References ___ *230*

CHAPITRE 5 - Synthèse et conclusion ___ *238*
5.1 Introduction ___ *239*
5.2 Sous-province d'Opinaca ___ *239*
5.2.1 La source des métasédiments ___ **239**
5.2.2 Présence d'un complexe d'injection ___ **240**
5.3 Principales implications globales ___ *241*
5.3.1 Terrain granulitique qui n'est pas déficitaire en granite ___ **241**
5.3.2 Réservoir de leucogranites évolués ___ **241**
5.3.3 Implications sur le régime thermique ___ **242**
5.3.4 Implications de la présence d'eau dans la croûte moyenne ___ **242**
5.3.5 Implications sur le processus général de différenciation crustale ___ **243**
5.3.6 Complexe d'injection comme des plutons diffus ___ **244**
5.4 Apports aux débats actuels ___ *244*
5.5 Investigations futures ___ *246*
5.6 Références ___ *248*

ANNEXES ___ *249*

LISTE DES FIGURES

CHAPITRE 1

Figure 1.1: Coupe schématique de la croûte continentale 6

Figure 1.2: Schéma du modèle conceptuel d'intrusion pervasive 8

Figure 1.3: Carte de localisation générale de la Sous-province d'Opinaca 14

CHAPITRE 2

Figure 2.1: Simplified map of the Superior Province showing the location of the Quetico, Nemiscau, Opinaca and Ashuanipi metasedimentary subprovinces 37

Figure 2.2: Regional map of the eastern James Bay area centered on the Opinaca Subprovince 40

Figure 2.3: Geological map of the two sectors from figure 2.2 43

Figure 2.4: Field pictures of the outcrops and sample positions 55

Figure 2.5: Paragenesis and microstructure of the samples 58

Figure 2.6: Selected representative cathodoluminescence images of zircon grains separated for each sample 60

Figure 2.7: Wetherhill Concordia plot and age distribution with the relative probability for each sample 62

Figure 2.8: Th/U vs Age (in Ma) from subconcordant zircons between 2550 and 2900 Ma 74

Figure 2.9: Distribution and relative probability of inherited ages 76

CHAPITRE 3

Figure 3.1: Outline of the Superior Province 99

Figure 3.2: Simplified geological map of the Superior Province east of James Bay 101

Figure 3.3: Simplified geological map of the study area shown in figure 3.2 103

Figure 3.4: Field aspect of the migmatites 109

Figure 3.5: Felsic veins in the granulite facies metasedimentary rocks 111

Figure 3.6: Morphology of the leucocratic veins 113

Figure 3.7: Cathodoluminescence images of representative zircons used for U-Pb SHRIMP analysis 117

Figure 3.8: Concordia diagram from zircon U-Pb SHRIMP analysis 118

Figure 3.9: Petrography and microstructure photographs and BSE images of the metasediments 123

Figure 3.10: Histogram of the percentage of outcrops versus the percentage of leucocratic veins 136

Figure 3.11: Schematic block diagram showing the injection complex at the crustal level presently exposed in the Opinaca Subprovince 137

Figure 3.12: Comparison of two temperature-depth profiles 145

CHAPITRE 4

Figure 4.1: Location of the Opinaca Subprovince 169

Figure 4.2: Simplified geological map of the Superior Province east of James Bay 171

Figure 4.3: Schematic representation of the interpreted time-temperatre path of

the Opinaca Subprovince 173

Figure 4.4: Geological map of the study area color-coded for the amount of leucocratic material per outcroup 176

Figure 4.5: Microstructure of the metagreywacke host rock and of various leucogranites 180

Figure 4.6: Field aspect of leucogranite dykes and veins in the Opinaca injection complex 183

Figure 4.7: Field photographs showing petrological features of the leucogranite 186

Figure 4.8: Feldspar triangle and Quartz - Alkali feldspar - Plagioclase plot 198

Figure 4.9: Harker diagrams for the major elements 199

Figure 4.10: Trace element (in ppm) Harker diagrams 201

Figure 4.11: Chondrite normalized REE patterns for the leucogranites 203

Figure 4.12: Whole rock $\delta^{18}O$ (relative to SMOW) results 208

Figure 4.13: Sketch of the mechanism leading to the evolved geochemical signature of leucogranites in the Opinaca injection complex 214

Figure 4.14: K_2O vs $CaO + Na_2O$ (wt. %) plot 216

Figure 4.15: Ba vs Sr (in ppm) plot of the composition of leucogranites from the Opinaca Subprovince 221

LISTE DES TABLEAUX

CHAPITRE 2

Table 2.1: SHRIMP Data 48

CHAPITRE 3

Table 3.1: U-Pb SHRIMP data 119

Table 3.2: Selected EPMA analysis of representative samples 125

Table 3.3: Content of heat-producing elements in rocks from the Opinaca 143

CHAPITRE 4

Table 4.1: Whole rock compositions of leucogranites from the Opinaca 191

Table 4.2: $\delta^{18}O$ (‰) composition of various rocks in the Opinaca and Ashuanipi 206

Table 4.3: Partition coefficient from Sample 4 in Nash and Creecraft (1985) 220

LISTE DES ANNEXES

Annexe 1: Exemples de structures de de veines leucogranitiques en affleurement 250

Annexe 2: Whole rock analysis quality control 251

Annexe 3: Whole rock analysis detection limits 252

CHAPITRE 1

INTRODUCTION

1.1 INTRODUCTION

1.1.1 IMPORTANCE DE LA DIFFÉRENCIATION CRUSTALE

La croûte continentale couvre près de 40% de la surface terrestre. Elle a comme différence fondamentale avec la croûte océanique de ne pas être recyclée dans le manteau, et donc elle enregistre des événements très anciens. Elle a commencé à se former dès l'Hadéen, et a continué de croître depuis (Rudnick, 1995). Parmi les différences majeures entre la croûte océanique et la croûte continentale, une est d'importance primordiale, sa composition. La croûte continentale a, en moyenne, une composition andésitique ce qui lui confère une densité plus faible que la croûte océanique (Taylor et McLennan, 1995; Rudnick et Gao, 2003).

Les sections suivantes présentent le contexte scientifique qui montre l'importance du transfert de magmas anatectiques dans la croûte continentale. Historiquement, vers la fin des années 1990, un ensemble de publications ont proposé la possibilité de la migration pervasive de magmas d'anatexie dans la croûte profonde (Collins et Sawyer, 1996; Weinberg et Searle, 1998; Brown et Solar, 1999). Ces publications fondatrices, basées sur des observations de terrain ont été suivies de modélisations numériques quelques années plus tard (Leitch et Weinberg, 2002; Hobbs et Ord, 2010). Ces modélisations, ainsi que les travaux les plus précoces, ont d'abord discuté de la possibilité qu'un tel mécanisme existe, et l'ont validé. Cependant, aucune recherche n'a mis l'emphase sur les conséquences que cela peut avoir sur la croûte et sur le phénomène de différenciation crustale. À la lecture de

la littérature sur le sujet, il ressort, de façon explicite ou implicite, que le mécanisme de transfert pervasif de magmas d'anatexie devrait avoir certains impacts sur la croûte. Dans le présent travail de recherche, nous proposons donc de retourner à l'étude d'un terrain naturel, pour étudier quels peuvent être certains de ces impacts. Dans un premier temps, l'importance du transfert de magmas d'anatexie, notamment par migration pervasive, sera présentée. Dans un deuxième temps, nous discuterons de la problématique spécifique de la thèse.

1.1.2 L'INFLUENCE DU TRANSFERT DE MAGMA SUR LA DIFFÉRENCIATION CRUSTALE

Le transfert des magmas d'anatexie, depuis leur source vers des niveaux plus superficiels, est l'un des mécanismes majeurs de la différenciation crustale (Fig. 1.1; Sawyer et al., 2011). D'autres mécanismes, comme le délaminage, sont également importants puisqu'ils empêchent la croûte continentale de devenir plus mafique. Dans ce cas, la différenciation se fait par une interaction entre le manteau et la croûte. En revanche, le transfert de magmas d'anatexie peut être un mécanisme interne à la croûte. Ce transfert de matériel granitique a pour effet de changer la distribution des éléments chimiques, le régime thermique, la distribution de la masse ainsi que celle des fluides. Ce transfert est donc un processus fondamental qui affecte de nombreux paramètres de la croûte continentale.

1.1.3 IMPORTANCE DE LA FUSION PARTIELLE DE LA CROÛTE ET SA DIFFÉRENCIATION

Dans certaines conditions, la croûte continentale peut atteindre des conditions de pression et de température suffisantes pour commencer à fondre partiellement (Clemens et Vielzeuf, 1987; White et al., 2011). Dans ce cas, il se forme une migmatite constituée d'un mélanosome et d'un leucosome. Ce dernier est le liquide silicaté produit par la fusion partielle (Sawyer, 2008). Malgré les différentes réactions possibles de fusion, le liquide silicaté a une composition globalement granitique (Clemens et Watkins, 2001; Clemens, 2006). Les gouttelettes de liquide ont tendance, lorsqu'elles sont soumises à un stress, à coalescer (Sawyer, 1994; Brown et al., 1995). Par la suite, la ségrégation entre le leucosome et le mélanosome se poursuit pour former des réseaux de conduits remplis de liquide silicaté. Dans des conditions typiques de métamorphisme régional associé à de la déformation, le réseau permet l'extraction des liquides de leur source. Le liquide produit, ayant une densité plus faible que sa roche mère, il est enclin à migrer, globalement, vers la surface (Rushmer, 2001). En effet, quoique le mouvement global des magmas d'anatexie est vers le haut, la direction de la migration est contrôlée avant tout par les gradients de pression locaux, de telle façon que les liquides migrent vers les zones de plus basse pression. Selon l'environnement tectonique, ce mouvement peut être latéral plutôt que vertical (Sawyer et al., 1999; Sawyer, 2001).

1.1.4 IMPORTANCE DE LA MIGRATION PERVASIVE COMME MÉCANISME DE TRANSFERT DES MAGMAS D'ANATEXIE

De nombreux débats ont eu lieu concernant le mécanisme selon lequel les magmas d'anatexie remontent dans la croûte. L'un des mécanismes initialement proposés est le phénomène de diapirs. De façon simplifiée, le mécanisme de diapir décrit un phénomène par lequel de larges volumes de magmas montent à travers la croûte sous la force de leur propre flottabilité (Arzi, 1978; Bateman, 1984). Selon ce mécanisme, les magmas contenus dans les diapirs peuvent théoriquement monter jusqu'à atteindre des niveaux où la densité de l'encaissant est la même, c'est-à-dire, généralement dans la croûte moyenne à supérieure. L'ascension de "bulles" de magmas est aujourd'hui considérée comme un mécanisme mineur (Rubin, 1993; Vigneresse et Clemens, 2000) et limité à des contextes spécifiques (Miller et Paterson, 1999; Olsen et al., 2004). Ainsi, le modèle de diapir a été remplacé par celui des dykes d'échelle crustale. Dans ce cas, les magmas anatectiques sont transportés à travers la croûte dans de grands dykes (Clemens et Mawer, 1992; Petford et al., 1994). Dans ce modèle, les magmas d'anatexie sont efficacement collectés à leur source et convergent vers de larges dykes où le transfert se fait rapidement vers les niveaux de mise en place (Petford et al., 1994; Cruden, 2006). La profondeur de mise en place est contrôlée par la capacité du dyke à se propager vers le haut et à transporter le magma suffisamment rapidement pour l'empêcher de cristalliser et de sceller le dyke. Typiquement, ces dykes alimentent des plutons ou des batholites dont la base se trouve à la limite fragile - ductile de la croûte. Ce modèle est encore aujourd'hui largement prédominant dans la littérature et est

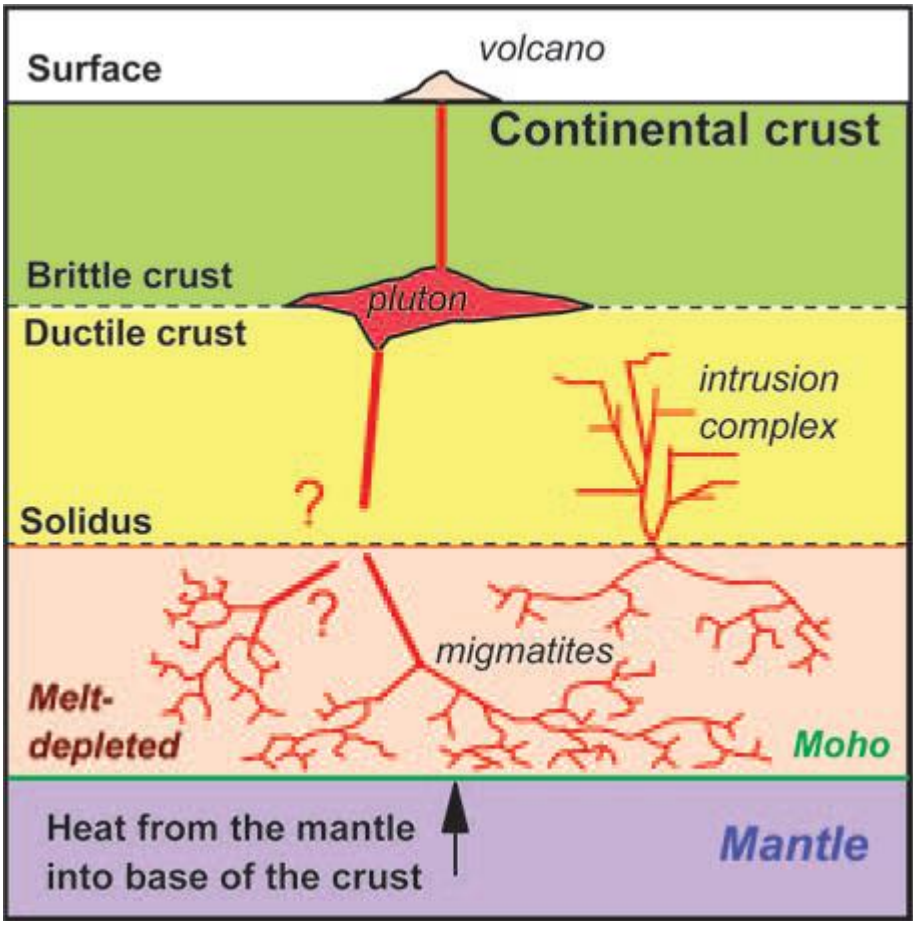

Figure 1.1: Coupe schématique de la croûte continentale montrant la distribution théorique des granites formés par anatexie. Le transfert vers la surface des magmas formés dans la partie inférieure est le mécanisme majeur de différenciation crustale. Cette illustration est possiblement la première figure disponible dans la littérature montrant un complexe d'injection dans un modèle schématique d'échelle crustale. Il est à noter que "intrusion complex" est un synonyme du concept de complexe d'injection utilisé dans cette thèse. Tiré de Sawyer et al., 2011.

celui qui explique le mieux le transfert de magma dans les niveaux supérieurs et froids de la croûte.

Vers la fin des années 1990, certaines observations ont montré que dans des terrains de haut grade métamorphique (faciès granulitique), proche des zones sources des magmas d'anatexie, les leucosomes ne convergent pas nécessairement pour former un réseau dendritique (Weinberg, 1999). Dans ces domaines où la température est suprasolidus, la migration des magmas d'anatexie peut se faire de façon pervasive, c'est-à-dire qu'un grand nombre de petites veines transportent le magma plutôt que quelques très gros dykes. Ce mécanisme n'est pas en contradiction avec le modèle de dykes (Brown et Solar, 1999; Weinberg et Searle, 1999) mais implique que, dans la croûte inférieure à moyenne, d'autres mécanismes peuvent être à l'œuvre. Le mécanisme de migration pervasive a surtout été étudié pour ses caractéristiques structurales et sa capacité à transporter les magmas. Cependant, les conséquences de ce mode de transfert n'ont été que partiellement modélisées (Fig. 1.2; Leitch et Weinberg, 2002; Hobbs et Ord, 2010). Ces modélisations restent peu ou pas validées à partir d'une étude de terrain.

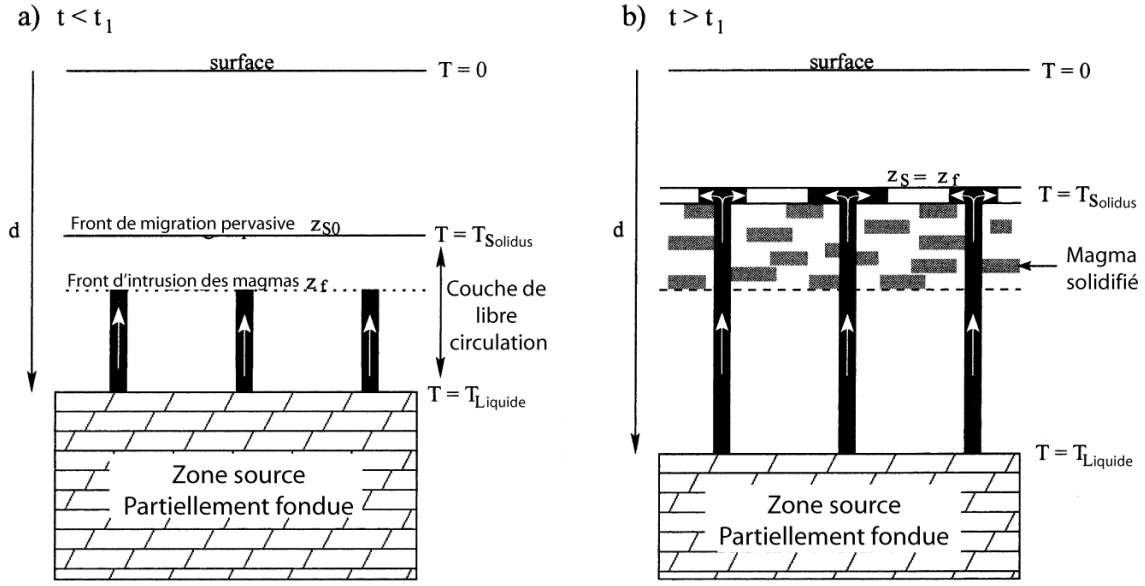

Figure 1.2 : Schéma du modèle conceptuel d'intrusion pervasive. Le modèle présente une zone source d'où proviennent les magmas (où T=$T_{liquidus}$) qui migrent dans une zone de libre circulation de façon pervasive jusqu'à la profondeur du solidus (Zs) où ils cristallisent (magmas solidifiés). Au cours du temps (schéma de droite), avec l'apport de chaleur par les magmas injectés, la profondeur du solidus diminue et les magmas peuvent migrer plus haut dans la croûte.

T: température, Zf: profondeur du front d'intrusion, Zs0 : profondeur du front de migration pervasive et Zs : profondeur du solidus. Modifiée d'après Leitch et Wienberg (2002).

1.1.5 LES COMPLEXES D'INJECTIONS: TERRAINS FORMÉS PAR LA MIGRATION PERVASIVE DE MAGMAS D'ANATEXIE

Dans le contexte géologique discuté dans cette thèse, c'est à dire un métamorphisme régional de haut grade et la migration de liquides silicatés felsiques, les complexes d'injections sont définis selon Weinberg et Searle (1998) comme la combinaison de 1) un hôte subissant un haut degré métamorphique et 2) d'innombrables veines et dykes felsiques qui s'injectent dans l'hôte. Les veines et dykes forment un réseau, de grande échelle, qui transportent le magma de façon pervasive depuis une source profonde vers des niveaux superficiels (Weinberg et Searle, 1998; Leitch et Weinberg, 2002). Le terrain hôte doit être à un haut grade métamorphique, typiquement au faciès des granulites. Un complexe d'injection est donc la trace laissée par la migration pervasive de magma dans un terrain de haut grade métamorphique. Ces terrains représentent typiquement des environnements profonds, environ 6 kbar, là où la température de la croûte est proche ou supérieure à celle du solidus des granites.

1.2 PROBLÉMATIQUE

Historiquement, les complexes d'injections ont été interprétés comme des zones de transfert pervasif de magma (Weinberg et Searle, 1998; Weinberg et Regenauer-Lieb, 2010). L'objet du présent travail consiste à analyser les impacts qu'a cette injection massive de magmas dans son hôte et d'en étudier les conséquences sur le phénomène global de différenciation

crustale. Il est en effet notable que, malgré sa fonction de transport de magma, les complexes d'injections contiennent encore de grands volumes de leucogranite observables sur le terrain. Ces volumes résiduels, qui n'ont pas été transporté hors de l'hôte, sont pris en compte dans les modélisations et sont importants pour la stabilité à long terme des complexes d'injection (Leitch et Weinberg, 2002; Hobbs et Ord, 2010). Il y a donc une partie du volume de magma transférée qui reste dans le complexe d'injection.

Si les surfaces considérées sont grandes et le volume de magma piégé dans le réseau formant le complexe d'injection est important, alors ceux-ci peuvent jouer un rôle non négligeable dans des processus crustaux. Ainsi, l'objet de ce travail de recherche est de déterminer quels sont les impacts de la mise en place d'un complexe d'injection.

1.3 HYPOTHÈSE

D'après des observations préalables de terrain, il semble que les complexes d'injections pourraient avoir un grand impact sur la croûte. En effet, nous postulons que les complexes d'injection ne sont pas seulement un ensemble de conduits transportant les magmas, mais constituent, en outre, un réservoir de magma de grande ampleur.

La présence de tels réservoirs de magma, à de telles profondeurs, n'est pas ou peu considérée dans la littérature. Nous faisons l'hypothèse que la présence d'un complexe

d'injection doit avoir des effets majeurs sur la croûte continentale et notamment sur le processus de différenciation crustale.

1.4 OBJECTIFS

L'étude se focalisera sur un complexe d'injection couvrant une grande surface.

Cette étude a pour but de :

- Identifier et caractériser le complexe d'injection
- Estimer et comparer les volumes de granites produits *in situ* vs. les granites injectés
- Estimer certains impacts d'un complexe d'injection sur la croûte dont:
    - Le bilan crustal des granites dans le contexte de métamorphisme granulitique régional
    - L'impact sur le transfert de chaleur dans la croûte
    - L'impact géochimique, particulièrement sur le degré d'évolution des leucogranites
    - L'impact de la présence d'H_2O contenue dans les granites

1.5 ZONE D'ÉTUDE

La section ci-dessous décrit les principales caractéristiques de la zone d'étude et les raisons du choix de celle-ci pour tester l'hypothèse générale. Cette thèse est sous forme d'un recueil d'articles, ce qui implique qu'une description de la zone d'étude sera répétée dans les différents chapitres. Néanmoins, chacun mettra l'emphase sur les particularités propres à leur problématique spécifique.

1.5.1 CONTEXTE GÉOLOGIQUE - LA SOUS-PROVINCE D'OPINACA DANS LA PROVINCE DU SUPÉRIEUR

La Sous-province archéenne d'Opinaca fait partie d'une série de quatre sous-provinces majoritairement métasédimentaires dans la Province du Supérieur (Fig. 1.3); cette série s'étend d'ouest en est sur plus de 2000 km et comprend les sous-provinces de Quetico, Nemiscau, Opinaca et Ashuanipi (Percival et al., 1992). Toutes ces sous-provinces présentent des similarités importantes parmi lesquelles (1) la composition principalement psamitique des roches métasédimentaires (Lapointe, 1996), (2) leurs âges et possiblement leurs environnements de dépôt ainsi que (3) leur quantité variable de veines leucogranitiques dans les métasédiments. Cependant, une caractéristique majeure différencie ces sous-provinces : chacune a atteint un pic de température métamorphique régional différent. Le grade métamorphique observé augmente depuis le faciès des schistes

vert à la bordure de la Sous-province de Quetico jusqu'au faciès des granulites dans l'Ashuanipi (Percival et al., 2006).

Dans le cadre de cette thèse, cette configuration régionale est importante, car elle permet l'étude de domaines géologiques comparables situés à différents niveaux crustaux. De plus, la grande taille de ces sous-provinces permet l'observation de phénomènes de grande ampleur affectant toute la croûte continentale. Grâce à ces caractéristiques, la Sous-province d'Opinaca permettra de vérifier l'hypothèse selon laquelle les complexes d'injections ont un impact sur la différenciation crustale.

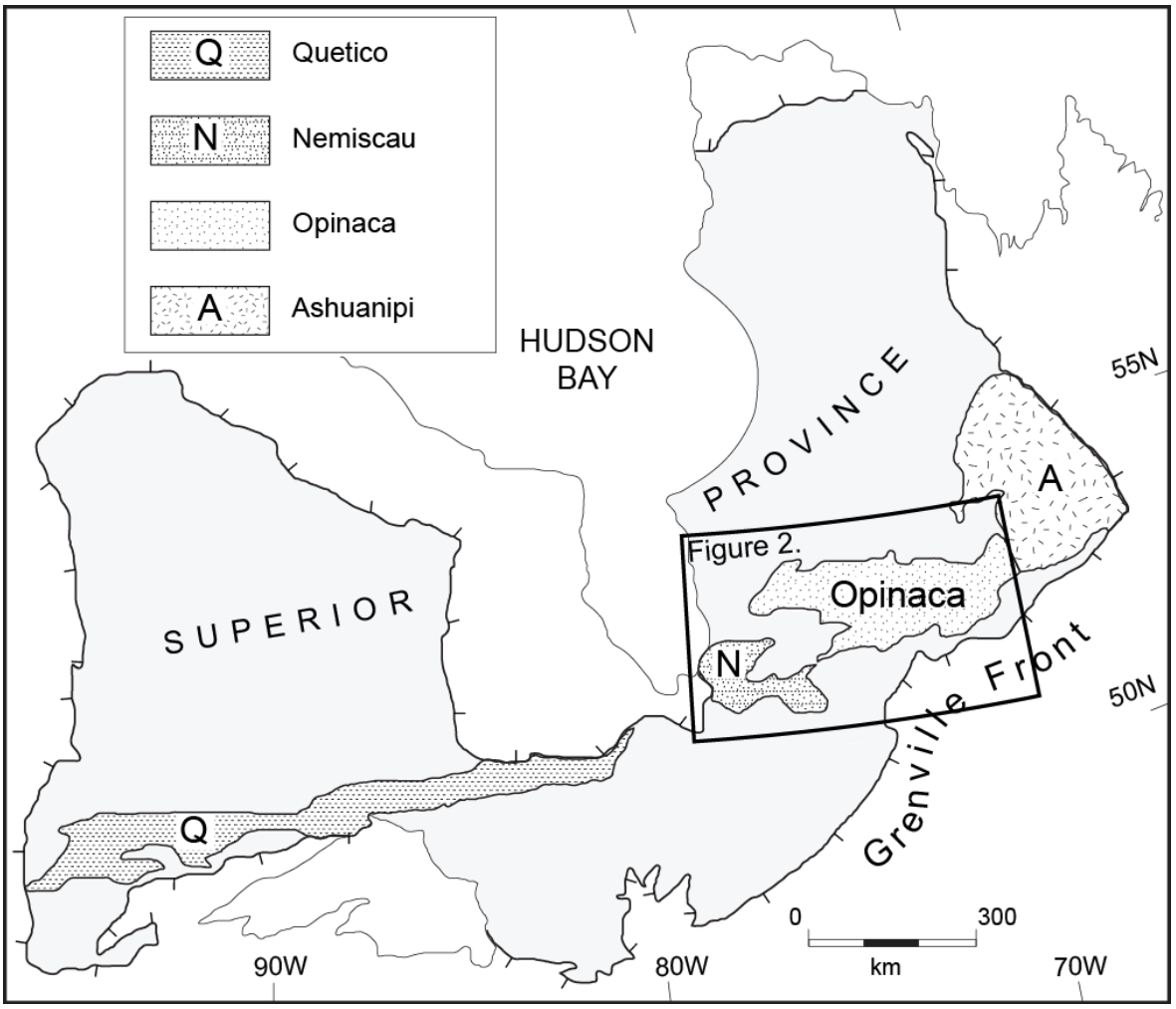

Figure 1.3: Carte de localisation générale de la Sous-province d'Opinaca dans la Province du Supérieur.

1.5.2 DESCRIPTION DE L'OPINACA

1.5.2.1 DESCRIPTION GÉNÉRALE

La Sous-province d'Opinaca est composée principalement d'unités métasédimentaires injectées par des quantités variables de fines veines leucogranitiques (Bandyayera et al., 2010, Bandyayera et al., 2011); cette combinaison forme le complexe d'injection (voir chapitre 3). Les veines leucogranitiques ont des épaisseurs variables mais sont généralement fines, soit entre 1 et 5 centimètres. Les veines qui sont plus large sont souvent composite, formées de multiples injections (voir chapitres suivants). Ces unités métasédimentaires montrent une schistosité principale S2, qui est accentuée par les injections de leucogranite subparallèles à S2. Des unités de roches mafiques métamorphisées, d'affinité tholéiitique, sont présentes dans les unités métasédimentaires. Leurs épaisseurs typiques sont de quelques dizaines de mètres, mais peuvent atteindre la centaine de mètres. Elles sont composées d'amphibole, plagioclase et clinopyroxène; l'orthopyroxène est parfois observé. De rares unités ultra-mafiques sont dispersées dans les unités métasédimentaires. Elles sont généralement de petite taille (dizaines de mètres en général) et montrent des évidences de métamorphisme et de réhydratation.

1.5.2.2 DESCRIPTION STRUCTURALE

Les structures sédimentaires originales sont rarement conservées. Cependant, des alternances de niveaux plus ou moins pélitiques caractérisés par des assemblages minéralogiques différents indiquent que le litage (S0) est subparallèle à la foliation principale (Bandyayera et al., 2010). Une structure planaire S1 est décrite dans l'ouest de l'Opinaca, mais n'est pas observée dans la zone d'étude spécifique à cette thèse (Bandyayera et al., 2010). La déformation principale est une schistosité (S2) orientée généralement est-ouest qui est observable dans toute la sous-province. Elle est subverticale et les linéations (qui sont parfois observables) plongent légèrement vers l'est ou l'ouest. Cette schistosité est principalement marquée par l'alignement des biotites dans les unités métasédimentaires. Elle est aussi rehaussée par les injections de leucogranites qui sont souvent subparallèles à S2. Une déformation tardive D3 est observée à l'échelle de la carte et plisse la foliation principale. Finalement, les flancs des plis F3 sont parfois tronqués par des zones de cisaillement est-ouest tardives (Bandyayera et al., 2010).

1.5.3 DESCRIPTION DES COMPOSANTES DU COMPLEXE D'INJECTION

Le complexe d'injection est la combinaison de l'hôte métasédimentaire et des multiples veines leucogranitiques qui l'injectent. Dans la section suivante, chaque composante est décrite de façon détaillée.

1.5.3.1 UNITÉS MÉTASÉDIMENTAIRES

Les unités métasédimentaires sont dominées par des compositions de métagreywacke et contiennent environ 10% de métapélites. Les métagreywackes ont une minéralogie simple composée de quartz + plagioclase + biotite (± grenat ± amphibole ± orthopyroxène ± tourmaline ± rare feldspath potassique). Leur structure est généralement granoblastique. Bien qu'il ne soit pas présent dans la plupart des métagreywackes (Simard et Gosselin, 1999; Bandyayera et al., 2010), l'orthopyroxène, qui est caractéristique du faciès granulitique, est observé dans toute la zone d'étude. Il est généralement remplacé par des phases hydratées telles que de la biotite, la cummingtonite ou l'anthophyllite, indiquant une réhydratation partielle au faciès supérieur des amphibolites. La présence de feldspath potassique (Kfs) est limitée à des grains qui ont la forme d'anciennes poches de liquide silicaté et est souvent associée aux assemblages contenant de l'orthopyroxène.

Les niveaux pélitiques sont plus rares, mais reconnaissables grâce à la présence de cordiérite et de sillimanite généralement associée à des assemblages péritectiques et à la présence de leucosomes. Les niveaux de métapélite étant plus fertiles que les métagreywackes (Nabelek et Bartlett, 2000), ces niveaux sont généralement plus riches en matériel leucocrate et la foliation principale y est plus souvent perturbée à cause de la quantité de liquide présente.

Ces unités sédimentaires forment l'hôte des injections de leucogranite. La prédominance de métagreywacke par rapport aux métapélites est un avantage dans l'optique de ce travail de recherche. La minéralogie y est simple et une seule réaction de fusion partielle est possible dans des conditions anhydres, celle-ci formant de l'orthopyroxène:

Biotite + Plagioclase + Quartz = Liquide silicaté + Orthopyroxène + Oxydes ± K-feldspath ± Grenat.

Il est donc plus facile d'estimer le taux de fusion partielle dans ce type de roche directement à partir de la quantité d'orthopyroxène (Guernina et Sawyer, 2003).

1.5.3.2 VEINES LEUCOGRANITIQUES

Les unités métasédimentaires ont atteint le faciès granulitique et ont été injectées de quantités variables de liquide leucogranitique sous forme de fines veines et de dykes. Ces veines sont généralement subparallèles à la foliation principale, mais peuvent être déformées de différentes façons en fonction du moment et de l'angle de leur mise en place vis-à-vis l'épisode de déformation principale. La granulométrie est très variable; la plupart des veines ont une granulométrie moyenne (taille des grains entre 2 et 10 mm), mais les textures pegmatitiques sont très communes. La minéralogie des veines leucogranitiques est simple, composée de quartz - plagioclase - K-feldspath dans différentes proportions (voir

chapitre 3); il y a très peu de minéraux mafiques et ceux-ci sont principalement de la biotite avec parfois du grenat et de la tourmaline.

1.6 MÉTHODOLOGIE

Le détail des procédures analytiques est fourni dans les parties portant sur les méthodes dans les différents articles. La partie qui suit met en évidence les relations entre les méthodes d'analyses et les différents objectifs spécifiques.

1.6.1 TRAVAIL DE TERRAIN

L'objectif du travail de terrain était de fournir une cartographie régionale contenant une estimation de la proportion des différents composants du complexe d'injection. Le terrain a aussi permis l'échantillonnage nécessaire pour les autres méthodes d'analyse décrites ci-dessous.

La grande surface cartographiée a permis de faire des interprétations qui ont des implications à l'échelle d'un niveau crustal, la croûte moyenne profonde. Cette échelle a une grande importance pour la compréhension du comportement de la croûte continentale.

Le travail de terrain a été effectué durant des campagnes de cartographie dirigées par le Bureau de l'Exploration Géologique du Québec durant les étés 2008 et 2009.

1.6.2 ANALYSE PÉTROGRAPHIQUE

L'analyse pétrographique permet de déterminer les assemblages minéralogiques et les microstructures des roches. Ces données permettent de déterminer le grade métamorphique en cherchant, par exemple, les évidences de fusion partielle dans les unités métasédimentaires. Elles permettent également d'estimer la production locale de liquide granitique. Cette estimation est indispensable pour la comparaison entre les volumes produits *in situ* et la quantité de leucogranites observée sur le terrain. Il s'agit d'un critère majeur pour l'identification du complexe d'injection. Les microstructures des leucogranites sont très importantes pour comprendre l'évolution pétrographique et géochimique des leucogranites qui forment le complexe d'injection. Par exemple, le feldspath principal des leucogranites est un critère majeur pour déterminer le processus et le degré de fractionnement. La minéralogie des assemblages rétrogrades dans les unités métasédimentaires permet de discuter l'importance des complexes d'injection en termes de réservoir d'H_2O dans la croûte continentale.

1.6.3 MICROSONDE

La microsonde a été utilisée pour déterminer la composition chimique des minéraux ainsi que pour confirmer des interprétations basées sur les observations pétrographiques. Les

résultats d'analyse sont aussi utilisés dans les équations de géothermomètres et de géobaromètres empiriques. Ceux-ci, couplées avec les observations pétrographiques, aident à déterminer les conditions métamorphiques.

L'analyse à la microsonde des leucogranites, la détermination de la calcicité des plagioclases en particulier, est utile dans l'interprétation de l'évolution des leucogranites formant le complexe d'injection.

1.6.4 LITHOGÉOCHIMIE

L'analyse des métasédiments de l'Opinaca montre que la composition des métagreywackes est similaire à celle de ceux de la Sous-province de Quetico qui est utilisée pour les pseudosections de Johnson et al. (2008).

La lithogéochimie est surtout utilisée pour illustrer le degré d'évolution des leucogranites qui forment le complexe d'injection, que ce soit grâce aux éléments majeurs, traces, ou bien de terres rares.

1.6.5 ISOTOPES D'OXYGÈNE

Déterminer les ratios d'isotopes d'oxygène ($\delta^{18}O$) sur des échantillons de roche totale permet d'estimer la source des fluides responsables de la réhydratation des assemblages

granulitiques. Ces analyses permettent d'étudier l'impact de la présence d'H_2O liée au complexe d'injection.

1.6.6 SHRIMP U/PB

Les ratios isotopiques d'uranium (U), plomb (Pb) et thorium (Th) ont été obtenus sur des zircons issus de métapélites, de métagreywackes, d'une veine leucogranitique et d'une veine pegmatitique. Les dates obtenues permettent de mieux comprendre les relations temporelles entre le haut grade métamorphique et les injections leucogranitiques. L'analyse des zircons détritiques apporte de nouvelles informations sur les sources potentielles des unités métasédimentaires et les processus antérieurs au complexe d'injection. L'ensemble des informations obtenues par la méthode SHRIMP offre une meilleure compréhension de la Sous-province d'Opinaca.

1.7 FORMAT DE LA THÈSE ET CONTRIBUTION DE CHAQUE AUTEUR

Cette thèse est présentée sous le format de recueil d'articles scientifiques. Pour chacun des articles, l'auteur principal est l'auteur de la présente thèse de doctorat. Chacun de ces articles est rédigé en anglais, car ils sont tous publiés ou prévus pour publication dans des

revues internationales. Le second chapitre de la thèse est intitulé “New geochronological constraints from SHRIMP U-Pb analysis in zircon from the Opinaca Subprovince, Superior Province, Quebec.” soumis et accepét dans la revue *Canadian Journal Of Earth Science* pour évaluation. Ce manuscrit présente des résultats d’analyse géochronologique U/Pb par la méthode SHRIMP dans le but de dater des zircons prélevés dans des unités métasédimentaires du complexe d’injection de l’Opinaca. Compte tenu de la relative faiblesse de la connaissance géochronologique dans la Sous-province d’Opinaca, les nouvelles donées apportées sont un ajout interessant à la compréhension de la région. Ce chapitre traite essentiellement des âges interprétés comme hérités de la source ainsi que des possibles perturbations du système isotopique qui ont pu affecter les zircons après l’épisode lié au complexe d’injection. Cet article ne se focalise pas sur la datation de l'évenement métamorphique principal, ni sur l'âge de crystallisation des veines leucogranitiques datées car ces aspects sont traités dans le chapitre 4. Dans cet article l'auteur principal est responsable de la rédaction de l'article, de l'analyses des résultats, du choix des points d'analyses en collaboration avec le personnel d'IBERSIMS et de la discussion. Le co-auteur est responsable de la discussion et du processus d'amélioration du manuscrit.

Le troisième chapitre est intitulé “Large volumes of anatectic melt retained in granulite facies migmatites: An injection complex in northern Quebec” et a été publié en mai 2013 dans le volume 168-169 de la revue *Lithos*. Cet article (Morfin et al. 2013) présente les évidences prouvant que les terrains d'Opinaca forment un complexe d’injection à partir

d’un travail de description de terrain basé sur une cartographie régionale. Des résultats de datation présentés montrent que l’épisode de haut grade métamorphique et la cristallisation des veines injectées se produisent simultanément. Cet article met en évidence la différence importante entre la quantité de matériel leucogranitique observée sur le terrain et cette même quantité estimée à partir d’une étude pétrographique et de modélisation thermodynamique. Le volume de matériel leucogranitique observé ne pouvant pas être expliqué par la simple fusion partielle des roches hôtes, il est conclu qu’une partie des leucogranites doit avoir été injectée. Cette observation fondamentale indique que l’Opinaca est un complexe d’injection et que celui-ci agit comme un réservoir de magmas anatectiques dans la croûte continentale moyenne. Certaines implications de cette découverte sont discutées, notamment concernant la distribution des éléments producteurs de chaleur dans la croûte continentale. L'auteur principal de cet article a participé au travail de terrain, a effectué certaines des analyses et est responsable de l'analyse des résultats. Il est l'auteur principal du manuscrit comprenant la rédaction, l'édition, ainsi que la discussion. Edward Sawyer a participé activement à la rédaction et aux corrections, ainsi qu'à la discussion scientifique générale. Daniel Bandyayera était responsable de la campagne de cartographie et a donc participé au travail de terrain, à la production de certaines figures ainsi qu'au processus de correction.

Le quatrième chapitre est intitulé “The geochemical signature of a felsic injection complex in the continental crust: Opinaca Subprovince, Quebec” et a été publié en 2014 dans le volume 196-197 de la revue *Lithos*. Cet article (Morfin et al. 2014)est basé sur l’analyse

pétrographique et géochimique des leucogranites constituant le complexe d'injection. Les résultats montrent que les magmas composant le complexe d'injection ont évolué par cristallisation fractionnée. Cela est important, car ces magmas évolués sont situés en profondeur dans la croûte continentale, ce qui n'est pas typique dans les modèles actuels. Le manuscrit discute de l'importance de la présence de larges volumes de magmas leucogranitiques évolués dans la croûte continentale moyenne. L'emphase est portée sur le bilan de distribution de la composante "granitique" dans la croûte, ainsi que sur les implications en termes de présence d'H_2O disponible pour réhydrater partiellement la coûte et/ou favoriser la fusion partielle; deux aspects fondamentaux du processus de différenciation crustale. L'auteur principal de cet article a participé au travail de terrain et est responsable de l'analyse des résultats et des modélisations géochimique. Il est l'auteur principal du manuscrit comprenant la rédaction, la discussion et l'édition. Edward Sawyer a participé activement à l'amélioration du manuscrit, aux corrections, ainsi qu'à la discussion scientifique. Daniel Bandyayera a participé au travail de terrain, à la production de certaines figures et au processus de correction.

Le cinquième chapitre est une synthèse des résultats présentés dans les articles. Cela permet une mise en perspective des impacts majeurs de la mise en place d'un complexe d'injection dans la croûte continentale pour la différenciation crustale. Cette partie conclut la thèse en proposant une actualisation des modèles classiques de distribution de granites dans la croûte et propose des pistes pour de futures recherches.

1.8 RÉFÉRENCES

Arzi, A.A., 1978. Critical phenomena in the rheology of partially melted rocks. Tectonophysics 44, 173-184.

Bandyayera, D., Burniaux, P., Morfin, S., 2011. Géologie de la région du lac Brune (33G07) et de la baie Gavaudan (33G10). Ministère des Ressources Naturelles du Québec, p. 25.

Bandyayera, D., Rhéaume, P., Maurice, C., Bédard, É., Morfin, S., Sawyer, E.W., 2010. Synthèse Géologique du Secteur du Réservoir Opinaca, Baie-James. Ministère des Ressources Naturelles du Québec, p. 44.

Bateman, R., 1984. On the role of diapirism in the, segregation, ascent and final emplacement of granitoid magmas. Tectonophysics 110, 211-231.

Brown, M., Averkin, Y.A., McLellan, E.L., Sawyer, E.W., 1995. Melt segregation in migmatites. Journal of Geophysical Research 100, 15655-15680.

Brown, M., Solar, G.S., 1999. The mechanism of ascent and emplacement of granite magma during transpression: a syntectonic granite paradigm. Tectonophysics 312, 1-33.

Clemens, J.D., 2006. Melting of the continental crust: fluid regimes, melting reactions, and source-rock fertility, in: Brown M, R.T. (Ed.), Evolution and Differentiation of the Continental Crust. Cambridge University Press, pp. 298-330.

Clemens, J.D., Mawer, C.K., 1992. Granitic magma transport by fracture propagation. Tectonophysics 204, 339-360.

Clemens, J.D., Vielzeuf, D., 1987. Constraints on melting and magma production in the crust. Earth and Planetary Science Letters 86, 287-306.

Clemens, J.D., Watkins, J., 2001. The fluid regime of high-temperature metamorphism during granitoid magma genesis. Contributions to Mineralogy and Petrology 140, 600-606.

Collins, W.J., Sawyer, E.W., 1996. Pervasive granitoid magma transfer through the lower-middle crust during non-coaxial compressional deformation. Journal of Metamorphic Geology 14, 565–579.

Cruden, A.R., 2006. Emplacement and growth of plutons: implications for rates of melting and mass transfer in continental crust, in: Brown M, R.T. (Ed.), Evolution and Differentiation of the Continental Crust. Cambridge University Press, pp. 455-519.

Guernina, S., Sawyer, E.W., 2003. Large-scale melt-depletion in granulite terranes: an example from the Archean Ashuanipi Subprovince of Quebec. Journal of Metamorphic Geology 21, 181–201.

Hobbs, B.E., Ord, A., 2010. The mechanics of granitoid systems and maximum entropy production rates. Philosophical Transactions of the Royal Society A: Mathematical, Physical and Engineering Sciences 368, 53-93.

Johnson, T.E., White, R.W., Powell, R., 2008. Partial melting of metagreywacke: a calculated mineral equilibria study. Journal of Metamorphic Geology 26, 837–853.

Lapointe, B., 1996. Un exemple de minéralisation aurifère en milieu profond :l'indice d'or du Lac Lilois dans le complexe d'Ashuanipi, Province du Supérieur, Nouveau-Québec. Chicoutimi : Université du Québec à Chicoutimi.

Leitch, A.M., Weinberg, R.F., 2002. Modelling granite migration by mesoscale pervasive flow. Earth and Planetary Science Letters 200, 131-146.

Miller, R.B., Paterson, S.R., 1999. In defense of magmatic diapirs. Journal of Structural Geology 21, 1161-1173.

Morfin, S., Sawyer, E.W., Bandyayera, D., 2013. Large volumes of anatectic melt retained in granulite facies migmatites: An injection complex in northern Quebec. Lithos 168–169, 200–218.

Morfin, S., Sawyer, E.W., Bandyayera, D., 2014. The geochemical signature of a felsic injection complex in the continental crust: Opinaca Subprovince, Quebec. Lithos 196–197, 339–355.

Nabelek, P.I., Bartlett, C.D., 2000. Fertility of metapelites and metagraywackes during leucogranite generation: an example from the Black Hills, U.S.A. Geological Society of America Special Papers 350, 1-14.

Olsen, S.N., Marsh, B.D., Baumgartner, L.P., 2004. Modelling mid-crustal migmatite terrains as feeder zones for granite plutons: the competing dynamics of melt transfer by bulk versus porous flow. Earth and Environmental Science Transactions of the Royal Society of Edinburgh 95, 49-58.

Percival, J.A., Mortensen, J.K., Stern, R.A., Card, K.D., Bégin, N.J., 1992. Giant granulite terranes of northeastern Superior Province: the Ashuanipi complex and Minto block. Canadian Journal of Earth Sciences 29, 2287-2308.

Percival, J.A., Sanborn-Barrie, M., Skulski, T., Stott, G.M., Helmstaedt, H., White, D.J., 2006. Tectonic evolution of the western superior province from NATMAP and lithoprobe studies. Canadian Journal of Earth Sciences 43, 1085-1117.

Petford, N., Lister, J.R., Kerr, R.C., 1994. The ascent of felsic magmas in dykes. Lithos 32, 161-168.

Rubin, A.M., 1993. Dikes vs. diapirs in viscoelastic rock. Earth and Planetary Science Letters 119, 641-659.

Rudnick, R.L., 1995. Making Continental Crust. Nature 378, 571-578.

Rudnick, R.L., Gao, S., 2003. Composition of the continental crust, in: Heinrich, D.H., Karl, K.T. (Eds.), Treatise on Geochemistry. Pergamon, Oxford, pp. 1-64.

Rushmer, T., 2001. Volume change during partial melting reactions: implications for melt extraction, melt geochemistry and crustal rheology. Tectonophysics 342, 389-405.

Sawyer, E.W., 1994. Melt segregation in the continental crust. Geology 22, 1019-1022.

Sawyer, E.W., 2001. Melt segregation in the continental crust: distribution and movement of melt in anatectic rocks. Journal of Metamorphic Geology 19, 291-309.

Sawyer, E.W., 2008. Atlas of Migmatites, Ottawa.

Sawyer, E.W., Cesare, B., Brown, M., 2011. When the continental crust melts. Elements 7, 229-234.

Sawyer, E.W., Dombrowski, C., Collins, W.J., 1999. Movement of melt during synchronous regional deformation and granulite-facies anatexis, an example from the Wuluma Hills, central Australia. Geological Society, London, Special Publications 168, 221-237.

Simard, M., Gosselin, C., 1999. Géologie de la région du Lac Lichteneger (SNRC 33B). Ministère des Ressources Naturelles du Québec, p. 25.

Taylor, S.R., McLennan, S.M., 1995. The geochemical evolution of the continental crust. Reviews of Geophysics 33, 241-265.

Vigneresse, J.L., Clemens, J.D., 2000. Granitic magma ascent and emplacement: neither diapirism nor neutral buoyancy. Geological Society, London, Special Publications 174, 1-19.

Weinberg, R.F., 1999. Mesoscale pervasive felsic magma migration: alternatives to dyking. Lithos 46, 393-410.

Weinberg, R.F., Regenauer-Lieb, K., 2010. Ductile fractures and magma migration from source. Geology 38, 363–366.

Weinberg, R.F., Searle, M.P., 1998. The Pangong Injection Complex, Indian Karakoram: a case of pervasive granite flowthrough hot viscous crust. Journal of the Geological Society 155, 883-891.

Weinberg, R.F., Searle, M.P., 1999. Volatile-assisted intrusion and autometasomatism of leucogranites in the Khumbu Himalaya, Nepal. Journal of Geology 107, 27.

White, R.W., Stevens, G., Johnson, T.E., 2011. Is the Crucible Reproducible? Reconciling Melting Experiments with Thermodynamic Calculations. Elements 7, 241-246.

CHAPITRE 2

NEW GEOCHRONOLOGICAL CONSTRAINTS FROM SHRIMP U-PB ANALYSIS IN ZIRCON FROM THE OPINACA SUBPROVINCE, SUPERIOR PROVINCE, QUEBEC

SAMUEL MORFIN[1], EDWARD W. SAWYER[1]

[1] UNIVERSITÉ DU QUÉBEC À CHICOUTIMI

CANADIAN JOURNAL OF EARTH SCIENCES, SOUMIS 2014

2.1 RÉSUMÉ

Les terrains de la Sous-province d'Opinaca, situés à la Baie James, au Québec, font partie de la Province du Supérieur et exposent un complexe d'injection d'échelle régionale. Ce dernier est composé d'unités métasédimentaires qui ont atteint le faciès des granulites, injectées d'innombrables petites veines de leucogranites. Des analyses U/Pb obtenues par SHRIMP (sonde ionique à haute résolution spatiale) sur quatre échantillons de métasédiments et sur un leucogranite sont présentées dans ce manuscrit. Les résultats améliorent l'âge du complexe d'injection qui est compris entre ca. 2670 Ma et ca. 2640, depuis des conditions granulitiques jusqu' aux conditions du solidus des granites. L'analyse de la fraction détritique des zircons montre que la transition entre les zircons hérités et la croissance de zircon métamorphique a lieu dans un court laps de temps (moins de 10 My entre 2680 et 2670 Ma). Bien que la plupart des âges hérités mesurés soient similaires aux âges de cristallisation des grandes unités géologiques situés autour de l'Opinaca à la Baie James, certains zircons ont retourné des âges mésoarchéens qui ne sont retrouvés que dans des unités situées au nord et au nord-ouest de l'Opinaca. Cela pourrait indiquer une vergence vers le sud pour la direction de la sédimentation. Cette direction de la sédimentation serait similaire à ce qui est proposé pour d'autres sous-provinces sédimentaires de la Province du Supérieur. Les droites de Discordia interceptent la Concordia à des âges qui, malgré de grandes marges d'erreur, indiquent une perturbation du système U/Pb à des âges grenvilliens, autour de 1000 Ma. Puisqu'aucune unité géologique grenvillienne n'est présente dans la région, une circulation de fluides provoquée par la

perturbation thermique associée à la mise en place de l'orogéne grenvillienne est envisagée. Ces fluides pourraient expliquer la perturbation isotopique enregistrée, et cela, à environ 250 km au nord du front de l'orogénie.

2.2 ABSTRACT

The Opinaca Subprovince, located in the James Bay area of Québec, is part of the Archean Superior Province. It exposes an injection complex composed of a granulite grade metasedimentary host injected by numerous thin (several centimeters thick) veins and dykes of leucogranites. U/Pb sensitive high-resolution ion microprobe (SHRIMP) analyses performed on zircons from four metasedimentary samples and from one injected leucogranite are presented in this contribution. The results allow for an improved understanding of the timing of the injection complex event which is bracketed between 2670 Ma at granulite condition and 2640 Ma at granite solidus conditions. Analysis of the detrital portions of the zircons yields information on the possible sources for the metasediments and indicates that the transition from detrital to high grade metamorphic zircon growth, which comprise the crystallisation of the igneous source, its exhumation, erosion and deposition as a sediment and the burial, occurs rapidly in less than 10 My between 2680 and 2670 Ma. Although most inherited zircons yield ages comparable to units across the James Bay area, several zircon record Mesoarchean ages which are only found in units situated to the north-northwest of the Opinaca Subprovince. Lower intercept

of the Discordias, despite having very large errors, are found to be within the range of ages from the Grenville Orogeny. Since there are no unit of that age in the vicinity of the Opinaca, a fluid circulation provoked by the thermal perturbation associated with the Grenville Orogen is inferred. These fluids could explain an isotopic perturbation at ca. 1000 Ma recorded 250 km north of the orogen front.

2.3 INTRODUCTION

Recent studies have shown that the relatively poorly studied Opinaca Subprovince of the Archean Superior Province is a large area where deep levels of the continental crust are exposed and that it contains an injection complex (Morfin et al. 2013). Injection complexes are defined as zones of high grade rocks which have been pervasively injected by granitic material (Weinberg and Searle, 1998). These structures are created by the pervasive migration of anatectic melts, which are produced in large volumes by partial melting of a deeper crustal source. The pervasive migration of anatectic magma is made possible in the suprasolidus crust by the fact that even small volumes of magma in small veins and dykes can exist for long period of time due to the high (supra solidus) temperature. This contribution presents and discusses new SIMS data obtained from zircons of the Opinaca Subprovince. The main objective of the discussion is to provide insight to the geochronological framework of the source material for the metasediments and to put it in a regional perspective. This publication is complementary to Morfin et al. (2013) where the

same samples were studied with a focus on the age of granulite conditions relative to the crystallisation of the leucogranites.

2.4 GEOLOGICAL CONTEXT

2.4.1 THE OPINACA SUBPROVINCE IN THE SUPERIOR PROVINCE

2.4.1.1 PART OF A LARGE SCALE SERIES OF METASEDIMENTARY BASINS

The Archean Opinaca Subprovince is part of a series of four metasedimentary subprovinces in the Superior Province (Fig. 2.1) stretching roughly east-west over 2000 km including, from east to west, the Quetico, Nemiscau, Opinaca and Ashuanipi Subprovinces. They have strong similarities, all are dominated by a metagreywacke that host various amounts of leucogranites. They also have similar ages of deposition and metamorphism (see below). The main variation between them is the peak metamorphic grade recorded by the metasediments in each. The metamorphic grade increases eastward from upper amphibolites facies in the Quetico Subprovince to Granulite facies in the Ashuanipi Subprovince. This regional configuration gives access to different crustal depth on a large scale.

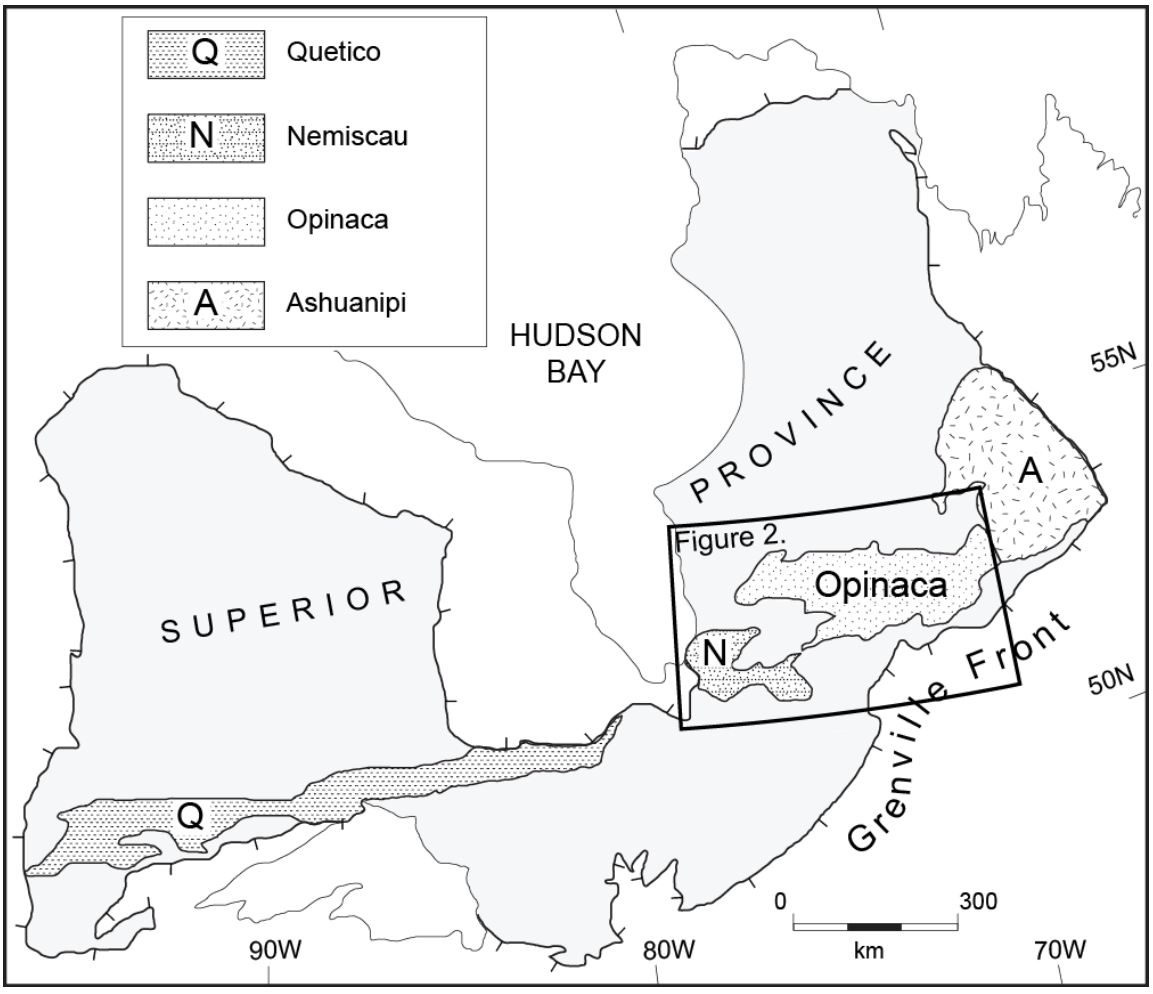

Figure 2.1: Simplified map of the Superior Province showing the location of the Quetico, Nemiscau, Opinaca and Ashuanipi metasedimentary subprovinces.

Deposition ages for metasediments in the Quetico Subprovince are <2698 Ma in the northern part and < 2692 Ma in the southern part. Deposition was followed by LP–HT metamorphism just reaching granulite facies in places in the central zone associated with partial melting. This event is coeval with the crystallisation of leucogranites in the high grade domains of the Quetico Subprovince between 2670 and 2650 Ma (Percival et al., 2006, see references therein for details).

Geochronological data from the Nemiscau Subprovince are scarce. Deposition age in the southern part is estimated at >2702 Ma (Davis et al., 1995) and <2706 ± 1 Ma in the northern part (Moukhsil and Legault, 2002). Titanite in a tonalite injected into the metasediments yield >2668 ± 2 Ma, which is interpreted as a metamorphic age for the surrounding metasediments (Moukhsil and Legault, 2002).

The Ashuanipi Subprovince is situated directly to the east of Opinaca Subprovince and the contact between the two is gradational, based on metamorphic grade, with the Ashuanipi Subprovince having reached higher peak conditions well into the granulite facies (Percival et al., 1992). The Ashuanipi Subprovince is a large granulite facies metasedimentary domain in which the average degree of partial melting reached ~31% (Guernina and Sawyer, 2003). Part of the melt produced from the metasediments is present in diatexite, mixed with various amounts of host residual metasediment. Some of the anatectic melt forms leucogranite bodies. Even with the presence of diatexites and leucogranitic bodies,

much of the leucogranite magma produced left the crustal level of the Ashuanipi so that the subprovince represent a large region of net melt-depletion (Guernina and Sawyer, 2003).

2.4.1.2 OPINACA SUBPROVINCE SURROUNDINGS

The Opinaca Subprovince is bounded (Fig. 2.2) by the La Grande Subprovince on its northern, western and south-western limits. The Opatica subprovince forms most of the southern contact. The limit to the east is transitional with the Ashuanipi Subprovince (Percival et al., 1992).

The Opatica Subprovince is a Neoarchan plutonic domain composed mainly of tonalite – trondhjemite – granodiorites orthogneisses (TTG) units which have been metamorphosed and partially melted at upper amphibolite facies (Sawyer, 2010). Crystallisation ages range from 2761 to 2702 Ma which was followed by metamorphic event between 2690 and 2677 Ma (Davis et al., 1995).

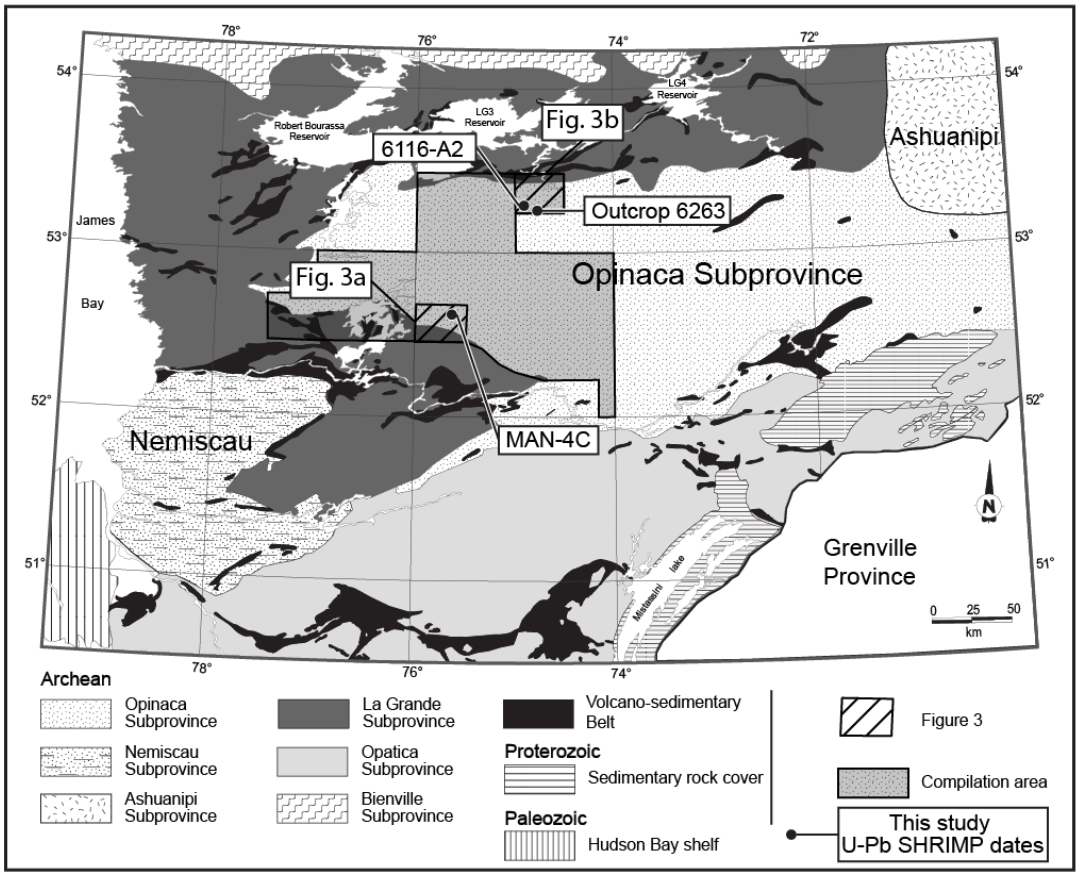

Figure 2.2: Regional map of the eastern James Bay area centered on the Opinaca Subprovince. Compilation area represents regions mapped by the MRNF for which some data is available. The positions of maps from figure 2.3 are shown together with the position of the samples used for zircon dating.

The plutonic and volcanic La Grande Subprovince is divided in two main domains, the La Grande volcanic domain in the north and the Eastmain volcanic domain in the south. The Eastmain volcanic domain lies to the south and west of the Opinaca Subprovince and consists of a series of Neoarchean tholeitic volcanic rocks, composed mostly of basalts, komatiites and felsic volcanic rocks. The volcanics are injected by TTG units. A synthesis of the geochronological events is presented in Moukhsil et al. (2003). The volcanism spans from 2751 to 2703 Ma, and is divided into four volcanic cycles. Synvolcanic felsic injections occurred between 2747 and 2710 Ma and were later intruded by syntectonic TTG between 2710 and 2697 Ma. Late tectonic granites and granodiorites emplaced post-deformation yield crystallization ages ranges from 2697 to 2618 Ma (Moukhsil et al., 2003).

The La Grande domain to the north and west of the Opinaca differs from the Eastmain domain mainly by the presence of Mesoarchean felsic crust. Most of the crustal basement is composed of the Langelier Complex consisting of banded tonalities and granodiorites ranging from 3360 +7/-5 to 2788 +4/-3 Ma (Goutier et al., 2001a). The Poste Le Moyne Pluton is also considered as part of the felsic basement and crystallised at 2881 ± 2 Ma (Goutier et al., 2001b). The La Grande domain records two main episodes of volcanism; the older Guyer Group between 2820 and 2806 (Bandyayera et al., 2011, Goutier et al., 2001b) and the Yasinski Group at 2732 +8-/-6 Ma (Goutier et al., 2001b) which have ages similar to those described in the Eastmain volcanic domain.

2.4.2 REVIEW OF THE OPINACA GEOCHRONOLOGY

Most of the geochronological data available is provided by reports from mapping campaigns by the geological survey of Quebec (BEGQ). The eastern part of the Opinaca, next to the well-studied Ashuanipi Subprovince has some geochronological information published contrary to the central Opinaca which has never been studied. The region of interest in the western Opinaca (Fig. 2.3) has few published geochronoligical data which is summarized in the next section.

The time of deposition of sediments in the eastern Opinaca Subprovince is bracketed by the 2721 Ma peak in detrital zircon ages and by the 2686 ± 1 Ma crystallisation age of a pyroxenite injected into them (Wodicka et al., 2009). In the western Opinaca, the minimum deposition age is constrained by intrusion of the Pluton de Bezier that yields a crystallisation age of 2674 ± 12 Ma (Goutier et al., 2001b, St. Seymour et al., 1989). The maximum age of deposition must be younger than 2700 Ma constrained by the pre-sedimentary 2699 ± 4 Ma Lac Taylor Granite (Goutier et al., 1999, Moukhsil et al., 2003).

In the east detrital zircons ages interpreted to represent source ages are scattered between 2721 and 2959 Ma (Wodicka et al., 2009), whereas some zircon cores record ages as old as 3284 Ma in the west (Moukhsil et al., 2003).

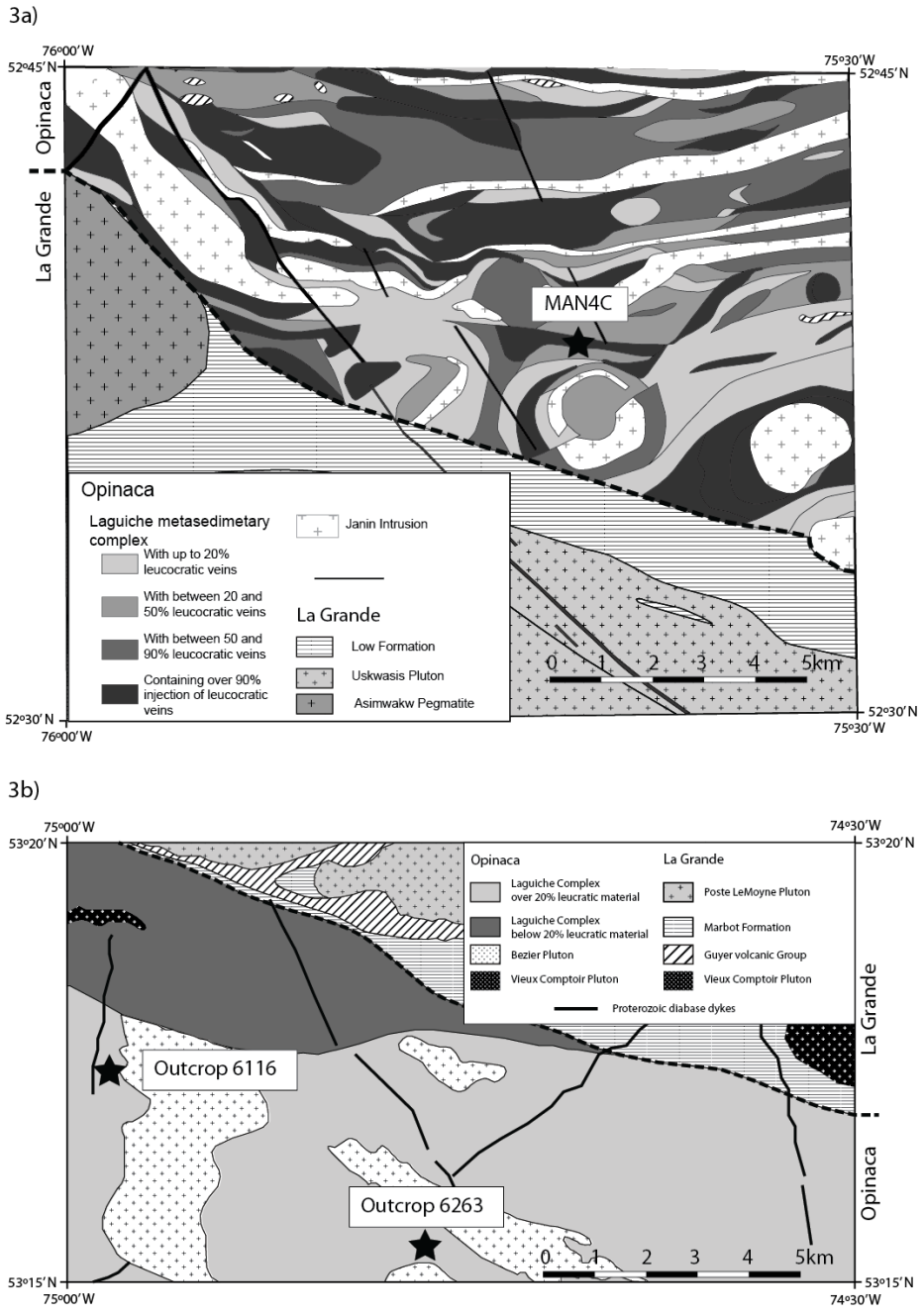

Figure 2.3: Geological map of the two sectors from figure 2.2 with the positions of the sampled outcrops indicated.

The metamorphic timeframe in the western Opinaca is constrained by a peak in zircon age population in a metagreywacke at 2647 Ma, which is interpreted as the age of metamorphism in a metagreywacke via ID-TIMS on zircon (David et al., 2010). SHRIMP analysis of metamorphic zircons from metapelitic samples 6116A and MAN4C (see sample description below) indicates that the main peak of zircon growth in these two metasediments occurred at 2660.6 ± 3.2 Ma and at 2663.6 ± 6.0 Ma respectively (Morfin et al., 2013). Sample MAN4C also shows a secondary peak in age distribution at 2637 ± 6.7 Ma, and this is interpreted as the end of the high grade event, possibly linked with H_2O released to the metasedimentary units from the crystallisation of the leucogranitic veins intruded into it (Morfin et al., 2013).

Zircon from a leucogranitic vein injected into the metasedimentary rocks studied by David et al. (2010) yield a crystallization age of 2671.6 ± 1.8 Ma (upper intercept of a linear regression line defined by three results and a lower intercept at 0 Ma). SHRIMP zircon analyses obtained in this study from leucogranite sample 6263C1 (see detailed description below) show two main peaks in the age distribution at 2665.9 ± 4.3 Ma and at 2646.0 ± 3.8 Ma (Morfin et al., 2013). These two age peaks are interpreted to represent two episodes of crystallisation, possibly due to the separate injection of batches of magma in to the vein as the field evidence suggests (Morfin et al., 2013).

The overlap between the metamorphic ages recorded in the metasedimentary units and the crystallisation ages recorded in the injected leucogranites leads to the interpretation that

cooling from the granulite facies metamorphic peak was contemporaneous with the crystallisation of the injected leucogranitic veins (Morfin et al., 2013; 2014).

In the eastern Opinaca the high-grade metamorphic event is constrained in metasedimentary units to be between 2668 and 2646 Ma; specifically at 2659 +4/-3 Ma from two different samples (Wodicka et al., 2009). In magmatic rocks the crystallisation of zircon is recorded at 2648 ± 1 and 2645 +5/-4 in a pyroxenite and from an upper Discordia intercept in zircon from a tonalitic vein, respectively (Wodicka et al., 2009). From these data, there is no clear simultaneity between metamorphism of the host rocks and the injection of magmatic units, although Wodicka et al. (2009) interpreted these events as similar.

2.5 SHRIMP METHODOLOGY

After the samples were crushed to millimetre sized grains, the zircons were separated and concentrated using standard separation techniques at the IBERSIMS laboratory at the University of Granada. Zircons were then mounted in epoxy with the 417 Ma TEMORA reference zircon (Black et al., 2003), and then polished. The position of the spots for analysis where selected from cathodoluminescence (CL) images. The analytical procedure at IBERSIMS follows that outlined in Williams and Claesson (1987). The TEMORA reference zircon was analyzed every fourth analysis for U-Pb ratio calibration. Point-to-point errors, calculated on replicates of the TEMORA standard at 95 % confidence interval,

range from 0.22 to 0.32 % for $^{206}Pb/^{238}U$, and 0.39 to 0.88 % for $^{207}Pb/^{206}Pb$, depending on the analytical session. Data reduction was done using the SHRIMPTOOLS software (available at www.ugr.es/~ibersims). Reduced data are plotted using ISOPLOT/EX 3.75 (Ludwig, 2012). $^{207}Pb/^{206}Pb$ ages (Table 2.1), corrected for common lead ^{204}Pb, are used for age distribution plots and age average calculations. Uncertainties are presented at the 2σ level (95 % confidence). Analyses yielding less than 5 % discordance are considered as subconcordant, and used in the discussion of ages, except if otherwise specified.

2.6 RESULTS

2.6.1 SAMPLE MAN4C: GRANULITE FACIES METAPELITE

2.6.1.1 SAMPLE DESCRIPTION

Sample MAN4C is a metapelite from the south-western Opinaca (Fig. 2.4a). The outcrop is situated 10 km north of the southern Opinaca – La Grande boundary, at the northern limit of a domain where the regional west-east schistosity is less pronounced. The unit is folded, and there is evidence for the migration of melt from fold limbs, which therefore become melt-depleted, towards the fold hinges which become melt-enriched, indicating effective melt segregation in this zone. The outcrop is composed of layers of partially melted metapelite that alternate with Fe-rich layers rich in garnet.

The sample itself is a typical metapelite which has partially melted; it is composed of melanocratic residuum and small patches of leucosomes (Fig. 2.4a).

Spot	Concentration (ppm)						Ratios (^{204}Pb Corrected)						Ages (^{204}Pb Corrected) in Ma							Spot position
	U	Th	^{206}Pb	f206_4%	f206_8%	^{232}Th/^{238}U	^{207}Pb/^{206}Pb	±err	^{207}Pb/^{235}U	±err	^{206}Pb/^{238}U	±err	^{207}Pb/^{206}Pb	±err	^{207}Pb/^{235}U	±err	^{206}Pb/^{238}U	±err	disc.(%)	
MAN4C - Metapelite																				
1.1	75	46	31	0.34	-2.27	0.63	0.189	0.001	12.510	0.258	0.480	0.009	2735	10	2644	20	2525	41	4.4	Core
1.2	290	4	128	0.04	-0.10	0.01	0.178	0.001	12.481	0.147	0.509	0.005	2633	7	2641	11	2652	23	-0.4	Rim
2.1	785	80	319	0.13	-0.40	0.10	0.177	0.001	11.489	0.056	0.470	0.000	2628	5	2564	5	2483	1	3.2	Rim
3.1	24	26	10	0.29	-6.13	1.10	0.189	0.005	12.058	0.427	0.464	0.012	2730	39	2609	34	2456	53	5.8	homog.
4.1	52	47	24	0.00	-0.68	0.93	0.188	0.001	13.784	0.246	0.532	0.009	2724	10	2735	17	2750	37	-0.6	Core
4.2	365	63	151	0.04	-0.68	0.18	0.181	0.000	11.967	0.112	0.479	0.004	2663	3	2602	9	2524	18	3	Rim
5.1	433	22	183	0.07	-0.56	0.05	0.177	0.001	11.874	0.077	0.487	0.002	2622	6	2595	6	2559	8	1.4	Rim
6.1	380	13	161	0.14	-0.27	0.03	0.178	0.000	12.038	0.085	0.491	0.003	2634	2	2607	7	2573	13	1.4	Rim
6.2	191	90	90	0.12	-0.08	0.48	0.202	0.001	15.143	0.090	0.545	0.002	2839	5	2824	6	2803	8	0.8	Core
7.2	1287	11	532	0.12	0.00	0.01	0.176	0.000	11.559	0.085	0.477	0.003	2615	4	2569	7	2512	12	2.2	Rim
8.1	419	485	183	0.04	-0.12	1.19	0.185	0.001	12.859	0.227	0.504	0.008	2700	7	2669	17	2630	36	1.4	Core
8.2	170	253	73	0.07	-1.17	1.53	0.184	0.001	12.560	0.118	0.496	0.004	2687	5	2647	9	2596	17	2	Core
9.1	718	130	310	0.09	-0.77	0.19	0.179	0.000	12.312	0.054	0.499	0.000	2644	4	2629	4	2609	2	0.8	Rim
9.2	719	356	303	0.07	-0.54	0.51	0.183	0.001	12.309	0.299	0.487	0.011	2682	9	2628	23	2560	50	2.6	Core
10.1	521	44	227	0.02	0.06	0.09	0.182	0.000	12.605	0.068	0.503	0.001	2670	4	2651	5	2626	6	1	Rim
10.2	256	216	112	0.06	-0.47	0.87	0.183	0.001	12.804	0.109	0.507	0.003	2681	6	2665	8	2644	15	0.8	Core
11.1	621	20	264	0.06	-0.24	0.03	0.179	0.000	12.155	0.123	0.491	0.005	2648	2	2617	10	2576	20	1.6	Rim
11.2	84	54	38	0.00	0.25	0.66	0.187	0.002	13.605	0.228	0.527	0.007	2717	14	2723	16	2731	31	-0.2	Core
12.1	571	986	249	0.03	-18.57	1.77	0.185	0.000	12.842	0.068	0.504	0.002	2698	3	2668	5	2629	7	1.4	Core
12.2	359	44	144	0.14	6.89	0.13	0.177	0.000	11.340	0.045	0.463	0.001	2629	2	2552	4	2455	3	3.8	Rim
13.1	570	178	271	0.03	5.68	0.32	0.205	0.000	15.535	0.067	0.549	0.001	2869	2	2849	4	2820	5	1	Core
13.2	291	216	141	0.04	0.30	0.76	0.216	0.001	16.715	0.169	0.562	0.005	2950	6	2919	10	2874	20	1.6	Rim
14.1	240	212	103	0.02	-3.53	0.90	0.186	0.001	12.649	0.125	0.494	0.004	2704	6	2654	9	2589	18	2.4	Core
14.2	359	23	161	0.18	7.50	0.07	0.174	0.000	12.396	0.053	0.517	0.001	2597	3	2635	4	2685	4	-1.8	Rim
15.1	286	198	120	0.06	-0.55	0.71	0.186	0.000	12.375	0.056	0.483	0.001	2704	4	2633	4	2542	4	3.4	Rim
16.1	492	278	219	0.03	1.41	0.58	0.189	0.001	13.391	0.169	0.514	0.006	2734	6	2708	12	2673	25	1.2	Core
16.2	502	24	219	0.05	7.91	0.05	0.179	0.001	12.423	0.076	0.503	0.001	2646	7	2637	6	2626	6	0.4	Rim
17.1	253	117	115	-0.02	2.86	0.47	0.190	0.001	13.734	0.156	0.525	0.005	2740	5	2732	11	2721	23	0.4	Core
17.2	373	4	158	0.03	8.21	0.01	0.178	0.000	12.023	0.064	0.490	0.002	2634	4	2606	5	2571	7	1.4	Rim
18.1	508	518	223	0.06	-5.80	1.04	0.184	0.000	12.856	0.075	0.507	0.002	2689	3	2669	6	2644	9	1	Rim
19.1	961	606	361	0.02	-0.16	0.65	0.180	0.000	10.760	0.050	0.435	0.001	2649	4	2503	4	2326	4	7	Rim
19.2	835	59	365	0.01	7.67	0.07	0.182	0.000	12.672	0.134	0.505	0.005	2671	4	2656	10	2635	21	0.8	Rim
20.1	874	216	341	0.03	5.33	0.25	0.181	0.001	11.222	0.127	0.450	0.005	2660	7	2542	11	2396	20	5.8	Rim
21.1	624	9	275	0.02	8.48	0.01	0.181	0.000	12.714	0.103	0.510	0.003	2661	5	2659	8	2656	15	0	Rim
21.2	179	200	73	0.22	-7.45	1.14	0.184	0.001	11.957	0.081	0.472	0.002	2686	4	2601	6	2494	10	4.2	Core
22.1	31	18	15	0.30	1.59	0.60	0.188	0.002	14.182	0.331	0.546	0.011	2727	20	2762	22	2810	45	-1.8	Core
22.2	278	1	121	0.02	8.33	0.01	0.177	0.001	12.295	0.110	0.503	0.004	2628	6	2627	8	2626	16	0	Rim
23.1	487	120	213	0.01	5.40	0.25	0.183	0.000	12.758	0.087	0.507	0.003	2677	4	2662	7	2643	11	0.8	Rim
24.1	351	15	152	0.00	7.84	0.04	0.177	0.001	12.249	0.112	0.501	0.004	2627	8	2624	9	2619	15	0.2	Rim
24.2	275	257	118	-0.01	-4.48	0.96	0.185	0.001	12.645	0.161	0.496	0.005	2699	9	2654	12	2595	23	2.2	Core
25.1	915	4	404	0.01	8.51	0.00	0.181	0.000	12.738	0.105	0.511	0.004	2662	3	2661	8	2659	16	0	Rim
25.2	132	107	60	-0.02	-2.38	0.83	0.184	0.001	13.362	0.129	0.525	0.004	2693	10	2706	9	2722	15	-0.6	Core
26.1	958	3	417	0.03	8.55	0.00	0.181	0.000	12.514	0.125	0.503	0.005	2659	2	2644	9	2625	20	0.8	Rim
26.2	242	315	106	0.00	-10.46	1.33	0.186	0.000	12.935	0.192	0.505	0.007	2705	1	2675	14	2635	31	1.4	Core
27.1	301	373	133	-0.01	-9.38	1.27	0.185	0.001	13.032	0.182	0.511	0.007	2698	7	2682	13	2661	28	0.8	Core

Spot	Concentration (ppm)						Ratios (^{204}Pb Corrected)						Ages (^{204}Pb Corrected) in Ma							Spot position
	U	Th	^{206}Pb	f206_4%	f206_8%	^{232}Th/^{238}U	^{207}Pb/^{206}Pb	±err	^{207}Pb/^{235}U	±err	^{206}Pb/^{238}U	±err	^{207}Pb/^{206}Pb	±err	^{207}Pb/^{235}U	±err	^{206}Pb/^{238}U	±err	disc.(%)	
28.1	90	77	40	0.04	-2.83	0.87	0.186	0.001	13.142	0.103	0.513	0.003	2707	7	2690	7	2668	12	0.8	Core
28.2	437	61	174	0.09	6.69	0.14	0.178	0.000	11.317	0.104	0.461	0.004	2636	3	2550	9	2443	17	4.2	Rim
29.1	432	98	171	0.28	4.90	0.23	0.166	0.001	10.399	0.141	0.456	0.006	2513	5	2471	13	2420	26	2	Rim
29.2	326	465	140	0.04	-13.00	1.47	0.185	0.001	12.631	0.170	0.496	0.006	2697	10	2653	13	2595	24	2.2	Core
30.1	147	99	68	0.07	-0.11	0.69	0.189	0.001	13.950	0.113	0.534	0.003	2737	7	2746	8	2759	13	-0.4	Core
31.1	60	89	22	0.48	-14.68	1.54	0.184	0.002	10.810	0.221	0.426	0.008	2688	16	2507	19	2290	34	8.6	homog.
32.1	125	144	45	0.08	-8.04	1.18	0.188	0.001	10.638	0.138	0.411	0.005	2724	6	2492	12	2218	22	11	homog.
33.1	157	23	64	0.07	6.89	0.15	0.185	0.002	12.051	0.120	0.473	0.002	2696	14	2608	9	2497	7	4.2	homog.
6116A2 - Metapelite																				
1.1	405	11	182	0.02	0.02	0.03	0.181	0.000	12.926	0.127	0.518	0.005	2662	2	2691	20	2674	9	-0.6	homog.
1.2	1087	756	436	0.06	-0.31	0.71	0.176	0.000	11.226	0.073	0.463	0.002	2614	3	2453	10	2542	6	3.4	homog.
2.1	546	35	235	0.03	0.05	0.07	0.178	0.003	12.181	0.192	0.496	0.001	2634	25	2599	4	2619	15	0.8	homog.
3.1	595	11	248	0.03	0.00	0.02	0.179	0.003	11.926	0.286	0.482	0.009	2647	24	2537	40	2599	23	2.4	homog.
3.2	746	6	296	0.05	0.03	0.01	0.176	0.001	11.131	0.127	0.459	0.005	2616	7	2433	20	2534	11	4.0	homog.
4.1	479	23	213	0.00	0.01	0.05	0.180	0.000	12.776	0.097	0.514	0.003	2656	2	2673	14	2663	7	-0.4	homog.
4.2	320	14	135	0.07	0.04	0.04	0.181	0.000	12.182	0.142	0.488	0.005	2663	4	2561	23	2619	11	2.2	homog.
5.1	604	63	231	0.18	-0.25	0.11	0.172	0.000	10.464	0.120	0.441	0.005	2579	4	2354	21	2477	11	5.0	homog.
5.2	614	78	242	0.57	-0.03	0.13	0.171	0.001	10.684	0.089	0.454	0.003	2564	5	2414	14	2496	8	3.4	homog.
7.1	460	20	186	0.28	0.03	0.04	0.180	0.002	11.553	0.239	0.466	0.008	2651	16	2466	37	2569	20	4	homog.
7.2	562	49	187	0.46	0.19	0.09	0.170	0.003	8.943	0.254	0.383	0.009	2553	25	2088	43	2332	26	10.4	homog.
8.1	599	25	262	0.03	-0.02	0.04	0.182	0.000	12.656	0.086	0.505	0.003	2668	2	2637	12	2654	6	0.6	homog.
9.1	831	148	320	0.12	0.06	0.18	0.165	0.001	10.128	0.127	0.444	0.005	2512	8	2369	22	2447	12	3.2	homog.
10.1	342	15	150	0.03	0.01	0.04	0.181	0.001	12.627	0.066	0.506	0.001	2661	5	2641	6	2652	5	0.4	homog.
11.1	1932	494	683	0.03	-0.35	0.26	0.139	0.001	7.852	0.083	0.408	0.004	2221	7	2207	17	2214	10	0.4	homog.
11.2	833	72	298	0.03	-0.16	0.09	0.154	0.001	8.762	0.140	0.414	0.006	2387	12	2231	26	2314	15	3.6	homog.
12.1	1046	465	425	0.06	-0.02	0.46	0.180	0.000	11.626	0.114	0.469	0.004	2651	4	2479	18	2575	9	3.8	homog.
13.1	501	115	198	0.22	0.32	0.24	0.177	0.000	11.132	0.159	0.456	0.006	2625	4	2422	28	2534	13	4.4	homog.
14.1	547	12	239	0.02	-0.01	0.02	0.181	0.001	12.587	0.107	0.505	0.004	2660	5	2636	15	2649	8	0.6	homog.
15.1	627	37	269	0.01	-0.01	0.06	0.181	0.001	12.371	0.103	0.495	0.003	2664	8	2593	12	2633	8	1.6	homog.
16.1	716	15	370	0.01	0.00	0.02	0.246	0.002	20.244	0.199	0.597	0.004	3160	10	3017	15	3103	10	2.8	homog.
18.1	514	5	222	0.13	0.06	0.01	0.180	0.000	12.393	0.083	0.498	0.003	2656	3	2607	11	2635	6	1.0	homog.
19.1	528	26	231	0.06	0.03	0.05	0.180	0.000	12.544	0.091	0.506	0.003	2650	4	2641	12	2646	7	0.2	homog.
20.1	629	12	270	-0.01	0.00	0.02	0.182	0.001	12.406	0.080	0.496	0.002	2667	5	2595	10	2636	6	1.6	homog.
6263A2 - Metagreywacke																				
2.1	243	359	106	0.45	-0.31	1.52	0.186	0.001	12.887	0.148	0.501	0.004	2711	10	2619	19	2671	11	2.0	Rim
2.2	150	147	65	0.64	0.26	1.00	0.183	0.001	12.542	0.211	0.496	0.008	2684	5	2596	35	2646	16	1.8	Core
3.1	72	37	33	-0.07	0.10	0.52	0.192	0.002	13.972	0.165	0.527	0.002	2761	17	2730	10	2748	11	0.6	Core
3.2	651	473	262	7.22	5.20	0.74	0.168	0.010	10.155	0.649	0.438	0.010	2539	97	2342	43	2449	61	4.4	Rim
4.1	864	569	302	0.83	-0.51	0.68	0.167	0.001	9.256	0.089	0.402	0.003	2529	10	2177	12	2364	9	8	Core
4.2	1999	29	404	8.81	9.51	0.01	0.124	0.019	3.661	0.591	0.215	0.013	2011	245	1253	68	1563	138	19.8	Rim
5.1	509	32	219	3.59	0.62	0.06	0.159	0.003	10.585	0.225	0.483	0.002	2444	34	2541	7	2487	20	-2.2	Rim
5.2	639	271	254	0.02	-0.55	0.43	0.184	0.000	11.622	0.075	0.459	0.002	2685	2	2436	11	2574	6	5.4	Core
6.1	464	379	181	0.65	0.35	0.84	0.178	0.001	11.028	0.130	0.449	0.005	2637	6	2390	21	2526	11	5.4	Core
6.2	516	457	187	0.44	-0.72	0.91	0.175	0.001	10.095	0.080	0.418	0.002	2609	7	2250	11	2444	7	8	Rim
7.1	392	235	167	0.29	-0.01	0.62	0.187	0.000	12.635	0.136	0.491	0.005	2712	4	2576	21	2653	10	2.8	Core

Spot	Concentration (ppm)						Ratios (^{204}Pb Corrected)						Ages (^{204}Pb Corrected) in Ma							Spot position
	U	Th	^{206}Pb	f206_4%	f206_8%	^{232}Th/^{238}U	^{207}Pb/^{206}Pb	±err	^{207}Pb/^{235}U	±err	^{206}Pb/^{238}U	±err	^{207}Pb/^{206}Pb	±err	^{207}Pb/^{235}U	±err	^{206}Pb/^{238}U	±err	disc.(%)	
7.2	479	32	179	0.20	0.23	0.07	0.177	0.000	10.522	0.056	0.431	0.001	2627	4	2308	6	2482	5	7	Rim
8.1	516	284	198	0.10	-0.47	0.56	0.178	0.000	10.873	0.063	0.442	0.002	2639	4	2359	8	2512	5	6.2	Rim
8.2	729	348	231	0.60	0.57	0.49	0.162	0.002	8.137	0.135	0.365	0.005	2476	16	2004	23	2246	15	10.8	Core
9.1	36	12	15	2.48	2.40	0.33	0.190	0.004	12.416	0.419	0.474	0.011	2741	38	2502	50	2636	32	5	Core
9.2	1181	34	250	0.29	0.26	0.03	0.115	0.001	3.864	0.058	0.244	0.003	1880	12	1406	17	1606	12	12.4	Rim
10.1	2218	26	470	0.33	0.27	0.01	0.119	0.001	3.994	0.063	0.244	0.004	1938	9	1407	18	1633	13	13.8	Rim
10.2	85	75	34	0.00	0.22	0.92	0.183	0.001	11.675	0.183	0.462	0.007	2681	6	2450	30	2579	15	5.0	Core
11.1	442	231	176	0.23	-0.10	0.54	0.169	0.001	10.712	0.058	0.458	0.001	2553	5	2433	5	2499	5	2.6	Rim
11.2	696	451	260	0.98	0.34	0.66	0.172	0.001	10.177	0.064	0.429	0.002	2580	5	2299	8	2451	6	6.2	Core
12.1	151	77	62	1.80	2.33	0.52	0.194	0.002	12.409	0.226	0.465	0.007	2772	13	2462	33	2636	17	6.6	Core
12.2	368	83	161	0.39	0.50	0.23	0.192	0.001	13.358	0.127	0.504	0.004	2760	8	2632	16	2705	9	2.6	Rim
13.1	318	80	127	0.26	0.49	0.26	0.195	0.001	12.363	0.195	0.460	0.006	2786	12	2437	28	2632	15	7.4	Rim
13.2	85	57	37	0.22	0.41	0.69	0.185	0.002	12.853	0.226	0.504	0.006	2698	19	2632	28	2669	17	1.4	Rim
14.1	519	132	206	0.83	0.60	0.26	0.174	0.001	10.918	0.080	0.456	0.002	2594	8	2594	8	2516	7	3.8	Rim
14.2	582	122	223	1.70	1.49	0.22	0.150	0.001	8.996	0.052	0.436	0.001	2341	7	2334	4	2338	5	0.2	Interm.
14.3	87	38	39	-0.04	-0.05	0.45	0.204	0.001	14.654	0.093	0.522	0.001	2857	7	2706	6	2793	6	3.2	Core
15.1	1269	519	411	0.36	-0.10	0.42	0.150	0.000	7.733	0.045	0.373	0.001	2349	4	2045	7	2200	5	7.0	Rim
15.2	1115	445	371	0.23	0.11	0.41	0.144	0.001	7.637	0.099	0.384	0.004	2281	9	2093	20	2189	12	4.4	Interm.
16.1	542	32	191	0.55	0.57	0.06	0.169	0.001	9.462	0.111	0.406	0.004	2547	10	2198	18	2384	11	8	Rim
16.2	151	154	66	-0.06	0.09	1.05	0.185	0.001	12.941	0.158	0.508	0.005	2696	11	2649	20	2675	12	1.0	Core
17.1	2180	579	874	6.04	5.58	0.27	0.163	0.005	9.934	0.326	0.441	0.007	2491	47	2355	31	2429	31	3.0	Core
17.2	868	35	278	2.35	1.86	0.04	0.166	0.004	8.313	0.253	0.362	0.006	2521	41	1994	30	2266	28	12.0	Rim
18.1	575	30	214	0.60	0.49	0.05	0.170	0.000	10.040	0.103	0.429	0.004	2555	3	2301	18	2439	10	5.6	Rim
18.2	287	168	120	0.91	0.89	0.60	0.186	0.001	12.332	0.132	0.481	0.004	2707	10	2532	17	2630	10	3.8	Core
19.1	646	31	271	0.19	0.13	0.05	0.175	0.000	11.702	0.078	0.484	0.002	2609	4	2546	11	2581	6	1.4	Rim
19.2	134	52	52	1.20	1.28	0.40	0.180	0.001	11.110	0.111	0.447	0.003	2657	9	2380	15	2532	9	6.0	Core
20.1	402	98	156	3.85	4.19	0.25	0.171	0.002	10.230	0.250	0.434	0.009	2568	21	2323	41	2456	23	5.4	Core
21.1	469	34	155	1.69	1.61	0.07	0.165	0.002	8.569	0.172	0.377	0.006	2507	17	2062	30	2293	18	10.0	Rim
21.2	106	95	46	0.08	0.00	0.92	0.186	0.001	12.959	0.111	0.507	0.002	2703	10	2642	10	2677	8	1.4	Core
22.1	284	131	118	0.16	0.36	0.47	0.182	0.001	12.010	0.103	0.478	0.003	2672	6	2520	14	2605	8	3.2	Rim
23.1	314	420	106	0.65	-0.03	1.37	0.171	0.001	9.158	0.142	0.389	0.005	2567	13	2116	23	2354	14	10.2	Core
23.2	517	722	191	0.40	1.62	1.43	0.179	0.000	10.465	0.046	0.424	0.001	2642	3	2280	3	2477	4	8.0	Rim
24.1	657	639	256	2.19	1.12	1.00	0.174	0.001	10.617	0.132	0.442	0.005	2600	8	2358	22	2490	12	5.4	Rim
25.1	385	358	150	0.08	-0.79	0.95	0.182	0.001	11.299	0.156	0.449	0.006	2676	7	2391	25	2548	13	6.2	Core
26.1	977	510	298	0.32	-0.51	0.54	0.154	0.002	7.479	0.194	0.352	0.008	2394	23	1942	36	2171	24	10.6	Interm.
27.1	272	46	118	2.64	2.43	0.18	0.180	0.002	12.201	0.186	0.493	0.006	2649	15	2582	25	2620	14	1.4	Core
27.2	1830	61	458	2.69	2.15	0.03	0.132	0.002	5.127	0.067	0.282	0.001	2120	20	1604	7	1841	11	12.8	Rim
28.1	503	119	177	0.61	0.71	0.24	0.173	0.001	9.623	0.090	0.404	0.003	2585	5	2186	15	2399	9	8.8	Rim
29.1	78	34	37	0.36	0.12	0.44	0.200	0.002	15.301	0.207	0.556	0.003	2823	19	2850	14	2834	13	-0.6	Core
1.1b	133	74	61	0.38	0.27	0.57	0.200	0.001	14.545	0.245	0.528	0.008	2824	8	2735	35	2786	16	1.8	Core
2.1b	90	110	40	0.00	-0.25	1.26	0.187	0.001	13.153	0.160	0.510	0.005	2715	8	2658	23	2691	12	1.2	Core
3.1b	92	69	38	0.74	0.68	0.77	0.183	0.001	11.846	0.194	0.469	0.007	2681	12	2481	29	2592	16	4.4	Core
4.1b	93	27	43	-0.04	0.00	0.29	0.191	0.002	14.157	0.243	0.537	0.006	2753	20	2770	25	2760	17	-0.4	Core
5.1b	157	133	73	0.02	-0.15	0.87	0.203	0.001	14.956	0.182	0.535	0.006	2850	6	2761	25	2812	12	1.8	Core
7.1b	89	43	42	-0.03	0.03	0.50	0.202	0.001	15.319	0.143	0.551	0.004	2840	8	2829	17	2835	9	0.2	Core

Spot	Concentration (ppm)						Ratios (^{204}Pb Corrected)						Ages (^{204}Pb Corrected) in Ma							Spot position
	U	Th	^{206}Pb	f206_4%	f206_8%	^{232}Th/^{238}U	^{207}Pb/^{206}Pb	±err	^{207}Pb/^{235}U	±err	^{206}Pb/^{238}U	±err	^{207}Pb/^{206}Pb	±err	^{207}Pb/^{235}U	±err	^{206}Pb/^{238}U	±err	disc.(%)	
8.1b	67	56	30	0.33	0.05	0.87	0.184	0.001	12.939	0.106	0.510	0.003	2688	7	2658	14	2675	8	0.6	Core
10.1b	107	93	47	0.32	0.24	0.89	0.183	0.001	12.813	0.147	0.507	0.005	2683	7	2644	22	2666	11	0.8	Core
11.1b	236	160	103	0.03	-0.02	0.69	0.188	0.000	13.087	0.161	0.506	0.006	2722	3	2638	25	2686	12	1.8	Core
12.1b	128	90	59	0.01	0.11	0.73	0.202	0.001	14.765	0.131	0.531	0.004	2839	4	2747	17	2800	8	1.8	Core
12.2b	66	28	32	0.00	0.00	0.44	0.200	0.005	15.294	0.375	0.554	0.003	2829	38	2840	14	2834	24	-0.2	Core
13.1b	127	33	56	0.02	-0.08	0.27	0.193	0.001	13.599	0.157	0.510	0.004	2772	11	2656	18	2722	11	2.4	Core
13.2b	108	65	50	-0.09	-0.21	0.61	0.197	0.001	14.565	0.077	0.537	0.001	2800	6	2770	4	2787	5	0.6	Core
15.1b	241	19	75	0.09	0.41	0.08	0.160	0.005	8.008	0.369	0.362	0.013	2461	49	1991	61	2232	42	10.8	Rim
6263A3 - Melted metagreywacke																				
1.1	2141	158	452	3.96	3.36	0.08	0.093	0.018	2.971	0.589	0.232	0.003	1486	334	1345	18	1400	163	4	Rim
2.1	2499	39	533	3.59	2.88	0.02	0.105	0.006	3.446	0.233	0.238	0.008	1713	106	1378	39	1515	55	9	Rim
2.2	582	559	229	5.34	5.30	0.98	0.174	0.002	10.422	0.220	0.436	0.008	2592	19	2331	34	2473	20	5.8	Core
3.1	2707	52	507	2.46	2.27	0.02	0.091	0.002	2.635	0.115	0.211	0.007	1441	50	1232	39	1311	33	6	Rim
4.1	1101	10	410	0.35	0.56	0.01	0.174	0.002	10.254	0.174	0.429	0.005	2592	19	2299	23	2458	16	6.4	Rim
5.1	1388	71	263	0.42	0.30	0.05	0.111	0.001	3.353	0.089	0.218	0.005	1824	23	1272	26	1493	21	14.8	Rim
6.1	755	183	289	10.55	10.07	0.25	0.158	0.004	8.793	0.279	0.404	0.007	2433	44	2187	32	2317	29	5.6	Rim
7.1	1226	17	250	0.69	0.86	0.01	0.128	0.001	4.136	0.086	0.234	0.004	2072	13	1357	23	1661	17	18.4	Rim
8.1	2192	137	528	1.44	1.44	0.06	0.123	0.002	4.654	0.079	0.275	0.002	1997	26	1565	10	1759	14	11	Rim
9.1	1940	656	535	0.51	0.31	0.35	0.134	0.000	5.883	0.061	0.317	0.003	2158	4	1776	15	1959	9	9.4	Rim
9.2	1180	591	399	0.06	-0.39	0.51	0.165	0.001	8.899	0.086	0.390	0.003	2512	6	2124	15	2328	9	8.8	Interm.
9.3	1110	531	373	0.18	-0.32	0.49	0.165	0.000	8.813	0.052	0.388	0.002	2506	4	2113	7	2319	5	8.8	Core
10.1	973	363	221	3.37	3.86	0.38	0.137	0.004	4.789	0.182	0.254	0.005	2184	54	1461	28	1783	32	18	Rim
11.1	1252	114	306	2.65	3.19	0.09	0.127	0.007	4.828	0.268	0.276	0.003	2054	93	1572	17	1790	48	12.2	Rim
12.1	1542	76	300	0.75	0.75	0.05	0.112	0.001	3.468	0.053	0.224	0.003	1840	15	1301	14	1520	12	14.4	Rim
13.1	1573	68	290	2.03	2.05	0.04	0.113	0.001	3.261	0.046	0.209	0.001	1853	22	1222	6	1472	11	17	Rim
14.1	1484	105	353	3.69	4.37	0.07	0.126	0.002	4.598	0.089	0.266	0.002	2036	30	1519	11	1749	16	13.2	Rim
15.1	2683	71	763	1.82	1.67	0.03	0.139	0.001	6.174	0.055	0.322	0.002	2215	7	1800	11	2001	8	10	Rim
16.1	1914	25	448	0.73	0.93	0.01	0.129	0.002	4.782	0.096	0.269	0.004	2086	25	1534	19	1782	17	13.8	Rim
16.2	844	627	322	1.01	0.42	0.76	0.173	0.002	10.405	0.333	0.437	0.013	2584	19	2338	59	2472	30	5.4	Core
17.1	2189	82	601	0.09	0.10	0.04	0.147	0.001	6.407	0.072	0.317	0.003	2306	9	1776	15	2033	10	12.6	Rim
18.1	1759	49	419	5.40	4.87	0.03	0.123	0.017	4.445	0.793	0.262	0.029	2000	230	1501	150	1721	160	12.8	Rim
19.1	1666	17	336	1.23	2.15	0.01	0.121	0.006	3.844	0.205	0.230	0.006	1974	82	1335	29	1602	44	16.6	Rim
20.1	926	32	305	4.90	5.20	0.04	0.147	0.002	7.408	0.144	0.365	0.004	2313	26	2007	21	2162	18	7.2	Rim
21.1	1654	43	370	2.03	2.65	0.03	0.126	0.015	4.409	0.620	0.254	0.020	2043	191	1458	106	1714	124	15	Rim
21.2	775	578	279	1.64	0.93	0.77	0.165	0.001	9.341	0.110	0.410	0.004	2510	12	2215	17	2372	11	6.6	Core
22.1	2642	34	539	0.67	0.65	0.01	0.117	0.000	3.767	0.054	0.234	0.003	1909	7	1354	16	1586	12	14.6	Rim
23.1	1002	55	277	5.23	6.34	0.06	0.142	0.002	5.990	0.140	0.305	0.006	2255	21	1718	29	1975	21	13	Rim
24.1	714	191	282	0.70	0.48	0.27	0.168	0.000	10.518	0.060	0.453	0.002	2542	4	2409	8	2482	5	3	Rim
27.1	783	39	174	0.54	0.53	0.05	0.134	0.000	4.726	0.028	0.256	0.001	2150	6	1469	4	1772	5	17	Rim
28.1	2213	31	498	0.50	0.70	0.01	0.116	0.003	4.121	0.260	0.259	0.015	1888	47	1483	76	1659	53	10.6	Rim
29.1	1171	868	539	4.85	5.61	0.76	0.177	0.001	12.501	0.073	0.512	0.002	2625	6	2666	7	2643	6	-0.8	Rim
30.1	494	71	211	7.19	7.36	0.15	0.179	0.009	11.430	0.636	0.464	0.012	2639	79	2459	54	2559	53	4	Rim
31.1	1279	846	423	1.06	0.36	0.68	0.152	0.002	7.947	0.098	0.379	0.002	2371	18	2070	9	2225	11	7	Rim
32.1	1215	78	328	1.80	3.70	0.07	0.135	0.005	5.702	0.413	0.307	0.019	2163	60	1724	96	1932	65	10.8	Rim
33.1	551	164	182	1.60	3.48	0.31	0.163	0.001	8.446	0.127	0.377	0.005	2484	10	2060	24	2280	14	9.6	Rim

Spot	Concentration (ppm)						Ratios (^{204}Pb Corrected)						Ages (^{204}Pb Corrected) in Ma							Spot position
	U	Th	^{206}Pb	f206_4%	f206_8%	^{232}Th/^{238}U	^{207}Pb/^{206}Pb	±err	^{207}Pb/^{235}U	±err	^{206}Pb/^{238}U	±err	^{207}Pb/^{206}Pb	±err	^{207}Pb/^{235}U	±err	^{206}Pb/^{238}U	±err	disc.(%)	
34.1	836	683	314	1.67	1.85	0.84	0.164	0.005	9.665	0.418	0.428	0.012	2496	53	2296	56	2403	41	4.4	Rim
35.1	2462	170	611	3.01	3.14	0.07	0.115	0.004	4.427	0.245	0.279	0.011	1879	68	1588	56	1718	47	7.6	Rim
35.2	2358	161	588	8.77	15.88	0.07	0.161	0.042	5.897	1.577	0.266	0.017	2466	382	1519	88	1961	264	22.6	Core
36.1	1671	51	384	1.72	2.68	0.03	0.120	0.007	4.322	0.281	0.261	0.008	1956	98	1497	43	1698	55	11.8	Rim
37.1	1212	300	393	0.36	0.02	0.25	0.155	0.001	7.951	0.125	0.373	0.005	2397	14	2044	22	2226	14	8.2	Rim
38.1	1176	373	280	1.52	2.11	0.33	0.139	0.002	5.201	0.097	0.272	0.002	2213	28	1549	12	1853	16	16.4	Rim
38.2	270	66	114	0.06	-0.07	0.25	0.184	0.001	12.428	0.151	0.489	0.005	2692	11	2566	20	2637	12	2.6	Core
39.1	549	237	199	5.09	5.90	0.44	0.157	0.009	8.696	0.717	0.402	0.023	2424	96	2176	107	2307	78	5.6	Rim
40.1	3315	273	669	3.02	3.03	0.08	0.099	0.002	3.052	0.140	0.223	0.009	1609	38	1299	48	1421	36	8.6	Rim
41.1	2147	173	408	0.05	-0.06	0.08	0.115	0.000	3.464	0.031	0.219	0.002	1873	2	1279	10	1519	7	15.8	Rim
42.1	1638	24	366	1.44	1.25	0.01	0.131	0.005	4.587	0.264	0.255	0.011	2107	64	1462	57	1747	49	16.2	Rim
43.1	190	56	118	16.46	16.75	0.30	0.180	0.006	15.739	0.645	0.635	0.015	2650	54	3171	60	2861	40	-10.8	Rim
44.2	427	233	185	1.60	1.60	0.56	0.186	0.001	12.625	0.158	0.493	0.005	2704	8	2585	24	2652	12	2.6	Core
45.1	2066	27	468	0.16	0.21	0.01	0.133	0.000	4.781	0.045	0.261	0.002	2134	5	1497	11	1782	8	16	Rim
45.2	550	500	226	0.03	0.42	0.93	0.185	0.001	12.074	0.127	0.474	0.004	2695	6	2502	19	2610	10	4.2	Core
46.1	1933	200	371	0.36	0.39	0.11	0.117	0.001	3.577	0.035	0.221	0.002	1917	8	1287	9	1544	8	16.6	Rim
46.2	857	215	248	0.37	0.42	0.26	0.156	0.001	7.172	0.088	0.333	0.004	2415	8	1853	17	2133	11	13.2	Core
47.1	850	206	261	1.59	2.11	0.25	0.163	0.001	7.885	0.110	0.351	0.004	2488	15	1938	17	2218	13	12.6	Rim
48.1	2472	65	453	1.34	1.03	0.03	0.111	0.008	3.198	0.246	0.209	0.008	1816	118	1223	41	1457	61	16	Rim
49.1	109	101	45	0.05	-0.38	0.95	0.200	0.001	13.200	0.130	0.478	0.004	2829	5	2518	18	2694	9	6.6	Rim
49.2	354	43	116	0.56	1.82	0.12	0.155	0.003	8.037	0.201	0.376	0.005	2403	36	2057	22	2235	23	8	Core
50.1	1202	111	341	0.49	0.38	0.09	0.152	0.001	6.838	0.051	0.326	0.002	2370	7	1819	8	2091	7	13	Rim
50.2	1162	1028	413	0.09	-0.59	0.91	0.168	0.003	9.482	0.278	0.410	0.010	2533	28	2217	45	2386	27	7	Core
51.1	2491	103	377	0.40	0.31	0.04	0.090	0.003	2.169	0.092	0.174	0.005	1434	62	1035	26	1171	30	11.6	Rim
52.1	1439	15	268	0.20	0.16	0.01	0.112	0.001	3.328	0.056	0.215	0.003	1838	12	1255	17	1488	13	15.6	Rim
53.1	2418	148	1357	12.98	14.17	0.06	0.162	0.017	13.118	1.824	0.588	0.051	2475	172	2982	212	2688	140	-11	Rim
53.2	845	64	179	0.17	0.17	0.08	0.132	0.001	4.432	0.061	0.244	0.003	2123	13	1406	14	1718	12	18.2	Interm.
54.1	597	20	179	1.60	2.24	0.03	0.163	0.002	7.671	0.080	0.341	0.001	2489	16	1891	2	2193	10	13.8	Rim
55.1	1907	50	353	0.77	0.60	0.03	0.104	0.001	3.055	0.056	0.212	0.003	1705	22	1240	15	1422	14	12.8	Rim
56.1	2628	29	515	0.63	0.90	0.01	0.118	0.003	3.669	0.203	0.225	0.011	1933	49	1307	57	1565	45	16.4	Rim
57.1	988	124	327	0.38	0.38	0.13	0.161	0.001	8.452	0.131	0.382	0.005	2462	11	2084	24	2281	14	8.6	Rim
57.2	3334	3390	1433	0.04	2.73	1.04	0.139	0.001	9.370	0.184	0.488	0.008	2217	16	2563	36	2375	18	-8	Interm.
57.3	4143	4702	1457	0.12	0.00	1.16	0.135	0.004	7.313	0.737	0.393	0.038	2165	50	2135	178	2150	94	0.8	Core
58.1	2447	32	372	1.17	1.29	0.01	0.097	0.001	2.329	0.030	0.174	0.001	1573	19	1032	6	1221	9	15.4	Rim
59.1	2235	43	434	2.11	2.75	0.02	0.102	0.005	3.094	0.152	0.220	0.004	1662	81	1281	22	1431	38	10.4	Rim
60.1	2059	38	453	2.21	2.17	0.02	0.107	0.006	3.675	0.217	0.249	0.003	1749	102	1434	15	1566	48	8.4	Rim
60.2	958	451	339	1.51	1.52	0.48	0.165	0.004	9.217	0.453	0.404	0.017	2512	44	2187	77	2360	46	7.4	Core
3.1b	1567	15	342	0.08	0.20	0.01	0.133	0.001	4.601	0.047	0.252	0.002	2133	8	1447	11	1750	9	17.2	Rim
4.1b	424	34	137	0.04	0.34	0.08	0.172	0.002	8.812	0.153	0.373	0.005	2573	17	2041	24	2319	16	12	Rim
6.1b	92	29	28	0.17	1.06	0.32	0.162	0.001	7.875	0.117	0.353	0.005	2473	7	1950	23	2217	14	12	Core

Spot	Concentration (ppm)						Ratios (^{204}Pb Corrected)						Ages (^{204}Pb Corrected) in Ma							Spot position
	U	Th	^{206}Pb	f206_4%	f206_8%	^{232}Th/^{238}U	^{207}Pb/^{206}Pb	±err	^{207}Pb/^{235}U	±err	^{206}Pb/^{238}U	±err	^{207}Pb/^{206}Pb	±err	^{207}Pb/^{235}U	±err	^{206}Pb/^{238}U	±err	disc.(%)	
6263C1 - Injected leucogranite																				
1.1	1559	258	494	0.50	0.41	0.17	0.157	0.006	7.903	0.536	0.364	0.020	2427	66	2220	63	2003	95	9.8	Rim
1.2	1380	180		0.01	0.00	0.13	0.186	0.003	12.902	0.813	0.503	0.030	2707	30	2673	61	2627	131	1.8	Rim
1.3	1627	212	643	0.01	-0.02	0.13	0.176	0.001	11.066	0.595	0.457	0.024	2613	10	2529	51	2425	109	4	Core
1.4	1067	125	450	0.01	-0.05	0.12	0.179	0.000	12.020	0.107	0.487	0.004	2644	3	2606	8	2558	17	1.8	Interm.
3.1	1101	151	358	0.08	0.37	0.14	0.163	0.000	8.403	0.046	0.375	0.001	2483	5	2276	5	2052	5	9.8	Interm.
3.2	401	121	161	0.51	-1.34	0.31	0.180	0.001	11.504	0.109	0.463	0.004	2654	6	2565	9	2454	16	4.4	Core
4.1	960	110	341	0.09	-0.02	0.12	0.172	0.000	9.734	0.147	0.410	0.006	2578	3	2410	14	2217	27	8	Rim
4.2	942	163	304	0.10	-0.37	0.18	0.162	0.000	8.341	0.049	0.372	0.001	2482	5	2269	5	2040	6	10	Core
5.1	984	165	327	0.21	-0.16	0.17	0.165	0.000	8.743	0.057	0.384	0.002	2509	4	2312	6	2095	9	9.4	Core
5.2	1018	188	333	0.55	0.03	0.19	0.168	0.000	8.690	0.061	0.376	0.002	2533	4	2306	6	2059	10	10.8	Interm.
6.1	1374	225	463	0.53	0.26	0.17	0.151	0.000	8.068	0.048	0.388	0.002	2356	5	2239	6	2113	7	5.6	Core
6.2	1321	162	481	0.00	-0.06	0.13	0.170	0.001	9.846	0.086	0.421	0.003	2555	5	2421	8	2264	14	6.4	Interm.
6.3	1253	164	480	4.97	10.01	0.13	0.162	0.008	9.459	0.553	0.425	0.013	2472	83	2384	55	2282	57	4.2	Interm.
6.4	631	58	263	0.00	-0.04	0.09	0.183	0.000	12.142	0.198	0.482	0.008	2677	3	2616	16	2537	33	3	Rim
7.1	2879	439	685	0.06	0.00	0.16	0.119	0.000	4.465	0.049	0.273	0.003	1938	7	1724	9	1554	13	9.8	Core
7.2	1040	123	317	0.12	-0.04	0.12	0.162	0.001	7.836	0.082	0.352	0.003	2473	6	2212	10	1942	15	12.2	Rim
8.1	1070	174	340	0.68	0.81	0.17	0.160	0.001	8.035	0.065	0.365	0.002	2452	7	2235	7	2006	11	10.2	Core
8.2	1540	230	304	0.22	0.21	0.15	0.117	0.001	3.655	0.035	0.227	0.002	1906	10	1562	8	1320	8	15.4	Rim
9.1	743	80	306	0.24	0.13	0.11	0.179	0.000	11.727	0.053	0.475	0.001	2645	3	2583	4	2505	5	3	Rim
9.2	676	72	288	0.03	0.01	0.11	0.182	0.002	12.373	0.227	0.493	0.008	2673	16	2633	17	2582	33	2	Core
10.1	1143	162	279	1.63	2.30	0.15	0.148	0.001	5.663	0.096	0.278	0.004	2322	17	1926	15	1579	19	18	Rim
11.1	804	106	344	0.16	0.00	0.14	0.179	0.002	12.214	0.411	0.494	0.015	2646	23	2621	32	2589	65	1.2	Core
11.3	574	82	209	0.07	-1.00	0.15	0.174	0.001	10.089	0.084	0.421	0.003	2596	6	2443	8	2264	13	7.4	Rim
12.1	879	95	351	1.02	1.15	0.11	0.179	0.002	11.315	0.610	0.457	0.024	2648	18	2550	52	2428	108	4.8	Core
12.2	812	86	343	0.02	-0.04	0.11	0.182	0.000	12.270	0.089	0.488	0.003	2675	4	2625	7	2562	12	2.4	Rim
13.1	952	150	369	0.63	0.68	0.16	0.174	0.001	10.714	0.071	0.446	0.002	2599	6	2499	6	2377	9	4.8	Core
13.2	1020	122	361	0.19	0.13	0.12	0.165	0.000	9.263	0.071	0.408	0.003	2506	4	2364	7	2204	12	6.8	Rim
14.1	840	281	330	0.42	-0.80	0.34	0.177	0.001	11.043	0.100	0.453	0.003	2623	7	2527	8	2409	14	4.6	Core
14.2	866	125	362	0.13	-0.34	0.15	0.181	0.000	12.058	0.055	0.483	0.001	2662	2	2609	4	2541	5	2.6	Rim
15.1	1990	310	639	0.03	-0.16	0.16	0.153	0.008	7.818	1.029	0.371	0.045	2378	89	2210	126	2035	213	8	Core
16.1	1193	144	327	0.05	0.12	0.12	0.153	0.005	6.688	0.555	0.317	0.024	2381	54	2071	76	1774	119	14.4	Core
16.2	1456	186	340	0.12	0.28	0.13	0.145	0.000	5.379	0.029	0.269	0.001	2286	4	1882	5	1538	5	18.2	Interm.
16.3	1013	132	282	0.08	0.10	0.13	0.154	0.001	6.843	0.079	0.321	0.003	2396	6	2091	10	1796	16	14.2	Interm.
16.4	1128	131	334	0.06	0.19	0.12	0.155	0.002	7.310	0.111	0.342	0.002	2401	23	2150	14	1898	9	11.8	Interm.
17.2	985	240	294	0.80	-0.63	0.25	0.162	0.000	7.632	0.032	0.342	0.000	2474	3	2189	4	1898	2	13.2	Interm.
18.1	969	151	394	0.02	-0.05	0.16	0.177	0.000	11.475	0.087	0.469	0.003	2629	4	2563	7	2480	13	3.2	Core
18.2	1377	283	347	1.29	1.21	0.21	0.140	0.001	5.582	0.054	0.288	0.001	2233	14	1913	8	1633	6	14.6	Interm.
18.3	984	187	292	0.46	-0.43	0.19	0.162	0.000	7.621	0.069	0.341	0.003	2477	2	2187	8	1892	14	13.6	Rim
19.1	1229	147	425	0.03	-0.03	0.12	0.169	0.000	9.285	0.045	0.399	0.001	2544	4	2367	5	2166	5	8.4	Rim
19.2	1723	260	389	0.03	-0.12	0.15	0.141	0.000	5.080	0.025	0.261	0.000	2244	5	1833	4	1493	2	18.6	Interm.
19.3	418	55	180	0.69	1.10	0.14	0.179	0.002	12.255	0.312	0.496	0.011	2645	22	2624	24	2597	46	1	Core
19.4	1056	169	342	0.26	-0.32	0.16	0.166	0.001	8.560	0.074	0.373	0.002	2520	7	2292	8	2046	12	10.8	Rim
20.2	1108	146	383	1.02	1.09	0.14	0.166	0.000	9.067	0.080	0.396	0.003	2517	4	2345	8	2152	14	8.2	Interm.
21.1	909	99	281	0.06	-0.01	0.11	0.166	0.000	8.182	0.097	0.357	0.004	2522	2	2251	11	1966	19	12.6	Rim
21.2	1414	201	331	0.89	1.24	0.15	0.144	0.001	5.318	0.078	0.268	0.003	2273	12	1872	13	1532	17	18.2	Core

Spot	Concentration (ppm)						Ratios (^{204}Pb Corrected)						Ages (^{204}Pb Corrected) in Ma							Spot position
	U	Th	^{206}Pb	f206_4%	f206_8%	^{232}Th/^{238}U	^{207}Pb/^{206}Pb	±err	^{207}Pb/^{235}U	±err	^{206}Pb/^{238}U	±err	^{207}Pb/^{206}Pb	±err	^{207}Pb/^{235}U	±err	^{206}Pb/^{238}U	±err	disc.(%)	
22.1	1492	193	479	0.02	-0.07	0.13	0.158	0.000	8.099	0.036	0.371	0.001	2439	4	2242	4	2033	3	9.4	Core
22.2	1199	128	427	0.01	-0.08	0.11	0.172	0.000	9.767	0.082	0.412	0.003	2577	3	2413	8	2223	14	7.8	Interm.
22.3	1266	144	433	0.09	-0.06	0.12	0.169	0.000	9.182	0.095	0.395	0.004	2544	4	2356	10	2146	17	9	Rim
23.1	1251	197	365	0.41	0.72	0.16	0.155	0.001	7.169	0.103	0.336	0.004	2397	11	2133	13	1870	20	12.4	Rim
23.2	1305	157	348	0.18	0.58	0.12	0.150	0.000	6.353	0.039	0.308	0.001	2342	3	2026	5	1731	7	14.6	Interm.
23.3	1134	147	403	0.04	-0.10	0.13	0.167	0.000	9.460	0.194	0.411	0.008	2529	4	2384	19	2217	38	7	Core
24.1	722	106	303	0.14	0.05	0.15	0.182	0.000	12.150	0.093	0.484	0.003	2673	3	2616	7	2544	13	2.8	Core
24.2	1037	130	326	0.03	0.02	0.13	0.164	0.000	8.215	0.091	0.364	0.004	2496	4	2255	10	1999	18	11.4	Interm.
24.3	649	152	240	1.18	1.94	0.24	0.173	0.000	10.122	0.071	0.424	0.002	2590	4	2446	7	2276	11	7	Interm.
24.4	1054	110	343	0.33	0.67	0.11	0.161	0.001	8.319	0.054	0.374	0.001	2468	6	2266	6	2050	7	9.6	Rim
25.1	613	106	234	0.40	-0.70	0.18	0.176	0.001	10.679	0.157	0.439	0.006	2619	10	2496	14	2347	25	6	Rim
25.2	2614	422	594	2.06	3.92	0.17	0.112	0.001	3.983	0.034	0.257	0.001	1838	9	1631	7	1475	8	9.6	Core
26.2	1070	229	356	1.35	1.55	0.22	0.158	0.016	8.281	0.860	0.380	0.004	2436	165	2262	99	2075	21	8.2	Interm.
26.3	573	110	223	0.38	-1.51	0.20	0.177	0.001	10.981	0.078	0.449	0.001	2629	10	2522	7	2390	5	5.2	Rim
27.1	1003	95	395	0.43	0.64	0.10	0.174	0.000	10.861	0.045	0.453	0.001	2596	1	2511	4	2408	4	4.2	Rim
27.2	1054	220	394	0.06	0.14	0.21	0.170	0.003	10.127	0.357	0.432	0.013	2559	28	2446	33	2313	60	5.4	Core
28.1	598	57	254	0.84	0.89	0.10	0.182	0.002	12.176	0.245	0.487	0.008	2667	18	2618	19	2556	35	2.4	Core
29.1	1211	237	310	2.82	4.24	0.20	0.143	0.001	5.682	0.067	0.289	0.002	2262	14	1929	10	1634	11	15.2	Interm.
30.2	849	106	351	0.01	-0.01	0.13	0.180	0.000	11.855	0.174	0.478	0.007	2650	3	2593	14	2521	30	2.8	Interm.
30.3	941	131	362	0.44	0.57	0.14	0.174	0.000	10.649	0.128	0.443	0.005	2601	3	2493	11	2363	22	5.2	Core
31.1	765	100	309	0.05	-0.01	0.13	0.175	0.001	11.261	0.141	0.467	0.005	2607	7	2545	12	2468	23	3	Core
32.1	2737	638	639	0.33	0.27	0.24	0.117	0.000	4.308	0.051	0.267	0.003	1908	5	1695	10	1528	15	9.8	Core
32.2	750	126	261	0.36	0.32	0.17	0.168	0.000	9.246	0.108	0.400	0.004	2534	3	2363	11	2170	20	8.2	Rim
33.1	1823	268	442	0.24	0.20	0.15	0.131	0.001	5.071	0.064	0.280	0.003	2118	12	1831	11	1590	14	13.2	Rim
33.2	2714	501	662	0.11	-0.06	0.19	0.126	0.001	4.885	0.042	0.280	0.002	2049	8	1800	7	1593	9	11.6	Core
34.2	2439	398	585	1.53	2.22	0.17	0.125	0.003	4.702	0.176	0.273	0.008	2024	41	1768	32	1558	40	11.8	Rim
1.1b	1321	153	443	0.05	-0.01	0.12	0.164	0.000	8.760	0.049	0.388	0.001	2497	4	2111	6	2313	5	8.8	Rim
2.1b	1940	286	436	0.46	0.87	0.15	0.131	0.004	4.676	0.135	0.258	0.002	2115	47	1481	12	1763	24	16	Interm.
3.1b	2126	367	459	0.45	0.22	0.18	0.126	0.001	4.309	0.060	0.248	0.003	2042	12	1429	15	1695	11	15.6	Core
6.1b	988	92	327	0.65	0.61	0.10	0.162	0.001	8.469	0.104	0.380	0.003	2472	15	2077	14	2283	11	9	Core
7.1b	988	98	344	0.05	-0.05	0.10	0.167	0.000	9.245	0.110	0.402	0.004	2526	4	2178	21	2363	11	7.8	Interm.
8.1b	608	106	262	0.22	-0.57	0.18	0.181	0.000	12.413	0.085	0.497	0.003	2665	1	2599	12	2636	7	1.4	homog.
8.2b	842	87	349	-0.01	-0.02	0.11	0.181	0.000	11.979	0.076	0.480	0.002	2664	4	2526	9	2603	6	3	homog.

Table 2.1: U-Pb SHRIMP data. f206_4% and f206_8% give the percentage of ^{206}Pb that is ^{204}Pb and of ^{206}Pb that is ^{204}Pb respectively. Disc% is the degree of discordance determined for the analysis. All values are at the 2-sigma confidence level. homog. and interm. indicate homogeneous zircons and spots situated in a intermediary position in the zircon. Spot number containing b indicates analysis done on a separate session compared to the main session for the given sample. Greyed lines correspond to data already published in Morfin et al. (2013).

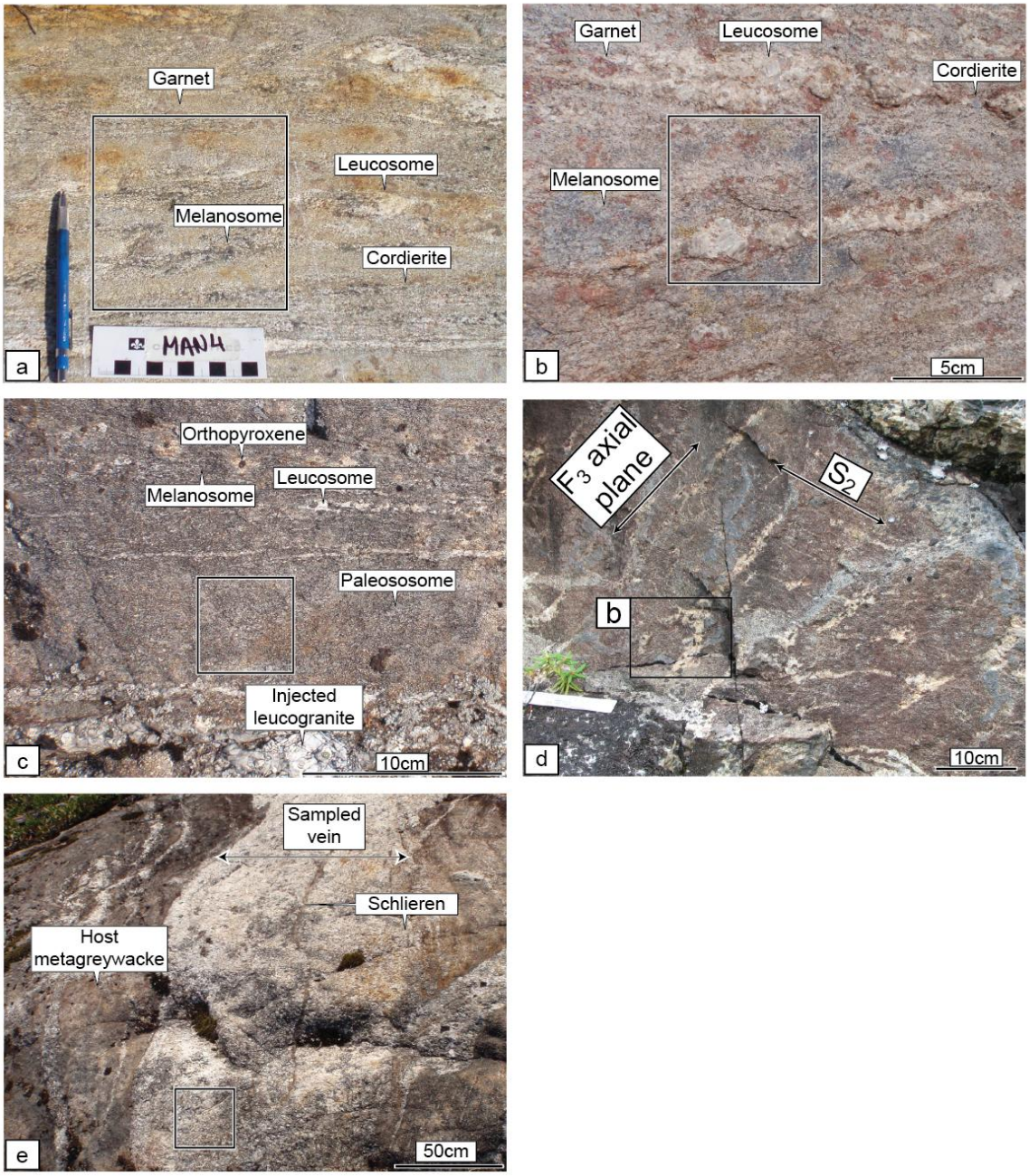

Figure 2.4: Field pictures of the outcrops and sample positions. a) Metapelite MAN4C. The sample contains both the garnet and cordierite-bearing melanosome and parts of the leucosome. b) Metapelite 6116A. The sample consists mainly of the melanosome with some leucosome. Note the numerous large peritectic *garnets left in the melanosome after melt was extracted. c) Metagreywacke sample 6263A2. The sample is taken from the domain free of leucosome and*

orthopyroxene, which indicates (together with the petrography) that the sample domain did not melt, although it is in close proximity with a domain with a low degree of partial melting. d) Outcrop of 6263A3 sample. The sample contains some leucosome, but is mostly composed of the orthopyroxene-bearing metagreywacke. e) Position of leucogranite sample 6263C1. The sample is taken from a wide leucocratic vein composed of multiple injections as evidenced by the multiple schlieren present parallel to the vein wall.

The matrix mineral assemblage is quartz + plagioclase + biotite + cordierite + garnet (Fig. 2.5a). Cordierite is replaced by pinnite and some minor, retrograde chlorite is present at the expense of biotite. K-feldspar is absent. The leucocratic patches contain quartz + plagioclase + garnet + minor biotite. Cordierite comprises about a third of some domains, reflecting the relatively high Mg number ([MgO]/{[MgO] + [FeO]}) for some metapelitic layers. Most zircons occur as inclusions in biotite and cordierite.

2.6.1.2 ZIRCON MORPHOLOGY

There are two types of zircon based on their colors (Fig. 2.6a): brownish ones and clear ones. However, this characteristic does not relate to any difference in the distribution of ages.

The size of zircons ranges from 50 to over 200 μm. The shape of zircon is varied, some are prismatic, whereas others (mostly the small ones) are rounded, or have irregular shapes. The cathodoluminescence images show that many zircons exhibit zonation between a rounded core and the rounded or prismatic outline. Zircons which do not show a zoned overgrowth on the core in the CL images, all yield ages similar to those from the cores of zoned zircons.

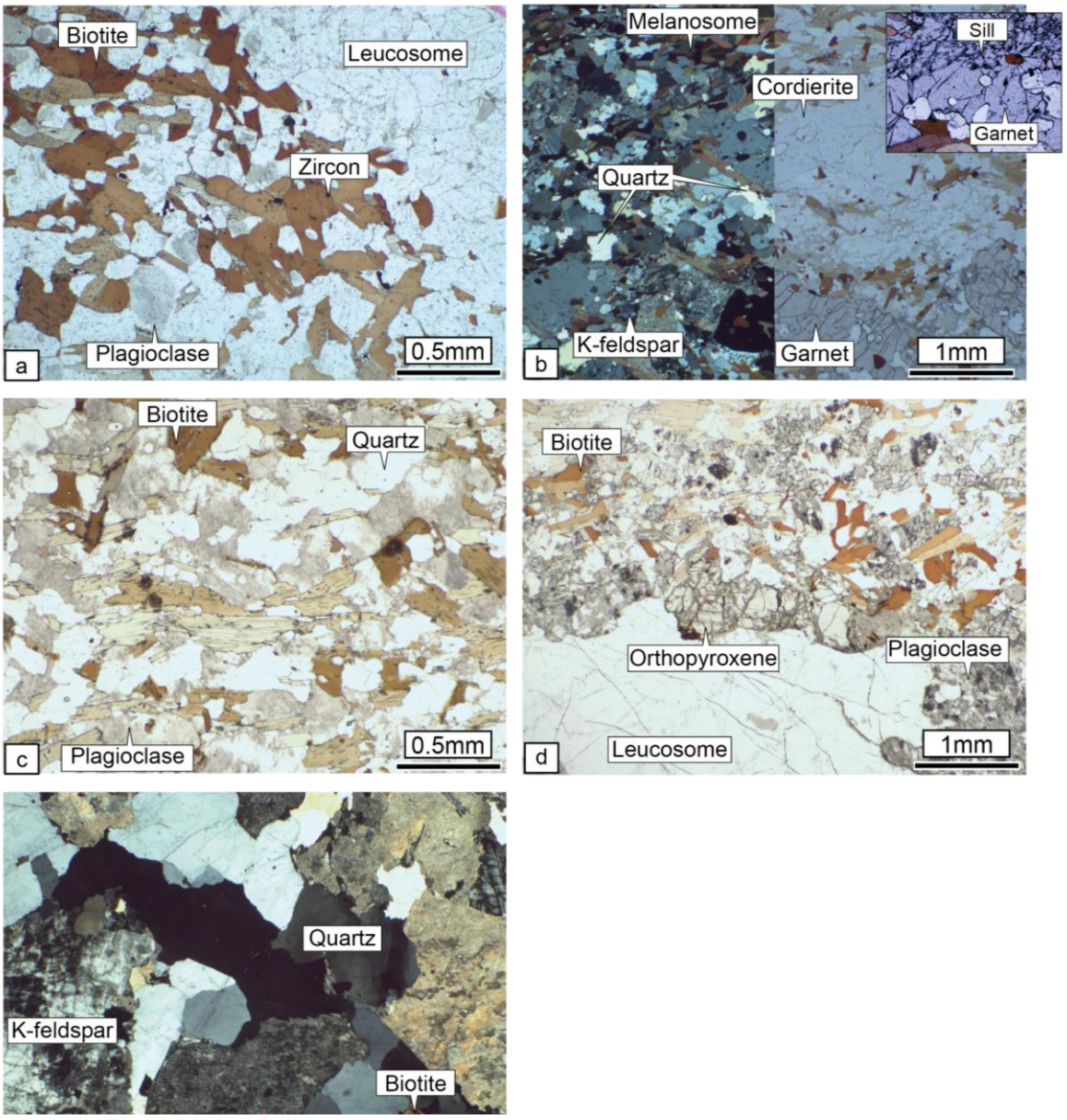

Figure 2.5: Microstructure in the paragneiss. a) Sample MAN4C: Metapelitic matrix composed of quartz + biotite + plagioclase. The image shows a leucogranitic leucosome, probably produced by in situ partial melting according to the field observation. b) Sample 6116A: Porphyroblasts of cordierite and garnet control the microstructure, the matrix is composed of quartz + K-feldspar + biotite. Some biotite-rich domains are interpreted as melanosome where the K-feldspar has been consumed. The insert shows sillimanite present as inclusion in garnets. c) Sample 6263A2: the sample is composed quartz + plagioclase + biotite. Aligned crystals of

biotite define the main schistosity. d) Sample 6263A3: the image shows a contact between the residual matrix, and a quartz-rich leucosome. The matrix contains orthopyroxene in addition to the main quartz + plagioclase + biotite assemblage, which is evidence for partial melting at granulite facies conditions. Orthopyroxene is present at the contact between the matrix and the leucosome. Most orthopyroxene shows evidence of partial retrogression into biotite / chlorite. e) Sample 6263C1: image of the leucogranite showing a very low modal proportion of mafic minerals.

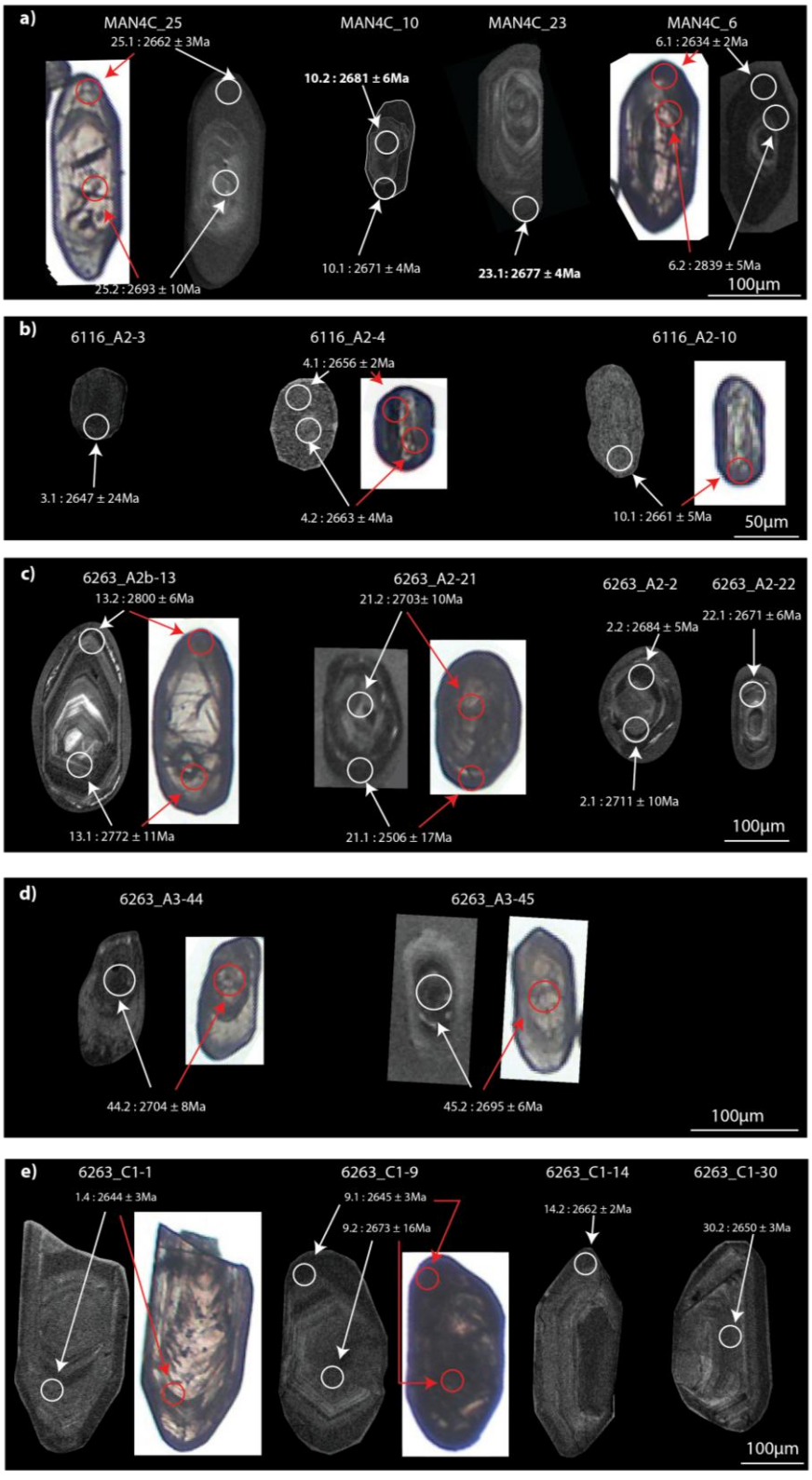

Figure 2.6: Selected representative cathodoluminescence and natural light images of zircon grains separated from each sample. The circle shows the approximate size of the analysis spot together with the reported ages. The bold font for sample MAN4C indicates age for the oldest rim and the youngest core analysed.

2.6.1.3 RESULTS

Some 50 analyses from 30 zircons have been obtained (Fig. 2.7a), 19 of which have already been published in Morfin et al. (2013). Analyses from the rims of zircons yield an average Th/U ratio of 0.08, whereas the average ratio for the cores is 0.87. Some spots, initially interpreted as rims based on the CL image, were re-interpreted as part of the zircon core set based to their Th/U ratios and the old ages obtained. Morfin et al. (2013) show that the distribution of high quality ages (below 3.2% discordance) from the rims is bimodal, the main peak is at 2663.6 ± 6.0 Ma and the second is at 2637 ± 6.7 Ma.

The cores of zircons have lower average U contents, 31 to 718 ppm (n = 19, excluding two high U outliers), compared to the rims which range from 277 to 1287 ppm (Table 2.1, Fig. 2.7b). The cores and homogeneous zircons give a range of $^{207}Pb/^{206}Pb$ age 2681 and 2950 Ma. All the ages obtained from the cores are older than 2681 Ma. A very old zircon is dated at 2950 ± 6 Ma (1.6% discordance). Two other zircon cores older than the main population yield ages of 2839 ± 5 and 2869 ± 2 (discordance of 0.8% and 1% respectively). The Concordia plot of the whole population of analyses (except for 5 outliers) indicates a lower Discordia intercept at 674 ± 360 Ma and the upper intercept crosses the Concordia at 2692 ± 16 Ma (Fig. 2.7a).

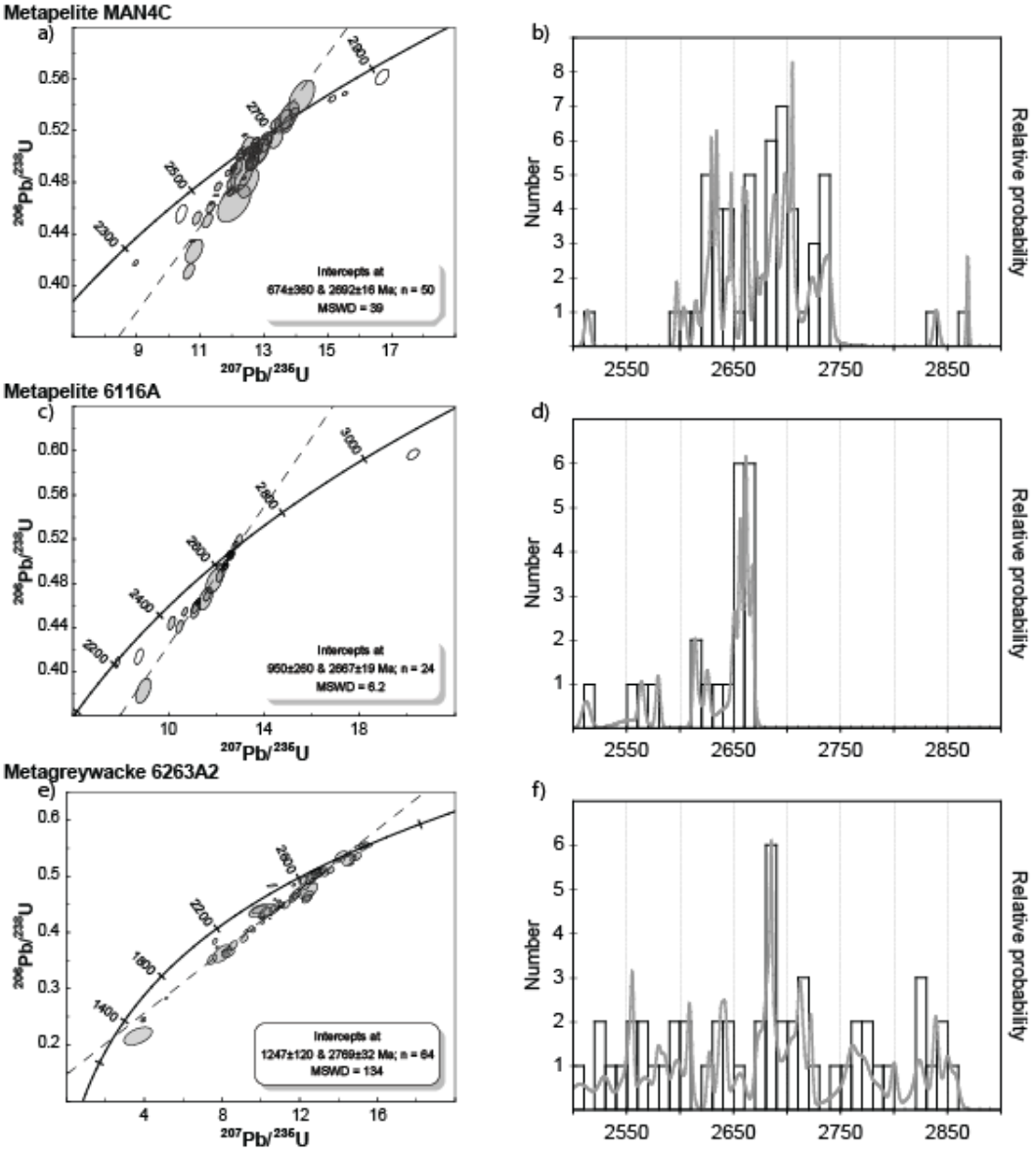
Metapelite MAN4C
a)
Intercepts at
674±360 & 2692±16 Ma; n = 50
MSWD = 59
$^{206}Pb/^{238}U$
$^{207}Pb/^{235}U$
b)
Number
Relative probability
Metapelite 6116A
c)
Intercepts at
950±260 & 2667±19 Ma; n = 24
MSWD = 6.2
d)
Metagreywacke 6263A2
e)
Intercepts at
1247±120 & 2769±32 Ma; n = 84
MSWD = 134
f)

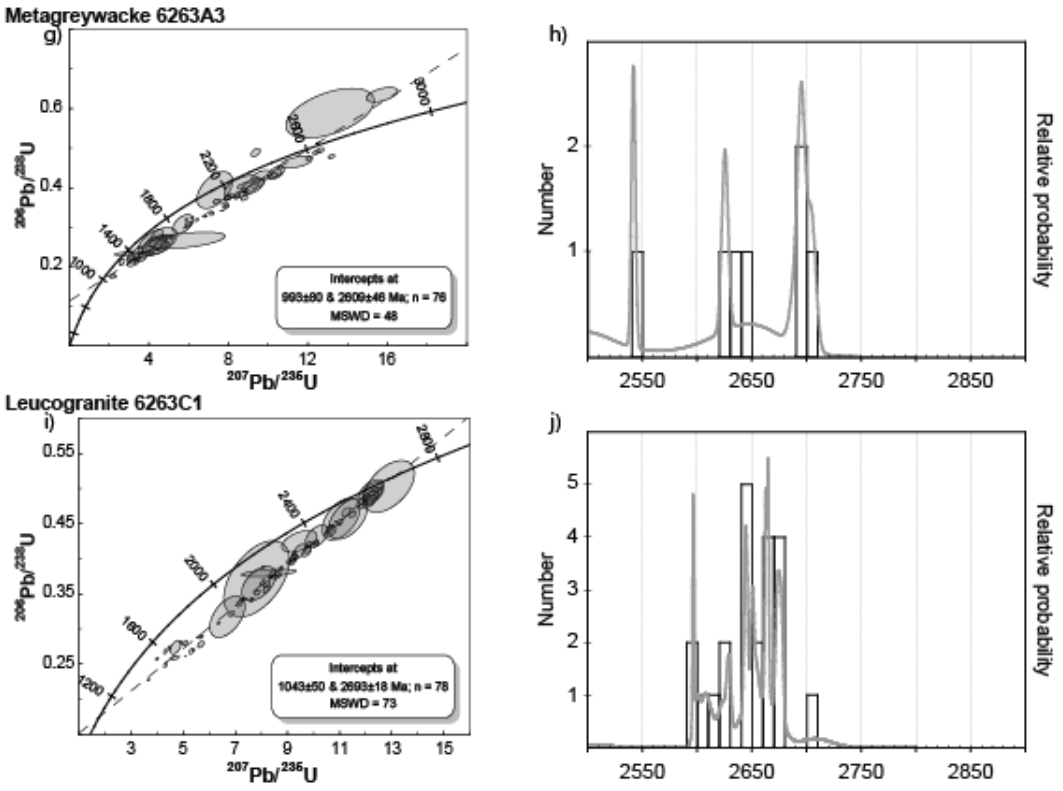

Figure 2.7: a), c), e) g), and i) Wetherhill Concordia plot. b), d), f), h), and j) age distribution with the relative probability for each sample. The Concordia plots feature the Discordia calculated for the respective sample. Note that the horizontal scale is the same for all age distribution / relative distribution plots to more easily facilitate comparisons between samples.

2.6.2 SAMPLE 6116A: GRANULITE FACIES METAPELITE

2.6.2.1 SAMPLE DESCRIPTION

Sample 6116A comes from the central-northern Opinaca (Fig. 2.3b), less than 5 km south of the boundary between the Opinaca and the La Grande subprovince. The outcrop consists of a metapelitic domain in which the main schistosity is disrupted due to the high volume of leucosome in it. Nevertheless, its general orientation is still evident. The outcrop contains both melt-rich domains, where leucosomes have accumulated, and melanosome domains from which melt has mostly been extracted and which are marked by the presence of large (up to 10cm) poikiolitic peritectic garnets and centimetre-sized crystals of cordierite. Sample 6116A contains both types of domain (Fig. 2.4b). In the outcrop there is no evidence for the presence of out-of-source injected veins, and the observed volume of leucocratic material present can be accounted for by *in situ* partial melting of the metapelite.

The mineral assemblage is quartz + plagioclase + cordierite + biotite + garnet with minor K-feldspar and sillimanite. Garnet occurs as porphyroblasts (Fig. 2.5b), and sillimanite only as inclusion in cordierite. Cordierite shows minor replacement by pinnite. Some coarser-grained, leucocratic domains occur parallel to the main schistosity and these are interpreted to be leucosomes. K-feldspar is rare, and it occurs only in the vicinity of garnet.

2.6.2.2 ZIRCON MORPHOLOGY

Zircons from sample 6116A are round or slightly elongated with rounded edges, slightly brownish and show no zonation, or the presence of a core (Fig. 2.7b). Few zircons retain a prismatic shape. The typical length of zircons is between 50 and 100 µm, this restricts multiple analysis on single grains to the largest examples due to the beam size of the SHRIMP.

2.6.2.3 RESULTS

Twenty-four analyses have been performed on 20 zircons (Table 2.1; Fig. 2.7c), 15 of which are already published in Morfin et al. (2013). The median U content is 599 ppm with the range between 320 and 1000 ppm (except for one outlier) and the average Th/U ratio is 0.12.

The Discordia (excluding three outliers) intercepts at 950 ± 260 Ma and 2667 ± 19 Ma (Fig. 2.7c).

A strong peak in relative probaility is observed at c.a. 2660 Ma (Fig. 2.7.d). Using a low discordance threshold of 3.2% to indentify the most concordant analysis, Morfin et al. (2013) calculated a weighted average age of 2660.2 ± 3 Ma for this subgroup and

interpreted it as the main episode of zircon growth after the peak granulite metamorphic condition.

Out of the three subconcordant outliers, one at and 2387 ± 12 Ma, does not appear to be related to any known geological unit in the region. An outlier at 2221 ± 7 Ma could be contemporary with the Senneterre paleoproterozoic diabase dyke swarm dated at 2214.3 ± 12.4 Ma (Buchan et al.,, 1993). The third outlier at 3160 ± 10 Ma could correlate with other Mesoarchean-age inherited zircon previously found in the Opinaca metasedimentary units (see discussion).

2.6.3 SAMPLE 6263A2: METAGREYWACKE

Outcrop 6263 is situated 10 km south of the central-northern Opinaca – La Grande boundary (Fig. 2.3b). The outcrop contains layers of metagreywacke (Fig. 2.4c), some of which have partially melted as indicated by the presence of orthopyroxene (Fig. 2.4d), whereas other layers seems to be free of both orthopyroxene and leucosome. However, the metagreywacke is injected by a series of leucogranitic veins (Fig. 2.4e). Most of the veins are parallel to the main foliation in the metasedimentary rocks and are coarse-grained leucogranite. Sample 6263C1 is taken from one of the larger of these veins (Fig. 2.4e). A pegmatitic vein crosses across the foliation and seems to occupy what might have been the feeder to the veins parallel to the foliation. Sample 6263C2 is from the large pegmatitic

vein, zircons have been separated and mounted but, due to their very high U content, they could not be used.

2.6.3.1 SAMPLE DESCRIPTION

Sample 6263A2 is taken from a metagreywacke layer that does not seem to have melted since no orthopyroxene or leucosome are observed based on the field (Fig. 2.4c). This un-melted layer is surrounded by metagreywacke layers which clearly have melted since they do contain orthopyroxene. The absence of partial melting in specific layers can be explained by a slightly more refractory, or infertile, bulk composition. If partial melting did occur in this layer, then it would have to have been of very minor extent since it did not change its generally homogeneous aspect and microstructure.

The thin section shows that the mineral assemblage is quartz, plagioclase and biotite, typical for a metagreywacke (Fig. 2.5c). The presence of biotite aggregates and some quartz-rich leucocratic domain could indicate that some partial melting occurred, in which case the biotite aggregates might represent the former peritectic orthopyroxene produced by biotite dehydration. Alternatively, the quartz-rich leucocratic domains and biotite aggregates could be the relics of earlier subsolius metamorphic segregation. Plagioclase is sericitized and biotite is partially chloritized.

2.6.3.2 ZIRCON MORPHOLOGY

Zircons from sample 6263A2 are elongated and rounded. Many zircons show oscillatory zoning (Fig. 2.6c). Zircons are generally large enough to analyze both the center and the rim of the grains.

2.6.3.3 RESULTS

Sixty-four analyses were performed on 29 zircons (Table 2.1; Fig. 2.7e), 34 of the analyses are subconcordant, the rims being generally more discordant than the cores. The average U content in the core is 326 ppm and 664 ppm in the rims. Thus, the average Th/U ratio is 0.68 for the cores, and twice that in the rims (0.35).

The Concordia plot of all the spots analysed indicates a lower Discordia intercept at 1247 ± 120 Ma and an upper intercept at 2769 ± 32 Ma (Fig. 2.7e).

The age distribution curve (Fig. 2.7f) shows a main peak at 2684 Ma, and this peak is mainly recorded by spots from high Th/U ratio cores of zircons. Consequently, this population of the data is not considered to represent the metamorphic event, but rather the age of the main source for the metasediments. Older populations of zircon are recorded at ca. 2720 and 2770 and 2820 Ma, again these represent the age of source material for the sediments. Smaller peaks in the age distribution are observed at younger ages, at ca. 2641 Ma, at ca. 2614 Ma and another at ca. 2555 Ma. Except for the 2641 Ma peak, which could

be connected to the granulitic episode recorded in the metapelites, the younger small peaks are not related to any know regional events.

2.6.4 SAMPLE 6263A3: OPX-BEARING METAGREYWACKE

2.6.4.1 SAMPLE DESCRIPTION

Sample 6263A3 is composed of an orthopyroxene-bearing metagreywackes and contains some patches of leucosome (Fig. 2.4d). Compared to sample 6263A2, this sample clearly shows evidence of partial melting. It is situated close to an F_3 fold hinge and the leucosomes are aligned parallel to the fold axial plane (Fig. 2.4d).

The thin section (Fig. 2.5d) shows the mineral assemblage plagioclase, quartz, orthopyroxene and biotite in the matrix, whereas the leucosome in the thin section is mostly composed of quartz with some sericitized plagioclase. Orthopyroxene located at the margin of the leucosome is larger than that located farther away in the matrix. Most orthopyroxene is partially retrograded to biotite, which has subsequently become chloritized.

2.6.4.2 ZIRCON MORPHOLOGY

The zircon crystals separated from the sample are elongate with rounded edges. Many have a homogeneous core surrounded by a thin, brighter rim in the CL images (Fig. 2.6d).

2.6.4.3 RESULTS

A total of 76 analyses have been obtained from 60 zircons (Table 2.1; Fig. 2.7g); only 9 are subconcordant. The U content is two to three times higher than in the zircons from the metagreywacke sample 6263A2. The average U content of the core is 1167 ppm and it is 1570 ppm in the rim. The average Th/U is four times higher in the core (0.57) than in the rims (0.14). Many rim analyses yield very low Th/U ratios which could indicate some loss of Th from the rims of the zircon grains. The loss of Th is also indicated by some very anomalous $^{208}Pb/^{232}Th$ ages, whereas the Pb/U ages are not (Table 2.1). Due to the high U content, the zircons may have suffered high degrees of radiation damage and this could explain the overall lower concordance of the analyses from this sample, and possibly the loss of Th. The Concordia plot of all analyzed spots indicates a lower intercept at 993 ± 80 Ma and an upper intercept at 2609 ± 46 Ma (Fig. 2.7g).

Amongst the subconcordant (Table 2.1) spots, 3 cores yield ages at 2692 ± 11 Ma, 2695 ± 6 Ma and 2704 ± 8 Ma respectively. These ages are similar to ages from the cores of zircon from samples MAN4C and 6263A2. The other low discordance analyses either have high error (e.g. spot 6263A3-30.1 at 2639 ± 79 Ma) or young ages that can not be correlated with any presently known geological event in the region (e.g. spot 6263A3-24.1 at 2542 ± 4 Ma).

2.6.5 SAMPLE 6263C1: INJECTED LEUCOGRANITE

2.6.5.1 SAMPLE DESCRIPTION

This sample is taken from the same outcrop as metagreywacke sample 6263A2 (see above). It consists entirely of a leucogranitic vein which was injected into the host metagreywacke (Fig. 2.4e). The vein is a meter wide, and contains multiple thin bands of leucogranite each separated by a biotite-rich schliere that is parallel to and close to the walls of the vein. This is interpreted as evidence that the meter-wide vein was constructed incrementally by multiple injections of small batches of leucogranitic magma, each time a new batch of magma was injected a small portion of the host wall rock was detached and partially assimilated and is preserved as a schliere on the interior side of each injection of magma (Morfin et al., 2013).

The mineralogy is of a simple leucogranite, it is composed of plagioclase (now sericitized), quartz and K-feldspar in approximately equal proportions (Fig. 2.5e). The mafic minerals consist of minor partially-chloritized biotite and rare small garnets.

2.6.5.2 ZIRCON MORPHOLOGY

The CL images show that the zircon grains are prismatic, can reach sizes up to 500 µm and display oscillatory zoning typical of magmatic zircons (Fig. 2.6e). No inherited cores are observed in the CL images.

2.6.5.3 RESULTS

A total of 78 analyses were obtained from 34 zircons (Table 2.1; Fig. 2.7i), 16 of which were already published in Morfin et al. (2013). Twenty-three of the analyses are subconcordant and have an average Th/U ratio of 0.15. The Concordia plot of all the points indicate a lower Discordia intercept at 1043 ± 50 Ma and an upper intercept at 2693 ± 18 Ma (Fig. 2.7i). The age distribution (Fig. 2.7j) of the subconcordant analyses shows a main group (n=16) of ages distributed in three main peaks between 2645 and 2673 Ma with a maximum at 2664 Ma (Fig. 2.7j). This distribution is interpreted to record successive episodes of zircon growth in the vein (Morfin et al., 2013). A smaller population of zircon ages (n = 6) range from 2596 Ma to 2630 Ma.

2.7 DISCUSSION

2.7.1 TRANSITION FROM INHERITED ZIRCON TO THOSE FORMED IN THE INJECTION COMPLEX

Of all the samples investigated, MAN4C is the only one in which the zircon clearly developed a metamorphic overgrowth (rims). The oldest rim age is 2671 ± 4 Ma and the youngest core age is 2681 ± 6 Ma (Table 2.1). The SHRIMP analyses also show that there is a significant decrease in Th/U ratios between 2680 and 2675 Ma zircon (Fig. 2.8). The

average Th/U value for subconcordant analyses with ages younger than 2680 is 0.17 ± 0.03 (one standard deviation), whereas the average for the analyses older than 2680 is 0.75 ± 0.04.

This pattern is consistent with a change from inherited magmatic zircon to new metamorphic zircon as overgrowths on the magmatic cores (Williams et al., 1996; Hartman and Santos 2004). This could suggest that the transition from zircon crystallisation in an igneous source to the growth of metamorphic zircon in the deep crust took only 10Ma. This short time interval thus contains the whole process of source crystallisation, exhumation, erosion, deposition as a sediment and finaly burial and subsequent metamorphism. This changeover from inherited to metamorphic zircon also corresponds to the oldest peak in the age distribution of zircon that crystallized from leucogranite sample 6263C1 at 2673 Ma. This leucogranitic vein is interpreted to be part of the injection complex in the Opinaca Subprovince, and corroborates the field-based observations that the formation of the injection complex event starts during peak metamorphism at ca. 2675 Ma.

This conclusion is similar to that from observed other metasedimentary subprovinces, such as the Ashuanipi (Guernina and Sawyer; 2003) and Quetico Subprovinces (Percival et al., 2006) where the main high-grade metamorphic event quickly followed the emplacement, crystallisation and erosion of the youngest igneous source rocks.

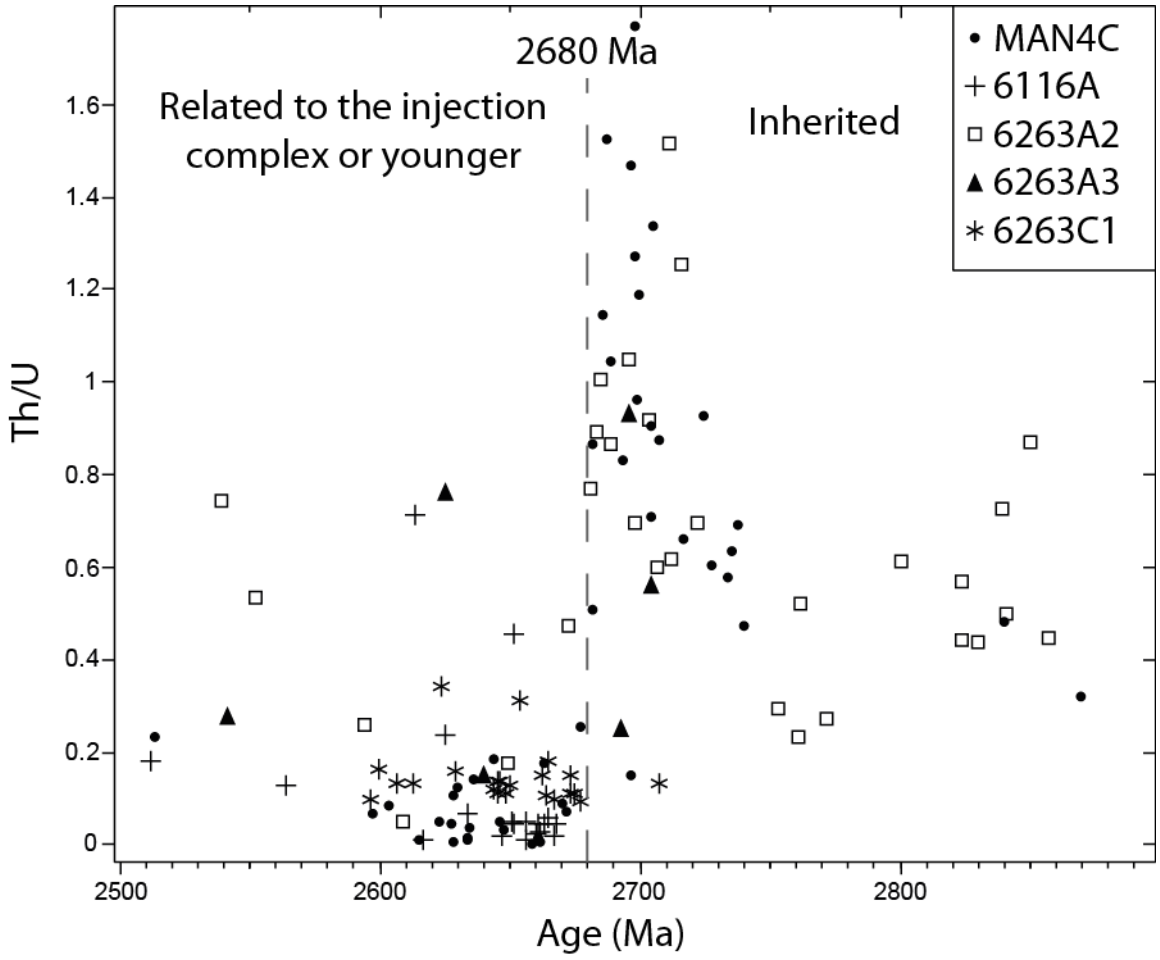

Figure 2.8: Th/U vs Age (in Ma) from subconcordant zircons between 2550 and 2900 Ma. The shift in Th/U at about 2680 Ma is interpreted to mark the transition from analyses of inherited zircon cores to analyses of zircon grown either by regional metamorphism or during crystallisation of the injection complex.

2.7.2 POPULATIONS OF INHERITED ZIRCON

The distribution of all the subconcordant (discordance below 5%) inherited ages >2680 Ma (n = 52) is presented in figure 2.9. The compilation also shows the available ages recorded in various geological units surrounding the Opinaca Subprovince and which constitute potential sources for the inherited zircons in the metasediments, i.e., the potential provenance area. The main population (n = 28) in the distribution of inherited (i.e., core) ages lies between ca. 2680 and 2710 Ma and can be seen to be coeval with many plutonic and volcanic suites situated in the region around the western Opinaca Subprovince (Fig. 2.9).

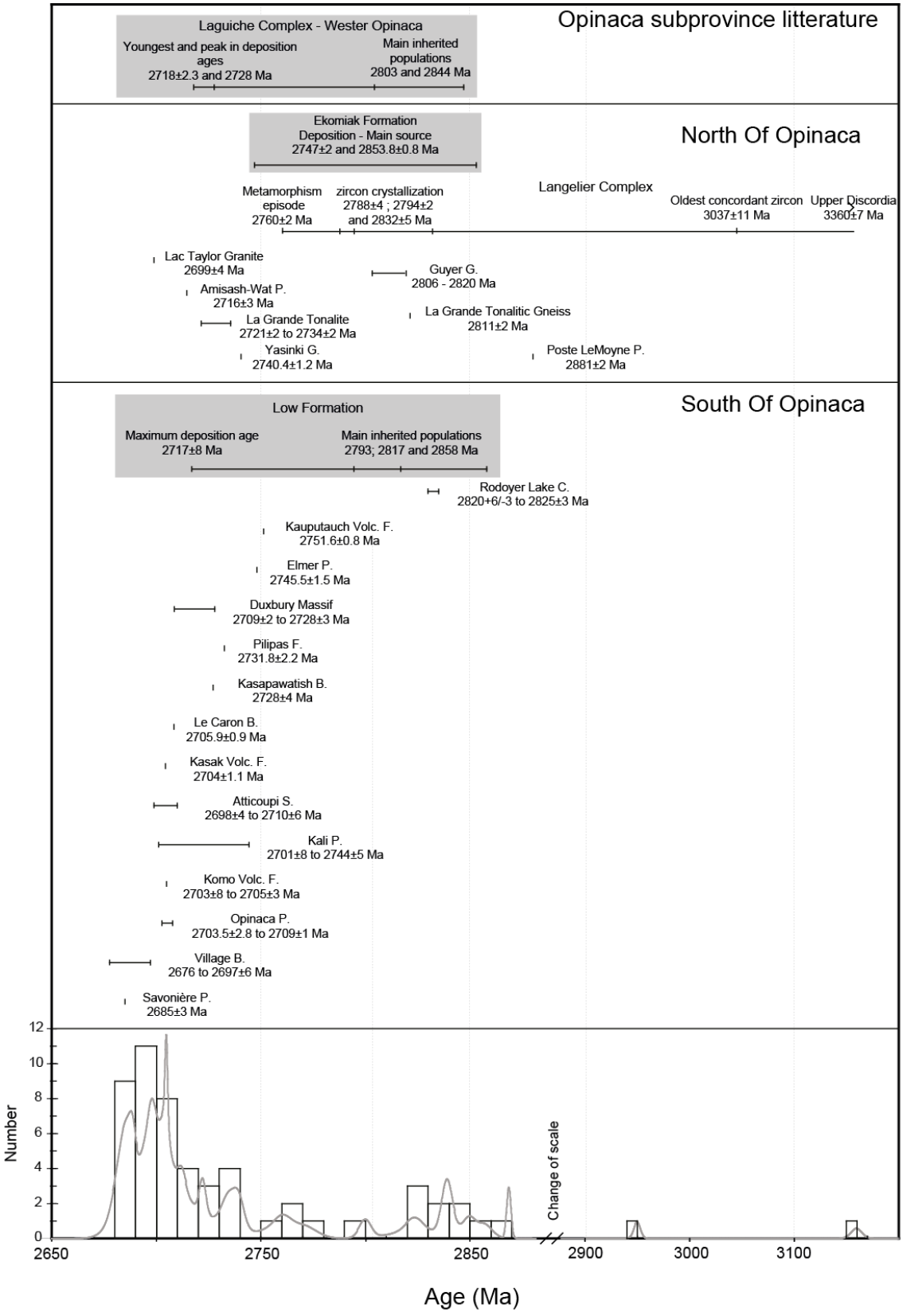
Opinaca subprovince litterature
Laguiche Complex - Wester Opinaca
Youngest and peak in deposition ages
2718±2.3 and 2728 Ma
Main inherited populations
2803 and 2844 Ma
North Of Opinaca
Ekomiak Formation
Deposition - Main source
2747±2 and 2853.8±0.8 Ma
Langelier Complex
Metamorphism episode
2760±2 Ma
zircon crystallization
2788±4 ; 2794±2 and 2832±5 Ma
Oldest concordant zircon
3037±11 Ma
Upper Discordia
3360±7 Ma
Lac Taylor Granite
2699±4 Ma
Amisash-Wat P.
2716±3 Ma
La Grande Tonalite
2721±2 to 2734±2 Ma
Yasinki G.
2740.4±1.2 Ma
Guyer G.
2806 - 2820 Ma
La Grande Tonalitic Gneiss
2811±2 Ma
Poste LeMoyne P.
2881±2 Ma
South Of Opinaca
Low Formation
Maximum deposition age
2717±8 Ma
Main inherited populations
2793; 2817 and 2858 Ma
Rodoyer Lake C.
2820+6/-3 to 2825±3 Ma
Kauputauch Volc. F.
2751.6±0.8 Ma
Elmer P.
2745.5±1.5 Ma
Duxbury Massif
2709±2 to 2728±3 Ma
Pilipas F.
2731.8±2.2 Ma
Kasapawatish B.
2728±4 Ma
Le Caron B.
2705.9±0.9 Ma
Kasak Volc. F.
2704±1.1 Ma
Atticoupi S.
2698±4 to 2710±6 Ma
Kali P.
2701±8 to 2744±5 Ma
Komo Volc. F.
2703±8 to 2705±3 Ma
Opinaca P.
2703.5±2.8 to 2709±1 Ma
Village B.
2676 to 2697±6 Ma
Savonière P.
2685±3 Ma
Number
0
2
4
6
8
10
12
Change of scale
Relative probability
2650
2750
2850
2900
3000
3100
Age (Ma)

Figure 2.9: Distribution and relative probability of inherited ages (i.e. analyses which yielded ages older than 2680 Ma) for all samples. Also shown is the age (or range of ages) for geological units in the region surrounding the western part of the Opinaca Subprovince based on geochronological data compiled by the Geological Survey of Canada (http://atlas.nrcan.gc.ca/site/english/maps/geochron/index.html#cgkb).
Note how the Mesoarchean ages are only recorded in units located to the north of the western Opinaca. Grey fields indicates a metasedimentary unit. Note the change in horizontal scale between 2850 and 2900 Ma.

A subgroup comprising the youngest inherited zircons in the Opinaca metasediments have ages similar (within the margin of error) to the youngest plutons around the Opinaca Subprovince (i.e., Village Batholith monzogranite, Savonière Pluton and Taylor Lake Pluton). A population of eleven analyses has ages between 2710 and 2740 Ma. This range of ages is very similar to the crystallisation ages obtained from several plutons and volcanic formations on either side of the Opinaca Subprovince, i.e., the La Grande Tonalite to the north and the Pilipas Formation to the south (Fig. 2.9).

A small population of four analyses is scattered between 2753 ± 20 and 2772 ± 11 Ma and do not correspond to known plutonic or volcanic events in the James Bay area. The only similar dates recorded in the area are interpreted to represent a metamorphic event in the Langelier Complex (Goutier et al., 1999). Figure 2.9 shows that of these four analyses, all of which are from sample 6263A2, three have low Th/U ratios in comparison to the >2680 Ma group average. This low Th/U ratio may be confirmation of the metamorphic origin of these detrital zircons. Thus, based on the Th/U ratios and their ages, these zircons may have come from the Langelier Complex.

One group of ages has no overlap with the others and ranges from 2800 ± 6 to 2869 ± 2 Ma, the weighted average age of the group is Mesoarchean at 2853 ± 15 (n = 10, MSWD = 85) while the rest of the recorded inherited zircons have Neoarchean ages. The younger part of this range of ages overlaps the range found in the Guyer Group (2806 to 2820 Ma) from the La Grande Domain. The oldest ages from the group are similar to those obtained from

the Poste LeMoyne Pluton (2881 Ma) which is also situated in the La Grande Domain north of the Opinaca (Fig. 2.9).

Two low-discordance analyses from metapelitic samples MAN4C and 6116A yield Mesoarchean ages of 2950 ± 5 Ma (1.6% discordance) and 3160 ± 10 Ma (2.8% discordance) respectively. These ages are similar to some units from the Langelier Complex (Fig. 2.9), which is presently the oldest known component of the La Grande Domain (Goutier et al., 2001a).

2.7.2.1 PROVENANCE OF THE SEDIMENTS

A total of 12 subconcordant analyses yielded Mesoarchean ages. As shown on figure 2.8, there are no known Mesoarchean rocks in the Opatica Subprovince, or in the southern part of the nearby Eastmain Domain of the La Grande Subprovince. The fact that Mesoarchean units are only found north of the Opinaca Subprovince suggests that the main source of metasedimentary material and detrital zircons was most probably situated to the north.

Viewed on a larger scale of the Superior Province, this interpretation is in agreement with the previous finding that the main source of material for the Quetico Subprovince, situated about 1000km farther to the west, was also from the north (Percival and Williams, 1989; Davis et al., 1990). This is also similar to the relation between some Abitibi metasediments and the Rodayer Lake pluton, a potential source situated to the north in the Opatica (Davis

et al. 1994). This similarity, together with the morphological, geochemical and geochronological ones is evidence that the Opinaca had a similar history and geological context as the well-studied Quetico Subprovince. The principal difference is the higher temperature and pressure of metamorphism in the Opinaca which reflects a deeper level in the crust.

2.7.3 TIMING OF THE INJECTION COMPLEX

The relative timing between the high grade metamorphism and injection of the leucogranitic veins is discussed in more details in Morfin et al. (2012).In summary, the time at which the injection complex formed has been determined in Morfin et al. (2013) from the dates obtained in metapelitic samples MAN4C and 6116A which record late-granulite conditions (Harley et al., 2007) and from leucogranite sample 6263C1 which records the crysatlisation of the veins. New data presented in the present contribution shows that metagreywacke sample 6263A2 also recorded zircon growth at ca. 2672 Ma. However, the peak in zircon growth at 2672 Ma in sample 6263A2 is partially occulted in the relative probability plots by the stronger peaks at 2685 Ma and 2642 Ma.

2.7.4 SIGNIFICANCE OF POST-INJECTION COMPLEX AGES

The end of the injection complex event is interpreted to be at ca. 2640 Ma, yet some samples record a small degree of zircon growth at younger ages. A secondary peak in the age distribution is observed at ca. 2629 Ma in sample MAN4C, at ca. 2614 Ma in sample 6116A and at ca. 2609 Ma in sample 6263A2. The significance of theses ages is not clearly understood. These ages are contemporary with some late-tectonic intrusions, such as the Vieux Comptoir Granite at 2618 ± 2 Ma (Goutier et al., 2000), which is considered as an S-type granite, possibly related to partial melting of metasediments (Goutier et al. 2000; Bandyayera et al. 2011). This could indicate that some minor, late crystallisation of S-type granite has occurred but the correlation with the main injection event is not known. The late zircon crystallisation recorded in the Opinaca metasediments could also be due to some late fluid circulation of unknown origin.

2.7.5 ISOTOPIC DISTURBANCE AND DISCORDIA INTERCEPTS

All samples contain zircons yielding discordant ages due to the loss of Pb. Lower intercepts on the Discordia have large age errors, but all intercept (within error) at Grenvillian ages (Fig. 2.7). Since no geological units of Grenvillian ages are found in the area, unlike the example described by Corfu and Muir (1989), the Pb loss is presumed to be due to the circulation of fluid, perhaps associated with the Grenville orogeny between 1190 and 980 Ma. The southernmost samples are located over 250 km away from the present day

Grenville Front. The effect of the major Grenvillian orogeny may have been recorded far into the Archean craton via the circulation of fluid. We are not arguing that the modifying fluids might come from the orogenic front itself, but rather that the thermal regime associated with the orogeny might have produced hydrothermal cells far off the orogenic front.

2.8 CONCLUSION

SHRIMP analysis was carried out on zircons from metasedimentary units and leucogranites from the Opinaca injection complex to improve our understanding of its regional context and especially the possible sources for the metasediments and to bracket the time of the granulite facies metamorphic event.

Based on the analysis of BSE images, Th/U ratios and ages, the transition from detrital to metamorphic overgrowth in zircon is constrained at ca. 2675 Ma. The age distribution of zircons older than 2675 Ma reflects that of the main geological units situated on all sides of the Opinaca subprovince, except for a small number of analysis yielding Mesoarchean ages which could only be related to units situated to the north-northwest. This observation, together with a comparison to the Quetico subprovince, leads to the interpretation that the main source of sedimentary material is from the north.

The combination of high grade metamorphism and pervasive injection and crystallisation of leucogranite define the Opinaca injection complex, the SHRIMP analysis bracket this event as occurring between 2670 and 2640 Ma, that is extending from peak granulite to near granite solidus conditions, indicating an overall cooling rate of ~6°C Ma^{-1}.

Analysis of the Discordias shows that most have lower intercept ages compatible with Grenvillian ages. A possible interpretation is proposed in which fluids might have circulated and interacted with rocks as far 250 km from the orogenic front.

This study focused on the western part of the large, and relatively poorly-known, Opinaca subprovince, more work, at a larger scale is still required to understand this subprovince which this study shows contains new features that provide a fuller understanding of the continental crust. This might provide insight on the relative timing of the metamorphic event across the Opinaca and link it with events in the better studied Ashuanipi Subprovince to the east.

2.9 ACKNOLEDGMENTS

This contribution is part of the first author's PhD. Funding for the SHRIMP analysis was met from a Natural Sciences and Engineering Research Council (NSERC) Discovery Grant to Sawyer. Fernando Bea at IBERSIMS is thanks for his help with the SHRIMP analysis and interpretation. We would like to thank Daniel Bandyayera at the BEGQ for his

comments which improved the manuscript. We also wish to thank the Bureau de l'Exploration Géologique du Québec for the financial and logistical support for the fieldwork. This is the IBERSIMS publication no. 18.

2.10 REFERENCES

Bandyayera, D., Burniaux, P., and Morfin, S. 2011. Géologie de la région du lac Brune (33G07) et de la baie Gavaudan (33G10). Ministère des Ressources Naturelles du Québec.

Bandyayera, D., Rhéaume, P., Maurice, C., Bédard, É., Morfin, S., and Sawyer, E.W. 2010. Synthèse Géologique du Secteur du Réservoir Opinaca, Baie-James. Ministère des Ressources Naturelles du Québec.

Black, L.P., Kamo, S.L., Allen, C.M., Aleinikoff, J.N., Davis, D.W., Korsch, R.J., and Foudoulis, C. 2003. TEMORA 1: a new zircon standard for Phanerozoic U–Pb geochronology. CHEMICAL GEOLOGY **200**(1–2): 155-170. doi: 10.1016/s0009-2541(03)00165-7.

Buchan, K.L., Mortensen, J.K., and Card, K.D. 1993. Northeast-trending Early Proterozoic dykes of southern Superior Province: multiple episodes of emplacement recognized from integrated paleomagnetism and U–Pb geochronology. Canadian Journal of Earth Sciences **30**(6): 1286-1296. doi: 10.1139/e93-110.

Corfu, F., and Muir, T.L. 1989. The Hemlo-Heron Bay greenstone belt and Hemlo Au‐Mo deposit, Superior Province, Ontario, Canada 1. Sequence of igneous activity determined by zircon U‐Pb geochronology. Chemical Geology: Isotope Geoscience section **79**(3): 183-200. doi: 10.1016/0168-9622(89)90029-8.

David, J., Vaillancourt, D., Bandyayera, D., Simard, M., Goutier, J., Pilote, P., Dion, C., and Barbe, P. 2010. Datations U-Pb effectuées dans les Sous-provinces d'Ashuanipi, de La Grande, d'Opinaca et d'Abitibi en 2008-2009. Ministère des Ressources Naturelles du Québec.

Davis, D.W., Pezzutto, F., and Ojakangas, R.W. 1990. The age and provenance of metasedimentary rocks in the Quetico Subprovince, Ontario, from single zircon analyses: implications for Archean sedimentation and tectonics in the Superior Province. Earth and Planetary Science Letters **99**(3): 195-205. doi: 10.1016/0012-821x(90)90110-j.

Davis, W.J., Gariépy, C., and Sawyer, E.W. 1994. Pre-2.8 Ga crust in the Opatica gneiss belt:A potential source of detrital zircons in the Abitibi and Pontiac subprovinces, Superior Province, Canada. Geology **22**(12): 1111-1114. doi: 10.1130/0091-7613(1994)022<1111:pgcito>2.3.co;2.

Davis, W.J., Machado, N., Gariépy, C., Sawyer, E.W., and Benn, K. 1995. U–Pb geochronology of the Opatica tonalite-gneiss belt and its relationship to the Abitibi

greenstone belt, Superior Province, Quebec. Canadian Journal Of Earth Sciences **32**(2): 113-127. doi: 10.1139/e95-010.

Goutier, J., Dion, C., David, J., and Dion, D.J. 1999. Géologie de la région de la passe Shimusuminu et du lac Vion (33F/11 et 33F/12). Ministère des Ressources Naturelles du Québec.

Goutier, J., Dion, C., and Ouellet, M.-C. 2001a. Géologie de la région de la colline Bezier (33G/12) et du lac de la Montagne du Pin (33G/13). Ministère des Ressources Naturelles du Québec.

Goutier, J., Dion, C., Ouellet, M.-C., David, J., and Parent, M. 2000. Géologie de la région des lacs Guillaumat et Sakami (33F/02 et 33F/07). Ministére des Ressources naturelles du Québec.

Goutier, J., Dion, C., Ouellet, M.-C., Davis, D.W., David, J., and Parent, M. 2001b. Géologie de la région du lac Guyer (33G05, 33G06 et 33G11). Ministère des Ressources Naturelles du Québec.

Guernina, S., and Sawyer, E.W. 2003. Large-scale melt-depletion in granulite terranes: an example from the Archean Ashuanipi Subprovince of Quebec. Journal of Metamorphic Geology **21**(2): 181-201.

Harley, S.L., Kelly, N.M., Möller, A. 2007. Zircon behaviour and the thermal histories of mountain chains. Elements **3**:25-30.

Hartmann, L.A., and Santos, J.O.S. 2004. Predominance of high Th/U, magmatic zircon in Brazilian Shield sandstones. Geology **32**(1): 73-76. doi: 10.1130/g20007.1.

Ludwig, K.R. 2012. Isoplot/Ex, v. 3.75. Berkeley Geochronology Center Special Publication No. 5, Berkeley.

Morfin, S., Sawyer, E.W., and Bandyayera, D. 2013. Large volumes of anatectic melt retained in granulite facies migmatites: An injection complex in northern Quebec. Lithos **168–169**(0): 200-218. doi: http://dx.doi.org/10.1016/j.lithos.2013.02.007.

Morfin, S., Sawyer, E.W., Bandyayera, D. 2014. The geochemical signature of a felsic injection complex in the continental crust: Opinaca Subprovince, Quebec. Lithos **196–197**: 339–355.

Moukhsil, A., and Legault, M. 2002. Géologie de la région de la Basse-Eastmain occidentale (33D/01, 33D/02, 33D/07 et 33D/08). Ministère des Ressources Naturelles du Québec.

Moukhsil, A., Legault, M., Boily, M., Doyon, J., Sawyer, E.W., and Davis, D.W. 2003. Synthése géologique et métallogénique de la ceinture de roches vertes de la Moyenne et de la Basse-Eastmain (Baie James). Ministère des Ressources Naturelles du Québec.

Percival, J.A., Mortensen, J.K., Stern, R.A., Card, K.D., and Bégin, N.J. 1992. Giant granulite terranes of northeastern Superior Province: the Ashuanipi complex and Minto block. Canadian Journal of Earth Sciences **29**(10): 2287-2308.

Percival, J.A., Sanborn-Barrie, M., Skulski, T., Stott, G.M., Helmstaedt, H., and White, D.J. 2006. Tectonic evolution of the western superior province from NATMAP and lithoprobe studies. Canadian Journal of Earth Sciences **43**(7): 1085-1117. doi: 10.1139/e06-062.

Percival, J.A., and Williams, H.R. 1989. Late Archean Quetico Accretionary Complex, Superior Province, Canada. Geology **17**(1): 23-25.

Sawyer, E.W. 2010. Migmatites formed by water-fluxed partial melting of a leucogranodiorite protolith: Microstructures in the residual rocks and source of the fluid. Lithos **116**(3-4): 273-286.

St. Seymour, K., Turek, A., Doig, R., Kumarapeli, S., and Fogal, R. 1989. First U–Pb zircon ages of granitoid plutons from the La Grande greenstone belt, James Bay area, New Quebec. Canadian Journal Of Earth Sciences **26**(5): 1068-1073. doi: 10.1139/e89-088.

Weinberg, R.F., and Searle, M.P. 1998. The Pangong Injection Complex, Indian Karakoram: a case of pervasive granite flowthrough hot viscous crust. Journal of the Geological Society **155**(5): 883-891.

Williams, I.S., Buick, I.S., and Cartwright, I. 1996. An extended episode of early Mesoproterozoic metamorphic fluid flow in the Reynolds Range, central Australia. Journal of Metamorphic Geology **14**(1): 29-47. doi: 10.1111/j.1525-1314.1996.00029.x.

Williams, I.S., and Claesson, S. 1987. Isotopic evidence for the Precambrian provenance and Caledonian metamorphism of high grade paragneisses from the Seve Nappes, Scandinavian Caledonides. Contributions to Mineralogy and Petrology **97**(2): 205-217. doi: 10.1007/bf00371240.

Wodicka, N., Lamothe, D., and Leclair, A. 2009. Géochronologie U-Pb du Projet Ashuanipi. Ministère des Ressources Naturelles du Québec.

CHAPITRE 3

LARGE VOLUMES OF ANATECTIC MELT RETAINED IN GRANULITE FACIES MIGMATITES: AN INJECTION COMPLEX IN NORTHERN QUEBEC

SAMUEL MORFIN[1], EDWARD W. SAWYER[1] & DANIEL BANDYAYERA[2]

[1] UNIVERSITÉ DU QUÉBEC À CHICOUTIMI

[2] BUREAU DE L'EXPLORATION GÉOLOGIQUE DU QUÉBEC

LITHOS, 2013, VOL. 168-169, P. 200-218

3.1 RÉSUMÉ

La Sous-province d'Opinaca fait partie de la Province du Supérieur dans le Nord du Québec. Elle est constituée de métagreywackes qui enregistrent un métamorphisme de grade granulitique tardi-Archéen et d'abondantes fines veines de leucogranite. Une étude à l'échelle régionale de cette sous-province apporte des informations importantes sur le budget de liquide anatectique (perte versus accumulation) dans la partie inférieure de la croûte continentale moyenne lors d'épisodes d'anatexie.

Une étude pétrologique indique que les métagreywakes ont partiellement fondu à des conditions de ~820^{o}C et ~7kbar, ce qui a pu générer jusqu'à 10 % de liquide anatectique en formant de l'orthopyroxène et/ou du grenat comme phase péritectique. Les métagreywackes contiennent des quantités variables de leucogranites présents sous forme de veines et de dykes sub-parallèles à la foliation principale E-W. L'étude de plus de 1070 affleurements indique qu'un affleurement « typique » contiendrait 63 % de matériel leucogranitique, ce qui est beaucoup plus que les 10 % maximum produits par fusion partielle de l'hôte métasédimentaire. Les âges de cristallisation obtenus par analyse U-Pb SHRIMP sur des zircons des migmatites et des leucogranites ont donné des âges entre 2666 Ma et 2636 Ma, suggérant que le haut grade métamorphique et les injections granitiques sont contemporains. Ces âges indiquent également un refroidissement lent d'environ 6^{o}C Ma^{-1} entre le pic métamorphique et le solidus des granites.

La grande différence (près de 50 %) entre le volume estimé de magma produit *in situ* et le volume observé sur le terrain suggère que les magmas anatectiques se sont accumulés dans la Sous-province d'Opinaca; il s'agit donc d'un complexe d'injection. La découverte que des terranes granulitiques peuvent être enrichis en magmas plutôt que déficitaires est importante et va à l'encontre du concept général selon lequel les terrains granulitiques sont déficitaires en magmas.

La présence d'un complexe d'injection dans la croûte profonde a plusieurs implications pour l'ensemble de la croûte continentale : 1) le fluide riche en H_2O libéré lors de la cristallisation des leucogranites peut réhydrater des assemblages anhydres granulitiques. C'est ce qui explique le remplacement de l'orthopyroxène par l'amphibole et la biotite. Ces roches réhydratées sont plus enclines à fondre de nouveau dans le cadre d'un évènement ultérieur de haut grade métamorphique que des assemblages anhydres; 2) la rétention de grands volumes de leucogranites dans le complexe d'injection a des conséquences thermiques sur la croûte. Les granites étant enrichis en éléments producteurs de chaleurs (Th, U et K), le complexe d'injection qui contient beaucoup de granite a une production de chaleur radiogénique accrue. De plus, la chaleur latente de cristallisation est libérée dans le complexe d'injection. Ces deux effets thermiques font que la croûte continentale inférieure est maintenue à des températures plus élevées pendant des périodes plus longues si un complexe d'injection est présent.

3.2 ABSTRACT

The Opinaca Subprovince in the Superior Province of northern Québec is a metasedimentary belt characterized by metagreywacke rocks that record a late Archean granulite facies metamorphism and contains abundant thin veins of leucogranite. Regional-scale study of this subprovince provides insight to the net budget of anatectic melt (loss *versus* accumulation) in the lower middle continental crust during anatexis.

A petrological study indicates that the metagreywackes partially melted at ~820^{o}C and ~7kbar and generated <10 % melt with orthopyroxene ± garnet as peritectic phases. The metagreywackes contain various amounts of leucogranite in thin veins, sills and dykes injected sub-parallel to the subvertical E-W striking main foliation. Study of more than 1070 outcrops indicates that the "typical outcrop" contains ~63 % of leucogranite; far more than the maximum 10 % of melt produced *in situ* from the host rocks. Crystallization ages obtained by U-Pb SHRIMP analysis of zircons from both the migmatites and the leucogranite veins indicate that the granulite facies metamorphism and the injection of veins were contemporary and occurred during slow cooling (6^{o}C My^{-1}) from the metamorphic peak at 2666 Ma to the granite solidus at 2636 Ma.

The large discrepancy (about 50 %) between the volume of anatectic melt produced locally (*in situ*) and the observed volume of leucogranite in the terrain indicates that anatectic melt accumulated in the Opinaca Subprovince; it is an injection complex. This finding that

granulite facies terranes can be enriched in melt contrasts with the general view that granulite terranes are melt-depleted.

The presence of an injection complex in the deep crust has several broad implications for the continental crust. 1) H_2O released as the injected melt crystallized rehydrated the adjacent granulite facies rocks which is evident from orthopyroxene replaced by amphibole and biotite. Consequently, these deep rocks would be more fertile in a subsequent anatectic event than non-rehydrated residuum. 2) The retention of voluminous leucogranite in the injection complex has thermal consequences for the crust. First, the bulk composition of the crust containing the injection complex is necessarily more felsic, thus the budget of heat-producing elements (Th, U and K) is locally enhanced and radiogenic heat production is higher. Secondly, latent heat of crystallization is released at a deeper level where the leucogranite solidifies. The combined effect of both maintains the lower crust several tens of degrees warmer for longer period of time.

3.3 INTRODUCTION

Partial melting has a profound effect on the continental crust (Sawyer et al., 2011). The formation of anatectic melt of granitic composition, its extraction and ascent is the main process by which the continental crust becomes differentiated and gravitationally stable with a denser lower part. The petrological and compositional links between the deep, partially melted, granulitic crust and granite plutons in the upper crust, called the granulite

– granite connection by some workers has been the subject of many studies (Brown, 1994, 2006; Clemens, 1990; Otamendi and Patiño Douce, 2001; Sawyer, 1998; Vielzeuf et al., 1990). In the last twenty years, attention has focused more on the mechanisms by which felsic anatectic magma moves through the continental crust. Clemens and Mawer (1992) argued that buoyancy in large dykes and not diapirism was how granitic magma traversed the middle crust to feed plutons in the upper crust. In addition, field observations from migmatite terranes show that some contain innumerable small, linked leucosomes, rather than a few large dykes. Thus, in some terranes the movement of anatectic melt may have been pervasive (Brown and Solar, 1999; Collins and Sawyer, 1996; Weinberg, 1999; Weinberg and Searle, 1998) rather than a strongly focused flow through a few large dykes.

Numerical modeling (Hobbs and Ord, 2010; Connolly and Podladchikov 2007; Leitch and Weinberg, 2002) provides insight into the large-scale link between segregation and transport of anatectic melt in the continental crust. The flow of melt from the grain boundaries and pores where it formed into small, elliptical leucosomes occurs over short distances, a few centimeters, and is driven by deformation of the solid matrix (Simakin and Talbot, 2001). The larger-scale problem of how far the melt can then move up from its source is controlled by how much melt, and thus heat, is advected (Leitch and Weinberg 2002; Hobbs and Ord, 2010) because this determines where the solidus of the melt lies in the crust. A large volume of melt rising through a wide dyke can ascend high in the crust before its heat is lost to the wall rocks, and it freezes (Petford et al., 1994). In contrast, the pervasive flow of melt through innumerable narrow channels is far more sensitive to the

loss of heat to the wall rocks as soon as it rises above the solidus and so the melt cannot rise as far before it freezes; it remains much nearer to the depth of the solidus as an injection complex (Leitch and Weinberg, 2002). The temperature difference between the source and the solidus, the volume of magma and the manner in which it moves, whether focused in a few dykes, or by pervasive flow, are key factors that determine how far up in the crust anatectic melt can migrate. At one extreme melt segregates, but barely leaves its source region, at the other it separates and can rise and form a pluton in the upper crust, or even be erupted. Both separate a granitic melt from a ferromagnesian residuum, but their consequences for the overall differentiation of the continental crust are quite different. The former affects only the lower crust, whereas the latter affects virtually its full thickness.

Most studies of the middle and deep levels of the continental crust have concentrated on the petrology and geochemistry of high-grade, melt-depleted rocks (e.g. Fornelli et al., 2002; Graessner and Schenk, 2001; Guernina and Sawyer, 2003; Slagstad et al., 2004; White and Powell, 2010), or on the short-range aspects of melt segregation (Marchildon and Brown, 2003; Oliver and Barr, 1997; Sawyer et al., 1999; Solar and Brown, 2001 White et al., 2004), rather than the volume and large-scale distribution of former anatectic melt in them. The lack of information on how much anatectic melt remained at deep levels in the crust has consequences for mass-balancing the process of crustal differentiation, because estimates of the bulk composition of the lower crust are based principally on the residual rocks (Rudnick and Fountain, 1995) and not on how much melt remained behind as leucosomes and leucogranitic veins. Therefore, this study addresses an important question

relevant to understanding the differentiation of the continental crust; how much of the anatectic melt that was formed in the deep crust remains there. To answer this question mapping has been conducted over a large region of granulite facies migmatites, derived from a metagreywacke (psammite) protolith in the Opinaca Subprovince of northern Quebec. The principal objectives of this paper are to: 1) document the distribution and location of leucosomes and veins of leucogranite that represent crystallized anatectic melt, 2) determine how much melt the protolith produced, 3) determine from mapping and a simple mass balance how much melt was added to, or lost from, the region and, 4) discuss some of the implications of these findings for our understanding of the continental crust.

3.4 OPINACA SUBPROVINCE IN THE SUPERIOR PROVINCE

The Opinaca Subprovince is one of four metasedimentary subprovinces that together cross the Archean Superior Province (Fig. 3.1). It is bounded to the west and north by the La Grande Subprovince (Fig. 3.2), which consists predominantly of mafic volcanic rocks intruded by plutons of tonalite and granodiorite, and to the south by the Opatica Subprovince, a plutonic belt which is dominated by tonalite, trondhjemite, granodiorite and migmatites derived from them (Sawyer, 1998; 2010). The Ashuanipi Subprovince, a granulite facies migmatite terrane (Guernina and Sawyer, 2003), lies to the east. The Ashuanipi and Opinaca Subprovinces form a contiguous sequence of siliciclastic rocks, which Percival et al. (1992) subdivided on the basis of a difference in metamorphic grade.

Strong similarities in rock types, bulk compositions and ages suggest that the sedimentary detritus for the Quetico, Nemiscau, Opinaca and Ashuanipi Subprovinces had very similar sources (Card, 1990), and were deposited in similar environments. The maximum temperature and pressure recorded in the four subprovinces increases from west to east, which indicates slight tilting and a deeper erosion level in the east (Percival et al. 2006).

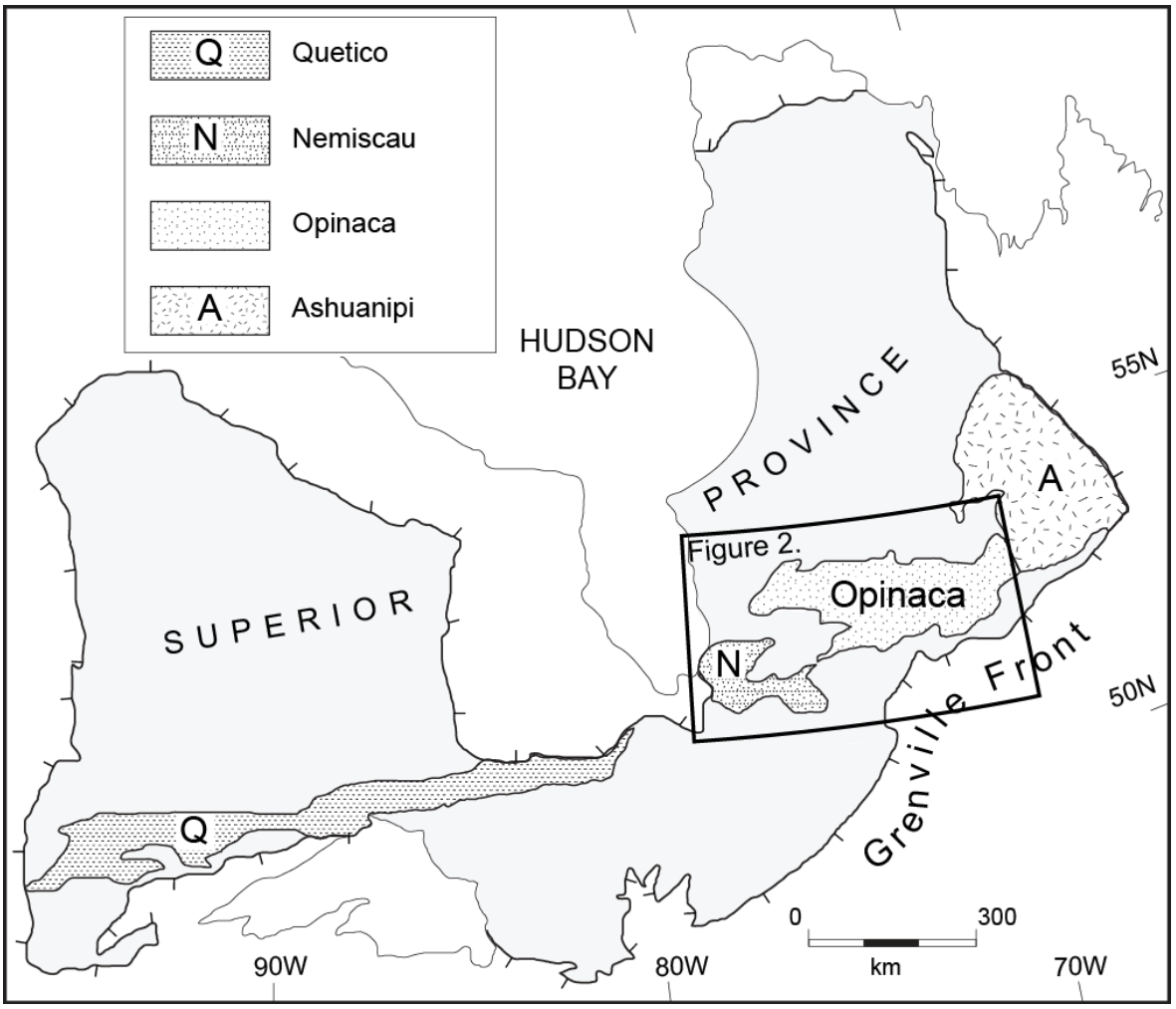

Figure 3.1: Outline of the Superior Province showing the location of the Quetico, Nemiscau, Opinaca and Ashuanipi metasedimentary subprovinces.

The age of deposition for the sedimentary rocks in the Opinaca Subprovince is constrained by intrusion of the Pluton de Bezier at 2674±12Ma (St. Seymour et al., 1989), and 2700Ma for the Lac Taylor Granite (Goutier et al., 1999) on which the sediments were deposited. The ages of detrital zircons indicate deposition occurred between 2698 and 2687Ma for the Quetico (Percival et al., 2006) and between 2700 and 2690Ma for the Ashuanipi subprovinces. The minimum age for deposition in the Nemiscau Subprovince is 2672Ma (Davis et al., 1995).

Deposition of sedimentary rocks in the four subprovinces was quickly followed by high-grade regional metamorphism and anatexis that lasted for tens of millions of years. In the Quetico Subprovince high-temperature metamorphism lasted from ca. 2670 to ca. 2650Ma and was coeval with intrusion of peraluminous granites (Pan et al., 1998; Percival et al., 2006; Zaleski et al., 1999). Granulite facies metamorphism occurred throughout the Ashuanipi Subprovince between 2682 and 2650Ma (Percival et al., 2003; Simard et al., 2009a; Simard et al., 2009b). To the south, amphibolite facies partial melting lasted from 2690 to 2655Ma in the Opatica Subprovince (Davis et al., 1995). Few ages are available for the Opinaca Subprovince; zircon crystallization ages of 2671.6±1.8Ma from vein of leucogranite and 2647Ma from a pegmatite were interpreted by David et al. (2010) to bracket regional anatexis.

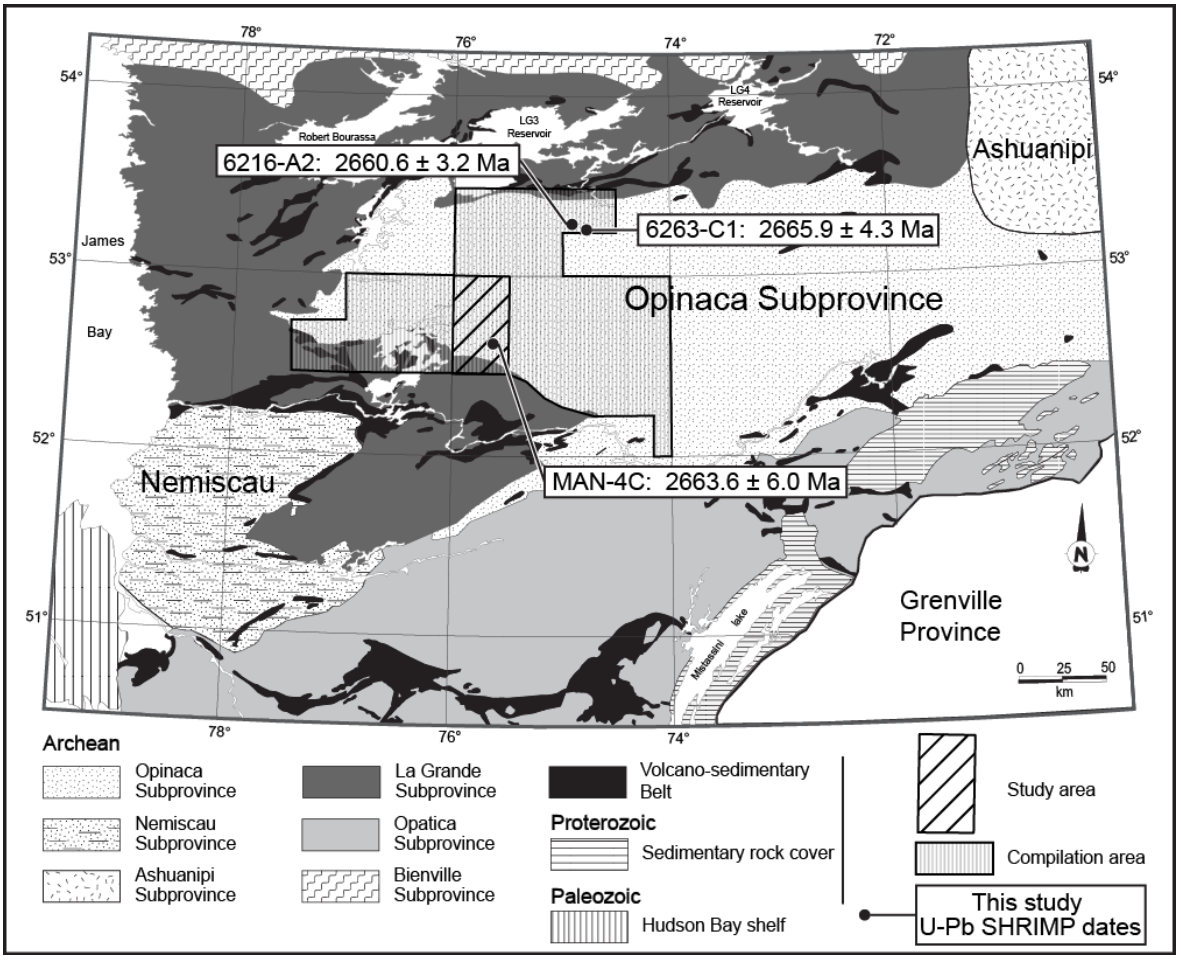

Figure 3.2: Simplified geological map of the Superior Province east of James Bay including location of samples used for U-Pb SHRIMP analysis, modified from Bandyayera et al. (2010). The map shows the present study area and the compilation areas mapped by Simard and Gosselin (1999), Bandyayera et al. (2010) and Bandyayera et al. (2011).

3.5 THE OPINACA SUBPROVINCE

Regional mapping (1:50000 scale) was carried out in the western third of the Opinaca Subprovince (Fig. 3.2) by the Bureau de l'Exploration Géologique du Québec and successive campaigns have mapped 15500km^2 (Bandyayera et al., 2011; Bandyayera and Fliszár, 2007; Bandyayera et al., 2010; Simard and Gosselin, 1999). Figure 3.3 shows the geology of the study area; a sub-region of the 15500km^2 mapped in more detail by the present authors. The Opinaca Subprovince is a belt of Archean siliciclastic metasedimentary rocks in which metagreywacke (psammite) dominate over pelite in a ratio of about 10:1 (see below for petrological and metamorphic details). Scattered metamafic units ranging from a meter to hundreds of meters in thickness occur within the metasedimentary rocks, and consist of amphibole + pyroxene (mostly clinopyroxene, but locally orthopyroxene) gneisses, commonly associated with minor banded iron formation. Rare, small ultra-mafic units also occur and underwent prograde metamorphism with their metagreywacke host rocks. Late- to post-tectonic felsic intrusive bodies in the Opinaca Subprovince have granodiorite to tonalite-enderbite compositions.

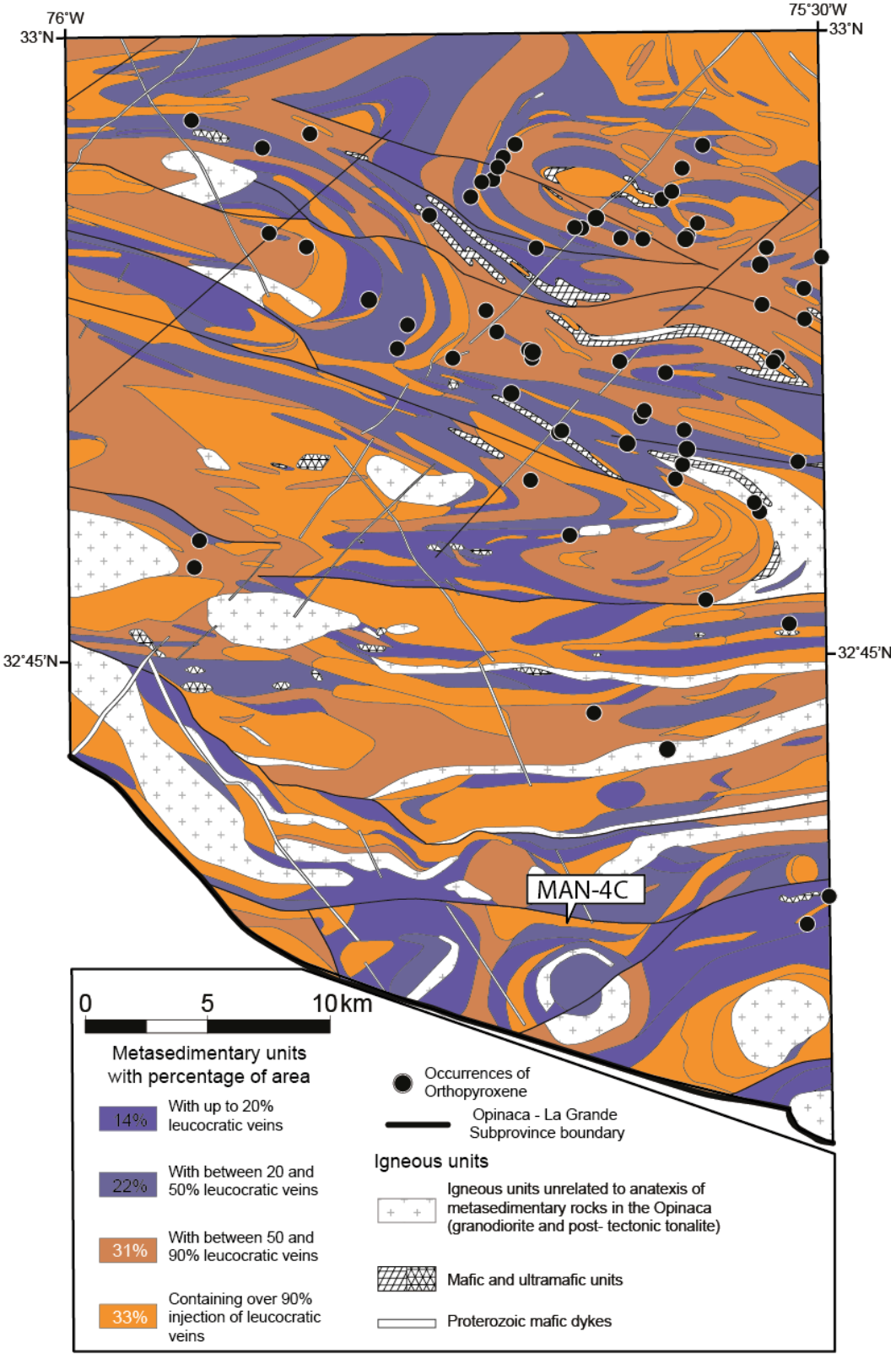
76°W
33°N
75°30'W
33°N
32°45'N
32°45'N
MAN-4C
0
5
10 km
Metasedimentary units
with percentage of area
14%
With up to 20%
leucocratic veins
22%
With between 20 and
50% leucocratic veins
31%
With between 50 and
90% leucocratic veins
33%
Containing over 90%
injection of leucocratic
veins
Occurrences of
Orthopyroxene
Opinaca - La Grande
Subprovince boundary
Igneous units
Igneous units unrelated to anatexis of
metasedimentary rocks in the Opinaca
(granodiorite and post- tectonic tonalite)
Mafic and ultramafic units
Proterozoic mafic dykes

Figure 3.3: Simplified geological map of the study area shown in Figure 3.2 modified from Bandyayera et al. (2010). The southern boundary of the Opinaca Subprovince is its contact with the La Grande Subprovince. The map is based on the description of over 1400 outcrops, which represent a grid of approximately one outcrop per square kilometer. The area of each outcrop range from several square meters to hundreds of square meters. The location of each outcrop could not be shown for reasons of map readability. Metasedimentary units are colored based on the proportion of leucocratic veins they contain. The relative area of each category is indicated in the legend. Black dots mark some locations where orthopyroxene is observed either in the field or in thin section. Position of SHRIMP sample MAN-4C is indicated.

3.5.1 STRUCTURAL CHARACTERISTICS

The rocks are pervasively deformed throughout the study area. Nevertheless, bedding in the metasedimentary rocks is evident as a variation in the grain size and proportion of minerals. Darker, coarse-grained layers rich in garnet, cordierite and biotite indicate beds of pelitic composition compared to metagreywackes which have smaller grain size and which have higher quartz and plagioclase contents. The main schistosity (S_2) is defined by oriented biotite and is commonly parallel to the pelite and greywacke layers (S_0). The S_2 schistosity is generally sub-vertical and contains a mineral lineation that plunges gently towards the east, or to the west (Bandyayera et al., 2010). A prominent compositional layering due to the presence of many thin, white quartzo-feldspathic veins in the metasedimentary rocks is evident in most outcrops, and is the result of the injection of felsic veins parallel, or sub-parallel, to the bedding or the S_2 planes. In the mafic and ultramafic rocks S_2 is defined by the orientation of amphibole.

The lithological units are folded and truncated at the map scale (Fig. 3.3). The folds are tight to isoclinal with subvertical axial planes and gently plunging hinges parallel to L_2 schistosity; these are interpreted as regional F_3 structures as they fold the S_2 schistosity. The bedding in metasedimentary rocks is steeply dipping in most outcrops. However, there are areas where it has gentle dips and these correspond to the hinge zones of folds.

The map units and the flanks of folds are truncated by broad, east-west striking, subvertical shear zones. These impose a strong, subvertical schistosity (S_4) on the adjacent rocks that is, in many places, sub-parallel to S_2.

Competent layers that are oriented approximately east-west show some degree of boudinage. However, felsic dykes oriented approximately north-south (i.e. orthogonal to layering) are commonly folded asymmetrically (either S or Z shapes depending on the direction of the plunge of the subhorizontal fold hinges). Overall this pattern is consistent with contraction oriented approximately north-south across the mapped areas.

In places, the felsic veins intruded along the S_2 schistosity or the bedding, follow the outline of F_3 folds and appear to have been folded during F_3. Close examination shows that a small proportion of these veins contain isoclinal intrafolial folds that have S_2 as their axial plane, thus they were folded prior to F_3, probably during the formation of the S_2 schistosity. Other, petrographically similar veins cross both the F_3 folds and the S_4 shear zones. Taken together these relationships indicate that felsic melt was intruded during the S_2 to S_4 deformation. Patches of neosome on the flanks of F_3 folds contain a high proportion of garnet and cordierite, whereas patches of leucosome in the hinges of F_3 folds contain less. This suggests that melting occurred as the F_3 folds developed and that melt migrated from the limbs to the hinges as the folds tightened. Leucosome also occurs in shear band structures that post-date F_3 folds and may be related to the S_4 shear zones. Thus, field relationships indicate that partial melting was contemporaneous with all the main phases of deformation recognizable in the field.

Some shear zones (Fig. 3.3) have been intruded by younger granodiorite and tonalite. In a few places, shear zones contain greenschist facies mineral assemblages, and thus were reworked at lower temperature.

3.5.2 MIGMATITES

Following the terminology of Sawyer (2008a, b), migmatites are crustal rocks formed by partial melting. The anatectic melt produced may be segregated and form *in situ* and "in source" leucosomes if still in its source layer, or leucocratic veins if the segregation distance was larger, but is still within the migmatite. Terminology becomes problematic when the source of the leucogranite in a vein is uncertain. A vein complex (Brown, 1973), or an injection complex (Weinberg and Searle, 1998), is formed when dykes or sills of granite are injected into a country rock that may, or may not, have melted. Thus, the dykes and sills in an injection complex are not necessarily leucosomes, consequently in this study they are called leucogranitic veins, dykes or sills as geometrically appropriate, to distinguish them from leucosomes which are demonstrably derived locally from partial melting of the host rocks.

In outcrop, the metasedimentary rocks resemble stromatic metatexite migmatites because they contain innumerable thin layers of leucogranite oriented sub-parallel to the main foliation (Bandyayera et al., 2010; Simard and Gosselin, 1999). Metagreywacke (or psammite) rocks in the mapped areas are fine-to medium-grained (~0.5mm, but some

outcrops contain coarse-grained (1 to 5mm) patches a few centimeters across in which quartz + plagioclase + K-feldspar encloses orthopyroxene (Fig. 3.4b) and more commonly garnet, but no cordierite. These patches are interpreted to be *in situ* neosome consisting of leucosome surrounding peritectic phases and are evidence of partial melting. In rocks where deformation was weak the patches are equant. However, in more deformed rocks the melt migrated into dilatant structures (Fig. 3.4a) and the morphology of the neosome is more complex. Most metagreywacke do not contain such obvious *in situ* neosome.

The metapelitic layers all contain macroscopic evidence for partial melting (Fig. 3.4c, d). Two varieties of small *in situ* neosome are common. In one, leucosome containing quartz + plagioclase + K-feldspar surrounds large crystals of pink garnet that are typically intergrown with quartz (Fig. 3.4c), and in the other an ellipsoidal leucosome is surrounded by a melanosome consisting of biotite + garnet + quartz + plagioclase. Some biotite-rich metapelitic layers contain large isolated pink garnets that have a small amount of quartz + plagioclase + K-feldspar leucosome around them; these are interpreted as neosome that has lost much of its melt (Fig. 3.4d). A few large (tens of square meters) outcrops show arrays of interconnected shear band structures that contain leucosome and scattered coarse-grained garnet or cordierite. These arrays are interpreted to be remnants of the network of channels through which melt escaped (e.g. Bons et al., 2001; Sawyer, 2001). Considering just the outcrops with *in situ* neosome and leucosome, the overall morphology is that of patch and net-structured metatexite migmatite.

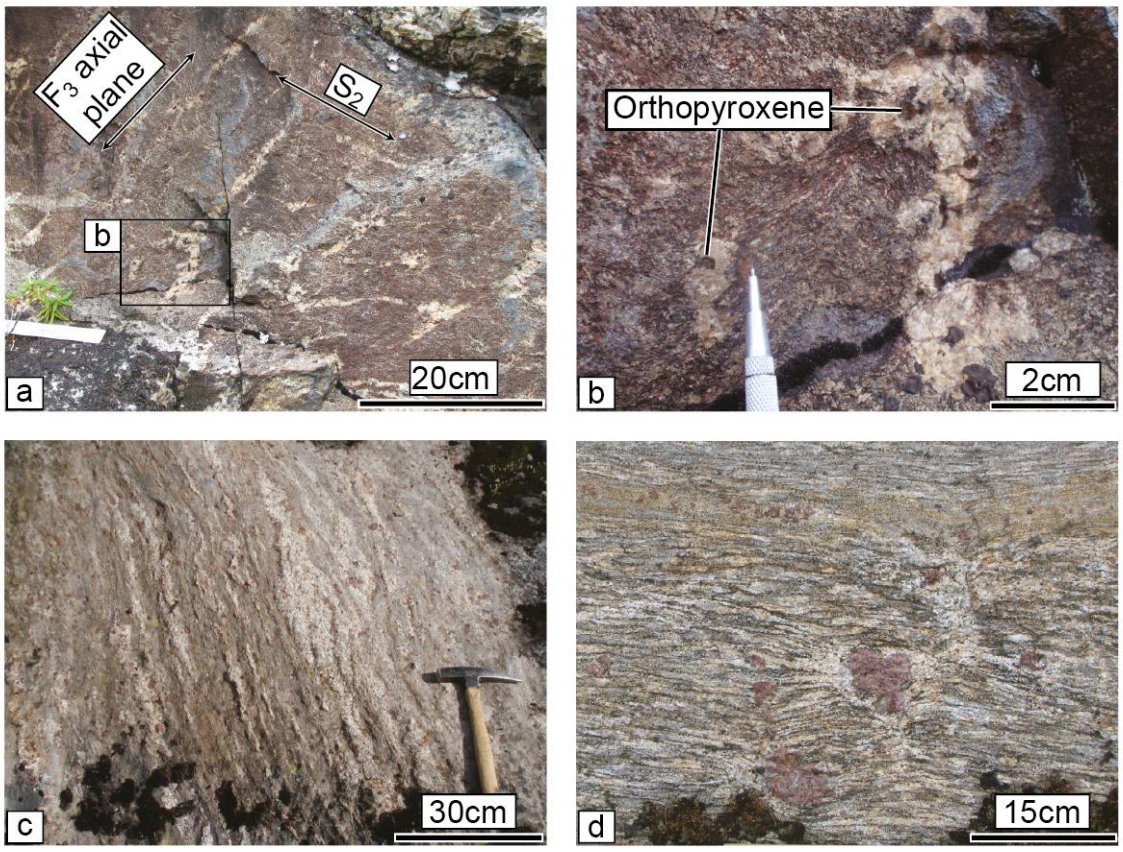

Figure 3.4: Field aspect of the migmatites. (a) Orthopyroxene-bearing metagreywacke with a network of leucosome in the hinge of a fold. Leucosomes are parallel to the main foliation (S_2) and to the F_3 axial plane, indicating melting was contemporaneous with D_3. (b) Neosome in a metagreywacke migmatite indicating in situ partial melting. Note orthopyroxene (melanosome) surrounded by the leucosome. (c) Typical garnet + cordierite stromatic metapelitic migmatite in the Opinaca Subprovince. (d) Large peritectic garnets surrounded by narrow leucosomes interpreted as evidence for the loss of melt from a metapelite and subsequent collapse of the channel through which melt escaped. Note the thin, yellowish, layer of fine grained garnet metagreywacke near the top of picture which contains much less leucosome than the coarser, partially melted metapelite.

3.5.3 THIN LEUCOCRATIC FELSIC VEINS IN MIGMATITES

The proportion of thin (<5cm) leucocratic veins varies greatly from outcrop to outcrop (Fig. 3.5). The veins range in composition from leucogranite to leucotonalite (a discussion of geochemical aspects of the leucogranites is in preparation) and most have a medium to coarse-grained granitic microstructure. The typical mineral assemblage is quartz + plagioclase + K-feldspar + biotite ± tourmaline ± garnet. Amphibole is very rare.

Most veins of leucogranite are oriented sub-parallel to S_2, or the bedding, in a *lit par lit* manner (Fig. 3.5). They do not have wide zones of residual rocks (melanosome) around them, and hence are not locally derived; they are not leucosomes. The veins are separated from their host by narrow (<5mm) selvedges composed of biotite which, in places, may also contain tourmaline and garnet. These melanocratic selvages are not interpreted as melanosomes in the sense of Sawyer (2008a, b) because: 1) they do not contain evidence of peritectic phases produced during biotite dehydration melting and, 2) crystals of biotite in the selvedges are a factor of 2 to 5 larger than those in the country rock.

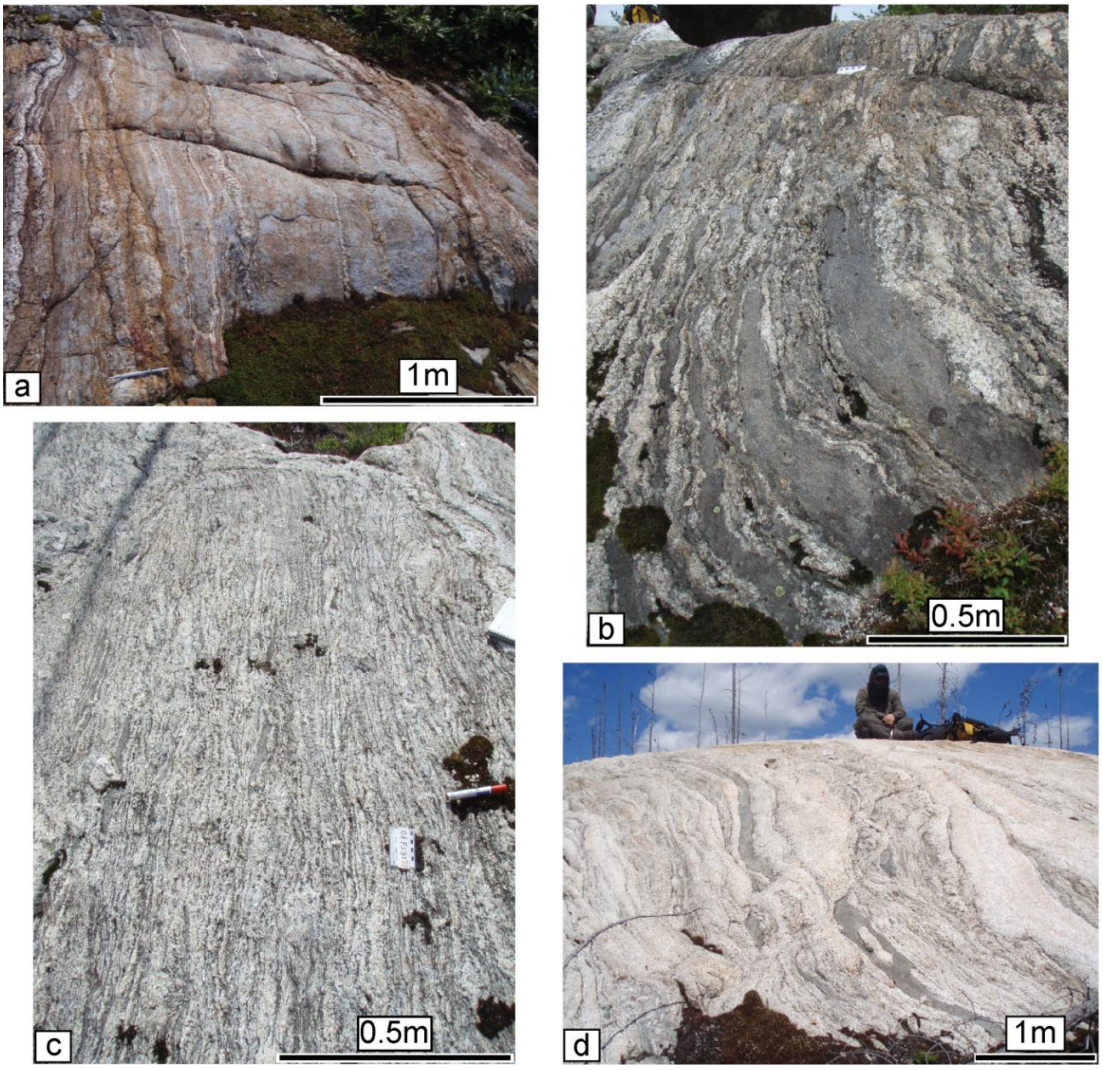

Figure 3.5: Felsic veins in the granulite facies metasedimentary rocks. (a) Stromatic migmatite with alternating metapelite and metagreywacke layers; orthopyroxene in the metagreywacke layers indicates that they partially melted. Note that the felsic veins are more abundant and wider in the weaker pelitic layers. (b) Injected felsic veins with schollen (screens) of metagreywacke preserved between the veins. (c) Outcrop showing abundant thin, sub-parallel leucogranitic veins with a few small remnants of metagreywacke among the anastomosing veins. (d) Outcrop with wide dykes of leucogranite. The dykes are typically multiple injections of various composition, grain size and microstructure. Schlieren and thin elongated metasedimentary enclaves commonly occur between injections.

Individual veins can be followed for many meters, and in some cases cross the foliation and bedding at a low angle, or step abruptly from one plane to another; features that indicate an intrusive origin. The veins commonly contain long, thin biotite-rich remnants of the host and differences in texture and modal mineralogy between the leucogranite on either side suggest multiple injections of slightly different magma into sub-parallel fractures in a crack-and-seal type of process (Fig. 3.6a). In most places the bedding and the S_2 foliation are subvertical, consequently the leucogranitic veins form thin, parallel subvertical sheets (Fig. 3.5); cross-cutting dykes are not obvious in these outcrops. However, where bedding and S_2 foliation have gentle dips in the hinges of F_3 folds, and the leucogranite veins intruded along these planes have gentle dips, the steeply dipping, discordant dykes of leucogranite are easily noticed (Fig. 3.6b). The steep dykes cross the bedding, but not the subhorizontal sheets of leucogranite. Rather, they are in petrographic continuity (term from Marchildon and Brown, 2003) with the layer-parallel sheets (Fig. 3.6b). This relationship indicates that the dykes and sheets were linked and contained melt at the same time.

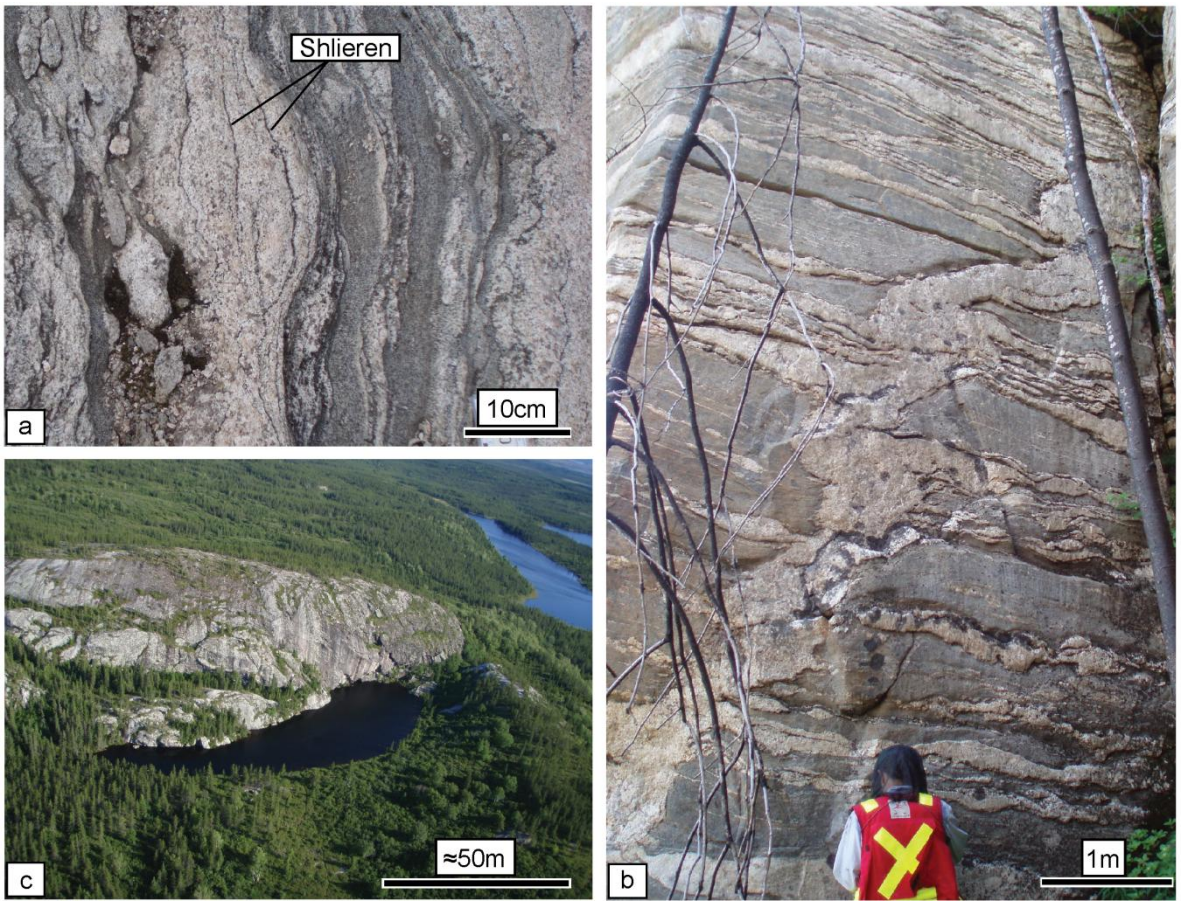

Figure 3.6: Morphology of the leucocratic veins. (a) Heterogeneous microstructure in a set of veins injected into metagreywacke. Note the crack and seal-like structure in the large vein with successive increments bounded by biotite schlieren. Note the mafic selvedges around small veins right of center. (b) Sills of leucogranite intruded sub-parallel to the gently dipping main (S2) foliation and bedding. The sills appear to be fed by a wider sub-vertical dyke since there are no truncations between the sills and the dyke. The sills show a weak pinch and swell structure, but the dyke is folded. (c) Elongate hill, hundreds of meters long composed of multiple dykes of leucogranite similar to those in figure 3.5d.

Some discordant dykes are planar and injected after the regional deformation indicating that most injections are syn- or pre-deformation, although some late injection occurred. However, most show a minor degree of deformation. For example, the vertical dyke in figure 3.6b has been shortened, whereas the sills parallel to the bedding show weak boudinage, or pinch and swell structure. The asymmetry of the folded veins changes with the orientation of the dyke relative to the normal to the S_2 foliation or bedding plane, consistent with a pure shear type of deformation (Price and Cosgrove, 1990, p. 12) contemporaneous with injection of the dykes and veins (sills).

3.5.4 LARGE LEUCOCRATIC DYKES AND SILLS

Areas with the highest proportion of thin felsic veins also contain some wider (~1m) dykes (or sills) of leucogranitic (leucogranite to leucotonalite) composition relative to the most common centimeter-scale veins (Fig. 3.5d), and this gives the outcrops the appearance of a "sheeted pluton". Rounded hills up to a kilometer in length occur throughout Opinaca (Fig. 3.6c) and indicate where these meter-wide dykes of leucogranite are more common. The wide dykes have compositions similar to the narrow ones, but their microstructure is more varied. The grain size and microstructure ranges from coarse-grained (10mm) granite to very coarse (>50cm) pegmatite and, more rarely, to fine-grained (1mm), which is generally the last intrusive phase. Biotite is the most common dark mineral, but small pink garnets (<2mm) occur in some leucogranites. Tourmaline occurs in some dykes near to the contact

with the host rocks. Hornblende occurs sparsely in some dykes of leucogranodiorite and leucotonalite. Muscovite occurs in some coarse-grained dykes.

Schlieren of biotite are present in some dykes, commonly with enclaves of the wall rocks (Figs. 3.5d, 3.6a), thus, a proportion of the biotite in the dykes came from the host rocks and represents contamination by the wall rocks. Thin, biotite-rich selvedges occur between the dykes and their host rocks.

3.6 U-PB SHRIMP GEOCHRONOLOGY

Field relations indicate that the injection of abundant leucocratic veins was coeval with regional anatexis and granulite facies metamorphism. In order to test this interpretation, zircons from migmatites and the leucocratic veins were dated by the U-Pb SHRIMP method.

Zircon was separated from three samples using conventional density and magnetic techniques, mounted in epoxy and then polished. Cathodoluminescence (CL) images obtained prior to analysis by SHRIMP at the IBERSIMS laboratory at the University of Granada. The spots for analysis on the zircon crystals were selected after examination of the cathodoluminescence (CL) images (Fig. 3.7). The analytical procedure at IBERSIMS follows that outlined in Williams and Claesson (1987). U-Pb ratios were calibrated using the 417Ma TEMORA reference zircon (Black et al., 2003) which was analysed every

fourth time. Point-to-point errors, calculated on replicates of the TEMORA standard at 95% confidence interval, range from 0.22 to 0.32% for $^{206}Pb/^{238}U$, and 0.39 to 0.88% for $^{207}Pb/^{206}Pb$, depending on the analytical session. Data reduction was done by the IBERSIMS laboratory using SHRIMPTOOLS software (downloadable from www.ugr.es/~ibersims) and plotted via ISOPLOT/EX 3.75 software (Ludwig, 2012, http://www.bgc.org/isoplot_etc/isoplot.html). Ages reported are $^{207}Pb/^{206}Pb$ corrected for common lead using ^{204}Pb. Uncertainties are presented at the 2σ level (95% confidence). For the purpose of this study, only the most concordant analyses are considered (Table 3.1, Fig. 3.8). A threshold value of 3.2% discordance was adopted as the best compromise between lowest discordance and the number of samples and only analysis under this threshold are considered in this contribution (3.2% allows a minimum of 15 analysis per sample).

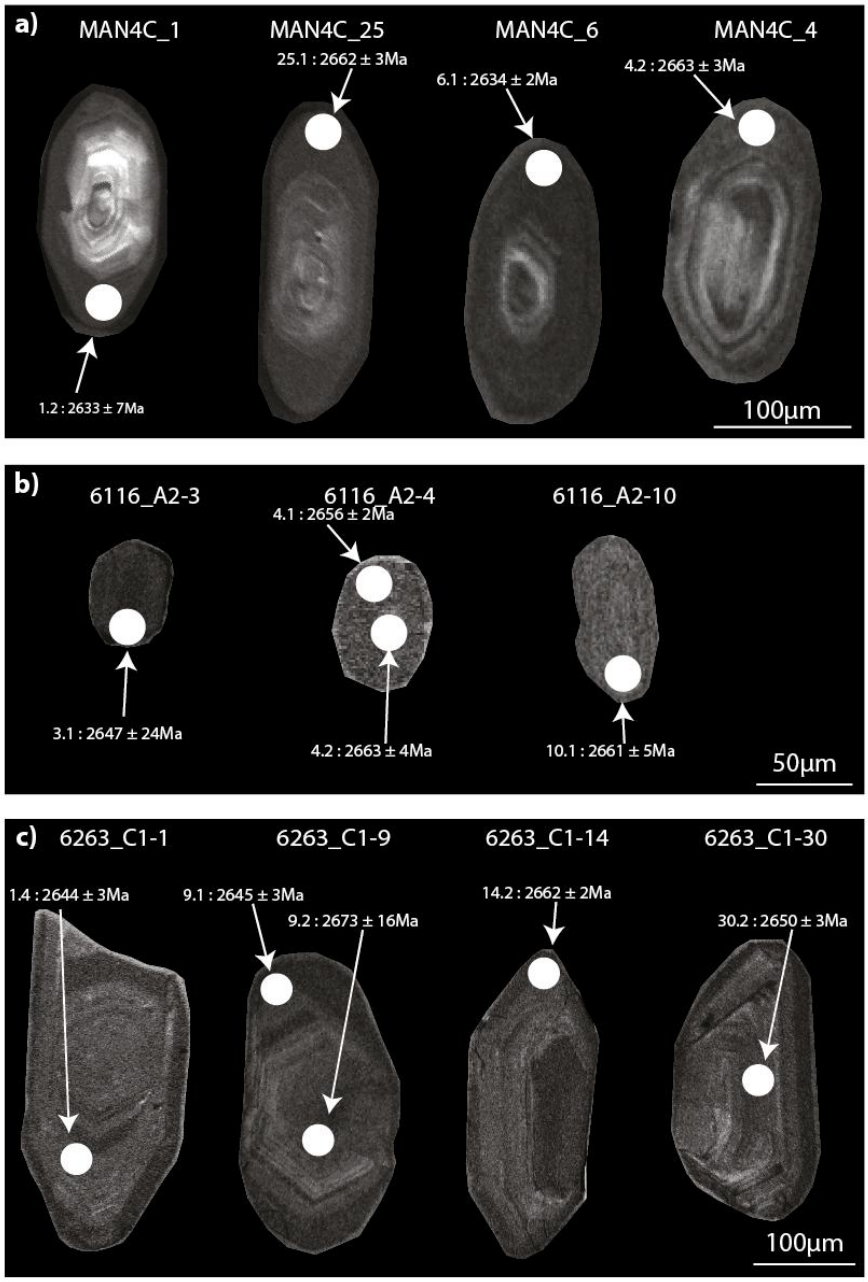

Figure 3.7: Cathodoluminescence images of representative zircons used for U-Pb SHRIMP analysis showing spot where analyses were taken for samples; a) metapelite MAN-4C, b) metapelite 6116-A2, and c) leucogranite 6263C1.

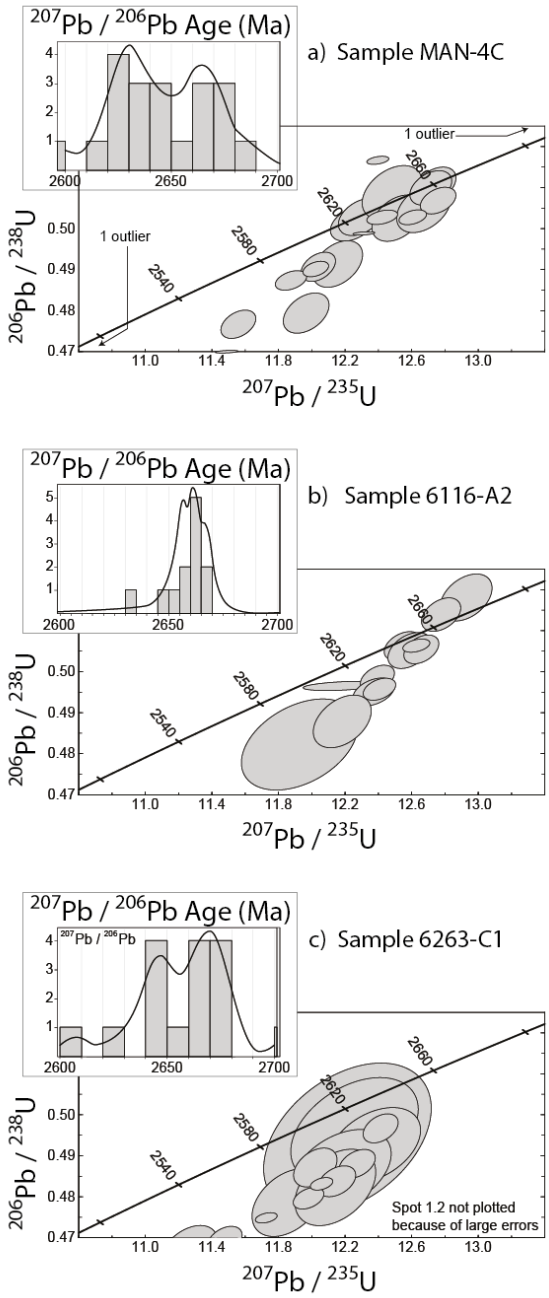

Figure 3.8: Concordia diagram from zircon U-Pb SHRIMP analysis for; a) metapelite MAN-4C, b) metapelite 6116-A2 and c) leucogranite 6263-C1. Inserts are $^{207}Pb/^{206}Pb$ age histogram and probability distribution for each sample. Scale is same for all three samples.

Spot	Concentration (ppm)						Ratios (^{204}Pb Corrected)						Ages (^{204}Pb Corrected)						
	U	Th	^{208}Pb	f206_4%	f206_8%	^{232}Th/^{238}U	^{207}Pb/^{206}Pb	±err	^{207}Pb/^{235}U	±err	^{206}Pb/^{238}U	±err	^{207}Pb/^{206}Pb	±err	^{207}Pb/^{235}U	±err	^{206}Pb/^{238}U	±err	disc.(%)
MAN4C - Metapelite				**52° 38' 27.9" N - 75° 40' 12.5" W**															
1.2	290	4	128	0.04	-0.10	0.01	0.1779	0.0007	12.4812	0.1468	0.5088	0.0053	2633	7	2641	11	2652	23	-0.4
2.1	785	80	319	0.13	-0.40	0.10	0.1773	0.0006	11.4888	0.0561	0.4699	0.0003	2628	5	2564	5	2483	1	3.2
4.2	365	63	151	0.04	-0.68	0.18	0.1811	0.0004	11.9671	0.1121	0.4793	0.0040	2663	3	2602	9	2524	18	3.0
5.1	433	22	183	0.07	-0.56	0.05	0.1767	0.0006	11.8740	0.0765	0.4873	0.0019	2622	6	2595	6	2559	8	1.4
6.1	380	13	161	0.14	-0.27	0.03	0.1780	0.0002	12.0380	0.0848	0.4906	0.0029	2634	2	2607	7	2573	13	1.4
7.2	1287	11	532	0.12	0.00	0.01	0.1759	0.0004	11.5586	0.0849	0.4766	0.0028	2615	4	2569	7	2512	12	2.2
9.1	718	130	310	0.09	-0.77	0.19	0.1790	0.0004	12.3115	0.0539	0.4988	0.0004	2644	4	2629	4	2609	2	0.8
10.1	521	44	227	0.02	0.06	0.09	0.1818	0.0005	12.6052	0.0676	0.5028	0.0015	2670	4	2651	5	2626	6	1.0
11.1	621	20	264	0.06	-0.24	0.03	0.1794	0.0002	12.1552	0.1232	0.4913	0.0046	2648	2	2617	10	2576	20	1.6
14.2	359	23	161	0.18	7.50	0.07	0.1740	0.0003	12.3960	0.0532	0.5166	0.0008	2597	3	2635	4	2685	4	-1.8
16.2	502	24	219	0.05	7.91	0.05	0.1792	0.0007	12.4232	0.0761	0.5027	0.0015	2646	7	2637	6	2626	6	0.4
17.2	373	4	158	0.03	8.21	0.01	0.1779	0.0004	12.0231	0.0636	0.4901	0.0015	2634	4	2606	5	2571	7	1.4
21.1	624	9	275	0.02	8.48	0.01	0.1808	0.0005	12.7139	0.1028	0.5099	0.0034	2661	5	2659	8	2656	15	0.0
22.2	278	1	121	0.02	8.33	0.01	0.1773	0.0006	12.2954	0.1101	0.5028	0.0037	2628	6	2627	8	2626	16	0.0
23.1	487	120	213	0.01	5.40	0.25	0.1826	0.0005	12.7584	0.0874	0.5068	0.0027	2677	4	2662	7	2643	11	0.8
24.1	351	15	152	0.00	7.84	0.04	0.1772	0.0008	12.2490	0.1116	0.5012	0.0035	2627	8	2624	9	2619	15	0.2
25.1	915	4	404	0.01	8.51	0.00	0.1809	0.0004	12.7379	0.1049	0.5106	0.0036	2662	3	2661	8	2659	16	0.0
26.1	958	3	417	0.03	8.55	0.00	0.1806	0.0002	12.5136	0.1247	0.5025	0.0046	2659	2	2644	9	2625	20	0.8
29.1	432	98	171	0.28	4.90	0.23	0.1656	0.0005	10.3988	0.1410	0.4556	0.0058	2513	5	2471	13	2420	26	2.0
6116-A2 - Metapelite				**53° 19' 48.9" N - 74° 58' 29.2" W**															
1.1	405	11	182	0.02	0.02	0.03	0.1809	0.0002	12.9256	0.1266	0.5181	0.0047	2662	2	2691	20	2674	9	-0.6
2.1	546	35	235	0.03	0.05	0.07	0.1779	0.0027	12.1811	0.1920	0.4965	0.0009	2634	25	2599	4	2619	15	0.8
3.1	595	11	248	0.03	0.00	0.02	0.1794	0.0026	11.9255	0.2856	0.4822	0.0091	2647	24	2537	40	2599	23	2.4
4.1	479	23	213	0.00	0.01	0.05	0.1803	0.0003	12.7755	0.0969	0.5139	0.0033	2656	2	2673	14	2663	7	-0.4
4.2	320	14	135	0.07	0.04	0.04	0.1811	0.0005	12.1815	0.1417	0.4878	0.0052	2663	4	2561	23	2619	11	2.2
8.1	599	25	262	0.03	-0.02	0.04	0.1816	0.0002	12.6559	0.0863	0.5054	0.0029	2668	2	2637	12	2654	6	0.6
9.1	831	148	320	0.12	0.06	0.18	0.1654	0.0007	10.1284	0.1268	0.4440	0.0049	2512	8	2369	22	2447	12	3.2
10.1	342	15	150	0.03	0.01	0.04	0.1809	0.0005	12.6271	0.0664	0.5063	0.0013	2661	5	2641	6	2652	5	0.4
11.1	1932	494	683	0.03	-0.35	0.26	0.1395	0.0006	7.8519	0.0834	0.4083	0.0037	2221	7	2207	17	2214	10	0.4
14.1	547	12	239	0.02	-0.01	0.02	0.1807	0.0005	12.5870	0.1070	0.5051	0.0036	2660	5	2636	15	2649	8	0.6
15.1	627	37	269	0.01	-0.01	0.06	0.1812	0.0009	12.3708	0.1032	0.4950	0.0028	2664	8	2593	12	2633	8	1.6
16.1	716	15	370	0.01	0.00	0.02	0.2460	0.0016	20.2437	0.1988	0.5967	0.0038	3160	10	3017	15	3103	10	2.8
18.1	514	5	222	0.13	0.06	0.01	0.1804	0.0003	12.3932	0.0826	0.4983	0.0027	2656	3	2607	11	2635	6	1.0
19.1	528	26	231	0.06	0.03	0.05	0.1797	0.0005	12.5442	0.0910	0.5063	0.0029	2650	4	2641	12	2646	7	0.2
20.1	629	12	270	-0.01	0.00	0.02	0.1815	0.0005	12.4063	0.0805	0.4957	0.0022	2667	5	2595	10	2636	6	1.6
6263-C1 - Leucogranite				**53° 15' 52.5" N - 74° 46' 25.3" W**															
1.2	1380	180		0.01	0.00	0.13	0.1860	0.0034	12.9022	0.8130	0.5031	0.0302	2707	30	2673	61	2627	131	1.8
1.4	1067	125	450	0.01	-0.05	0.12	0.1790	0.0003	12.0204	0.1068	0.4871	0.0039	2644	3	2606	8	2558	17	1.8
6.4	631	58	263	0.00	-0.04	0.09	0.1826	0.0003	12.1424	0.1981	0.4822	0.0076	2677	3	2616	16	2537	33	3.0
9.1	743	80	306	0.24	0.13	0.11	0.1791	0.0003	11.7265	0.0531	0.4748	0.0010	2645	3	2583	4	2505	5	3.0
9.2	676	72	288	0.03	0.01	0.11	0.1822	0.0017	12.3732	0.2266	0.4926	0.0075	2673	16	2633	17	2582	33	2.0
11.1	804	106	344	0.16	0.00	0.14	0.1793	0.0025	12.2143	0.4109	0.4942	0.0151	2646	23	2621	32	2589	65	1.2
12.2	812	86	343	0.02	-0.04	0.11	0.1824	0.0004	12.2703	0.0894	0.4880	0.0029	2675	4	2625	7	2562	12	2.4
14.2	866	125	362	0.13	-0.34	0.15	0.1810	0.0002	12.0584	0.0549	0.4831	0.0012	2662	2	2609	4	2541	5	2.6
18.1	969	151	394	0.02	-0.05	0.16	0.1774	0.0004	11.4753	0.0869	0.4692	0.0029	2629	4	2563	7	2480	13	3.2
19.3	418	55	180	0.69	1.10	0.14	0.1792	0.0024	12.2550	0.3120	0.4961	0.0105	2645	22	2624	24	2597	46	1.0
24.1	722	106	303	0.14	0.05	0.15	0.1822	0.0004	12.1501	0.0926	0.4838	0.0031	2673	3	2616	7	2544	13	2.8
28.1	598	57	254	0.84	0.89	0.10	0.1815	0.0020	12.1763	0.2454	0.4865	0.0081	2667	18	2618	19	2556	35	2.4
30.2	849	106	351	0.01	-0.01	0.13	0.1797	0.0003	11.8554	0.1741	0.4785	0.0068	2650	3	2593	14	2521	30	2.8
31.1	765	100	309	0.05	-0.01	0.13	0.1750	0.0007	11.2606	0.1406	0.4666	0.0052	2607	7	2545	12	2468	23	3.0
8.1b	608	106	262	0.22	-0.57	0.18	0.1813	0.0002	12.4130	0.0854	0.4967	0.0029	2665	1	2599	12	2636	7	1.4
8.2b	842	87	349	-0.01	-0.02	0.11	0.1812	0.0005	11.9792	0.0758	0.4796	0.0021	2664	4	2526	9	2603	6	3.0

Table 3.1: U-Pb SHRIMP data. Columns f206_4% and f206_8 give the percentage of ^{206}Pb that is ^{204}Pb and of ^{206}Pb that is ^{208}Pb respectively. Column Disc% is the degree of discordance determined for the analysis. All values are at the 2-sigma confidence level.

3.6.1 RESULTS

Samples MAN-4C and 6116-A2 are partially melted garnet + cordierite metapelites. Zircons from MAN-4C are up to 300µm long and commonly show a finely banded, prismatic overgrowth on a rounded core (Fig. 3.7a). The results reported here are from the overgrowths which are interpreted to be linked to the anatexis event. Zircons from sample 6116-A2 are smaller (up to 150µm), mostly rounded and do not show, evidence for compositional zoning in the overgrowth on the CL images (Fig. 3.7b).

Sample 6263-C1 is a leucogranite dyke injected into a metagreywacke. It contains prismatic zircons, up to 500µm across, that display oscillatory zoning (Fig. 3.7c) and are interpreted to indicate growth from a melt. Some 20% of the analysed points from zircons of this sample show evidence for the loss of lead; these are not considered further. As expected (Vavra et al., 1999), Th/U ratios (Table 3.1) are higher on average (Th/U=0.13) in the zircons from leucogranite sample than in zircons from metapelitic samples (average Th/U=0.06 and 0.07 for 6116-A2 and MAN-4C, respectively). This is interpreted to indicate that the former have an igneous origin and the latter a metamorphic origin.

Pelitic migmatite sample 6116-A2 displays an age probability distribution that is bell-shaped with a $^{207}Pb/^{206}Pb$ weighted mean of 2660.6±3.2Ma (12 out of 15 analyses considered, MSWD=9.7, Fig. 3.8b). The $^{207}Pb/^{206}Pb$ probability density plots for metapelite migmatite sample MAN-4C shows two small peaks from which weighted $^{207}Pb/^{206}Pb$ ages of 2663.6±6.0 and 2637±6.7Ma (based on 18 out of 20 analyses, MSWD=105 and 38

respectively, Fig. 3.8a) can be calculated. The high MSWDs and the relative weakness of the peaks suggest that crystallization of zircon occurred over a ~25Ma period with two main periods of crystallization.

The probability density plot (Fig. 3.8c) for leucogranite vein 6263-C1 shows two peaks of zircon growth (i.e. crystallization), one at 2665.9±4.3Ma and another at 2646.0±3.8Ma (13 out of 16 analyses considered, MSWD=16 and 3.2, respectively). These are considered to be crystallization ages of the vein. The presence of two age populations is consistent with field evidence for multiple injections to form the vein, similar to the case described in Fig. 3.6a.

3.7 PETROLOGY OF THE MIGMATITES

3.7.1 METAGREYWACKE PALEOSOME

The common mineral assemblage in the metagreywacke/psammite rocks of the Opinaca Subprovince is quartz + plagioclase + biotite ± garnet ± tourmaline (Fig. 3.9a). K-feldspar is not present. An equilibrated granoblastic-polygonal microstructure with a grain size of 0.5mm is widely developed; quartz and plagioclase (median An_{29}, Table 2) are equant or slightly elongated in the S_2 schistosity that is defined by the orientation of biotite. Garnet forms idioblastic crystals up to 5mm across and typically displays small pressure shadows filled with quartz (Fig. 3.9b). Biotite is in textural equilibrium with garnet and does not

replace it. In some rocks, the cores of garnet contain straight inclusion trains of biotite and quartz that are oblique to the external foliation (Fig. 3.9b). Thus, growth of garnet may have started before the main D_2 deformation. Dravite tourmaline is a minor, but common phase in the metagreywackes (Fig. 3.9a). A minor amount of magnesio-hornblende occurs in some metagreywackes. Metagreywackes with the common assemblage do not contain microstructures, such as cuspate grain boundaries, or corroded quartz, plagioclase or biotite (e.g. Sawyer, 2001, 2008a) indicative of partial melting. Such microstructures may have been erased by subsequent textural re-equilibration, but the absence of more robust macrostructures, such as neosomes, makes it unlikely that these rocks melted; hence they are inferred to represent paleosome.

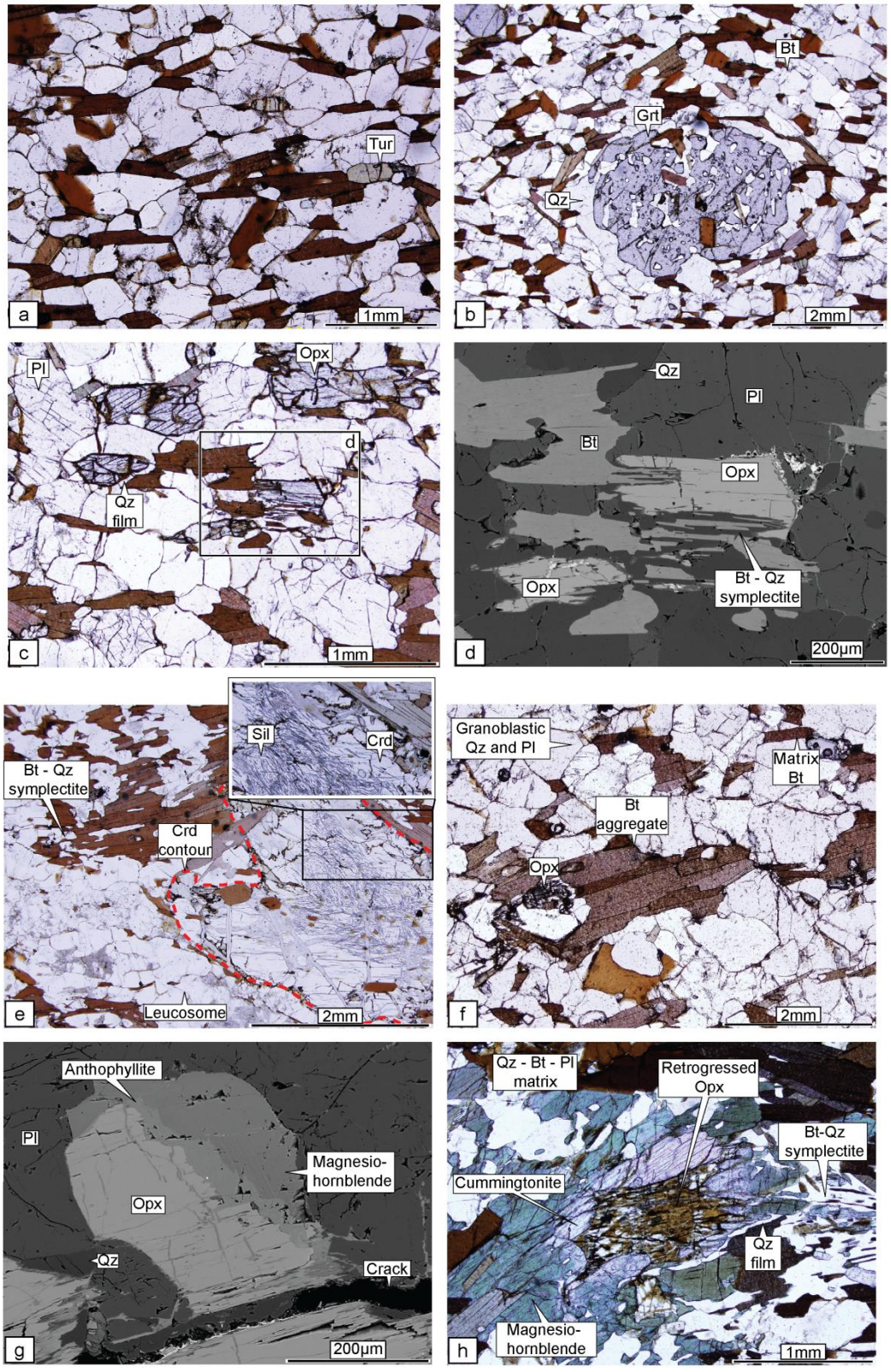
a
Tur
1mm
b
Bt
Grt
Qz
2mm
c
Pl
Opx
d
Qz
film
1mm
d
Qz
Pl
Bt
Opx
Opx
Bt - Qz
symplectite
200µm
e
Sil
Crd
Bt - Qz
symplectite
Crd
contour
Leucosome
2mm
f
Granoblastic
Qz and Pl
Matrix
Bt
Bt
aggregate
Opx
2mm
g
Anthophyllite
Pl
Magnesio-
hornblende
Opx
Qz
Crack
200µm
h
Qz - Bt - Pl
matrix
Retrogressed
Opx
Bt-Qz
symplectite
Cummingtonite
Qz
film
Magnesio-
hornblende
1mm

Figure 3.9: (a) Typical non-melted metagreywacke paleosome with a granoblastic-polygonal microstructure composed of plagioclase, quartz, biotite and minor tourmaline. The alignment of biotite defines the S_2 foliation. (b) Garnet-bearing metagreywacke in which porphyroblasts of garnet have inclusions of biotite and elongated quartz that define an internal fabric oriented at a high angle to the external S_2 fabric. Garnet is not replaced by biotite. (c) Xenoblastic to subidioblastic orthopyroxene in a metagreywacke. Thin films of quartz surround some orthopyroxene crystals and indicate the former presence of melt along grain boundaries. (d) Back scattered electron (BSE) image from (c) showing biotite + quartz symplectite replacing a subidioblastic crystal of orthopyroxene. This microstructure is interpreted as a reaction between the interstitial melt and orthopyroxene. Note the rounded outline on the right edge of the large orthopyroxene in the center. (e) Cordierite + garnet-bearing metapelitic migmatite. Poikiloblast of peritectic cordierite with abundant inclusions of biotite, quartz and sillimanite. Note the biotite-free leucosome next to the cordierite. (f) High-grade replacement of orthopyroxene by an aggregate of biotite crystals larger than those in the matrix. (g) BSE image of orthopyroxene partially replaced by anthophyllite and magnesio-hornblende. (h) High-grade replacement of orthopyroxene by cummingtonite and magnesio-hornblende. Note that elsewhere orthopyroxene is partially replaced by a biotite + quartz symplectite.

		wt.%										a.p.f.u.																		
		SiO_2	TiO_2	Al_2O_3	FeO	MnO	MgO	CaO	Na_2O	K_2O	Total	Si	Ti	Al	Fe(ii)	Mg	Mn	Ca	Na	K	X_{Mg}	Al^{IV}	Al^{VI}					T° (Ti-in-Bt)	Grt-Bt T° GBPQ P°
Non-melted metagreywacke																								*An*	*Ab*	*Or*				
Pl	Matrix	57.95	0.01	26.31	0.05	0.00	0.02	7.96	7.18	0.05	99.55	2.60		1.45	0.00			0.40	0.65	0.00				*37.90*	*61.83*	*0.27*				
Bt		37.06	2.73	17.63	17.28	0.07	12.47	0.01	0.10	7.90	95.58	5.52	0.31	3.10	2.15	2.77	0.01	0.00	0.03	1.50	0.56	2.48	0.62					684		
Amp		47.14	0.88	7.43	14.67	0.22	13.22	11.84	0.83	0.60	97.11	6.72	0.09	1.25	1.75	2.81	0.03	1.81	0.23	0.11	0.62	1.22	0.00	*Gross*	*Pyr*	*Alm*	*Sper*			
Grt		37.27	0.01	21.51	33.01	2.97	4.03	1.78	0.01		100.65	5.94	0.00	3.03	2.20	0.48	0.20	0.15	0.00		0.18	0.06	2.96	*0.05*	*0.16*	*0.73*	*0.07*			
Tl		35.73	1.21	32.23	5.42	0.03	7.74	1.66	1.64	0.03	100.00	5.84	0.15	6.21	0.74	1.89	0.00	0.29	0.52	0.01										
Grt	Porphyroblast	37.72	0.00	21.08	32.35	2.51	4.80	1.60	0.01		100.61	6.01	0.00	2.97	2.15	0.57	0.17	0.14	0.00		0.21	0.00	2.97	*0.04*	*0.19*	*0.71*	*0.06*			
Bt	Inclusion in Grt	38.17	2.12	18.16	15.06	0.02	14.36	0.04	0.23	7.63	96.18	5.57	0.23	3.12	1.84	3.12	0.00	0.01	0.07	1.42	0.63	2.43	0.69					659		T° 623 P° 6803
Melted metagreywacke																								*Wo*	*En*	*Fs*	*Ac*			
Opx	Matrix	51.21	0.12	0.56	30.14	1.38	15.82	0.42	0.00	0.00	99.71	2.00	0.00	0.03	0.98	0.92	0.05	0.02	0.00	0.00	0.48	0.00	0.02	*0.01*	*0.47*	*0.52*	*0.00*			
Bt		35.76	3.55	15.38	18.91	0.11	12.16	0.00	0.07	9.86	96.22	5.45	0.41	2.76	2.41	2.76	0.01	0.00	0.02	1.92	0.53	2.55	0.21	*An*	*Ab*	*Or*		718		
Pl		59.57	0.01	25.28	0.07	0.03	0.00	6.65	7.94	0.32	100.07	2.66		1.39	0.00			0.33	0.72	0.02				*31.08*	*67.13*	*1.79*				
Kfs		61.65	0.00	18.92	0.05	0.00	0.02	0.04	0.33	16.19	98.57	2.94		1.04	0.00			0.00	0.03	0.96				*0.22*	*3.03*	*96.75*				
																								Gross	*Pyr*	*Alm*	*Sper*			
Grt	Matrix	35.83	0	21.58	31.36	2.868	4.538	2.776	0.027		99.045	5.80	0.00	3.09	2.12	0.55	0.20	0.24	0.00		0.04	0.20	2.89	*0.08*	*0.18*	*0.68*	*0.06*			
Bt		35.59	3.828	15.75	18.85	0.102	11.5	0.003	0.111	9.566	99.567	5.44	0.44	2.84	2.41	2.62	0.01	0.00	0.03	1.86	0.52	2.56	0.27					727		T° 676
High-grade assemblages retrogression in metagreywacke																								*Wo*	*En*	*Fs*	*Ac*			
Opx	Porphyroblast	51.50	0.03	0.39	30.96	0.72	15.99	0.67	0.02	0.00	100.30	2.00	0.00	0.02	1.00	0.92	0.02	0.03	0.00	0.00	0.48	0.00	0.01	*0.01*	*0.47*	*0.52*	*0.00*			
Bt		35.40	3.47	14.51	21.94	0.09	11.45	0.02	0.03	8.87	96.39	5.45	0.40	2.63	2.83	2.63	0.01	0.00	0.01	1.74	0.48	2.55	0.08					707		
Amp1	Opx	47.57	0.62	6.65	15.48	0.22	13.23	11.70	0.69	0.44	96.83	6.79	0.07	1.12	1.85	2.82	0.03	1.79	0.19	0.08	0.60	1.09	0.00							
Amp2	Retrogression	51.66	0.00	0.28	25.36	0.58	17.02	0.61	0.02	0.00	95.60	7.51	0.00	0.05	3.08	3.69	0.07	0.10	0.01	0.00	0.54	0.05	0.00							
Cl	Matrix	29.62	0.00	16.35	24.30	0.21	18.14	0.03	0.01	0.13	88.83	6.09	0.00	3.97	4.11	5.56	0.04	0.01	0.00	0.07	0.58	1.91	2.07							
Bt		36.62	3.91	14.78	19.59	0.08	11.13	0.01	0.06	9.49	96.16	5.58	0.45	2.65	2.50	2.53	0.01	0.00	0.02	1.84	0.50	2.42	0.23	*An*	*Ab*	*Or*				
Pl		58.78	0.02	26.03	0.04	0.00	0.00	7.58	7.42	0.18	100.18	2.63		1.43	0.00			0.38	0.67	0.01				*35.71*	*63.27*	*1.02*				
Metapelite																														
Tl	Matrix	34.85	1.15	31.08	6.00	0.00	7.66	1.38	1.79	0.02	100.00	5.83	0.15	6.13	0.84	1.91	0.00	0.25	0.58	0.00	0.69									
Bt		36.55	4.28	18.02	15.13	0.00	12.33	0.03	0.11	9.71	96.88	5.41	0.48	3.14	1.87	2.72	0.00	0.00	0.03	1.83	0.59	2.59	0.55	*An*	*Ab*	*Or*		752		T° 629 P° 6829
Pl		60.64	0.00	25.29	0.03	0.00	0.01	6.36	8.08	0.27	100.73	2.68		1.39	0.00			0.32	0.73	0.02		0.00		*29.85*	*68.64*	*1.52*				
Grt	Core	38.09	0.00	22.04	30.77	0.69	8.08	1.19	0.02		100.88	5.90	0.00	3.02	1.99	0.93	0.05	0.10	0.00		0.07	0.10	2.93	*0.03*	*0.30*	*0.65*	*0.01*			
Crd	Matrix, pinnitised	48.37	0.00	33.23	6.43	0.12	8.77	0.01	0.65	0.00	97.58	4.98	0.00	4.04	0.55	1.35	0.01	0.00	0.13	0.00	0.71	3.02	1.02							
Crd	Porphyroblast	47.72	0.00	32.83	6.11	0.15	8.58	0.00	1.14	0.00	96.54	4.98	0.00	4.03	0.53	1.33	0.01	0.00	0.23	0.00	0.71	3.02	1.01	*Gross*	*Pyr*	*Alm*	*Sper*			
Grt	Rim	36.60	0.03	21.84	33.48	0.84	6.00	1.13	0.02		99.98	5.83	0.00	3.07	2.23	0.71	0.06	0.10	0.00		0.05	0.17	2.90	*0.03*	*0.23*	*0.72*	*0.02*			
Bt	Inclusion in Grt	37.48	3.28	17.89	11.56	0.02	15.80	0.03	0.32	8.97	96.25	5.47	0.36	3.08	1.41	3.44	0.00	0.00	0.09	1.67	0.71	2.53	0.54					*749*		
Mv	Crd retrogression	50.30	0.11	35.91	1.07	0.00	1.05	0.01	0.32	7.32	96.13	6.45	0.01	5.42	0.11	0.20	0.00	0.00	0.08	1.20	0.64	1.55	3.87							

Table 3.2: Selected EPMA analysis of representative samples. Beam conditions are 15kV acceleration voltage and 20nA sample current on Cameca SX100 at Université Laval. Counting times are 20 seconds on peak and 10 on background. Atoms per formula unit (a.p.f.u.) calculated with 8 oxygen for feldspar, 18 for cordierite, 22 for biotite and muscovite, 23 for amphiboles, 24 for garnet, 24.5 for tourmaline, 28 for chlorite. Ti-in-biotite thermometer after Henry et al. (2005). Garnet-biotite thermometer and GBPQ barometer follow calibration from Wu and Cheng (2006).

3.7.2 MIGMATITES

The rocks which contain macroscopic *in situ* neosomes contain mineral assemblages and microstructures indicative of partial melting. Metagreywacke bulk compositions have the mineral assemblage biotite + quartz + plagioclase + orthopyroxene + Fe oxides (ilmenite or magnetite) ± garnet ± K-feldspar (Fig. 3.9c). Plagioclase (Table 3.2) in the migmatites is slightly more calcic (median An_{32}) than in the paleosome metagreywackes. The composition of plagioclase within individual samples varies <3%An. Small (<1mm), typically subidioblastic crystals of orthopyroxene occur throughout the matrix (Fig. 3.9c, d), but larger grains occur near *in situ* neosome. Although variable between thin sections, orthopyroxene has a homogeneous composition in a given thin section with X_{Mg} between 0.46 and 0.51 (Table 3.2). Garnet is generally present in samples with orthopyroxene, but occurs alone in metagreywackes with slightly more aluminous bulk compositions.

K-feldspar occurs in both leucosome and residuum. Rare, irregularly-shaped, cuspate grains of K-feldspar in the residual rocks are interpreted to pseudomorph pores formerly filled with anatectic melt (Holness, 2008; Sawyer, 1999, 2001). Many rocks contain a symplectic intergrowth of biotite + quartz (Fig. 3.9d) that replaces orthopyroxene, or occurs between orthopyroxene and K-feldspar. This symplectite texture is only observed around orthopyroxene and is interpreted to be the result of a reaction between peritectic (residual) orthopyroxene and the last-remaining anatectic melt in the rock (e.g. Waters, 2001 and Fig. F78 in Sawyer, 2008a), and thus as a late-stage anatectic phenomenon. The mineral

assemblage and microstructure in these metagreywackes is consistent with the melting reaction

biotite + plagioclase + quartz = orthopyroxene + melt + Fe-oxide ± K-feldspar ± garnet (R1).

The common mineral assemblage in metapelitic rocks is quartz + biotite + plagioclase + garnet + cordierite ± K-feldspar (Fig. 3.9e). The composition of plagioclase ranges between An_{24} and An_{34} (Table 3.2); variation within a sample is <2% An. K-feldspar is rare in the matrix, it occurs mostly in leucosome. Porphyroblasts of garnet and cordierite are up to several centimeters across and are commonly poikilitic. Biotite and quartz are common inclusions; sillimanite occurs rarely in cordierite (Fig. 3.9e). Inclusions of sillimanite, biotite and quartz are not in mutual contact. Thus, garnet and cordierite are peritectic phases, and the general melt-producing reaction in the metapelites is of the form:

quartz + biotite + plagioclase + sillimanite = melt + garnet/cordierite ± K-feldspar (R2)

Matrix biotite, whether in metapelite or metagreywacke, has a uniform X_{Mg} (median value 0.54) within samples. Biotite inclusions in garnet are more magnesian (X_{Mg}~0.60), and have lower Ti contents than the matrix biotite. The median Ti content of biotite in the metagreywackes (0.31 Ti a.p.f.u.) is notably higher than in the biotite from metapelites (0.24 Ti a.p.f.u.).

3.7.3 REHYDRATION OF HIGH TEMPERATURE MINERAL ASSEMBLAGES

Relatively few orthopyroxene-bearing rocks contain fresh orthopyroxene. Besides the biotite + quartz symplectite, orthopyroxene in the Opinaca subprovince is also widely replaced by a decussate aggregate of a few large grains of biotite (Fig. 3.9f), or by anthophyllite + magnesio-hornblende or cummingtonite + magnesio-hornblende (Fig. 3.9g, h). A few rocks (Fig. 3.7h) contain both types of replacement; the decussate aggregates overprint the symplectite.

Orthopyroxene that is partially replaced by amphibole and biotite, is more magnesian (X_{Mg}>0.60) than fresh orthopyroxene (X_{Mg}~0.48). The replacive biotite is generally slightly poorer in Ti, but richer in Fe (~0.05 Ti a.p.f.u. and 0.5 Fe a.p.f.u.) than biotite in the matrix (Table 3.2). Garnet is rarely replaced by biotite. Cordierite in some metapelitic rocks is partially replaced by biotite + muscovite, or is pseudomorphed by pinnite.

Orthopyroxene in extensively replaced by amphibole or biotite in many parts of the Opinaca Subprovince (Bandyayera et al., 2011; Bandyayera et al., 2010; Simard and Gosselin, 1999) and these areas coincide with where dykes and sills of leucogranite and pegmatite are especially abundant. Particularly extensive replacement occurs in the area mapped by Simard and Gosselin (1999) where little macroscopic orthopyroxene remains, and rocks can be mistaken in the field for amphibolite-facies metasedimentary units. The former existence of a granulite facies mineral assemblage throughout that area is revealed only in thin section by rare, relics of orthopyroxene within the patches of amphibole or

biotite. This spatial association suggests the hydration of orthopyroxene to amphibole, or biotite, involved the aqueous fluid released during to the crystallization of leucogranite magma intruded into the migmatites (see discussion).

3.7.4 TEMPERATURE AND PRESSURE DURING ANATEXIS

Although widely distributed, the modal amount of orthopyroxene in the least retrogressed rocks is low (few %) and abundant prograde (foliation-defining) biotite remains. Thus, metamorphic conditions did not reach "biotite-out" in the Opinaca Subprovince. Experimental investigations of metagreywacke bulk compositions show that orthopyroxene appears through a partial melting reaction between biotite, plagioclase and quartz at about 810^{o}C (orthopyroxene-in) for pressures >3kbar. Biotite disappears (biotite-out) from these bulk compositions over the temperature interval of 850 to 920^{o}C (e.g. Stevens et al., 1997; Vielzeuf and Montel, 1994).

Temperatures calculated with the Ti-in-biotite thermometer of Henry et al. (2005) on matrix biotite from an orthopyroxene-bearing metagreywacke and a garnet + cordierite-bearing metapelite from localities 50km apart yield maximum temperatures of 718°C and 752°C, respectively (Table 3.2). Application of the Wu and Cheng (2006) formulation for the Fe-Mg exchange thermometer between garnet and biotite in an orthopyroxene-bearing metagreywacke yields a maximum temperature of 676°C at 7kbar (Table 3.2). As expected (Frost and Chacko, 1989; Pattison et al., 2003), both geothermometers yield temperatures

well below that for the appearance of orthopyroxene determined from melting experiments since cooling from peak temperature was slow.

Metamorphic temperature may also be estimated by comparing the mineral assemblages observed in natural rocks with the calculated phase equilibria for the particular bulk composition. Greenschist facies metagreywacke rocks in the Quetico Subprovince have been shown to be reasonable proxies of the major element composition of the protolith to granulite-facies metagreywackes in the Ashuanipi (Guernina and Sawyer, 2003), and by extension for the Opinaca Subprovince. Johnson et al. (2008) modeled mineral assemblages in the NCKFMASHTO (NaO-CaO-K_2O-Fe_2O-MgO-Al_2O_3-SiO_2-H_2O-TiO_2-O) system produced by partial melting in the three representative metagreywacke rocks (samples S1/ES356, S2/ES36 and S3/ES355) from the Quetico Subprovince. Their modeling predicts that orthopyroxene could appear in these rocks at temperatures close to 750°C, whereas biotite disappears between 850 and 870°C (Johnson et al., 2008). Furthermore, the modeling shows that these bulk compositions do not contain cordierite at pressures above about 6kbars and since the metagreywackes do not contains cordierite metamorphic pressures in the Opinaca were likely >6kbar.

Considering the widespread occurrence of orthopyroxene, the maximum observed mode of orthopyroxene of 10% and the presence of biotite, metamorphic temperatures across the mapped part of the Opinaca Subprovince are estimated to have been approximately 820°C.

The estimated metamorphic pressure from the Garnet – Biotite – Plagioclase – Quartz barometer using the method in Wu and Cheng (2006) lies between 6 and 7kbar at 820°C (e.g. Table 3.2), consistent with the absence of cordierite in the metagreywacke bulk compositions.

3.8 DISCUSSION

The core question to address is whether the leucocratic material in the outcrops represents redistributed local anatectic melt, or was intruded from a deeper crustal source. The amount of anatectic melt that Opinaca rocks have produced *in situ* is evaluated first and then compared to the observed proportion of felsic veins, dykes and sills.

3.8.1 TIMING OF GRANULITE FACIES METAMORPHISM AND INJECTION OF LEUCOGRANITE

Crystallization ages obtained in the leucogranite sample are, within error, the same as those obtained from the two metapelitic migmatite samples and confirm ages obtained in the Opinaca Subprovince by David et al. (2010). We conclude that the high grade metamorphic event was contemporaneous with injection of the bulk of the leucogranitic veins and dykes.

Growth of zircon in metapelite and metagreywacke is interpreted to have occurred when cooling began at about 2665 Ma; whereas the last crystallization of zircon in the leucogranites occurred with the latest injections, when the temperature was very close to the granite solidus at ca. 2637 Ma. Thus, cooling from the peak of high grade metamorphism in the Opinaca Subprovince lasted some 30 Ma, consistent with results from other metasedimentary belts in the Superior Province. Assuming a peak metamorphic temperature of 820^{o}C and 650^{o}C for the granite solidus, the average cooling rate is about 6^{o}C My^{-1} for the late Archean granulite facies metamorphism in the Opinaca Subprovince.

3.8.2 PERCENTAGE OF MELT PRODUCED BY LOCAL ANATEXIS

The Opinaca metasedimentary rocks reached granulite facies. The initial composition of the sediments (protolith) is thus unknown since it could have been changed due to loss of some melt. Similarities between the metasedimentary rocks of the Quetico, Nemiscau, Opinaca and Ashuanipi Subprovinces have been previously noted, and the composition of greenschist facies metagreywackes from the Quetico Subprovince were used as a proxy for the protolith for the granulite facies migmatites in the Ashuanipi Subprovince and adequately reproduced the petrographic and geochemical features of anatexis in that subprovince (Guernina and Sawyer, 2003; Johnson et al., 2008). The same similarities apply between metagreywacke rocks from the Quetico and Opinaca Subprovinces. For these reasons, samples S1/ES356, S2/ES36 and S3/ES355 (Johnson et al., 2008; Sawyer,

1986) are considered to represent plausible protolith compositions for the metagreywackes the Opinaca Subprovince. At the disappearance of biotite (~860^{o}C), Figure 5 of Johnson et al. (2008) indicates that about 25 mol% melt would have been produced from the metagreywackes. At 820^{o}C, a temperature mid-way between the appearance of orthopyroxene and the disappearance of biotite, samples S1/ES356, S2/ES36 would have produced 10 mol% melt, an amount consistent with the small proportion of *in situ* leucosome present and low modal proportion of orthopyroxene in the metagreywackes. Sample S3/ES355 would also have produced about 10 mol% melt, but without orthopyroxene. Thus, some or all of the orthopyroxene-absent metagreywackes may have produced a little anatectic melt and consequently would not be paleosome. However, these rocks contain no microstructures indicative of melting. If the maximum temperature was only 800^{o}C, then the volume of melt produced from the metagreywacke will have been less (~7%). To summarize, the maximum amount of melt produced from metagreywackes in the Opinaca Subprovince was ~10%.

Metapelitic bulk compositions would produce significantly more melt (~30 mol%) at 820^{o}C than metagreywacke (Nabelek and Bartlett, 2000). However, their contribution to the overall volume of anatectic melt is small because metagreywackes are 10 times more voluminous in the Opinaca Subprovince. Similarly, the contribution of anatectic melt (of tonalite composition) from metamafic rocks is neglected because they represent <5% of the study area and would not produce much melt by hydrate breakdown reactions. Partial melting owing to an influx of H_2O via a reaction such as

quartz + plagioclase + K-feldspar + H_2O = melt

can produce a large volume of melt at low temperatures (~700^oC) from granitic protoliths (Sawyer 2010). Archean metagreywackes from the Superior Province are K_2O- and Al_2O_3 deficient (Sawyer, 1987) and would have contained little or no K-feldspar, and therefore are not able to generate granitic melt by low-temperature H_2O-fluxed partial melting by a reaction such as that above. In addition, there is no microstructural evidence of H_2O-fluxed melting in thin section. For these reasons, anatexis is not considered to have occurred by H_2O-fluxed partial melting in the Opinaca Subprovince. Thus, *in situ* partial melting at 820^oC of the metasedimentary rocks in the Opinaca Subprovince may have produced as much as 12% melt, but more likely <10%.

3.8.3 ACCUMULATION OF FELSIC MELT IN THE OPINACA SUBPROVINCE

The percentage of felsic veins, dykes, sills and leucosomes was estimated in the field at 1070 outcrops in the 1500km^2 mapped area (Fig. 3.3). Outcrops were typically 500m to 2000m apart. The estimate of the amount felsic material in each outcrop is believed to be accurate to ±5%. Results (Fig. 3.10) indicate that only 7% of the area contains less than 10% of felsic material, whereas over 60% of the study area consists of outcrops with >50% felsic material. The "typical" outcrop in the study area contains 63% felsic material. Similar results are obtained for the adjacent 15500km^2 (Fig. 3.2) based on the percentage of the

felsic material estimated in each outcrop from previous mapping (Simard and Gosselin, 1999; Bandyayera et al., 2010; Bandyayera et al., 2011).

Thus, the "typical" outcrop in the Opinaca Subprovince contains five times as much felsic material in the form of leucogranitic veins and dykes than could have come from hydrate-breakdown partial melting of the host metagreywacke and metapelitic rocks. Hence, the present surface through the Opinaca Subprovince exposes a level in the continental crust where a considerable volume of felsic magma has collected. The Opinaca Subprovince constitutes a large-scale injection complex in the sense of Leitch and Weinberg (2002) that formed in granulite facies migmatites (Fig. 3.11). An implication of this finding is that a significant proportion of the anatectic melt produced in deep crustal granulite-facies anatexis does not necessarily rise through the continental crust to form plutons at, or near, the brittle-ductile transition (e.g. Cruden, 2006). A large proportion of the anatectic melt may remain in the deeper parts of the crust, possibly as an injection complex.

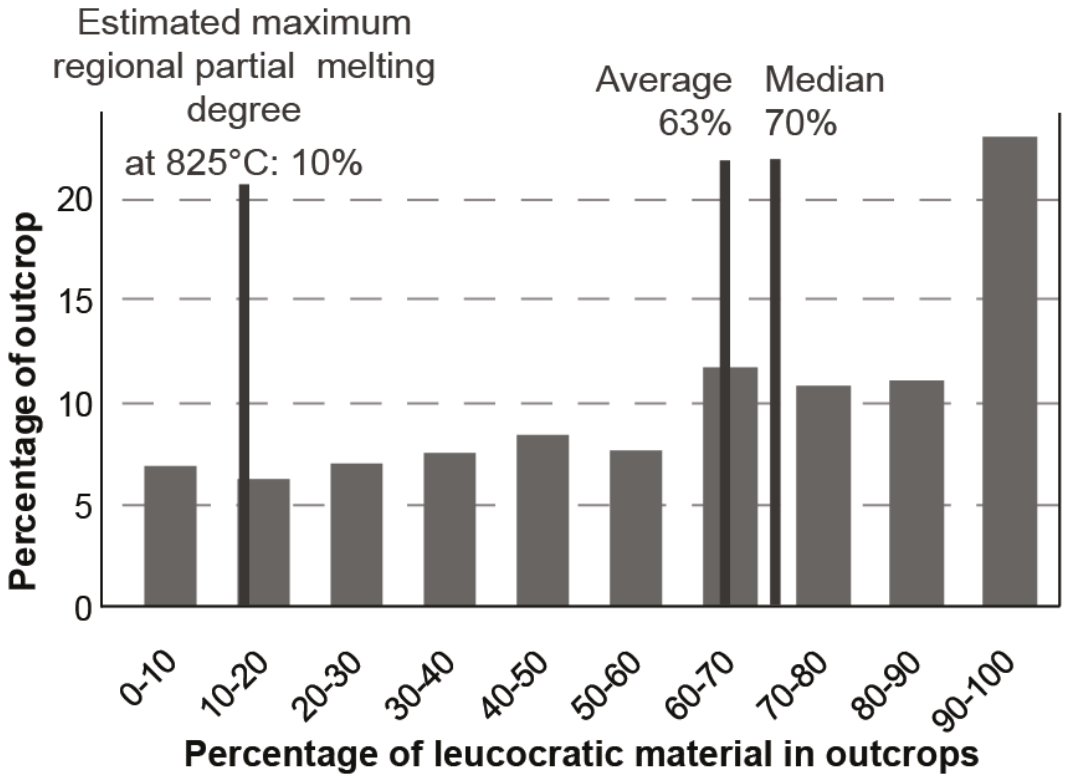

Figure 3.10: Histogram of the percentage of outcrops versus the percentage of leucocratic veins, dykes and sills present in them for 1070 outcrops in the study area. The mean proportion of leucocratic material per outcrop is more than 5 times the estimated amount of melt that could be produced from the metasedimentary rocks in the Opinaca Subprovince.

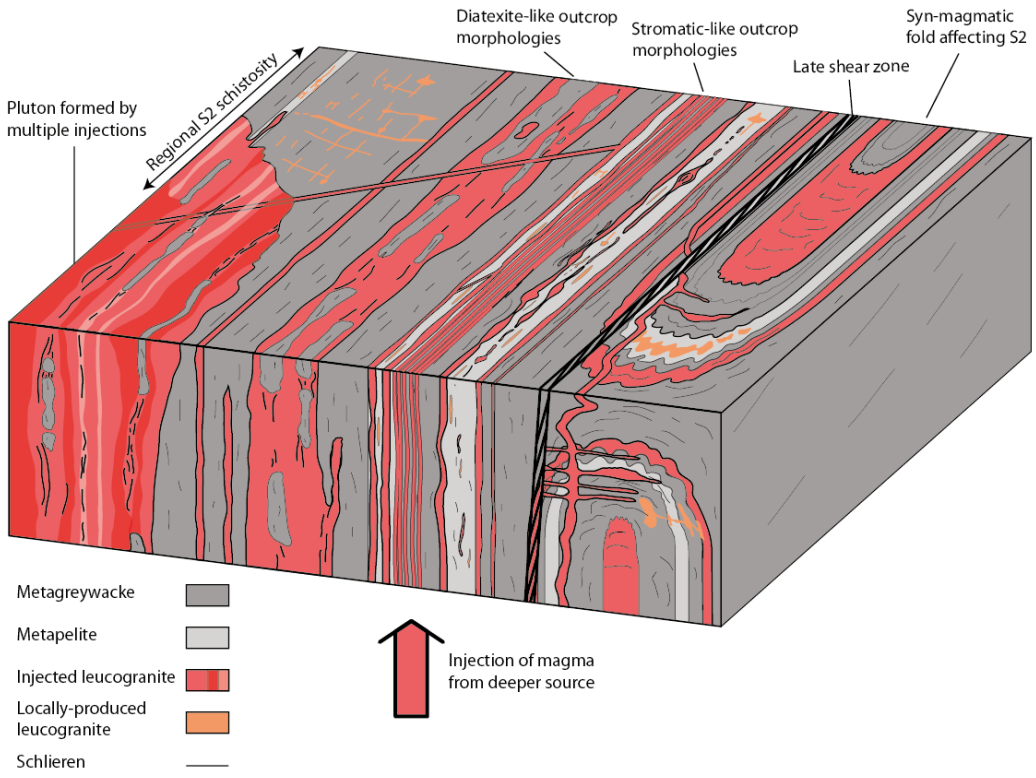

Figure 3.11: Schematic block diagram showing the injection complex at the crustal level presently exposed in the Opinaca Subprovince. The metasedimentary host rocks are granulite facies and partially melted and produced a local network of in situ leucosomes, but accounts for no more than 10% of the total leucogranite present. Most leucogranitic material present was intruded from deeper crustal source, possibly similar to the Ashuanipi Subprovince.

3.8.4 POTENTIAL SOURCE OF THE FELSIC MAGMA

Granitic magma migrates because of pressure gradients and has an overall upward movement because of its buoyancy, thus the source of the excess felsic magma lies below the present exposure level in the Opinaca. The Ashuanipi Subprovince located to the east (Fig. 3.1) may resemble a potential source region. Metagreywacke rocks there contain more orthopyroxene and record higher temperatures than in the Opinaca and, consequently, underwent a significantly higher degree (average ~31%) of partial melting (Guernina and Sawyer, 2003). The bulk composition and microstructure of the metagreywacke rocks in the Ashuanipi Subprovince indicate that they lost most of the anatectic melt that was generated in them (Guernina and Sawyer, 2003); some of this extracted melt may have moved to higher crustal levels. Assuming that rocks similar to those in the Ashuanipi exist below the Opinaca Subprovince, then a large volume of anatectic magma would be readily available to be emplaced into it.

3.8.5 WHY AN INJECTION COMPLEX?

Numerical modeling (Hobbs and Ord, 2010; Leitch and Weinberg, 2002) demonstrates that the buoyant rise of anatectic melt by pervasive flow could be arrested close to the depth of the solidus. This is because the low volume to surface ratio in small conduits means that the melt looses heat rapidly to the wall rocks and solidifies before it can move far. The frozen remnants of the pervasive flow network are the multitude of small veins that comprise an

injection complex. If anatectic melt is to rise higher in the crust, then the flow of melt must be concentrated into much larger dykes such that the magma can rise faster than it solidifies (Petford et al., 1994). The ascent of anatectic melt described by Weinberg and Regenauer-Lieb (2010) requires a transition from ductile fractures in the high grade source to a brittle-elastic behavior in the colder crust. In the approximately 30Ma duration of the injection process, both mechanisms are possible depending on the timing; ductile fracture are likely at the peak metamorphic conditions and brittle-elastic fracturing at the end when the crust had cooled substantially.

3.8.6 WHY THIN VEINS AND DYKES?

The expulsion of melt from the deep crust that is undergoing anatexis is a consequence of compaction (loss of volume) there. The crust immediately above this region dilates to accommodate the flux of magma from below (Connolly and Podladchikov, 2007; Hobbs and Ord, 2010) driven by melt pressure from below.

Rosenberg and Handy (2005) showed that the presence of just a few percent melt can considerably weaken rocks. Dilation (decompaction) of rocks containing a few percent of melt drives flow of the melt through the pores from the regions with the lowest fraction of melt to create a narrow zone, or channel, where the fraction of melt is somewhat higher (Connolly and Podladchikov, 1998). These channels then provide a pathway along which melt from a deeper source is focused as it rises through the crust (Connolly and

Podladchikov, 2007; Bouilhol et al, 2011), the Opinaca injection complex could be a natural example of this mechanism at work. Field and petrological evidence indicates that the metapelitic layers, and some metagreyacke layers, partially melted. Thus, each partially melted layer in the Opinaca Subprovince is a potential plane along which melt can be more easily injected, consistent with the field evidence (Figs. 3.5 and 3.6b).

On a macroscopic scale, the movement of melt can be described as pervasive and involved a very large volume of melt. The schlieren and screens of country rock in dykes of leucogranite (Fig. 3.5d) and the 30% of outcrops that comprise >80% narrow felsic veins both indicate the multiple injection of melt in very close proximity. Thus, there was some degree of focusing of melt movement into favorable pathways. However, channeling of the melt into wide (larger than several meters) dykes capable of transporting melt to the upper crust did not occur. This indicates that injection along a multitude of thin dykes parallel to the pre-existing bedding and/or main foliation was energetically favorable. Given that the net volume of melt emplaced into the Opinaca was large, and its cooling history very long (>30 Ma), then this suggests that the instantaneous flux of magma entering Opinaca was very low. Effectively, each small batch of melt that arrived either created a new dyke or reactivated a previously used dyke (Fig. 3.6a; Hassalová et al., 2011) depending on whether or not the previous ones had, largely or completely, solidified

3.8.7 SOME CONSEQUENCES OF AN INJECTION COMPLEX IN THE DEEP MIDDLE CRUST

Partial melting deep in the continental crust and migration of that melt to the upper crust is widely viewed as the principal mechanism by which the continental crust became differentiated (e.g. Fyfe, 1973; Rudnick and Gao, 2003). Overall, such a process leaves the deep, granulite facies region of the continental crust with a bulk composition depleted in those elements that partition into the melt. However, this study shows that some levels within granulite facies regions actually accumulated large volumes of melt and so cannot have melt-depleted bulk compositions. This section examines two consequences of the retention of melt at depth in the crust on its subsequent development, specifically: 1) the effect on long term heat production, and 2) the role of the H_2O released as the felsic melt crystallized.

3.8.7.1 TRANSFER OF HEAT PRODUCING ELEMENTS INTO THE INJECTION COMPLEX

The main heat producing elements (HPE) in the continental crust are Th, U and K. These elements strongly partition into felsic melts during anatexis. Once the lower crust starts to melt, there is a general upward transfer of the melt and thus of the HPE. The HPE are thus redistributed in the crust depending on the depth of emplacement of the melt. In the case of an injection complex, accumulation of melt occurs deeper in the crust compared to a

scenario where melt is transported via large crustal dykes to the upper crust. In this section we investigate with simple models, the effect of the accumulation of HPE in the lower middle crust rather than in the upper crust. The typical felsic vein rock contains 2ppm U, 15ppm Th and 4.04wt% K (Table 3.3), whereas the typical metasedimentary host rock contains half as much; 1.3ppm U, 6.9ppm Th and 2.05wt% K. Radiogenic heat production (A) for the granitic and metasedimentary rocks are 4.92 and 2.12μWm^{-3} respectively, using the isotopic ratios for 2500Ma (Fowler, 1990) and a density of 2700 $kg.m^{-3}$.

	Granite, pegmatite and aplite				Metasediment			
	Median	Average	Std. dev.	n	Median	Average	Std. dev.	n
U (ppm)	2.0	4.2	5.3	35	1.3	1.8	1.9	31
Th (ppm)	15.4	23.9	25.0	35	6.9	7.3	3.4	31
K (%)	4.0	3.8	1.7	35	2.0	2.5	1.1	31
Modern A ($\mu W\ m^{-3}$)	3.37				1.02			
Archean A ($\mu W\ m^{-3}$)	4.92				2.12			

Table 3.3: Content of heat-producing elements in rocks from the Opinaca Subprovince. Modern heat production (A) corrected to Archean isotopic ratios (Emsley, 1989). The density of the rocks is assumed to be 2700kg.m^{-3}. Compilation is based on whole rock geochemical data archived in the Québec Geoscientific database Sigeom (sigeom.mrnf.gouv.qc.ca/).

Considering that at the present exposure level the Opinaca Subprovince is composed of ~60% leucogranite and ~40% metasedimentary country rock, the weighted heat production is 3.85μWm^{-3} in the injection complex. Temperature-depth profiles for conductive heat transfer were calculated for a 40km thick model crust without an injection complex (Model 1) where melt is ponded in the upper 15km of the crust and with an injection complex (Model 2) where melt is ponded between 20 and 25km depth (Fig. 3.12). A three layer model was used for the injection complex derived from equations in Fowler (1990); see figure 3.12 for model parameters. Results indicates that the presence of HPE-rich melt ponded in the middle crust rather than in plutons in the upper crust keeps the lower half of the crust warmer. The accumulation of leucogranites provides a long term heat source at depth which can result in slower cooling rates; explaining the broad range of zircon crystallization ages in the metagreywacke and leucogranite. The distribution and migration of HPE has an important impact on the rheology of the crust. A warmer lower crust is weaker and will delay cratonisation which is in part controlled by the transfer of HPE out of the lower crust (Sandiford and McLaren, 2002; Sandiford et al., 2002).

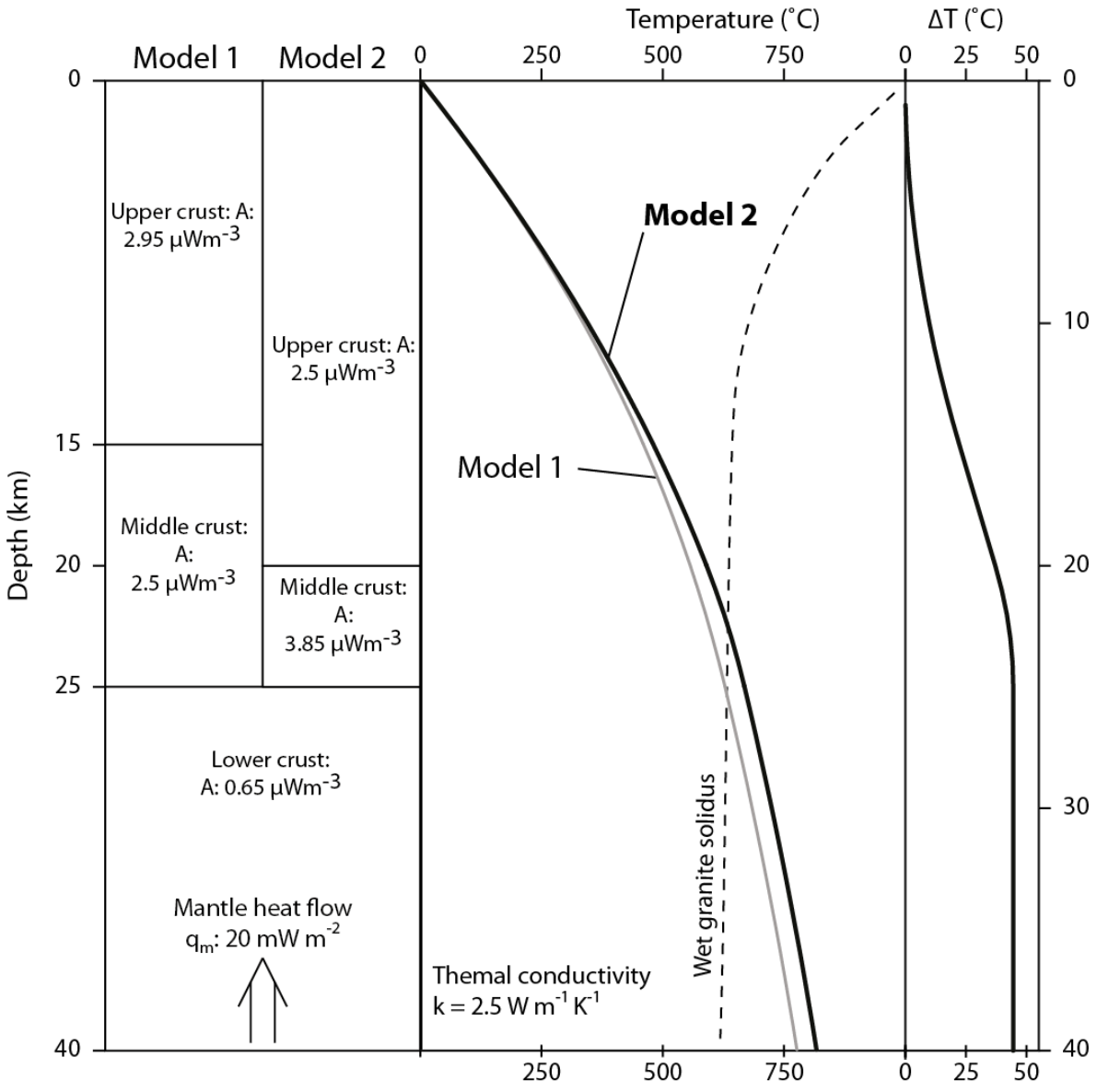

Figure 3.12: Comparison of two temperature-depth profiles for conductive heat transfer for a model crust without (Model 1) and with (Model 2) a 5km thick layer representing the presence of an injection complex in lower middle crust. Thermal conductivity and mantle heat flow from Rudnick et al. (1998). Heat-producing elements in the injection complex raise the temperature of the deep crust by ~40°C.

3.8.7.2 LATENT HEAT OF CRYSTALLIZATION

An additional source of heat is provided by the crystallization of the melt in the injection complex. Melting is an endothermic process that consumes heat (Stüwe, 1995), but upon crystallization latent heat (~300kJkg^{-1}) is released. The latent heat released buffers the temperature during cooling (Zhang et al., 2008) and with the large volume of magma retained in the injection complex deep in the crust (e.g. Fig. 5 in Leitch and Weinberg, 2002), higher temperature were maintained in the Opinaca than would have been the case had all the anatectic melt been transported to the upper crust.

3.8.7.3 ADDITION OF H_2O

The H_2O content of melt derived from a metagreywacke by biotite dehydration melting is typically 3 to 4% (Holtz et al., 2001; Montel and Vielzeuf, 1997). Some of this H_2O becomes bound in hydrous minerals that crystallize from the melt, but the excess is exsolved from the melt. The larger the volume of magma, the larger the volume of fluid released. This exsolved fluid, and any components dissolved in it, can interact with the host rocks.

The widespread replacement of orthopyroxene by biotite, or amphibole, throughout the Opinaca Subprovince, provides evidence that an aqueous fluid interacted pervasively with the granulites. Moreover, the degree of replacement is greatest where the proportion of

felsic veins is greatest. The accumulation of anatectic magma in the deep crust has the potential to cause extensive rehydration of high grade, residual mineral assemblages there, and this may have implications for the subsequent evolution of the crust. For example, Clark et al. (2011) argue that ultra-high temperature (UHT, >900°C) metamorphism is more likely to be attained if the lower continental crust has already experienced partial melting. This is because partial melting produces residual mineral assemblages that are not very fertile, thus in a subsequent melting event temperature could rise higher because the buffering of the temperature due to a large degree of melting is diminished. This study suggests if melt is retained, and the exsolved H_2O rehydrates the country rocks, then the fertility of the crust may not be reduced greatly and consequently melting in a subsequent metamorphic event may still be sufficient to buffer temperature and prevent UHT conditions being attained. Thus, the amount of melt left in so-called melt-depleted granulite terrains may be a critical factor that needs to be fully assessed in developing models for UHT metamorphism.

3.9 CONCLUSION

The granulite facies metamorphic terrain in the Opinaca Subprovince contains ~63% leucogranite in narrow dykes, veins and sills. This amount of leucogranite is far in excess of the <10% produced by partial melting of metagreywacke and pelitic protoliths at 800 to 825^{o}C and 7kbar pressure. Thus, the present exposure level in the terrain represents an

injection complex where the buoyant rise of anatectic melt from deeper levels was arrested. Consequently, granulite facies metamorphic terranes should not be viewed just as regions of melt-depletion; large parts of them may actually be regions of net accumulation of melt. There are three consequences of the accumulation of leucogranite there; 1) the terrain has a higher content of heat producing elements (K, Th, and U) than a granulite terrain that has a net depletion in anatectic melt, 2) the crystallization of a large volume the felsic magma in abundant thin dykes and sills exsolves H_2O that results in the extensive rehydration of the surrounding granulite facies rocks, and 3) the leucogranite constitutes a rock type that is potentially a fertile source in a subsequent metamorphic event. Thus, deep levels of the continental crust which contain felsic injection complexes may produce more radiogenic heat and be considerably more fertile in a subsequent partial melting event than an adjacent granulite facies terrain that is depleted in melt.

3.10 ACKNOWLEDGMENTS

This study represents part of the first author's Ph.D research. This project was possible because of the financial and logistical support through two seasons of field mapping in northern Quebec and we express our gratitude to the Bureau d'exploration géologique du Quebec for this support and their unwavering encouragement. We would like to thank Roberto Weinberg and an anonymous reviewer for their comments which substantially improved this manuscript. Mike Brown is thanked for his informal review and comments.

We also thank Fernando Bea at IBERSIMS for his invaluable assistance in obtaining, treating and interpreting the zircon data. The cost of SHRIMP analyses was met from a Natural Sciences and Engineering Research Council (NSERC) Discovery grant to Sawyer. This is the IBERSIMS publication nº6 and MRNF publication number 8439-2012-2013-5.

3.11 REFERENCES

Bandyayera, D., Burniaux, P., Morfin, S., 2011. Géologie de la région du lac Brune (33G07) et de la baie Gavaudan (33G10). Ministère des Ressources Naturelles du Québec, RG 2011-01.

Bandyayera, D., Fliszár, A., 2007. Géologie de la région de la baie Kasipasikatch (33C09) et du lac Janin (33C16). Ministère des Ressources Naturelles du Québec, RP 2005-09.

Bandyayera, D., Rhéaume, P., Maurice, C., Bédard, É., Morfin, S., Sawyer, E.W., 2010. Synthèse Géologique du Secteur du Réservoir Opinaca, Baie-James. Ministère des Ressources Naturelles du Québec, RG 2010-02.

Black, L.P., Kamo, S.L., Allen, C.M., Aleinikoff, J.N., Davis, D.W., Korsch, R.J., Foudoulis, C., 2003. TEMORA 1: a new zircon standard for Phanerozoic U–Pb geochronology. Chemical Ggeology 200, 155-170.

Bons, P.D., Dougherty-Page, J., Elburg, M.A., 2001. Stepwise accumulation and ascent of magmas. Journal of Metamorphic Geology 19, 627-633.

Bouilhol, P., Connolly, J.A.D., Burg, J.-P.2011. Geological evidence and modeling of melt migration by porosity waves in the sub-arc mantle of Kohistan (Pakistan) Geology, 39, 1091-1094.

Brown, M., 1973. The definition of metatexis, diatexis and migmatite. Proceedings of the Geologists' Association 84, Part 4, 371-IN372.

Brown, M., 1994. The generation, segregation, ascent and emplacement of granite magma: the migmatite-to-crustally-derived granite connection in thickened orogens. Earth-Science Reviews 36, 83-130.

Brown, M., 2006. Melt extraction from lower continental crust of orogens: the field evidence, in: Brown M, R.T. (Ed.), Evolution and Differentiation of the Continental Crust. Cambridge University Press, pp. 331-383.

Brown, M., Korhonen, F.J., Siddoway, C.S., 2011. Organizing Melt Flow through the Crust. Elements 7, 261-266.

Brown, M., Solar, G.S., 1999. The mechanism of ascent and emplacement of granite magma during transpression: a syntectonic granite paradigm. Tectonophysics 312, 1-33.

Card, K.D., 1990. A review of the Superior Province of the Canadian Shield, a product of Archean accretion. Precambrian Research 48, 99-156.

Clark, C., Fitzsimons, I.C.W., Healy, D., Harley, S.L., 2011. How Does the Continental Crust Get Really Hot? Elements 7, 235-240.

Clemens, J.D., 1990. The granulite - granite connection, in: Vielzeuf, D., Vidal, P. (Eds.), Granulites and Crustal Evolution. Kluwer Academic Publ, Dordrecht, pp. 25-36.

Clemens, J.D., Mawer, C.K., 1992. Granitic magma transport by fracture propagation. Tectonophysics 204, 339-360.

Collins, W.J., Sawyer, E.W., 1996. Pervasive granitoid magma transfer through the lower-middle crust during non-coaxial compressional deformation. Journal of Metamorphic Geology 14, 565-579.

Connolly, J.A.D. Podladchikov, Y.Y. 1998. Compaction-driven fluid flow in viscoelastic rock. Geodynamica Acta.11, 55-84.

Connolly, J.A.D., Podladchikov, Y.Y. 2007. Decompaction weakening and channeling instability in ductile porous media: Implications of asthenoshereic melt segregation. Journal of Geophysical Research 112, B10205.

Cruden, A.R., 2006. Emplacement and growth of plutons: implications for rates of melting and mass transfer in continental crust, in: Brown M, R.T. (Ed.), Evolution and Differentiation of the Continental Crust. Cambridge University Press, pp. 455-519.

David, J., Davis, D.W., Bandyayera, D., Simard, M., Moukhsil, A., Dion, C., 2010. Datations U-Pb effectuées dans les sous-provinces d'Ashuanipi, de Minto et de La Grande. MRNF, RP 2010-03.

Davis, W.J., Machado, N., Gariépy, C., Sawyer, E.W., Benn, K., 1995. U–Pb geochronology of the Opatica tonalite-gneiss belt and its relationship to the Abitibi greenstone belt, Superior Province, Quebec. Canadian Journal of Earth Sciences 32, 113-127.

Emsley, J., 1989. The Elements. Clarendon Press, Oxford, p. 231.

Fornelli, A., Piccarreta, G., Del Moro, A., Acquafredda, P., 2002. Multi-stage Melting in the Lower Crust of the Serre (Southern Italy). Journal of Petrology 43, 2191-2217.

Fowler, C.M.R., 1990. The Solid Earth. Cambridge University Press, New York. pp 472.

Frost, B.R., Chacko, T., 1989. The Granulite Uncertainty Principle: Limitations on Thermobarometry in Granulites. The Journal of Geology 97, 435-450.

Fyfe, W.S. 1973. The granulite facies, partial melting and the Archaean crust. Philosophical Transactions of the Royal Society of London, Series A 273, 457-461.

Goutier, J., Dion, C., David, J., Dion, D.J., 1999. Géologie de la région de la passe Shimusuminu et du lac Vion (33F/11 et 33F/12). Ministère des Ressources Naturelles du Québec, RG 98-17.

Graessner, T., Schenk, V., 2001. An Exposed Hercynian Deep Crustal Section in the Sila Massif of Northern Calabria: Mineral Chemistry, Petrology and a P–T Path of Granulite-facies Metapelitic Migmatites and Metabasites. Journal of Petrology 42, 931-961.

Guernina, S., Sawyer, E.W., 2003. Large-scale melt-depletion in granulite terranes: an example from the Archean Ashuanipi Subprovince of Quebec. Journal of Metamorphic Geology 21, 181-201.

Hasalová, P., Weinberg, R.F., Macrae, C., 2011. Microstructural evidence for magma confluence and reusage of magma pathways: implications for magma hybridization, Karakoram Shear Zone in NW India. Journal of Metamorphic Geology 29, 875-900.

Henry, D.J., Guidotti, C.V., Thomson, J.A., 2005. The Ti-saturation surface for low-to-medium pressure metapelitic biotites: Implications for geothermometry and Ti-substitution mechanisms. American Mineralogist 90, 316-328.

Hobbs, B.E., Ord, A., 2010. The mechanics of granitoid systems and maximum entropy production rates. Philosophical Transactions of the Royal Society A: Mathematical, Physical and Engineering Sciences 368, 53-93.

Holness, M.B., 2008. Decoding Migmatite Microstructures, in: Sawyer, E.W., Brown, M. (Eds.), Working with Migmatites. Mineralogical Association of Canada, pp. 57-76.

Holtz, F., Johannes, W., Tamic, N., Behrens, H., 2001. Maximum and minimum water contents of granitic melts generated in the crust: a reevaluation and implications. Lithos 56, 1-14.

Jessop, A.M., 1990. Thermal geophysics, Developments in Solid Earth Geophysics. Elsevier, Amsterdam.

Johnson, T.E., White, R.W., Powell, R., 2008. Partial melting of metagreywacke: a calculated mineral equilibria study. Journal of Metamorphic Geology 26, 837-853.

Leitch, A.M., Weinberg, R.F., 2002. Modelling granite migration by mesoscale pervasive flow. Earth and Planetary Science Letters 200, 131-146.

Ludwig, K.R., 2012. Isoplot/Ex, v. 3.75. Berkeley Geochronology Center Special Publication No. 5, Berkeley.

Marchildon, N., Brown, M., 2003. Spatial distribution of melt-bearing structures in anatectic rocks from Southern Brittany, France: implications for melt transfer at grain- to orogen-scale. Tectonophysics 364, 215-235.

Montel, J.-M., Vielzeuf, D., 1997. Partial melting of metagreywackes, Part II. Compositions of minerals and melts. Contributions to Mineralogy and Petrology 128, 176-196.

Nabelek, P.I., Bartlett, C.D., 2000. Fertility of metapelites and metagraywackes during leucogranite generation: an example from the Black Hills, U.S.A. Geological Society of America Special Papers 350, 1-14.

Oliver, N.H.S., Barr, T.D., 1997. The geometry and evolution of magma pathways through migmatites of the Halls Creek Orogen, Western Australia. Mineral Magazine 61, 3-14.

Otamendi, J.E., Patiño Douce, A.E., 2001. Partial melting of aluminous metagreywackes in the Northern Sierra de Comechingones, Central Argentina. Journal of Petrology 42, 1751-1772.

Pan, Y., E. Fleet, M., Heaman, L., 1998. Thermo-tectonic evolution of an Archean accretionary complex: U–Pb geochronological constraints on granulites from the Quetico Subprovince, Ontario, Canada. Precambrian Research 92, 117-128.

Pattison, D.R.M., Chacko, T., Farquhar, J., McFarlane, C.R.M., 2003. Temperatures of granulite-facies metamorphism: constraints from experimental phase equilibria and thermobarometry corrected for retrograde exchange. Journal of Petrology 44, 867-900.

Percival, J., Stern, R., Rayner, N., 2003. Archean adakites from the Ashuanipi complex, eastern Superior Province, Canada: geochemistry, geochronology and tectonic significance. Contributions to Mineralogy and Petrology 145, 265-280.

Percival, J.A., 1991. Orthopyroxene–poikilitic tonalites of the Desliens igneous suite, Ashuanipi granulite complex, Labrador–Quebec, Canada. Canadian Journal of Earth Sciences 28, 743-753.

Percival, J.A., Mortensen, J.K., Stern, R.A., Card, K.D., Bégin, N.J., 1992. Giant granulite terranes of northeastern Superior Province: the Ashuanipi complex and Minto block. Canadian Journal of Earth Sciences 29, 2287-2308.

Percival, J.A., Sanborn-Barrie, M., Skulski, T., Stott, G.M., Helmstaedt, H., White, D.J., 2006. Tectonic evolution of the western superior province from NATMAP and lithoprobe studies. Canadian Journal of Earth Sciences 43, 1085-1117.

Petford, N., Lister, J.R., Kerr, R.C., 1994. The ascent of felsic magmas in dykes. Lithos 32, 161-168.

Price, N.J., Cosgrove, J.W., 1990. Analysis of geological structures. Cambridge University Press, Cambridge.

Rosenberg, C.L., Handy, M.R., 2005. Experimental deformation of partially melted granite revisited: implications for the continental crust. Journal of Metamorphic Geology 23, 19-28.

Rudnick, R.L., Fountain, D.M., 1995. Nature and composition of the continental crust: A lower crustal perspective. Reviews of Geophysics 33, 267-309.

Rudnick, R.L., McDonough, W.F., O'Connell, R.J., 1998. Thermal structure, thickness and composition of continental lithosphere. Chemical Geology 145, 395-411.

Rudnick, R.L., Gao, S., 2003. The composition of the continental crust. In: Rudnick, R.L. (ed) The Crust: Treatise on Geochemistry 3, Elsevier-Pergammon, Oxford, pp.1-64.

Sandiford, M., McLaren, S., 2002. Tectonic feedback and the ordering of heat producing elements within the continental lithosphere. Earth and Planetary Science Letters 204, 133-150.

Sandiford, M., McLaren, S., Neumann, N., 2002. Long-term thermal consequences of the redistribution of heat-producing elements associated with large-scale granitic complexes. Journal of Metamorphic Geology 20, 87-98.

Sawyer, E.W., 1986. The influence of source rock type, chemical-weathering and sorting on the geochemistry of clastic sediments from the Quetico meta-sedimentary belt, Superior Province, Canada. Chemical Geology 55, 77-95.

Sawyer, E.W., 1987. The role of partial melting and fractional crystallization in determining discordant migmatite leucosome compositions. Journal of Petrology 28, 445-473.

Sawyer, E.W., 1998. Formation and evolution of granite magmas during crustal reworking: the significance of diatexites. Journal of Petrology 39, 1147-1167.

Sawyer, E.W., 1999. Criteria for the recognition of partial melting. Physics and Chemistry of the Earth, Part A: Solid Earth and Geodesy 24, 269-279.

Sawyer, E.W., 2001. Melt segregation in the continental crust: distribution and movement of melt in anatectic rocks. Journal of Metamorphic Geology 19, 291-309.

Sawyer, E.W., 2008a. Atlas of migmatites. The Canadian Mineralogist. In: Special Publication, vol. 9. NRC Research Press, Ottawa, Ontario, p. 371.

Sawyer, E.W., 2008b. Working with Migmatites: Nomenclature for the Contituent Parts, in: Sawyer, E.W., Brown, M. (Eds.), Working with Migmatites. Mineralogical Association of Canada, Short Course Volume 38, pp. 1-28.

Sawyer, E.W., 2010. Migmatites formed by water-fluxed partial melting of a leucogranodiorite protolith: Microstructures in the residual rocks and source of the fluid. Lithos 116, 273-286.

Sawyer, E.W., Cesare, B., Brown, M., 2011. When the Continental Crust Melts. Elements 7, 229-234.

Sawyer, E.W., Dombrowski, C., Collins, W.J., 1999. Movement of melt during synchronous regional deformation and granulite-facies anatexis, an example from the Wuluma Hills, central Australia. Geological Society, London, Special Publications 168, 221-237.

Simakin, A., Talbot, C., 2001. Tectonic pumping of pervasive granitic melts. Tectonophysics 332, 387-402.

Simard, M., Gosselin, C., 1999. Géologie de la région du Lac Lichteneger (SNRC 33B). Ministère des Ressources Naturelles du Québec, RG 98-15.

Simard, M., Gosselin, C., Lafrance, I., 2009a. Géologie de la région de la Riviére Sérigny (24C - 23N). MRNF Québec, RG 2009-02.

Simard, M., Parent, M., Paquette, L., Lafrance, I., 2009b. Géologie de la région du Réservoir de Caniapiscau (SNRC 23K - 23N). MRNF Québec, RG 2009-04.

Slagstad, T., Hamilton, M.A., Jamieson, R.A., Culshaw, N.G., 2004. Timing and duration of melting in the mid orogenic crust: Constraints from U-Pb (SHRIMP) data, Muskoka and Shawanaga domains, Grenville Province, Ontario. Canadian Journal of Earth Sciences 41, 1339-1365.

Solar, G.S., Brown, M. 2001. Petrogenesis of Migmatites in Maine, USA: Possible Source of Peraluminous Leucogranite in Plutons? Journal of Petrology 42, 789-823.

St. Seymour, K., Turek, A., Doig, R., Kumarapeli, S., Fogal, R., 1989. First U–Pb zircon ages of granitoid plutons from the La Grande greenstone belt, James Bay area, New Quebec. Canadian Journal of Earth Sciences 26, 1068-1073.

Stevens, G., Clemens, J.D., Droop, G.T.R., 1997. Melt production during granulite-facies anatexis: experimental data from "primitive" metasedimentary protoliths. Contributions to Mineralogy and Petrology 128, 352-370.

Stüwe, K., 1995. Thermal buffering effects at the solidus. Implications for the equilibration of partially melted metamorphic rocks. Tectonophysics 248, 39-51.

Vavra, G., Schmid, R., Gebauer, D., 1999. Internal morphology, habit and U-Th-Pb microanalysis of amphibolite-to-granulite facies zircons: geochronology of the Ivrea Zone (Southern Alps). Contributions to Mineralogy and Petrology 134, 380-404.

Vielzeuf, D., Clemens, J.D., Pin, C., Moinet, E., 1990. Granites, granulites, and crustl differentiation, in: Vielzeuf, D., Vidal, P. (Eds.), Granulites and Crustal Evolution. Kluwer Academic Publ, Dordrecht, pp. 59-85.

Vielzeuf, D., Montel, J.M., 1994. Partial melting of metagreywackes. Part I. Fluid-absent experiments and phase relationships. Contributions to Mineralogy and Petrology 117, 375-393.

Waters, D.J., 2001. The significance of prograde and retrograde quartz-bearing intergrowth microstructures in partially melted granulite-facies rocks. Lithos 56, 97-110.

Weinberg, R.F., 1999. Mesoscale pervasive felsic magma migration: alternatives to dyking. Lithos 46, 393-410.

Weinberg, R.F., Searle, M.P., 1998. The Pangong Injection Complex, Indian Karakoram: a case of pervasive granite flow through hot viscous crust. Journal of the Geological Society 155, 883-891.

White, R.W., Powell, R., 2010. Retrograde melt–residue interaction and the formation of near-anhydrous leucosomes in migmatites. Journal of Metamorphic Geology 28, 579-597.

White, R.W., Powell, R., Halpin, J.A., 2004. Spatially-focussed melt formation in aluminous metapelites from Broken Hill, Australia. Journal of Metamorphic Geology 22, 825-845.

Williams, I.S., Claesson, S., 1987. Isotopic evidence for the Precambrian provenance and Caledonian metamorphism of high grade paragneisses from the Seve Nappes, Scandinavian Caledonides. Contributions to Mineralogy and Petrology 97, 205-217.

Wu, C.-M., Cheng, B.-H., 2006. Valid garnet–biotite (GB) geothermometry and garnet–aluminum silicate–plagioclase–quartz (GASP) geobarometry in metapelitic rocks. Lithos 89, 1-23.

Zaleski, E., van Breemen, O., Peterson, V.L., 1999. Geological evolution of the Manitouwadge greenstone belt and Wawa-Quetico subprovince boundary, Superior Province, Ontario, constrained by U-Pb zircon dates of supracrustal and plutonic rocks. Canadian Journal of Earth Sciences 36, 945-966.

Zhang, B., Wu, J., Ling, H., Chen, P., 2008. Estimating influence of crystallizing latent heat on cooling-crystallizing process of a granitic melt and its geological implications. Acta Geologica Sinica - English Edition 82, 438-443.

CHAPITRE 4

THE GEOCHEMICAL SIGNATURE OF A FELSIC INJECTION COMPLEX IN THE CONTINENTAL CRUST: OPINACA SUBPROVINCE, QUEBEC

SAMUEL MORFIN[1], EDWARD W. SAWYER[1] & DANIEL BANDYAYERA[2]

[1] UNIVERSITÉ DU QUÉBEC À CHICOUTIMI

[2] BUREAU DE L'EXPLORATION GÉOLOGIQUE DU QUÉBEC

LITHOS, 2014, VOL. 196-197, P. 339-355

4.1 RÉSUMÉ

La Sous-province d'Opinaca qui fait partie de la Province du Supérieur d'âge archéen dans le Nord du Québec constitue un complexe d'injection. Celui-ci est composé d'unités métasédimentaires injectées par un grand volume de liquides leucogranitiques sous forme de fines veines et dykes. La présence de l'orthopyroxène montre que les métasédiments ont atteint le faciès des granulites.

La microstructure typique des leucogranites peut être séparée en deux groupes; 1) le premier groupe forme un réseau ouvert de feldspath potassique (Kfs) dont les interstices sont remplis de plagioclase riche en albite et de quartz; 2) le second groupe se présente sous la forme d'une charpente de plagioclase riche en albite dont les interstices sont remplis de quartz et parfois de petits grenats rosés. Sur le terrain, les textures pegmatitiques et aplitiques sont communes.

Géochimiquement, les leucogranites qui forment le complexe d'injection sont riches en SiO_2 (au-delà de 70 wt. %) et ont un faible contenu en (FeO + MgO + TiO_2) comparativement aux liquides expérimentaux similaires. Les minéraux mafiques ont été fractionnés du magma avant la mise en place dans le complexe d'injection. Les leucogranites forment une suite dans les diagrammes en éléments majeurs qui s'explique par l'extraction d'un cumulat dominé par le feldspath potassique depuis une composition de "liquide initial". Les cumulats sont enrichis en K_2O tandis que les liquides résiduels sont enrichis en SiO_2 et en Na_2O.

À partir de ces résultats, les leucogranites à charpente de Kfs sont interprétés comme des cumulats. Ces leucogranites ont des signatures en Éléments de Terres Rares (REE) typiques de l'accumulation de feldspaths. Les liquides résiduels extraits de ces cumulats à charpente de Kfs sont les leucogranites à charpente de plagioclase riche en albite. Ces derniers ont des signatures en REE qui sont typiques des liquides très évolués dont les minéraux accessoires ont déjà été fractionnés.

Le caractère très évolué des leucogranites d'Opinaca associé au fait qu'ils furent injectés dans des terrains granulitiques a de grandes implications pour l'évolution de la croûte. 1) Ces grands volumes de magma évolués qui se mettent en place en profondeur peuvent libérer de grandes quantités d'H_2O dans leur environnement. Les complexes d'injections peuvent donc agir comme des sources d'H_2O dans la croûte moyenne, et cette H_2O peut réhydrater les assemblages de haut grade environnant. 2) Si des granites aussi évolués sont présents à des niveaux aussi profonds de la croûte, alors des évidences de fractionnement devraient être observables à plus grande profondeur, proche de la source des magmas. 3) Ces exemples naturels confirment des modèles numériques qui suggèrent que l'ensemble des processus subis par les leucogranites (fusion partielle, évolution, cristallisation) peut se passer en dessous, ou juste au-dessus, de la profondeur du solidus des granites. Ceci a un impact majeur sur la compréhension globale des processus de transfert de leucogranites dans la croûte, qui est lui même un des mécanismes majeurs de la différenciation crustale.

4.2 ABSTRACT

The Archean Opinaca Subprovince of the Superior Province in northern Québec is an injection complex consisting of lower granulite facies metasedimentary terrane that was pervasively injected with a large volume of leucogranitic melt which form innumerable thin dykes and veins.

The typical microstructure of the leucogranites can be divided into two groups, 1) the first has an open framework of K-feldspar in which the interstices are filled with albite-rich plagioclase and quartz and, 2) a microstructure defined by an albite-rich plagioclase framework where the interstices are filled by quartz and, in some cases, small pink garnets. In the field, pegmatitic and aplitic textures are common.

Geochemically, leucogranites that form the injection complex are all SiO_2-rich (above 70 wt %) and have a low content of (FeO + MgO + TiO_2) compared to experimental melts. The mafic minerals were fractionated from the magma before its emplacement into the injection complex. The leucogranites form a coherent trend on major element diagrams that is best explained by the removal of a cumulate dominated by K-feldspar from an "initial melt" composition. The cumulate rocks are enriched in K_2O whereas the residual melts are richer in SiO_2 and Na_2O.

Based on these results, leucogranites with a K-feldspar framework are interpreted as cumulate rocks. This indicates that the early-crystallizing calcic plagioclase had already been fractionated from the magma before injection into the complex. The leucogranites

have rare earth element (REE) patterns typical of feldspar accumulation. The residual melts extracted after the K-feldspar framework developed are those that have an albite-rich plagioclase framework. These have REE patterns typical of highly evolved melts from which the accessory minerals have also been fractionated.

The highly evolved nature of the leucogranites from the Opinaca which were injected in a granulite facies environment has several important implications for crustal evolution. 1) The large volume of evolved melts emplaced at depth released a significant amount of H_2O into the adjacent crust, and thus injection complexes should be considered as a potentially important source of H_2O in the middle crust that is capable of rehydrating the granulitic terranes into which they are injected. 2) A corollary of the evolved nature of the leucogranite in the injection complex is that there should be evidence of accumulation of the early fractionated material still deeper in the crust. 3) These findings are natural examples that corroborate predictions from numerical modelling which suggest that the whole process from melting to crystallisation of leucogranite can be confined to deep levels of the crust, below, or close to, the solidus. This has important impact on our general view on the transfer of leucogranites in the continental crust which is the main mechanism of crustal differentiation.

4.3 INTRODUCTION

The continental crust is chemically differentiated; the upper crust is enriched in K_2O, Na_2O, H_2O and SiO_2 relative to the lower crust which is correspondingly enriched in Al_2O_3, FeO and MgO (Rudnick and Gao, 2003; Taylor and McLennan, 1995). Based on field observations, the main physical mechanism through which this differentiation occurs is the ascent of granitic melts created by anatexis of the lower crust (Brown et al., 2011; Sawyer et al., 2011). These observations confirm older interpretations of the geochemical difference between granulite facies metamorphic terrains and the upper crust (e.g. Fyfe, 1973; Lambert and Heier, 1968).

Many studies have examined the mechanism by which granitic melt ascends through the crust and have shown that large dykes are a very efficient means of transporting magma to feed granitic plutons in the upper crust (Cruden, 2006; Petford et al., 1994). The progressive chemical evolution of the anatectic magma during its transport to the upper crust results in a range of evolved magma compositions at the level of emplacement where plutons are formed (e.g. Johnson et al., 2003; Tartèse and Boulvais, 2010).

Field studies in high grade metamorphic terranes have shown that anatectic melt can also migrate in a pervasive fashion through a network of small veins in the suprasolidus crust (the part of the crust situated at temperature higher than the granitic solidus) (Collins and Sawyer, 1996; Connolly and Podladchikov, 1998; Weinberg and Searle, 1998). Pervasive migration of melt gives rise to the complex pattern of leucosomes and leucogranitic veins

typical of many migmatites. Numerical modelling (Hobbs and Ord, 2010; Leitch and Weinberg, 2002) has shown that a large number of small magma-filled veins can propagate out of their source by heating the wall rocks as they rise. However, because the veins are small and lack sufficient thermal energy to propagate high into the subsolidus crust they cannot transport felsic melt very far before solidification occurs. Thus, pervasive migration can create an extensive zone of narrow, granite-filled dykes and such a zone has been termed an injection complex (Weinberg and Searle, 1998). Injection complexes are characterized by large volumes of magma injected into high-grade rocks as a network of interlinked small leucogranitic veins and dykes. Generally, injection complexes are viewed as the vestigial remnants of a formally more pervasive network of channels through which melt moved (Bons et al., 2010; Weinberg, 1999). Recently, Morfin et al. (2013) showed that an injection complex in the middle crust is not simply the collapsed relic of a melt transfer zone. Rather, because it contains such a large number of felsic dykes, it can also be viewed as a site where a large volume of anatectic melt accumulated in the crust. Consequently, injection complexes can be considered as magmatic reservoirs (Weinberg et al., 2009), albeit one that is more diffuse and located at greater depth.

Injection complexes form because small volumes of anatectic melt rising in narrow dykes solidify before they can migrate great distances (Leitch and Weinberg, 2002). However, the melt did migrate some distance and crystallised along the way, therefore, the geochemical signature of an injection complex is expected to reflect this. Hence, in this contribution we look at an injection complex through the geochemical composition of its leucogranites.

Specific objectives are; 1) to describe the geochemical characteristics of the leucogranites comprising the injection complex, focusing on their degree of evolution, and 2) to assess the processes responsible for their geochemical characteristics. Then the implications of the presence of large volumes of magma in the lower middle crust and for the differentiation of the continental crust are discussed. In order to address these problems, regional-scale mapping and sampling of leucogranitic veins was conducted in a large injection complex located in the Opinaca Subprovince of northern Quebec (Morfin et al., 2013).

4.4 GEOLOGICAL CONTEXT

4.4.1 REGIONAL GEOLOGY

The Opinaca Subprovince is part of a 2000 km long series of four metasedimentary subprovinces that crosses the Archean Superior Province (Fig. 4.1) in Canada. The metasedimentary rocks in all four subprovinces have strong similarities in composition and deposition ages, but show an increase in metamorphic grade eastwards (Card, 1990; Percival et al., 2006). This suggests similar provenance and history, but different degrees of exhumation.

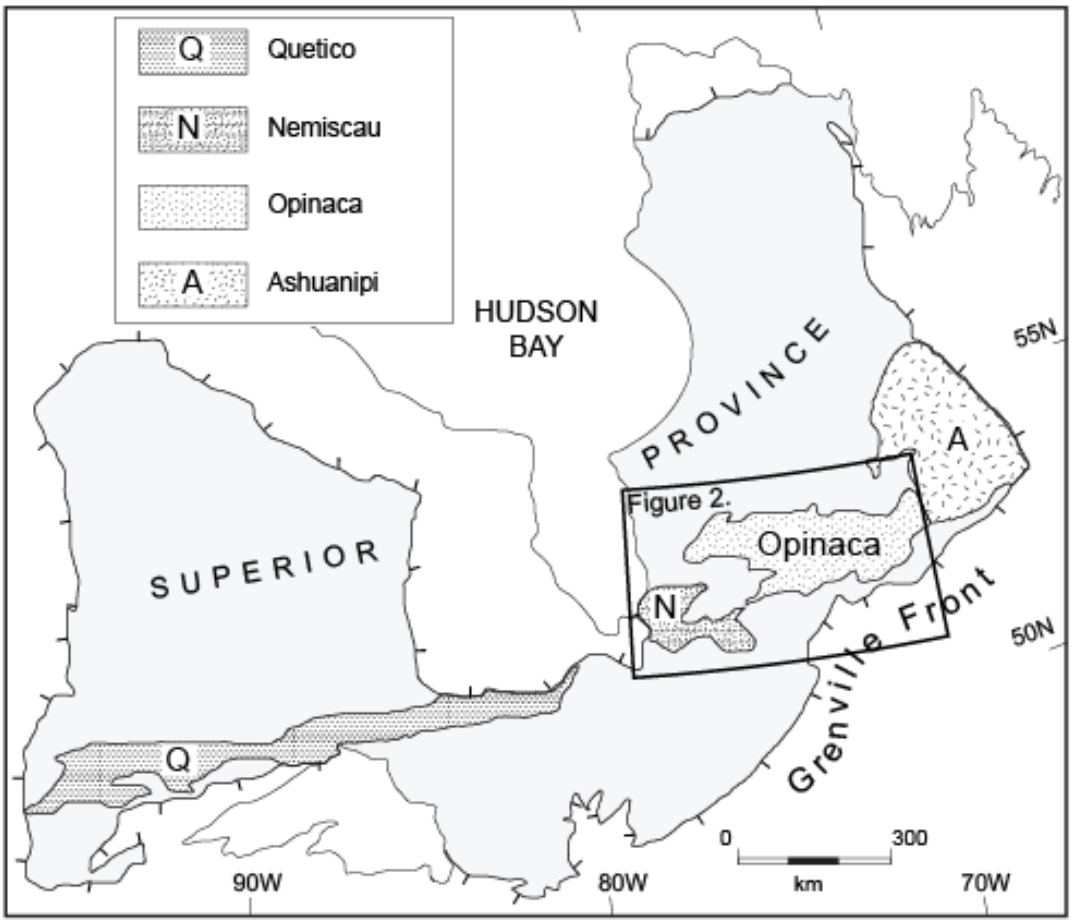

Figure 4.1: Location of the Opinaca Subprovince and its relation to Quetico, Nemiscau and Ashuanipi metasedimentary belts, modified from Sawyer (2010).

The Opinaca Subprovince covers over 35000 km^2, although only about 15000 km^2 have been mapped at a scale better than regional reconnaissance. The Opinaca Subprovince is bounded (Fig. 4.2) to the north and west by the La Grande Subprovince which is a plutonic terrane dominated by tonalite-granodiorite units separated by thin belts of amphibolite facies metavolcanic and metasedimentary rocks (Bandyayera et al., 2011; Bandyayera et al., 2010). The southern edge of the Opinaca Subprovince is against the Opatica Subprovince which consists principally of tonalite, trondhjemite and granodiorite rocks (TTG), and their anatectic products (Sawyer, 2010). The eastern boundary with the Ashuanipi Subprovince is gradational (Percival et al., 1992) and defined by increasing metamorphic grade; the Ashuanipi Subprovince reached conditions well into the granulite facies (Guernina and Sawyer, 2003).

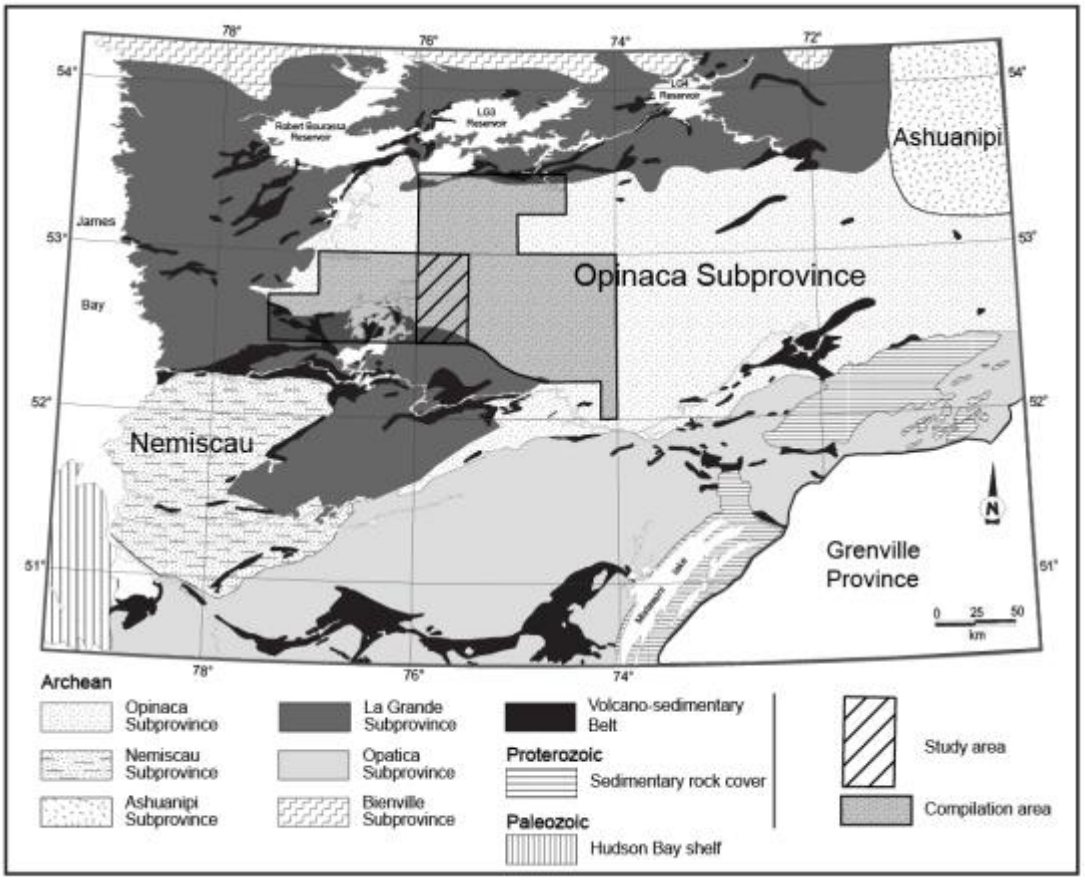

Figure 4.2: Simplified geological map of the Superior Province east of James Bay. The bold striped zone represent the area of this study, the shaded area shows the compiled areas mapped by Simard and Gosselin (1999), Bandyayera et al. (2010) and Bandyayera et al. (2011). Map modified from Bandyayera et al. (2010).

4.4.2 GEOCHRONOLOGY

The age of deposition for sediments in the Opinaca Subprovince is poorly constrained. Minimum and maximum ages of deposition are bracketed by the 2674 ± 12 Ma Pluton de Bezier (Goutier et al., 2001; St. Seymour et al., 1989) and the ca. 2700 Ma Lac Taylor granite (Goutier et al., 1999), respectively. Thus, deposition ages are likely to be similar to deposition ages between 2698 and 2687 Ma and 2700 and 2690 Ma obtained for the Quetico and Ashuanipi Subprovinces, respectively (Percival, 1991).

Deposition of sedimentary rocks in the Quetico, Opinaca and Ashuanipi Subprovinces was quickly followed by deformation and high-grade regional metamorphism of the Kenoran Orogeny and lasted for several tens of millions years. In the Quetico Subprovince, regional metamorphism is at the greenschist facies but locally reached the granulite facies which was coeval with the injection of peraluminous leucogranites between ca. 2670 and 2650 Ma (Pan et al., 1998; Percival et al., 2006). In the Ashuanipi Subprovince widespread granulite facies partial melting and the formation of migmatites and leucogranites occurred between 2682 and 2650 Ma (Guernina and Sawyer, 2003; Percival et al., 2003; Percival, 1993; Percival et al., 1992; Simard et al., 2009a; Simard et al., 2009b). The time of granulite facies metamorphism in the Opinaca Subprovince is constrained by zircon growth in residual metapelites to occur at 2663.6 ± 6.0 Ma (Morfin et al., 2013). This coincides with the oldest zircon crystallisation recorded in an injected leucogranitic vein at 2671 Ma, which indicates that injection and incipient crystallisation of the leucogranitic melt started at granulite conditions.

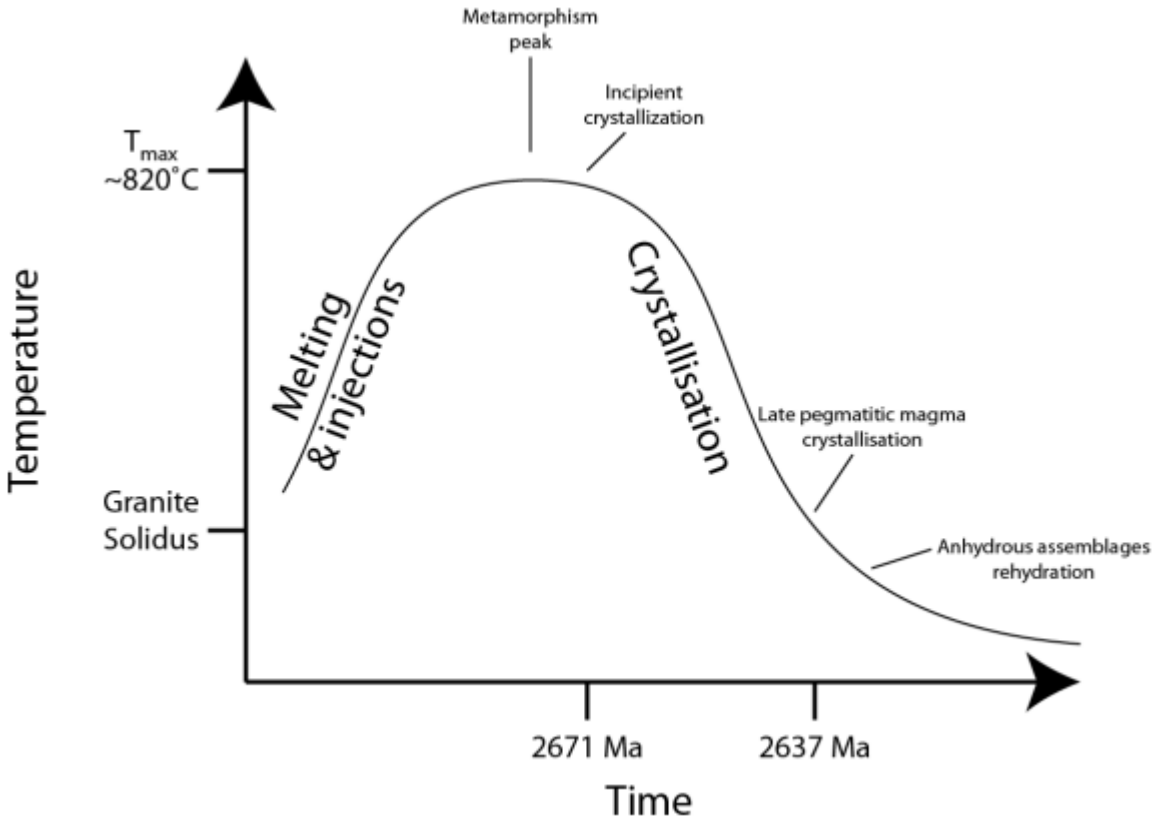

Figure 4.3: Schematic representation of the interpreted time-temperature path of the Opinaca Subprovince. The rise in temperature allows small volumes of leucogranitic melts to exist for a long period of time. At peak temperature some melt is produced in situ by the metagreywackes. Crystallisation of the leucogranitic veins occurred between 2671 and 2637 Ma. The H_2O released in the late stages of leucogranite crystallisation partially rehydrates the anhydrous, high grade, orthopyroxene-bearing assemblages.

The field relations and geochronology indicates that granulite facies metamorphism was synchronous with the injection of leucogranitic veins in the Opinaca Subprovince (Fig. 4.3). This is to be expected in an injection complex setting; Leitch and Weinberg (2002) show that the injection of anatectic magma increases the temperature of the crust situated just above, allowing a positive feedback effect where the next batches of magma can rise slightly higher in the crust. The Opinaca shows the same timing relationship in which high grade metamorphism is quickly followed by the injection of the leucogranitic magmas during the main deformation event. Cooling of the terrane and subsequent crystallisation of the leucogranite started around 2670-2665 Ma.The youngest leucogranite dyke associated with the injection complex crystallised at 2637 Ma (Fig. 4.3, David et al., 2010). Assuming that this occurred close to the granite solidus, then temperature dropped from the peak (~820°C at ca 2665 Ma; Morfin et al. (2013)) to granite solidus (~650°C) in approximately 30 My, which gives an average cooling rate of 6°C My^{-1}.

4.4.3 LOCAL GEOLOGY

This study focuses on a 30 by 50 km area mapped at the 1:50 000 scale (Bandyayera et al., 2010), but includes mapping work in adjacent area for a total of over 15 000km^2 (Bandyayera et al., 2011; Bandyayera et al., 2010; Simard and Gosselin, 1999).

The Opinaca Subprovince consists largely of high-grade metasedimentary rocks which are pervasively injected by thin felsic leucocratic veins and dykes striking parallel to the main east-west foliation (Fig. 4.4). Metagreywacke bulk compositions dominate over metapelite ones by a ratio of about 10 to 1. Minor metamafic and ultramafic layers concordant within the metasedimentary rocks occur in parts of the Opinaca Subprovince. The metasedimentary rocks are intruded by late to post-tectonic tonalite-enderbite, granodiorite and monzodiorite plutons (Bandyayera et al., 2010).

Bedding (S_0) is indicated by darker metapelitic layers in the metagreywackes. Regionally, an S_1 schistosity is described west of the study area, but is not observed in the field (Bandyayera et al., 2010). However, the most prominent structural feature is a pervasive (S_2) schistosity that affects all the metasedimentary rocks, and is defined by the alignment of biotite. The S_2 schistosity is subvertical and strikes E-W, commonly sub-parallel to the bedding (S_0). It contains a mineral lineation that plunges gently to the east or the west. Many leucogranitic veins injected into the metasedimentary rocks also record the S_2 deformation event. Veins oriented parallel to foliation typically show boudinage, but those initially at high angle with the foliation are asymmetrically folded.

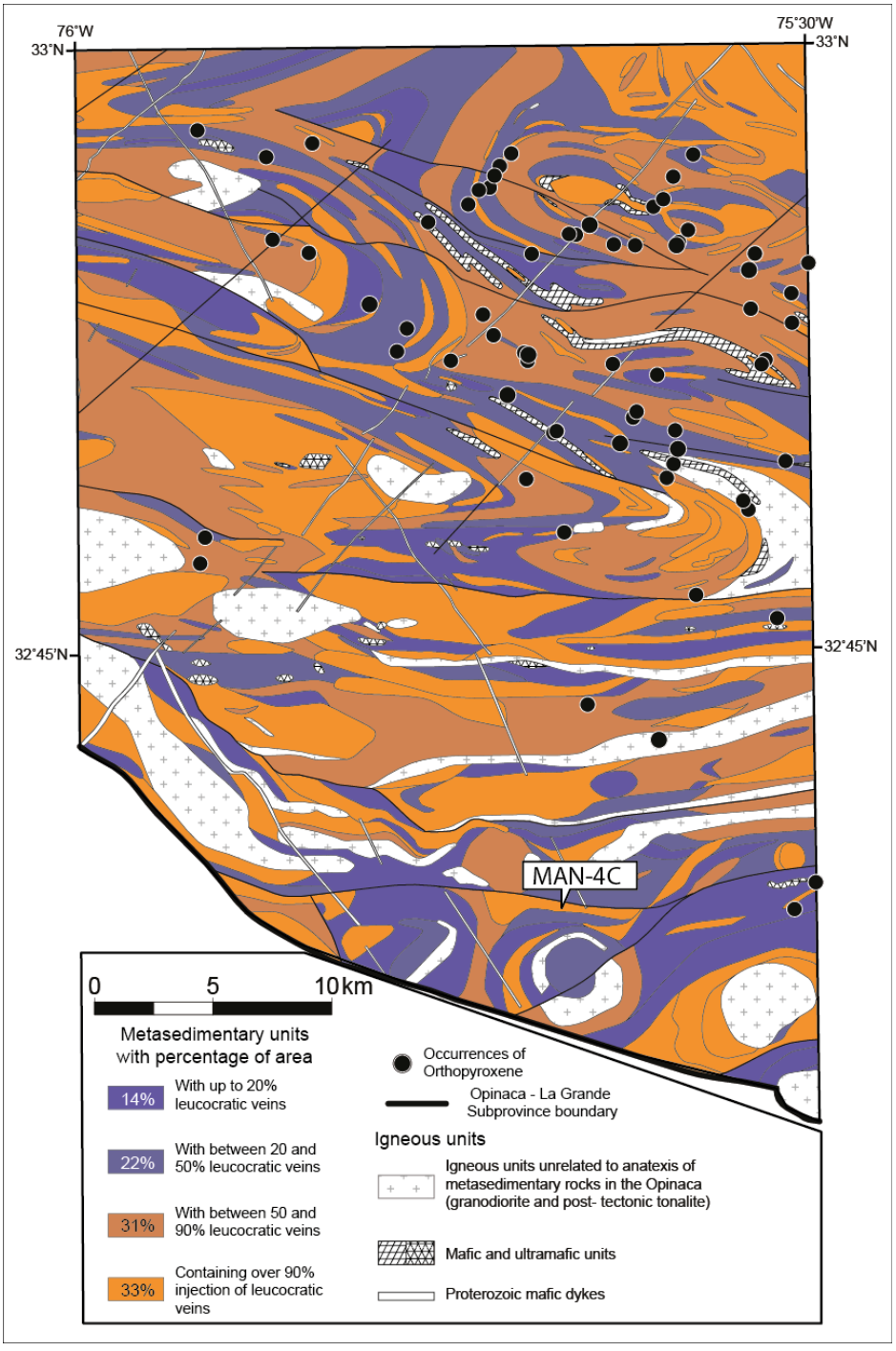

Figure 4.4: Geological map of the study area color-coded for the amount of leucocratic material present in the metasedimentary host, modified from Bandyayera et al. (2010).

The D_3 deformation event folded and truncated the main schistosity as shown in figure 4.4 where some fold flanks and contacts are shifted. The F_3 folds have subvertical E-W axial planes and subhorizontal hinges; the flanks of some F_3 folds are truncated by E-W S_3 shear zones that are sub-parallel to S_2. Compared to D_2, D_3 is much less pervasive and is spatially restricted to where F_3 folds are developed. Late intermediate to felsic plutons follow the structural pattern produced by D_2 and D_3, but are interpreted to be late to post-deformation in age because they show minor internal deformation.

4.4.3.1. METAMORPHIC CONDITIONS

Although not abundant, orthopyroxene occurs in metagreywackes across the whole study area, and indicates that granulite facies conditions were attained throughout the Opinaca Subprovince (Fig. 4.5a; Morfin et al., 2013). The typical assemblage of the metagreywackes is quartz + plagioclase + biotite ± garnet ± orthopyroxene ± tourmaline, and many of these rocks contain small *in situ* neosome or leucosome patches, indicating that they partially melted via a reaction such as

biotite + plagioclase + quartz = orthopyroxene + melt + Fe-oxides ± garnet (R1)

K-feldspar is generally not observed in the matrix, except as rare cuspate-shaped grains that pseudomorph the former melt-filled pores in orthopyroxene-bearing domains in the

residuum. The general microstructure is granoblastic with schistosity defined by oriented biotite (see Morfin et al., 2013 for details). Orthopyroxene is commonly partially, or completely, replaced by anthophyllite + hornblende, cummingtonite + hornblende or biotite (Fig. 4.5b), indicating rehydration of the peritectic phase (Morfin et al., 2013).

At the outcrop scale all the pelitic layers contain leucosomes, and in thin section contain assemblages, or microstructures, that indicate partial melting via

quartz + biotite + plagioclase + sillimanite = melt + garnet / cordierite ± K-feldspar (R2)

(see Morfin et al., 2013). In contrast some metagreywacke layers show no evidence for melting whereas others do (e.g. *in situ* patch neosome). Thus, peak metamorphic conditions in the Opinaca Subprovince are estimated at ~820ºC and 6-7 kbar (Morfin et al., 2013). At these conditions an estimated maximum of 10% partial melting of a typical Opinaca metagreywacke could occur, based on the comparison of observed modal composition with the results of THERMOCALC modelling by Johnson et al. (2008). However, a typical outcrop contains 63% leucogranite in veins and thin dykes, the overall proportion of veins per outcrop ranges from none to almost 100% (Morfin et al., 2013). Thus, most of the leucogranite observed in outcrops must have been injected into the Opinaca Subprovince because local partial melting generated no more than 10% granitic melt. This observation indicates that the granulites in the Opinaca Subprovince have accumulated melt rather than being melt-depleted as are some other granulite terranes, and that this melt accumulation

started while the terrane was at granulite conditions (Brown and Solar, 1999; Guernina and Sawyer, 2003).

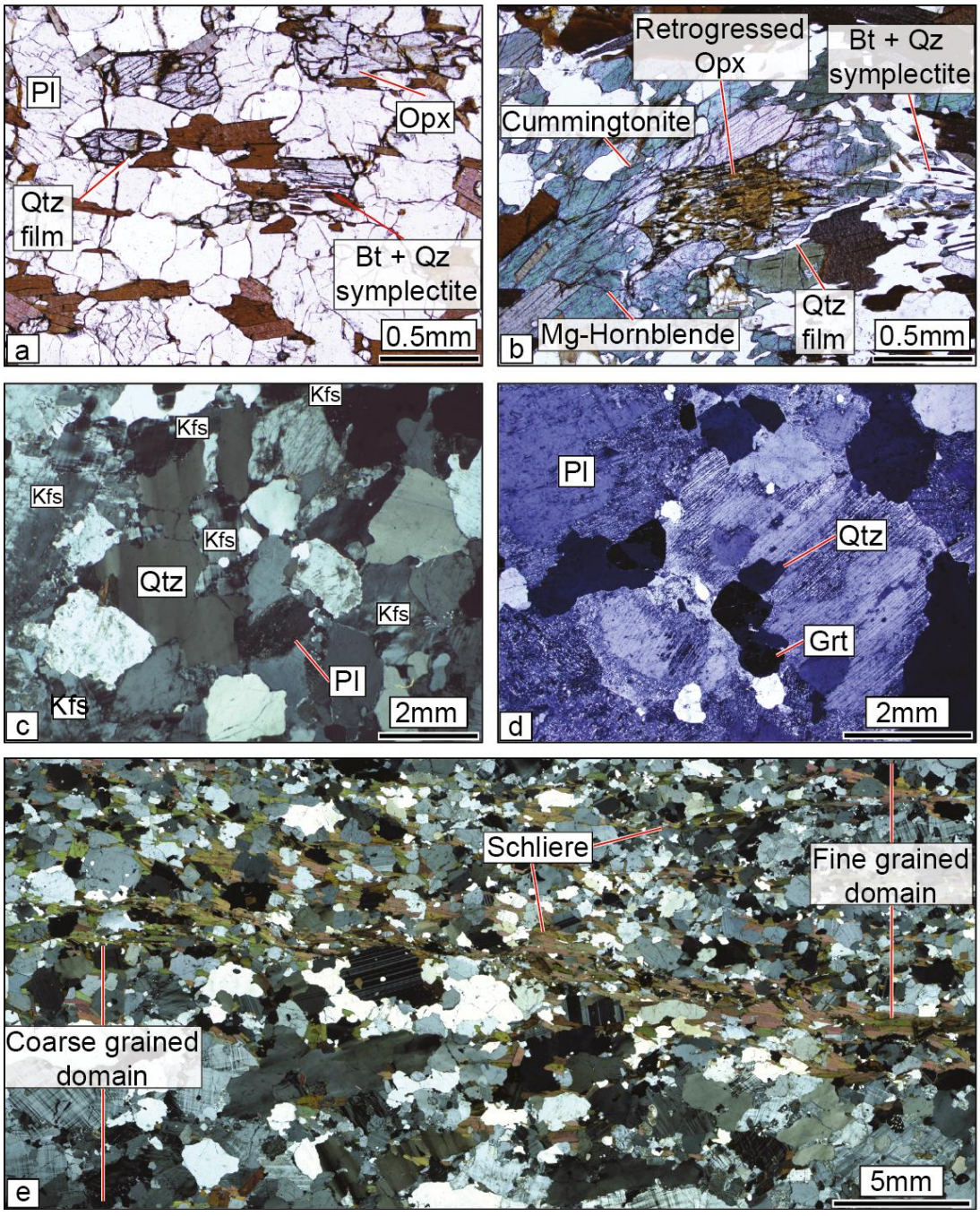

Figure 4.5: Microstructure of the metagreywacke host rock and of various leucogranites. a) Example of an orthopyroxene-bearing assemblage in a metagreywake. Films of quartz around the orthopyroxene indicate the former presence of melt along grain boundaries. b)

Cummingtonite and magnesio-hornblende replacing orthopyroxene at upper amphibolite condition. Orthopyroxene can also be replaced by a biotite + quartz symplectite. c) Example of a K-feldspar framework leucogranite.The feldspar crystals form an open framework of touching subhedral grains and the interstices are filled with anhedral quartz and plagioclase. d) Example of a microstructure formed by an open framework of very sodic plagioclase (~An15).The interstices are filled with anhedral quartz and euhedral small pink garnets. This is interpreted as the crystallisation of a highly evolved melt, after K-feldspar has been fractionated. e) Biotite schlieren delimit zones of different grain size in a leucogranite. This is interpreted as evidence of multiple injections of magma. The schlieren are the main source of mafic minerals in the leucogranites. Note how larger grains with higher aspect ratio are elongated parallel to the foliation.

4.5 THE LEUCOGRANITIC VEINS AND DYKES

4.5.1 MACROSCOPIC FEATURES

Veins and dykes of leucogranite are common throughout the Opinaca Subprovince, and in some outcrops they are abundant (Fig. 4.6). Most leucogranitic veins are simple subvertical sheets that were injected parallel to the main schistosity S_2 (Fig. 4.6a). The exceptions are small (few 10s cm wide), irregular bodies of leucogranite located in fold hinges and other low-pressure sites interpreted to be accumulations of local anatectic melt. Some veins cross the schistosity (mostly at low angles) and link between layer-parallel veins to create an anastomosing network. Most of the leucogranite occurs as thin veins or dykes from a centimeter to several tens of centimeters wide. Veins wider than several tens of centimeters typically contain textural evidence of multiple injection of leucogranite, such as the presence of multiple schlieren parallel to the vein wall, abrupt variations in texture, or crack and seal type structures (Fig. 4.5e & 4.6c). Thus, wider veins are built by multiple, small volume injections of magma.

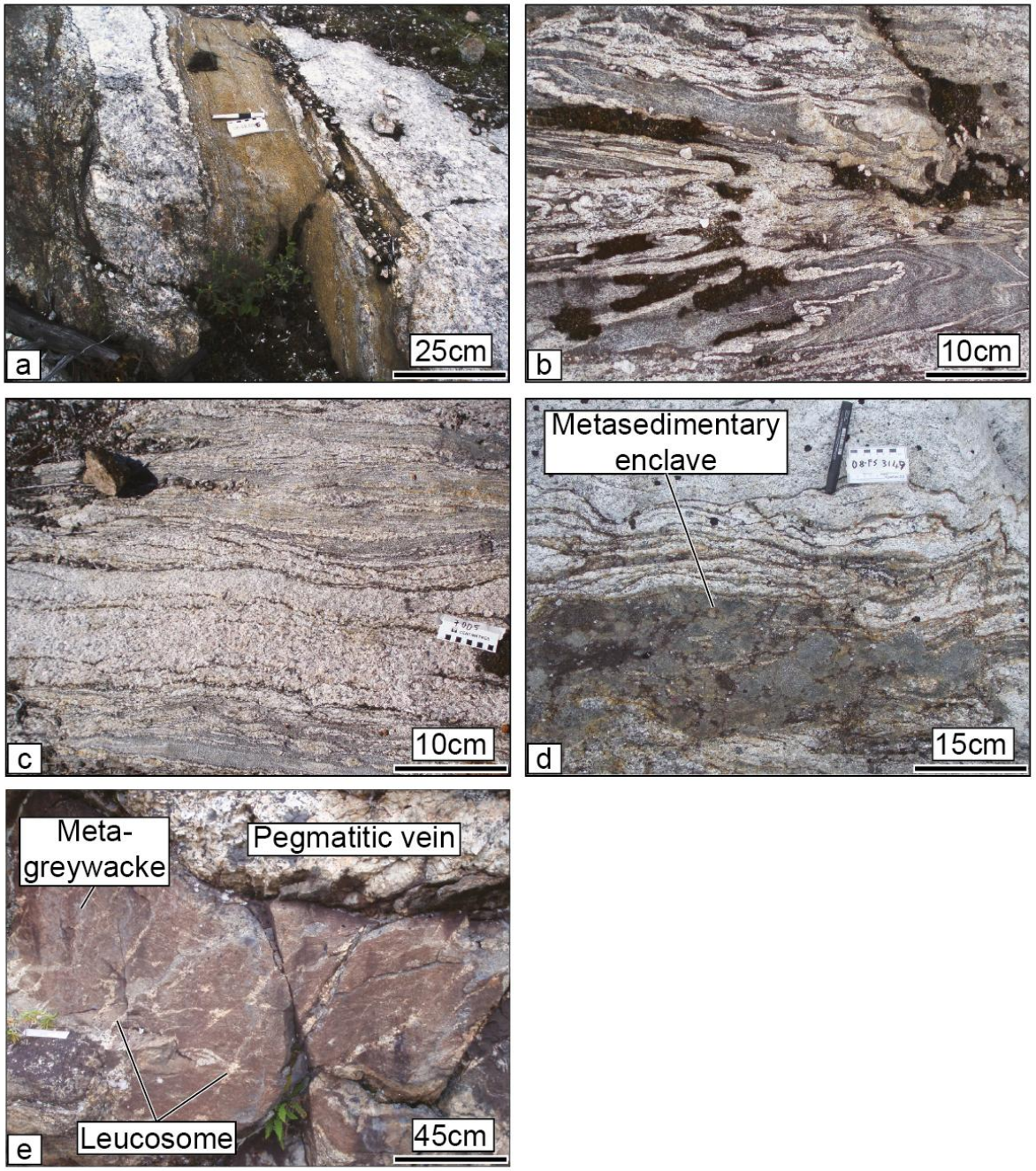

Figure 4.6: Field aspect of leucogranite dykes and veins in the Opinaca injection complex. a) Simple vertical leucogranite sheets injected into metagreywacke. Note the presence of schlieren and elongated enclaves along the host-dyke contact. b) Folded veins of leucogranite. Veins injected parallel to the foliation in the metasedimentary rocks are boudinaged (top of picture) whereas veins injected perpendicular to it, are folded with some dextral shearing. c) Typical

leucogranitic vein constructed by multiple injections which are separated by biotite schlieren. d) Irregular-shaped metasedimentary enclave in a leucogranite host. The contact between enclave and granites is marked by multiple schlieren roughly following the shape of the enclave. Note the heterogeneous texture of the host granite (see top right of picture). e) Linked and coalesced in situ leucosomes; some patches of former melt are linked to each other, but they do not connect with the pegmatitic vein located at the top of picture.

Some large outcrops, typically situated on top of small hills, are dominated by somewhat wider (~1m) veins of leucogranite. In these, the leucogranite no longer has a banded appearance, but is a more homogeneous leucogranite with patches of pegmatite and irregularly shaped enclaves of host rock (Fig. 4.6d). A relative chronology can be deduced for the leucocratic veins and dykes. Early crystallised veins are either boudinaged if initially parallel to S_2, or asymmetrically folded if initially at angle with S_2 (Fig. 4.6b). Veins which are straight and cross the foliation are clearly late as they post-date the main deformation event; these typically have pegmatitic or aplitic textures. The various geometrical and deformation features indicate that the injection of leucogranite veins and dykes started before, and ended after the main (D_2) regional deformation event.

4.5.2 PETROLOGY OF THE LEUCOCRATIC VEINS

Typical leucocratic veins have medium to coarse-grained microstructure (Fig. 4.7). Pegmatite texture is very common. Aplites are less common and restricted to thin (<10cm), late veins in outcrops that have abundant leucogranitic veins.

The typical mineral assemblage in leucogranitic veins is quartz + plagioclase + K-feldspar + biotite ± garnet ± tourmaline, with rare amphibole. The modal composition ranges from granite to tonalite. Biotite is by far the most abundant mafic mineral, nevertheless, its mode is <5%. Moreover, much of the biotite in the leucocratic veins appears to be derived from

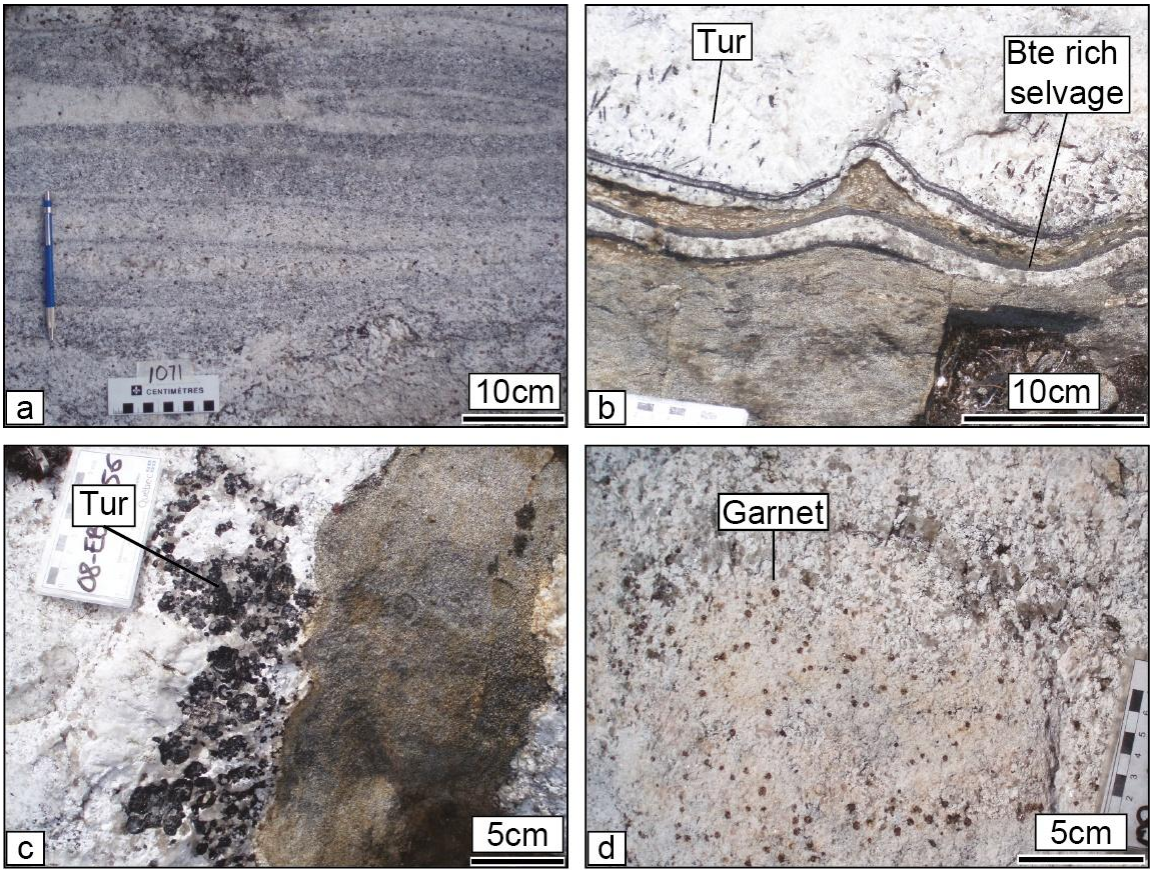

Figure 4.7: Field photographs showing petrological features of the leucogranite. a) Various changes in grain size and composition in leucogranite from a single outcrop. White bands are richer in feldspar compared to the quartz-rich darker bands. b) Interaction between a leucogranite vein and the metasedimentary host resulting in the development of a dark selvage mostly composed of biotite. Tourmaline needles grow close to and perpendicular to the vein/host contact. c) Tourmaline-rich selvage to a pegmatitic vein. The tourmaline is restricted to areas close to the contact with the metasediment and is more common in and adjacent to pegmatitic veins. d) Small patches rich in pink almandine garnet (up to 5mm) in a leucogranitic aplitic patch inside a pegmatite.

the break-up of biotite-rich schlieren and the disaggregation and assimilation of enclaves of the metasedimentary host rocks. Many thin isolated leucogranite veins have a biotite-rich selvage that is a few millimeters wide (Fig. 4.7b). These melanocratic selvages are interpreted to be the result of diffusional exchange between the leucogranite and its host rather than a melanosome (residuum), because there is no evidence for partial melting in the immediately adjacent metasedimentary units. Tourmaline is commonly developed at the contacts with leucogranitic veins and the metasedimentary host rocks, but also occurs in some pegmatite-textured veins (Fig. 4.7b & c). Garnet typically occurs as small (up to a few millimeters) pink crystals in highly leucocratic veins of aplite and pegmatite (Fig. 4.5d & 4.7d). The typical assemblage of accessory minerals is zircon, apatite, monazite and titanite.

4.5.3 MICROSTRUCTURE OF THE LEUCOGRANITE

The quartz in most leucogranites commonly displays weak undulose extinction and the development of some lobate grain boundaries indicates recovery and recrystallisation after moderate deformation. Nevertheless, the original magmatic microstructure is preserved, particularly in the medium grained to coarse grained (3 to 8 mm) veins of leucogranite. Typically, the microstructure in these veins consists of a well-developed framework of subhedral crystals of feldspar (Fig. 4.5c) that is filled with interstitial quartz; this is interpreted to be a primary magmatic microstructure. There are two variants of this

microstructure. In one the framework consists predominantly of larger crystals of sodic plagioclase to which quartz and, less commonly, K-feldspar are interstitial (Fig. 4.5d). In the other, more common variety, the framework comprises of crystals of subhedral K-feldspar (Fig. 4.5c). No systematic structural relationships that could have indicated a relative chronology between the two vein types was observed in the field. In some leucogranites the feldspars that construct the framework are also weakly aligned. However, the main indicators of an alignment of minerals are the scattered flakes of biotite, or, where present, the schlieren of biotite (Fig. 4.5e). Both microstructures indicate that some of the leucogranite veins preserve a magmatic flow fabric.

Other veins of leucogranite have a smaller (2 to 4 mm), and more uniform, grain size and crystals of quartz are equant, or slightly elongate, with irregular lobate (rounded) bulges. In these rocks recovery followed by grain boundary migration in response to the main D_2 phase of deformation has reduced the grain size and largely destroyed the initial magmatic fabric (Fig. 4.5d), which has been replaced by a weak shape-preferred orientation of quartz, feldspar and biotite that is parallel to the regional S_2 schistosity.

The great variability of microstructure amongst the leucogranitic veins indicates that each vein has a different temporal relationship to the deformation. Early crystallising veins which have experienced the regional deformation for a longer time would also have experienced a longer period of time at high temperature, and thus more time for its initial texture to completely re-equilibrate. Samples with the least textural maturation are interpreted to have been injected and crystallised later in the development of the injection

complex. The nature of the feldspar framework structure provides significant information for the interpretation of the leucogranites because it indicates which feldspar crystallised first.

4.6 GEOCHEMISTRY OF THE LEUCOGRANITES

4.6.1 SAMPLING AND ANALYTICAL METHODS

Sampling the veins and dykes of leucogranite from the metasedimentary rocks in the Opinaca Subprovince is unlikely to have been truly representative because of the difficulty in extracting sufficient material from very thin (<10mm) veins of leucogranite. Consequently, the thinnest leucogranites are under-represented in the geochemical data base (but not amongst the thin sections). In total 39 samples of leucogranitic veins collected during our mapping of the Opinaca Subprovince (Bandyayera et al., 2010). Four additional samples of leucogranitic veins from the adjacent area (see Fig. 4.1) that was mapped and reported by Simard and Gosselin (1999) and Bandyayera et al. (2011) are also included in this study.

The major and trace element compositions determined for the 39 samples of leucogranites are given in Table 4. 1 along with some relevant metasediments from the Quetico and Opinaca Subprovinces. Standard whole rock analyses were performed on 32 samples by X-Ray Fluorescence for the major elements and via ICP-MS for the trace elements at ACME

labs in Vancouver, Canada. Seven samples were analysed at COREM laboratory in Québec city by X-Ray Fluorescence for the major elements and by Instrumental Neutron Activation Analysis (INAA) for the trace elements.

Whole rock oxygen $^{18}O/^{16}O$ ratios were determined on 17 samples from the study area, four additional, previously unpublished, analysis of leucogranites from the Ashuanipi Subprovince are included (Table 4.2). Analyses were performed by the conventional fluorination method at the Facility for Isotope Research of Queen's University. Results are in standard $\delta^{18}O$ notation relative to SMOW (per mil). Analytical error is 0.1-0.2‰.

Sample	06-AF-3007A	06-AF-3097A	06-AF-3116A	06-AF-3145A	06-AF-3153A	06-AF-3166A	06-DB-1081A	06-MA-4129B2	06-NT-8012A
Field description	Tonalite	Granite	Granodiorite	Granodiorite	Tonalite	Granodiorite	Granodiorite	Tonalite	Tonalite
REE Group	3	3	1	2	3	2	1	1	1
Major Oydes (wt%)									
SiO2	76.38	74.76	73.76	75.23	70.41	76.04	74.00	75.06	72.89
TiO2	0.04	0.04	0.21	0.08	0.17	0.02	0.13	0.11	0.23
Al2O3	13.56	14.42	14.17	13.83	16.81	13.69	14.14	13.85	14.71
FeOt	0.45	0.51	1.58	1.13	1.27	0.42	1.64	0.91	1.20
MnO	0.01	0.01	0.03	0.05	0.01	0.01	0.02	0.01	0.01
MgO	0.16	0.18	0.38	0.21	0.71	0.10	0.31	0.30	0.51
CaO	1.16	1.27	1.11	0.82	2.79	0.90	0.90	1.00	1.25
Na2O	3.15	3.33	3.96	3.71	4.68	3.52	3.46	3.50	2.75
K2O	5.07	5.46	4.73	4.88	3.05	5.27	5.37	5.23	6.36
P2O5	0.02	0.03	0.07	0.05	0.10	0.03	0.04	0.03	0.08
LOI	0.20	0.30	0.10	0.50	0.60	0.40	2.00	0.60	0.70
ASI	1.06	1.05	1.04	1.07	1.04	1.04	1.08	1.05	1.07
Mg#	36.40	36.54	27.97	23.17	47.34	28.02	23.51	35.03	41.02
ICPW Norm									
Q	36	31	30	33	25	33	30	32	29
Or	30	32	28	29	18	31	31	31	37
Ab	27	28	33	31	39	30	29	29	23
An	6	6	5	4	13	4	4	5	6
C	1	1	1	1	1	1	1	1	1
Trace Elements (ppm)									
Cs	3.2	1.3	1.7	7.5	0.9	0.4	1.0	1.1	1.9
Rb	118	119	218	273	81	107	142	117	176
Sr	472	497	201	106	558	88	253	243	415
Ba	950	1241	602	437	705	186	505	1162	1024
Y	2.40	1.50	7.30	21.80	4.80	13.60	6.20	5.00	5.40
Zr	76.7	80.6	213.5	104.5	211.4	45.0	155.0	90.0	61.8
Hf	2.7	3.0	6.4	3.9	6.7	2.0	5.4	3.2	1.9
Nb	1.9	1.3	9.5	13.6	4.0		2.8	4.1	5.3
Ta	0.3	0.1	0.6	2.0	0.2		0.1	0.2	0.2
Th	18.9	8.2	15.7	36.3	2.4	17.0	79.5	29.9	13.1
U	2.7	1.8	0.9	7.3	0.8	2.7	5.4	2.9	0.5
Pb	11.9	5.3	11.0	13.6	4.9	14.1	24.1	17.8	7.4
V	9.0	6.0	15.0	5.0	26.0		14.0	10.0	16.0
Ni	2.9	1.2	3.6	1.8	2.8	0.9	1.4	1.9	5.8
Co	1.0	1.3	2.3	1.4	4.2	0.5	1.6	2.6	2.8
Cu	3.0	0.9	8.3	1.5	3.6	1.1	1.9	11.2	2.0
Zn	7.0	7.0	28.0	24.0	20.0	4.0	25.0	19.0	18.0
Ga	15	16	19	20	20	16	18	16	16
Sn	1.0		2.0	5.0			1.0		
W	0.1	0.1		0.1				0.1	0.1
REE (ppm)									
La	9.1	17.0	29.9	33.1	14.0	13.7	74.6	28.9	69.4
Ce	25.6	32.4	72.5	71.3	27.1	29.5	158.8	57.7	134.1
Pr	1.99	2.95	6.56	7.51	2.72	3.17	15.83	5.47	14.51
Nd	6.0	8.7	21.6	24.9	9.4	10.9	57.7	17.7	46.2
Sm	1.0	1.1	2.8	5.5	1.7	2.7	8.6	3.0	5.2
Eu	0.71	0.65	0.49	0.27	0.78	0.20	0.66	0.66	1.21
Gd	0.55	0.46	1.60	4.54	1.37	2.46	4.41	1.71	2.56
Tb	0.08	0.07	0.25	0.75	0.17	0.42	0.47	0.24	0.33
Dy	0.43	0.31	1.18	3.66	0.98	2.18	1.68	0.94	1.21
Ho	0.08		0.23	0.66	0.15	0.40	0.20	0.17	0.17
Er	0.25	0.14	0.62	1.99	0.41	1.20	0.48	0.41	0.41
Tm			0.11	0.34		0.16	0.06	0.06	0.06
Yb	0.27	0.17	0.64	2.46	0.39	1.00	0.37	0.40	0.31
Lu	0.05	0.03	0.10	0.41	0.07	0.16	0.06	0.07	0.06
Rb/Sr	0.2	0.2	1.1	2.6	0.1	1.2	0.6	0.5	0.4
K/Rb	35.7	38.1	18.0	14.9	31.2	41.0	31.4	37.3	30.1
Nb/Ta	6.3	13.0	15.8	6.8	20.0		28.0	20.5	26.5
Eu/Eu*	2.4	2.1	0.6	0.2	1.5	0.2	0.3	0.8	0.8
La/Yb norm	22.8	67.6	31.6	9.1	24.3	9.3	136.2	48.8	151.3

Sample	08-CC-8010B	08-CM-2044B	08-CM-2045B	08-DB-1071A	08-EB-5079A	08-EB-5107A	08-EB-5163A	08-EB-5165A
Field description	Pegmatite	Granite	Granite	Pegmatite	Granite	Granodiorite	Tonalite	Aplite
REE Group	1	3	3	2	2	1	1	2
Major Oydes (wt%)								
SiO2	69.89	77.57	74.44	76.43	76.99	73.86	72.82	76.22
TiO2	0.33	0.07	0.02	0.01	0.03	0.06	0.29	0.02
Al2O3	15.99	13.49	14.74	13.81	13.63	14.66	14.30	13.65
FeOt	1.69	0.60	0.46	0.65	0.64	0.72	2.29	0.41
MnO	0.01	0.01	0.01	0.10	0.01	0.01	0.03	0.01
MgO	1.03	0.42	0.19	0.08	0.12	0.33	1.17	0.09
CaO	1.58	1.72	1.62	0.46	1.42	0.82	2.76	0.83
Na2O	3.67	4.22	3.36	4.98	4.84	3.10	3.40	3.74
K2O	5.67	1.88	5.13	3.44	2.30	6.41	2.81	4.99
P2O5	0.13	0.02	0.03	0.02	0.02	0.02	0.12	0.04
LOI	1.80	1.20	0.60	0.80	0.50	0.70	0.40	0.30
ASI	1.06	1.11	1.05	1.08	1.05	1.08	1.05	1.04
Mg#	50.03	52.90	40.15	16.66	23.26	42.95	45.29	25.92
ICPW Norm								
Q	22	41	31	33	37	29		33
Or	33	11	30	20	14	37		29
Ab	30	35	28	42	41	26		32
An	7	8	8	2	7	4		4
C	1	1	1	1	1	1		1
Trace Elements (ppm)								
Cs	2.8	0.5	0.8	5.3	2.0	1.1	5.2	1.2
Rb	145	46	92	216	70	117	95	84
Sr	456	411	584	11	92	468	557	41
Ba	1390	428	2229	17	42	2475	992	58
Y	7.70	1.30	0.80	17.50	45.40	3.60	7.60	27.50
Zr	292.9	393.6	79.8	14.7	64.3	97.2	150.9	89.1
Hf	7.9	10.7	2.6	1.3	4.1	2.4	4.1	4.7
Nb	6.4	1.4	0.5	1.7	2.9	1.3	7.9	7.2
Ta	0.3	0.2	0.1	0.4	0.3	0.1	0.7	0.4
Th	50.5	3.7	1.9	2.7	17.6	29.9	14.9	22.8
U	3.1	1.2	0.7	1.6	9.0	2.1	2.4	8.1
Pb	9.5	4.7	5.4	1.7	7.7	14.4	7.0	3.6
V	39.0	12.0	8.0	8.0	8.0	8.0	28.0	8.0
Ni	10.9	7.3	2.7	0.7	0.7	1.4	13.8	0.6
Co	5.3	2.2	1.0	0.3	0.4	1.8	5.5	0.4
Cu	0.6	17.1	2.6	1.1	3.2	1.2	6.0	2.3
Zn	24.0	8.0	5.0	1.0	7.0	8.0	33.0	3.0
Ga	18	14	13	21	20	12	15	19
Sn	1.0	1.0	1.0	2.0	1.0	1.0	1.0	1.0
W	0.5	0.5	0.5	0.5	0.5	0.5	0.5	0.5
REE (ppm)								
La	94.9	11.4	6.2	4.2	1.8	58.8	28.3	6.0
Ce	158.5	16.0	9.5	10.0	3.4	112.4	52.3	11.3
Pr	17.34	1.62	0.90	1.29	0.40	12.57	6.08	1.37
Nd	55.1	5.0	2.6	5.5	1.9	40.1	20.0	4.9
Sm	6.9	0.6	0.4	1.5	1.1	5.3	2.8	1.3
Eu	0.97	0.69	1.14	0.03	0.19	1.19	0.67	0.12
Gd	4.33	0.36	0.25	1.44	2.88	3.04	2.21	2.40
Tb	0.50	0.04	0.03	0.28	0.79	0.28	0.23	0.50
Dy	1.90	0.20	0.16	2.34	5.20	1.03	1.38	4.17
Ho	0.27	0.04	0.02	0.48	1.34	0.11	0.28	0.92
Er	0.67	0.14	0.08	1.83	4.61	0.27	0.78	2.95
Tm	0.07	0.03	0.02	0.50	0.71	0.03	0.13	0.50
Yb	0.44	0.23	0.11	4.15	4.54	0.20	0.88	3.22
Lu	0.06	0.05	0.03	0.73	0.70	0.03	0.12	0.46
Rb/Sr	0.3	0.1	0.2	19.5	0.8	0.2	0.2	2.1
K/Rb	32.6	34.0	46.1	13.2	27.3	45.7	24.7	49.3
Nb/Ta	21.3	7.0	5.0	4.3	9.7	13.0	11.3	18.0
Eu/Eu*	0.5	4.1	10.8	0.1	0.3	0.8	0.8	0.2
La/Yb norm	145.7	33.5	38.1	0.7	0.3	198.7	21.7	1.3

Sample	08-FS-3018A	08-FS-3153A	08-GR-4110A	08-GR-4119B	08-PR-6018A	08-PR-6049A	09-EB-2108D	09-SB-5011B
Field description	Granite	Pegmatite	Tonalite	Pegmatite	Pegmatite	Granite	Granodiorite	Granite
REE Group	1	2	2	3	1	3	1	3
Major Oydes (wt%)								
SiO2	73.93	74.44	77.12	74.57	73.88	75.21	75.16	75.87
TiO2	0.14	0.03	0.01	0.06	0.10	0.01	0.11	0.03
Al2O3	14.36	14.39	13.60	14.43	14.29	13.91	13.68	13.94
FeOt	1.12	0.41	0.68	1.02	0.95	0.32	0.86	0.36
MnO	0.01	0.01	0.20	0.02	0.01	0.01		
MgO	0.37	0.15	0.09	0.36	0.37	0.07	0.44	0.17
CaO	1.30	0.52	1.75	1.50	0.85	0.83	1.19	0.88
Na2O	3.21	3.11	5.36	3.84	3.09	2.88	2.88	3.60
K2O	5.51	6.88	1.18	4.17	6.39	6.75	5.62	5.13
P2O5	0.04	0.06	0.02	0.03	0.07	0.02	0.06	0.02
LOI	0.40	0.80	0.50	0.80	0.40	0.20	0.70	0.40
ASI	1.05	1.06	1.02	1.06	1.05	1.03	1.05	1.06
Mg#	34.88	37.48	17.70	36.67	38.75	26.33	45.48	43.24
ICPW Norm								
Q	31	29	37	32	29	31	34	33
Or	32	40	7	24	37	40	33	30
Ab	27	26	45	32	26	24	24	30
An	6	2	9	7	4	4	5	4
C	1	1	0	1	1	0	1	1
Trace Elements (ppm)								
Cs	1.7	2.4	0.6	1.9	1.2	1.7	0.7	0.7
Rb	148	125	54	82	151	156	113	96
Sr	275	116	141	291	293	108	379	276
Ba	869	299	40	735	870	142	1319	740
Y	3.10	47.10	32.40	3.00	8.00	5.60	7.20	1.10
Zr	190.9	46.1	69.5	156.9	178.4	62.7	183.3	99.8
Hf	6.3	1.7	2.9	5.3	5.7	3.5	6.0	3.7
Nb	2.0	0.9	0.4	1.3	4.2	0.1	2.3	
Ta	0.1	0.1	0.1	0.1	0.4	0.1		
Th	37.0	15.0	9.2	26.5	31.6	12.6	50.3	3.8
U	2.1	2.7	1.8	3.0	2.2	10.2	2.6	1.7
Pb	10.5	4.5	11.8	10.3	13.8	3.6	14.5	8.8
V	16.0	8.0	8.0	18.0	15.0	8.0		
Ni	2.5	0.9	0.8	5.4	2.9	0.7	6.4	3.3
Co	1.9	0.5	0.4	2.2	1.9	0.3	2.6	
Cu	1.0	1.3	3.8	4.6	1.9	0.6	2.7	1.8
Zn	13.0	6.0	4.0	12.0	13.0	3.0	11.0	4.0
Ga	15	14	16	14	14	16	12	14
Sn	1.0	1.0	1.0	1.0	1.0	1.0		
W	0.5	0.5	0.5	0.5	0.5	0.5		
REE (ppm)								
La	29.2	9.6	16.1	24.1	73.1	3.3	74.5	5.6
Ce	64.9	21.2	29.5	51.9	109.9	5.4	152.7	9.1
Pr	6.03	2.60	3.32	5.23	13.86	0.54	15.64	0.87
Nd	19.2	9.3	9.7	13.8	44.4	2.6	52.1	3.0
Sm	2.6	2.8	1.6	1.9	5.2	0.6	8.1	0.4
Eu	0.63	0.24	0.16	0.73	0.68	0.29	1.10	0.68
Gd	1.38	3.60	1.61	1.11	3.20	0.75	5.77	0.37
Tb	0.16	0.90	0.35	0.11	0.36	0.13	0.58	0.04
Dy	0.72	5.98	3.61	0.57	1.51	0.82	2.16	0.24
Ho	0.11	1.42	1.03	0.10	0.23	0.18	0.22	
Er	0.30	4.28	4.53	0.31	0.63	0.44	0.55	0.09
Tm	0.05	0.68	1.08	0.05	0.10	0.08		
Yb	0.39	3.93	8.90	0.37	0.69	0.46	0.52	0.15
Lu	0.06	0.55	1.58	0.06	0.12	0.07		
Rb/Sr	0.5	1.1	0.4	0.3	0.5	1.4	0.3	0.3
K/Rb	31.0	45.7	18.1	42.2	35.2	36.0	41.3	44.3
Nb/Ta	20.0	9.0	4.0	13.0	10.5	1.0		
Eu/Eu*	0.9	0.2	0.3	1.4	0.5	1.4	0.5	5.2
La/Yb norm	50.6	1.7	1.2	44.0	71.6	4.8	96.8	25.2

Sample	09-SM-6255A	09-SM6263C1	09-SM-6263C2	98-MB-12	98-MB-12	98-SL-3018A	98-SL-3029A	CG-1175-3A-97
Field description	Granite	Granite	Granite	Granite	Granite	Monzogranite	Granodiorite	Granite
REE Group	1	1	3	n.d.	n.d.	1	n.d.	1
Major Oydes (wt%)								
SiO2	72.72	75.35	73.14	77.45	75.07	74.83	75.44	74.71
TiO2	0.07	0.18	0.04	0.00	0.00	0.12	0.13	0.09
Al2O3	14.80	13.02	14.84	13.95	14.97	14.04	14.10	13.97
FeOt	1.14	1.59	0.39	0.00	1.21	1.17	1.05	0.81
MnO	0.02	0.03	0.01			0.01	0.01	0.01
MgO	0.61	0.82	0.12	0.00	0.00	0.26	0.36	0.21
CaO	0.98	0.93	0.52	0.00	1.76	0.38	2.30	1.04
Na2O	2.65	3.15	3.79	4.01	5.08	4.13	3.87	3.63
K2O	6.87	4.87	7.12	4.58	1.90	4.97	2.69	5.51
P2O5	0.15	0.06	0.03	0.00	0.00	0.08	0.05	0.02
LOI	0.60	0.94	0.42	1.10	1.03	0.59	0.43	0.20
ASI	1.09	1.07	1.00	1.21	1.10	1.09	1.05	1.01
Mg#	46.39	45.22	32.68			26.62	35.78	
ICPW Norm								
Q	28	35	23			31	37	30
Or	40	29	42			29	16	33
Ab	22	27	32			35	32	31
An	4	4	2			1	11	5
C	2	1	0			1	1	0
Trace Elements (ppm)								
Cs	1.0	1.0	6.6		16.0			2.9
Rb	133	120	260	89	52	227	72	164
Sr	477	400	199	120	242	99	210	119
Ba	2501	1631	828	410	480	510	770	414
Y	9.00	16.28	2.16	18.00	9.00	15.00	4.00	10.00
Zr	93.6	296.0	11.0	20.0	96.0	114.0	96.0	92.0
Hf	2.7	8.0	0.3		27.0	4.0	3.2	3.4
Nb		3.7	10.8	58.0	4.0	11.0	3.0	9.0
Ta		0.3	1.3					0.9
Th	21.7	60.8	10.4	97.0	87.0	30.0	9.8	22.9
U	1.6	2.7	1.0	2.0	27.0	5.2		7.2
Pb	8.7	32.8	34.7	32.0	17.0			
V		26.6	2.4					
Ni	2.0	14.2						
Co	2.3	5.3	0.7					0.8
Cu	1.3	9.5	2.7		150.0			
Zn	15.0	27.0	12.0	10.0	18.0			
Ga	12	13	20	17	17	18	14	17
Sn		0.8	1.4					
W		0.2	2.2					
REE (ppm)								
La	49.8	119.6	17.9	73.0	16.0	43.0	12.0	23.4
Ce	104.6	238.8	32.1	14.0	25.0	87.0	21.0	41.8
Pr	10.87	26.16	3.18	15.00	25.00			
Nd	39.2	88.9	9.9	52.0	83.0	18.0	5.0	16.1
Sm	6.1	13.0	1.4	15.0	14.0	3.7	1.2	3.0
Eu	1.22	1.24	0.60			0.60	0.80	0.32
Gd	3.73	7.33	0.75		13.00			
Tb	0.49	0.73	0.09					0.34
Dy	2.14	3.36	0.44	28.00	12.00			
Ho	0.30	0.61	0.07					1,5149
Er	0.74	1.79	0.19	18.00				
Tm		0.29	0.02			1,0	0.90	
Yb	0.47	2.03	0.17	15.00		0.80		1.03
Lu		0.33	0.03			0.10		0.17
Rb/Sr	0.3	0.3	1.3	0.7	0.2	2.3	0.3	1.4
K/Rb	42.8	33.7	22.7	42.8	30.4	18.2	31.0	27.9
Nb/Ta		12.7	8.1					9.8
Eu/Eu*	0.7	0.3	1.5					0.3
La/Yb norm	71.6	39.8	72.5	3.3		36.3		15.3

Sample	JP-5136-3C-97	MS-125-3A-97(3)	MS-176-3A-97	MS-71-3A-97	MS-88-3B-97	PB-4161-3B-97
Field description	Granite	Granite	Diatexite	Granite	Granite	Granite
REE Group	1	3	n.d.	3	n.d.	1
Major Oydes (wt%)						
SiO2	76.85	76.49	73.10	77.17	78.31	73.66
TiO2	0.00	0.01		0.02	0.03	0.14
Al2O3	14.18	13.47	14.66	13.21	12.55	14.37
FeOt		0.18	1.55	0.40	0.32	0.93
MnO						
MgO		0.07	0.00	0.00	0.10	0.30
CaO	2.00	1.48	2.04	0.76	0.98	1.29
Na2O	4.83	3.37	8.00	4.13	2.66	3.20
K2O	2.11	4.91	0.65	4.31	5.03	6.06
P2O5	0.03	0.02		0.00	0.01	0.05
LOI	1.27	0.37	2.25	0.27	0.48	0.39
ASI	1.02	0.99	0.83	1.03	1.08	1.01
Mg#		38.39			33.21	34.29
ICPW Norm						
Q		35			41	29
Or		29			30	36
Ab		29			22	27
An		7			5	6
C		0			1	0
Trace Elements (ppm)						
Cs	1.0	0.6		0.6	0.8	1.8
Rb	59	103		77	127	149
Sr	174	380	1200	181	402	249
Ba	214	1077				
Y	8.00	1.20		3.00		4.00
Zr	104.0	111.0	93.0	62.0	121.0	155.0
Hf	4.2	3.7	2.8	2.3	4.7	5.2
Nb		0.4				
Ta	0.5					0.1
Th	43.3	1.0		6.4	71.0	36.0
U	5.1	1.1		4.5	6.6	3.6
Pb		23.1				
V		2.4				
Ni		1.9				
Co	0.7	0.8				
Cu		3.1				
Zn						
Ga	17	13	26	17	13	15
Sn		0.3				
W						
REE (ppm)						
La	29.0	6.0	4.2	8.1	3.8	40.0
Ce	44.3	9.0	8.0	14.0	8.0	77.0
Pr		0.84				
Nd	18.5	2.7	5.0	2.0		21.0
Sm	3.0	0.5		0.5		3.9
Eu	0.48	0.78	0.30	0.40	1.00	0.80
Gd		0.31				
Tb	0.28	0.04			0.10	0.30
Dy		0.21				
Ho	0,9928	0.04				1,3
Er		0.12				
Tm		0.02				
Yb	0.28	0.17		0.20		0.20
Lu	0.12	0.03				0.06
Rb/Sr	0.3	0.3	0.0	0.4	0.3	0.6
K/Rb	29.7	39.5		46.6	32.9	33.8
Nb/Ta	0.0					0.0
Eu/Eu*	0.5	5.8				0.7
La/Yb norm	69.2	24.2		27.4		135.1

Sample	ES356	Opinaca Average	Quetico low grade average
Field description	Metagreywacke	Metagreywacke	Metagreywacke
REE Group	n.a.	n.a.	n.a.
Major Oydes (wt%)			
SiO2	65.49	65.54	61.52
TiO2	0.57	0.53	0.61
Al2O3	15.73	15.74	16.33
FeOt	5.69	5.36	5.36
MnO	0.09	0.08	0.09
MgO	3.54	3.05	3.30
CaO	2.72	3.42	2.21
Na2O	3.96	3.72	2.77
K2O	2.01	2.38	3.06
P2O5	0.19	0.18	0.17
LOI	1.66	1.26	1.87
ASI	1.15	1.05	1.37
Mg#	50.44	48.28	40.76
ICPW Norm			
Q	24	23	20
Or	12	14	18
Ab	33	31	23
An	12	15	10
C	3	1	4
Trace Elements (ppm)			
Cs	6.0	8.2	5.4
Rb	72	97	102
Sr	440	570	287
Ba	514	687	650
Y	12.00	12.34	15.52
Zr	139.0	131.1	134.6
Hf	3.1	3.7	3.1
Nb	-5.0	6.1	
Ta	0.4	0.5	
Th	5.7	8.4	6.5
U	1.8	2.1	2.2
Pb	0.0	5.6	
V	-5.0	103.7	
Ni	-5.0	52.9	
Co	-5.0	16.0	6.0
Cu	-5.0	33.1	
Zn	72.0	51.1	94.1
Ga	0	19	
Sn	0.0	1.4	
W	0.0	0.8	
REE (ppm)			
La	29.4	19.5	28.2
Ce	54.0	40.0	56.3
Pr		4.80	
Nd	23.5	18.1	26.5
Sm	4.5	3.2	4.7
Eu	1.20	0.96	1.27
Gd	0.00	2.74	
Tb	0.47	0.38	0.46
Dy	0.00	2.21	
Ho	0.00	0.43	
Er		1.20	
Tm	0.00	0.19	
Yb	1.40	1.22	1.53
Lu	0.22	0.18	0.24
Rb/Sr	0.2	0.2	0.4
K/Rb	23.2	20.3	25.1
Nb/Ta		11.9	
Eu/Eu*	0.9	1.0	0.9
La/Yb norm	14.2	10.7	12.4

Table 4.1: Whole rock compositions of leucogranites from the Opinaca and two metasedimentary samples. The full data set from our mapping in the Opinaca Subprovince is available from Sigéom, the online portal of the Bureau de l'Exploration Géologique du Québec (sigeom.mrnf.gouv.qc.ca).

4.6.2 MAJOR OXIDES

Leucogranites from the Opinaca Subprovince have alumina saturation index (ASI = molar $Al_2O_3/\{CaO + Na_2O + K_2O\}$) between 0.99 and 1.11, with one outlier at 1.21 (Table 4.1). Based on their mesonorm normative modes plotted on a QAP (Quartz, Alkali-feldspar and Plagioclase) triangle (Fig. 4.8a), 29 of the samples are granite, 8 are granodiorite, one is a tonalite and one is a quartz-monzodiorite. Based on their normative modes, leucogranites from the Opinaca appear to define two main groups, one dominated by K-feldspar and albite plagioclase and another group which is enriched in albitic plagioclase.

The SiO_2 contents of the leucogranites ranges from 69.99 to 78.32 wt.%. The Harker variation diagrams (Fig. 4.9) show negative correlations with Al_2O_3, K_2O, (FeO_t + MgO + TiO_2) with increasing SiO_2; CaO shows no clear correlation, whereas Na_2O increases with silica. An important feature of the composition of the Opinaca leucogranites is that (FeO_t + MgO + TiO_2) is typically lower than, or close to 2 wt.% (except for 3 outliers), and thus consistently lower than in melts produced by the experimental partial melting of appropriate metagreywacke bulk compositions at temperatures of 800 to 900°C and pressures of 5-7 kbar, and which still contained biotite in the end-products (Fig. 4.9).

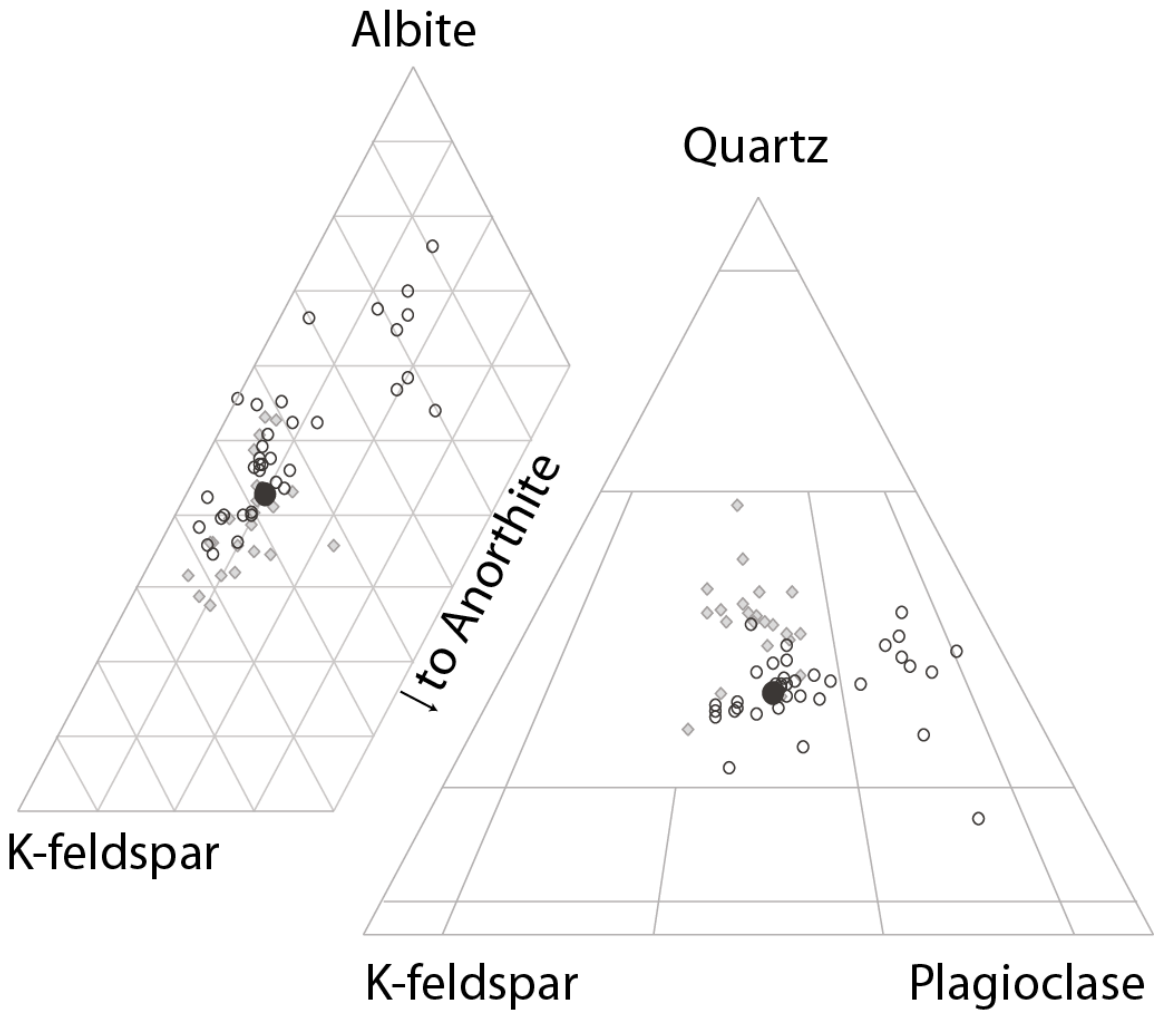

Figure 4.8: Feldspar triangle (left) and Quartz - Alkali feldspar - Plagioclase (right) plot based on mesonorm mineral modes. The figure presents the position of the leucogranites from the Opinaca (open circles) and of the experimental melts (diamonds) produced by partial melting of a metagreywacke between 800 and 900°C, and between 5 and 7 kbar that still contained biotite (Koester et al., 2002; Montel and Vielzeuf, 1997; Patiño Douce and Beard, 1995, 1996; Stevens et al., 1997). The position of sample FS-3018 is marked by the bold, filled circle.

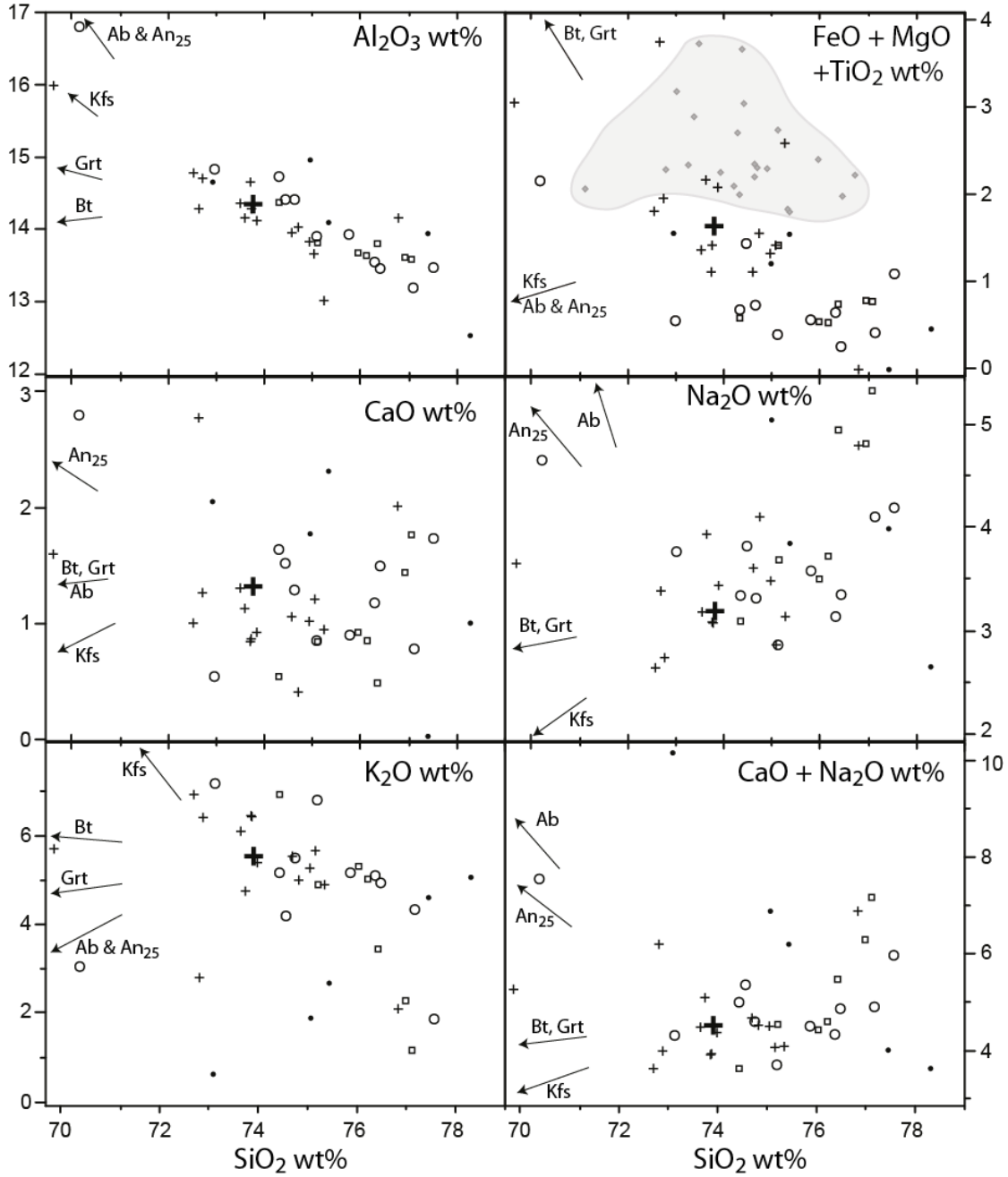

Figure 4.9: Harker diagrams for the major elements: Samples are grouped based on REE groups (see text), group 1, 2 and 3 are crosses, squares and circles, respectively. Sample FS-3018 is represented by the bold cross. Dots are samples for which no REE group was attributed. Major elements trends relative to SiO2 are broadly consistent with fractional crystallisation. The SiO2 vs FeO+MgO+TiO2 plot shows the field (grey) of the same experimental melts as in figure 4.8; most of the leucogranites from the Opinaca are less mafic than the experimental melts.

4.6.3 TRACE ELEMENTS

To differentiate leucogranites produced by partial melting of metasedimentary rocks from other felsic intrusive rocks, such as the late TTG suite injected into the Opinaca, a cut-off at 15ppm Ni was used. Samples with Ni >15ppm are interpreted to be fractionated from a mafic source of the same type as the Deslien Suite in the Ashuanipi Subprovince (Percival et al., 2003) and are thus excluded from the dataset. Samples from the Janin intrusive suite of Bandyayera et al. (2010) were not considered except for the Ajni1 sub-unit samples which are interpreted to be derived from melting of metasedimentary rocks.

The concentration of LILE (large-ion lithophile elements, Rb, Sr and Ba) decreases with increasing SiO_2 (Fig. 4.10). This is consistent with the fact that these elements are mainly partitioned into feldspars, the mode of which decreases as the melt becomes more siliceous, i.e. quartz / (plagioclase + K-feldspar) ratio increases (Fig. 4.9 & 4.10).

The similarity between TiO_2 vs SiO_2 and Zr vs SiO_2 correlations and between Th vs SiO_2 and La vs SiO_2 (Fig. 4.10) are consistent with the presence of the accessory phases titanite, zircon and monazite in the leucogranites. Zr and Hf correlate strongly, which is to be expected since zircon is present, with an average Zr/Hf ratio of 28. Uranium increases with increasing SiO_2 and correlates with both Zr and TiO_2, rather than with La and this indicates control by zircon rather than by monazite.

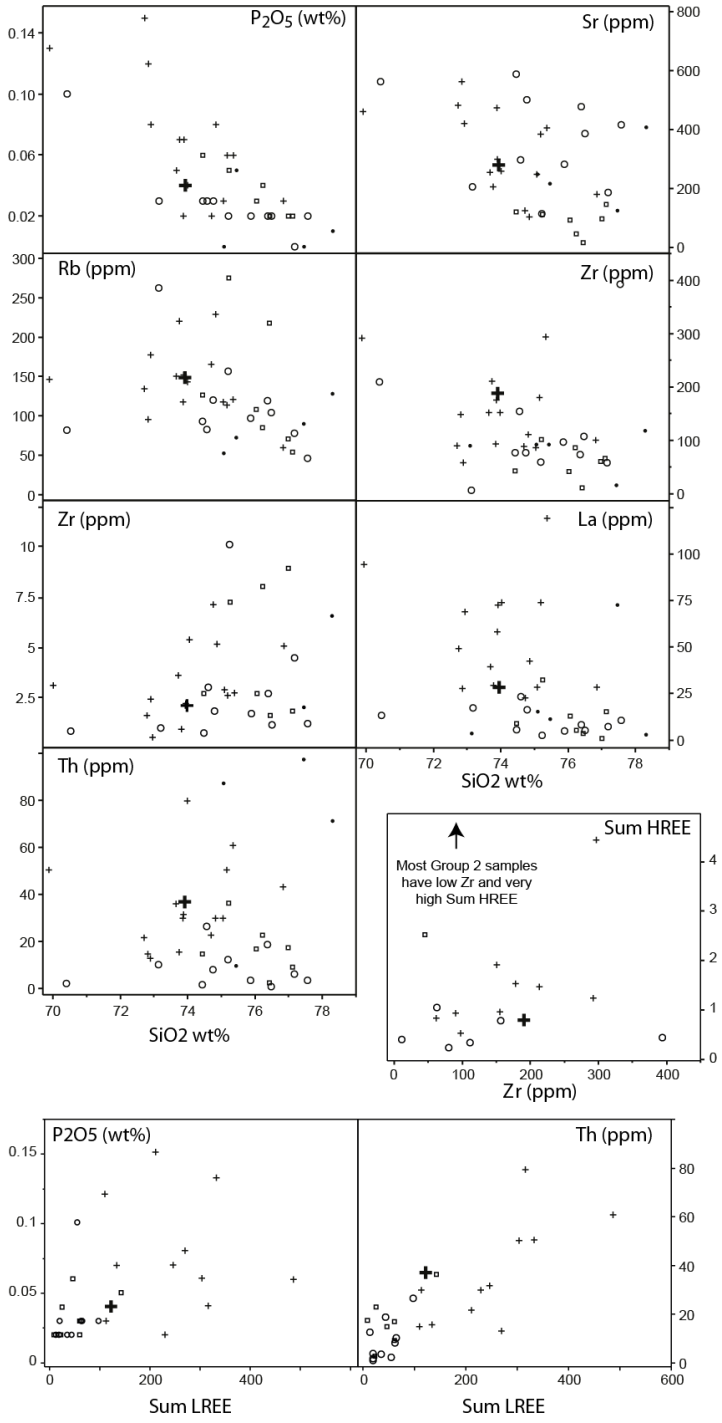

Figure 4.10: Trace element (in ppm) Harker diagrams for leucogranites of the Opinaca Subprovince. Symbols as in figure 4.9. See text and table 4.1 for definition of Group 2.

The light rare earth elements (LREE) are associated with monazite or with apatite because of the generally good correlation with P2O5, but the correlation with Th (Fig. 4.10) indicates that monazite is the main control. The concentration of the heavy rare earth elements (HREE) correlates with Zr (Fig. 4.10), except for garnet-bearing samples from Group 3 (see below).

Based on their chondrite-normalized REE contents (all values and ratios reported are normalised to the factors given by Taylor and McLennan,1995), the leucogranites from the Opinaca can be subdivided into three main groups based on the type of Eu anomaly (where $Eu/Eu^* = Eu_N/(Sm_N.Tb_N)^{1/2}$), the slope of the REE pattern, i.e. La/Yb_N (Fig. 4.11), and their total content of REE ($\sum$REE calculated only for the samples analyzed by ICP-MS). Five samples in the data set are from an older study and were not attributed to a group because fewer of the REE were determined by the INAA method.

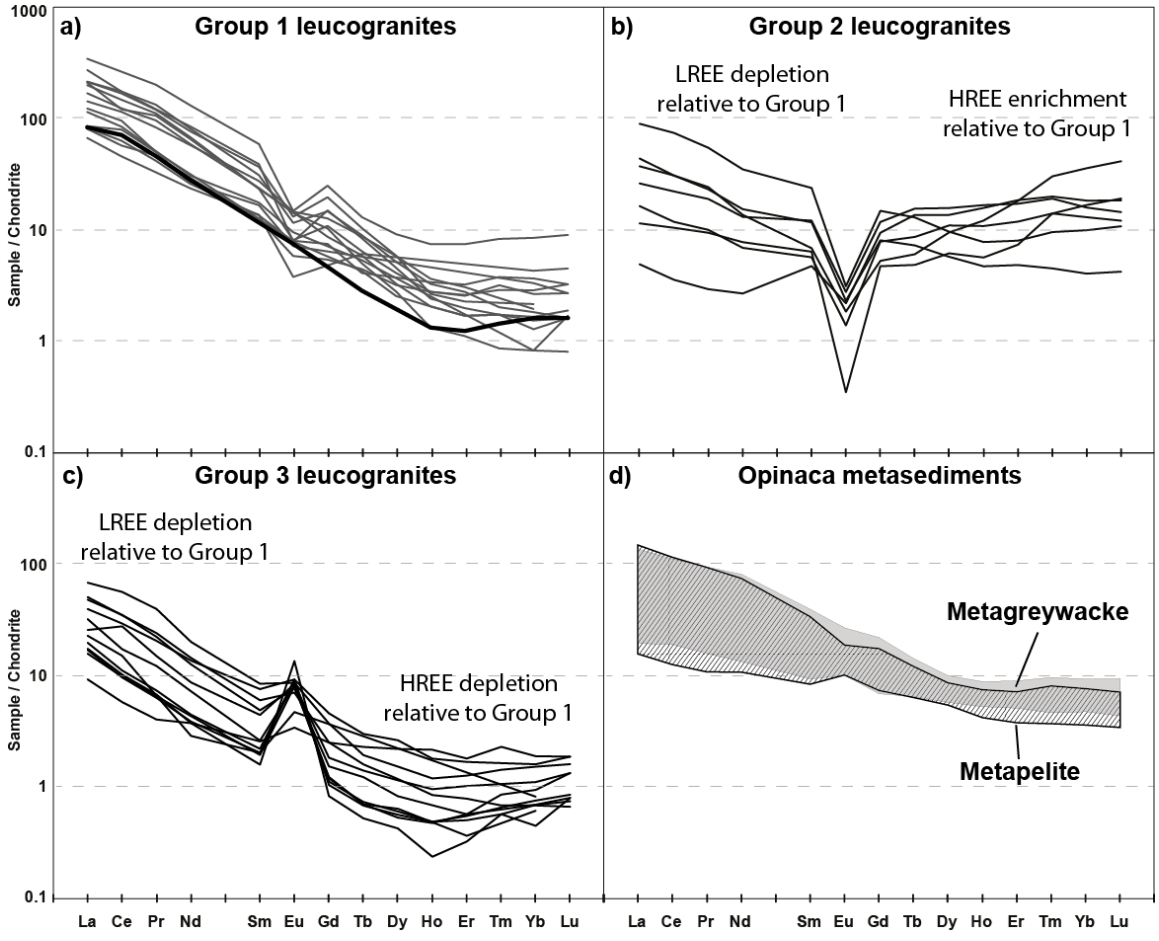

Figure 4.11: Chondrite normalized REE patterns. a, b and c) for the leucogranites and grouped by shape of the REE pattern and, d) Opinaca metagreywacke and metapelites. Sample FS-3018 is shown with a bold line in figure 4.11a.

Group 1 (Fig. 4.11a) is characterized by no, or a small negative Eu anomaly (Eu/Eu* = 0.3 to 0.86) and high La/Yb_N ratios (15.3 to 198.7). This group contains the samples with the highest total REE (average ∑REE = 245). Samples in Group 1 have essentially parallel patterns, except for some variation in the HREE (Ho to Lu). Group 1 samples have REE patterns that most closely resemble those from the Opinaca metasedimentary rocks (Fig. 4.11d). This indicates that they may be the least modified melts, although they have steeper pattern with higher LREE and lower HREE than the potential source. The REE signature of this group of leucogranites indicates that they crystallised from mildly fractionated magmas. The Rb/Sr values of this group are intermediate between the ratios for groups 2 and 3.

Group 2 (Fig. 4.11b) is defined by the presence of a strong negative Eu anomaly (Eu/Eu* < 0.3) and a relatively flat REE pattern (La/Yb_N = 0.3 to 9.3), some display a positive slope. Most samples have HREE values that are slightly higher than Group 1, and this may be linked to the presence of garnet in group 2 leucogranites. Group 2 samples represent leucogranites that crystallised from magmas that are more fractionated than Group 1, and had already crystallised an Eu-bearing phase, such as K-feldspar or plagioclase, after fractionation of LREE-bearing phases such as monazite and/or apatite. The result is an enrichment of HREE and depletion of the middle rare earth elements (MREE, Gd and Tb) which gives the group its characteristic shallow, V-shaped REE patterns. Leucogranites from Group 2 have the highest Rb/Sr and the highest Rb/Ba ratios, which are both consistent with these granites being strongly evolved with low modal plagioclase content,

and as also indicated by their low (Na_2O + CaO) contents. Petrographically, Group 2 contains the highest proportion of pegmatitic leucogranite.

Group 3 (Fig. 4.11c) is characterized by positive Eu anomalies, some of which are large (Eu/Eu* = 1.3 to 10). The REE patterns have moderate, negative slopes (La/Yb_N = 4.8 to 72.5), but at lower levels of REE than samples in Group 1 (except Eu in a few cases). Thus, samples in Group 3 have the lowest average ∑REE content (40.9). Most samples have REE patterns with a marked depletion in Dy, Ho, Er and Tm relative to Yb and Lu. Leucogranites from Group 3 have the lowest Rb/Sr ratios, and this suggests that they formed from less fractionated melts than the other groups. The trace element signature of Group 3 samples is consistent with these leucogranites being accumulations of feldspar, and specifically of K-feldspar.

Sample	Rock Type	Subprovince	SGDAC[a]	$\delta^{18}O$ (‰)[b]
08-EB-5079A	Leucogranite	Opinaca	2008039054	9.0
08-CM-2045B	Leucogranite	Opinaca	2008039005	9.3
08-FS-3129A	Metagreywacke	Opinaca	2008039019	5.3
08-EB-5111 B	Metagreywacke	Opinaca	2008039057	5.7
08-EB-5030B	Metagreywacke	Opinaca	2008039049	8.2
08-EB-5055A	Metagreywacke	Opinaca	2008046523	8.4
08-FS-3238A	Metagreywacke	Opinaca	2008039087	8.8
08-CM-2066A	Metagreywacke	Opinaca	2008039010	8.9
08-CM-2027C	Opx-bearing Metagreywacke	Opinaca	2008039002	9.5
08-SM-7032B	Metagreywacke	Opinaca	2008039064	9.6
08-EB-5062A	Metagreywacke	Opinaca	2008039051	10.2
08-EB-5069B	Metapelite	Opinaca	2008039053	7.8
08-EB-5203B	Metapelite	Opinaca	2008039062	9.6
08-EB-5116D	Metamafite	Opinaca	2008039058	7.0
08-SM-7038A	Metamafite	Opinaca	2008046532	7.5
08-SM-7056D	Ultramafic	Opinaca	2008046534	7.1
1115	Leucogranite	Ashuanipi	199817148	8.5
2009	Leucogranite	Ashuanipi	199817113	8.7
1023	Leucogranite	Ashuanipi	199817118	8.9
1009	Leucogranite	Ashuanipi	199817115	9.1

[a] SGDAC is MNRF sample unique number.
[b] Relative to SMOW.

Table 4.2: $\delta^{18}O$ (‰) composition of various rocks. The last four samples are leucogranites from the Ashuanipi Subprovince

4.6.4 OXYGEN ISOTOPES

Samples of granulite facies metasedimentary rocks yield $\delta^{18}O$ values ranging from 7.8 to 9.6‰ (average 9‰, n=8) excluding two samples at $\delta^{18}O$ of 5.3 and 5.7‰, respectively (Fig.12), which come from late shear zones that contain low-grade mineral assemblages (i.e. retrogressed granulite). Two samples of leucogranite have $\delta^{18}O$ values of 9.0 and 9.3‰ similar to the metasedimentary rocks, and are considered typical for Archean S-type granites (Eiler, 2001). Leucogranites from the Ashuanipi Subprovince have $\delta^{18}O$ values between 8.5 and 9.1‰ (Table 4.2 and Fig. 4.12), similar to those for leucogranites from the Opinaca Subprovince. Two samples of metabasite have $\delta^{18}O$ of 7.0 and 7.5‰, and a metamorphosed ultramafic rock yielded a $\delta^{18}O$ value of 7.1‰. Thus, both the metamorphosed mafic and ultramafic rocks have higher $\delta^{18}O$ than expected for the basaltic (5.3 to 6.1‰, Harmon and Hoefs, 1995) and ultramafic (5.4 to 5.6‰, Eiler, 2001) mantle reservoirs.

4.7 DISCUSSION

The following sections discuss how the leucogranites acquired their composition in the context of the mechanisms occurring during transport and crystallisation. Then, the release of water into the granulite terrane, one of the major consequences of crystallising the injected leucogranite magma, is discussed.

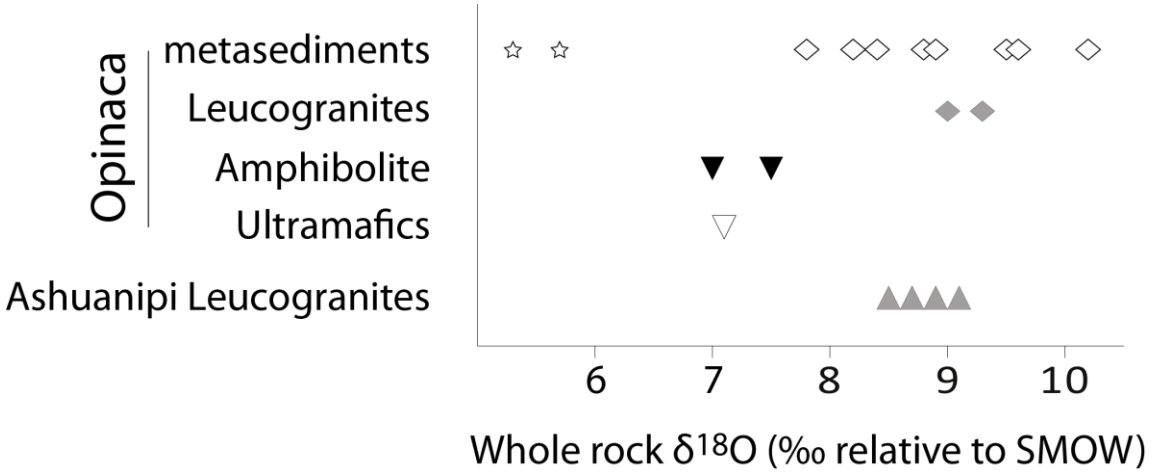

Figure 4.12: Whole rock δ18O (relative to SMOW) results for various rock types in the Opinaca Subprovince and leucogranites from the Ashuanipi Subprovince. The star symbol represents a metasedimentary rock highly retrogressed which contains secondary muscovite and is from a late regional shear zone.

4.7.1 MODELLING MAJOR ELEMENT COMPOSITIONS

4.7.1.1 COMPOSITION OF THE SOURCE MATERIAL

The original bulk composition of the metasedimentary rocks in the Opinaca Subprovince is not precisely known because they have all been modified during granulite facies regional metamorphism, and for many samples this involved the loss of anatectic melt. Nevertheless, the similarity in the composition of metasedimentary rocks from the Quetico, Opinaca and Ashuanipi Subprovinces has been noted by others (Guernina and Sawyer, 2003; Johnson et al., 2008; Lapointe, 1996) and used to argue that the low-grade metasediments from the Quetico Subprovince can be used as a first-order proxy for the original source composition of the sediments in the high-grade terranes where low grade rocks are no longer present. Similarly, the Ashuanipi can be considered as a proxy for crustal levels situated below the Opinaca Subprovince, and thus as a proxy for the source region of the leucogranite injected in the Opinaca injection Complex.

Low-grade metagreywackes from the Quetico Subprovince contain quartz + plagioclase + biotite ± chlorite ± garnet; muscovite is a rare, minor constituent. The average composition of 10 metagreywackes recording greenschist or lower amphibolite facies from Sawyer (1986) is given in Table 4.1 together with representative sample ES356 used in the petrogenetic modelling carried out by Johnson et al. (2008). In addition, the average composition of metagreywacke from the Opinaca Subprovince is similar in most respects, but has slightly higher CaO and lower K_2O contents, consistent with some loss of anatectic

melt (Morfin et al., 2013). There is no petrological evidence for partial melting by any reaction other than fluid-absent breakdown of biotite (R1).

None of the metasedimentary rocks sampled is depleted in either of quartz, plagioclase or biotite. Although R1 is the main melting reaction observed in the Ashuanipi Subprovince, Guernina and Sawyer (2003) found that some metagreywackes are lacking biotite and thus that the reaction R1 was completed and melt with different initial composition produced by other reactions might have formed.

Despite the fact that various protolith melted, and that several melting reaction might have occured in the deep-seated metagreywackes, the vast majority of the leucogranitic melts produced by the metasedimentary rocks in the Opinaca and below was produced by R1, and the geochemical variations shown by the suite of leucogranites are attributed to post-melting processes.

4.7.1.2 COMPOSITION OF THE INITIAL MELT

In order to interpret the compositions of the leucogranites found the Opinaca Subprovince it is necessary to identify, what the starting composition of the anatectic melt derived from the protolith greywacke metasediments might have been. Figure 4.8 shows the compositions of quenched glasses (anatectic melts) from partial melting experiments conducted on metagreywacke bulk compositions at pressures and temperatures similar to

the *P-T* conditions estimated for the granulite facies metamorphism in the Opinaca Subprovince. Among the various metagreywacke bulk compositions (mostly synthetic) that have been used in experiments to explore partial melting, the SBG and SMAG starting materials of Patiño-Douce and Beard (1995, 1996) are particularly relevant because these starting materials are chemically similar to the Opinaca metagreywackes (Table 4.1). The leucogranites from the Opinaca Subprovince are also plotted on figure 4.8 and of these samples FS-3018 is most similar to the composition of the experimental melts produced from SBG and SMAG. In addition, sample FS-3018 has a smooth REE pattern (Group 1; Fig. 4.11) consistent with what is expected for an initial melt derived from the Opinaca metasediments which also have smooth REE patterns (Fig. 4.11d). However, FS-3018 has a lower content of mafic components FeO_t, MgO and TiO_2 than the experimental melts (Fig. 4.9). Nevertheless, sample FS-3018 is considered to be the closest natural sample to an "initial melt", and will be used as a starting composition in the modelling (see sections below) since in addition to major elements, analysis of the natural sample also gives the trace element composition.

4.7.1.3 LOW TIO_2, FEO AND MGO

Whole rock analyses (Table 4.1) show that all the leucogranites from the Opinaca Subprovince have low contents of TiO_2, FeO and MgO relative to the experimental melts (Fig. 4.9). This compositional trait is contrary to that generally found in granites, which

typically have higher concentrations of TiO_2, FeO and MgO than experimental melts obtained from appropriate starting materials. The discrepancy is commonly attributed to the entrainment of peritectic phases (i.e. orthopyroxene, garnet, cordierite and Fe-Ti oxides) at the time when the granitic melt was segregated from its complementary residuum (e.g. Stevens et al., 2007). Alternatively, this general compositional trend is explained by contamination with xenocrysts from the wall rocks during ascent and emplacement of the magma (e.g. Erdmann et al., 2004).

Leucogranites are a special case because they contain less mafic components than expected. The Himalayan leucogranites were derived from pelitic source rocks and yet have low contents of TiO_2, FeO_t and MgO, and this has been attributed to hydrate melting of muscovite, rather than biotite (e.g. Harris et al., 1995; Le Fort et al., 1987). Other anatectic leucogranites, such as those in the nearby Opatica Subprovince, were derived by melting of the quartz, plagioclase and K-feldspar in a leucogranite protolith (Sawyer, 1998; 2010). Neither of these mechanisms are applicable to the Opinaca leucogranites where the presence of orthopyroxene indicates melting of metagreywacke via the breakdown of biotite at temperatures >800^oC (Morfin et al. 2013). Field observation shows the presence of biotite-rich schlieren in the leucogranites (Fig. 4.5e) and crack and seal structures (Fig. 4.6c); thus, the schlieren are interpreted to have been originally screens of country rock between successive injections of felsic magma (e.g. Lavaure and Sawyer, 2011). Disaggregation of the schlieren can increase the content of TiO_2, FeO_t and MgO in the leucogranite by contamination, but this is a minor and local effect. Consequently, the

leucocratic nature of the granite veins in the Opinaca is interpreted to arise because the phases that contain TiO_2, FeO_t and MgO (and any xenocrystic zircon) had already been separated from the anatectic magma prior to its final emplacement as veins. This implies that anatectic melt crystallised as it moved (ascended) through the Opinaca.

4.7.1.4 EVOLUTION OF LEUCOGRANITES BY FRACTIONAL CRYSTALLISATION

The fractional crystallisation mechanism as described by Bowen (1928) was conceived mainly as crystallisation at the walls of dykes with the residual melt moving along the dyke, and this mechanism may be applicable to the veins and dykes forming the Opinaca injection complex (Fig. 4.13). In such a scenario, a framework of first-formed minerals (calcic plagioclase) forms and traps some melt and various entrained minerals in its interstices and the rest of the evolved melt continues to flow along the dyke or vein (Yamato et al., 2012). The control on the subsequent chemical evolution of granitic magma that results from prior crystallisation of plagioclase, which then forms a cumulate with trapped biotite, has been described from the migmatites at St. Malo by Milord et al. (2001) and from granites in Maine by Solar and Brown (2001). In the present case, we focus on what happens to the evolved melt.

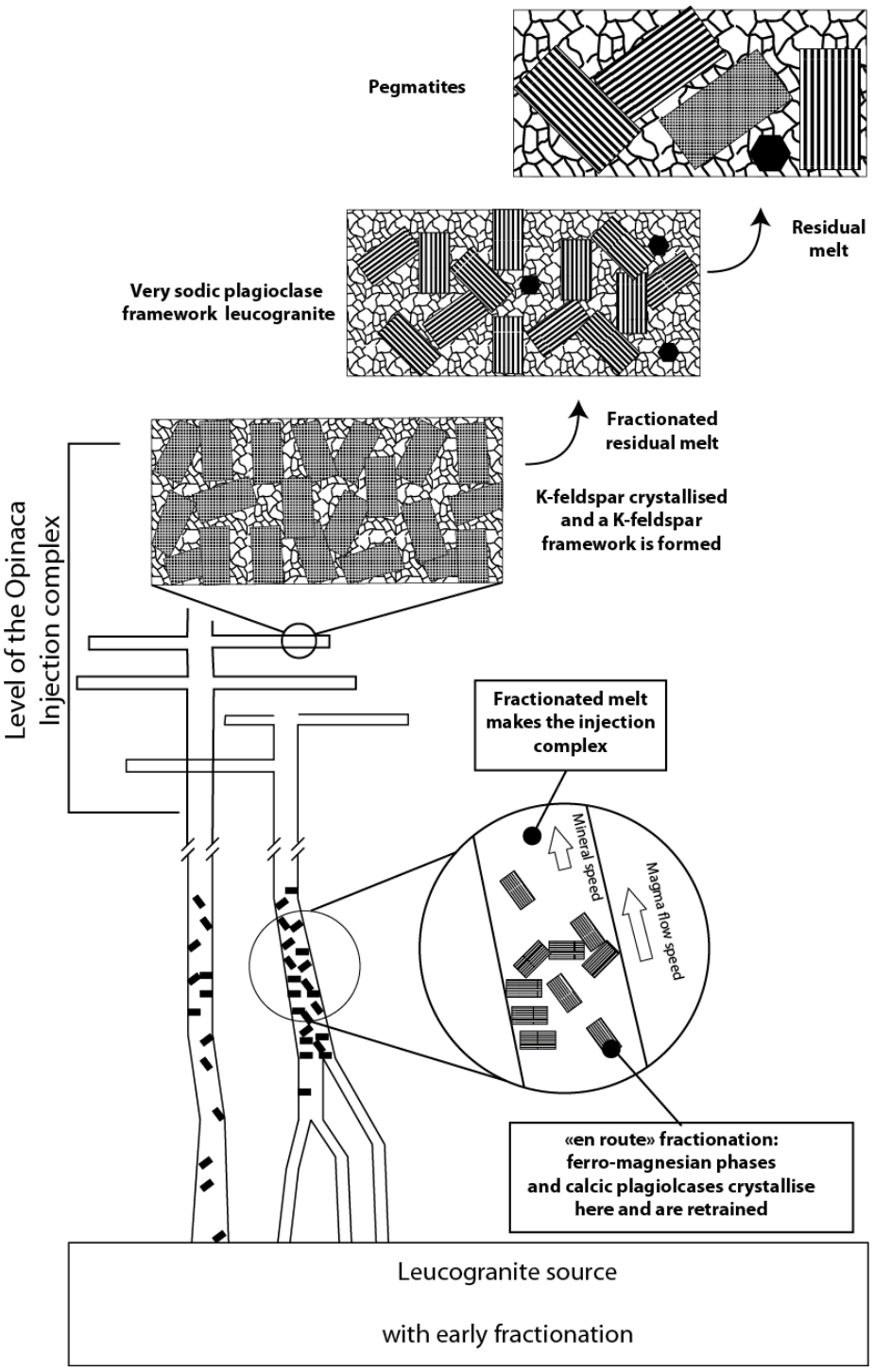

Figure 4.13: Sketch of the mechanism and spatial relationships leading to the evolved geochemical signature of leucogranites in the Opinaca injection complex.

The injection complex is formed by a multitude of small magma batches, and each batch follows its own fractional crystallisation trend. When modelling the evolution of the whole magmatic suite no single combination of measured, or estimated, cumulate composition and starting material is capable of reproducing the whole range of leucogranite compositions found in the Opinaca. If it did, that would imply that a single melt composition entered the injection complex and only one cumulate was formed, which is unrealistic given the size of the complex.

The leucogranites form a single coherent trend on a K_2O vs ($CaO + Na_2O$) plot (Fig. 4.14) which indicates that they shared and have the same phases, K-feldspar, quartz and sodic plagioclase on the liquidus. From the distribution of the leucogranite samples and the mineral vectors shown on figure 4.14, two main trends can be defined relative to the position of sample FS-3018. Samples plotting below FS-3018 can be explained by the crystallisation and removal of K-feldspar, a process which enriched the remaining melt in $CaO + Na_2O$ (but, mostly Na_2O, Table 4.1). However, the vector drawn by the samples is steeper than what would be expected from crystallisation of pure albite, meaning that another phase not in the composition space of figure 4.14 is involved; this mineral is quartz. Samples that plot above FS-3018 can be explained as enriched in K-feldspar. The sample trend is less steep than the vector to K-feldspar, and thus must also contain a phase with less K_2O and without CaO or Na_2O. That mineral could be biotite, but the very small amount of $FeO_t + MgO$ in the whole rock compositions strictly limits the modal proportion of biotite in the leucogranites.

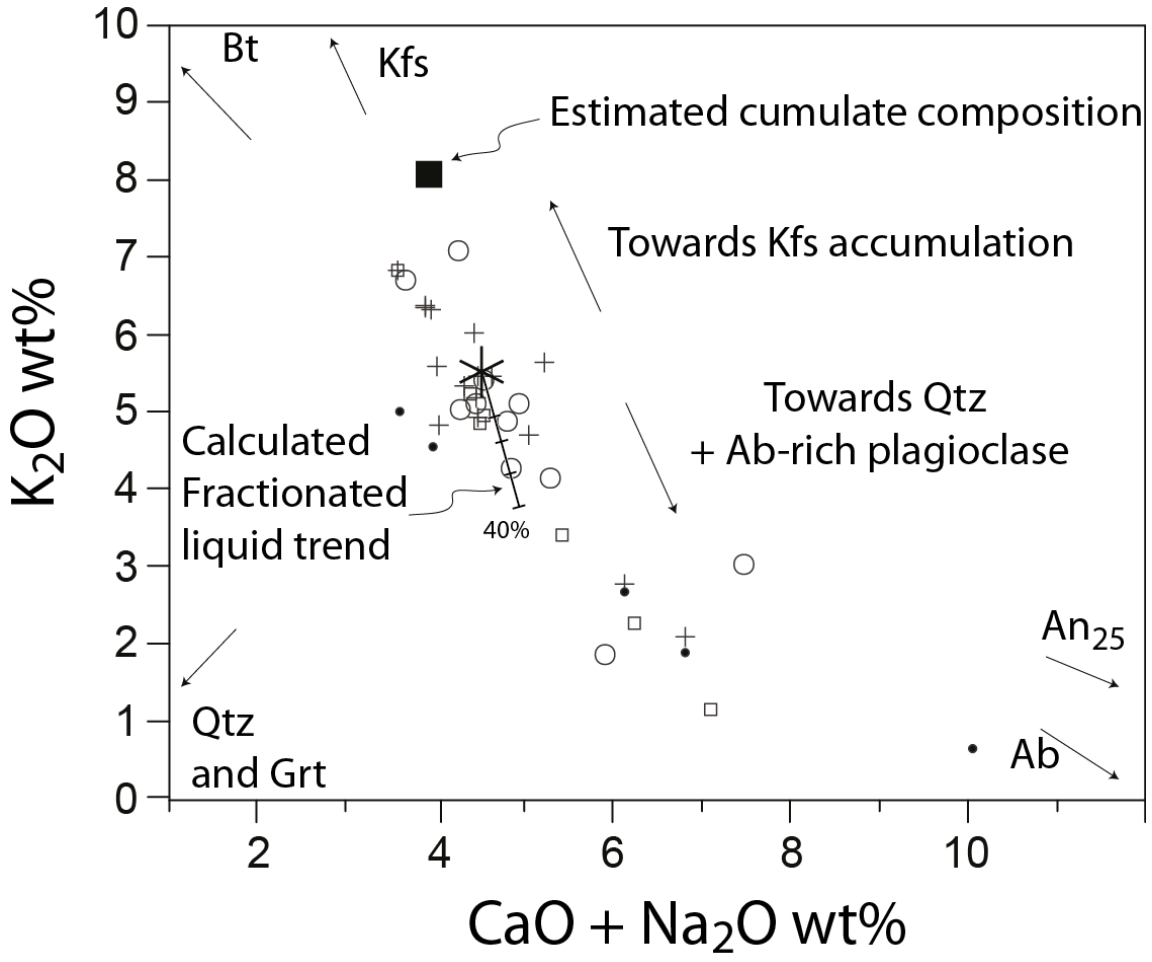

Figure 4.14: K_2O vs $CaO + Na_2O$ (wt. %) plot. Symbols for the leucogranites from the Opinaca follow those of figure 4.9. The star indicates the position of sample FS-3018.

Alternatively, the crystallisation of quartz along with K-feldspar would have the same effect on the trend in figure 4.14. Based on the thin sections examined, the modal proportion of quartz is far superior to that of biotite (e.g. Fig. 4.5c), thus the later proposition is preferred.

In the following section we model a possible fractional crystallisation trend as an example of what happened for a batch of leucogranitic magma, this is only one of multiple possibilities but is representative of the general fractionation trend. A typical cumulate composition is estimated graphically from the trends defined in the Harker diagrams (Fig. 4.9) and yields approximately 45% K-feldspar, 23% albite, 5% anorthite, 20% quartz, 5% biotite and 2% garnet. Removal of this model cumulate composition from sample FS-3018 yields a fractionated liquid composition modelled at intervals of 10% (solid line with ticks extending from star symbol in figure 4.14) that adequately reproduces the general trend observed in the leucogranite samples. The fractionated melts tend toward a plagioclase + quartz composition while the natural cumulate rocks are a combination of the K-feldspar rich cumulate and various amount of trapped melt as shown in figure 4.5c and, therefore, plot at lower K_2O, but above the star symbol (FS-3018).

Overall, the compositional trend of the Opinaca leucogranites is explained by the crystallisation and removal of K-feldspar from already fractionated melts. The compositions of the leucogranites thus fall into two groups; those which are K-feldspar-

dominated cumulates (Fig. 4.5c) and those which crystallised from a highly evolved Na_2O and SiO_2-rich magma (Fig. 4.13), these contain an albite-rich plagioclase (Fig. 4.5d).

The mesonorm QAP plot (Fig. 4.8) shows that the majority of leucogranites define a trend from granodiorites to monzogranite consistent with all the samples being the result of fractionation of a relatively uniform initial melt composition. The mesonorm QAP plot (Fig. 4.8) also shows that leucogranites from the Opinaca are depleted in quartz relative to the majority of relevant experimental melts. This is explained by the two trends defined above, in the first case, the cumulative feldspar framework is filled by melt, but the overall composition is depleted in quartz because of volume occupied by the feldspar framework (Fig. 4.5c & d), these are the points situated to the bottom-left side of the QAP plot and at the bottom-left hand side of the feldspar triangle (Fig. 4.8). In the second case the overall composition is of a quartz and Ab-rich plagioclase which are represented by the compositions on the right-hand side of the QAP triangle and plot closer to the top of the feldspar triangle (Fig. 4.8).

The composition of the majority of leucosomes is dominated by K-feldspar, and indeed the feldspar framework in these consists of microcline (Fig. 4.5c), consequently the "K-feldspar cumulate" leucogranites in the Opinaca are completely different from the cumulates formed at the start of crystallisation of granitic melts which are dominated by relatively calcic plagioclases (Milord & Sawyer, 1998: Solar & Brown 2001) and to a lesser extent by mafic minerals such as biotite or orthopyroxene. Therefore, the magma from which the Opinaca leucogranites formed from had already gone through this early stage of

the fractional crystallisation of plagioclase before they were injected, they were crystallising mainly K-feldspar or very sodic plagioclase. These results indicate that the magma, from which the Opinaca leucogranites formed, already had fractionated compositions before they were emplaced as veins in the injection complex. It also implies that the fractionation process started at a depth below that of the Opinaca Subprovince, and thus at an early stage in the process of segregation and transport of anatectic magmas whilst still in their source area.

4.7.1.5 TRACE ELEMENTS

The composition of residual melts resulting from Raleigh fractionation from sample FS-3018 was calculated (Table 4.3) using the same representative cumulate composition and the partition coefficients for plagioclase, biotite and K-feldspar given by Nash and Creecraft (1985). The plot of Ba vs Sr (Fig. 4.15) shows that the trend defined by the modeled fractionated melts after 10% increments of fractional crystallisation is consistent with the trend defined by the most evolved of the leucogranite samples. Samples plotting towards the top-right of figure 4.15 are thus interpreted as being mostly accumulation of K-feldspar. This is in agreement with the interpretation based on the major elements.

	Rb	Sr	Ba
Kd plagioclase	0.09	6.8	0.63
Kd biotite	1.6	4.7	7.2
Kd K-feldspar	1.5	5.9	7.3

Table 4.3: Partition coefficients from sample 4 in Nash and Crecraft (1985) that are used for the calculations in figure 4. 15.

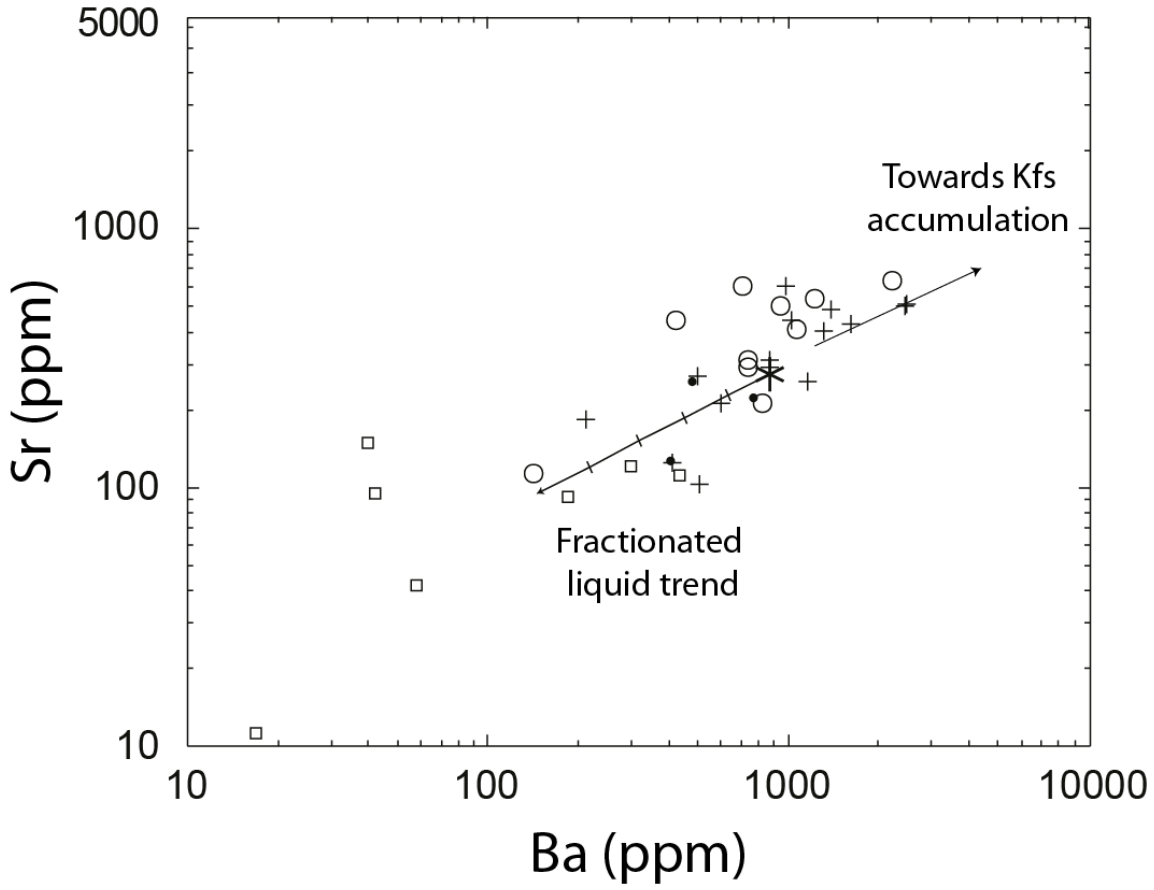

Figure 4.15: Ba vs Sr (in ppm) plot of the composition of leucogranites from the Opinaca Subprovince. Samples are grouped based on their REE pattern (same symbols as figure 4.9). The bold line show the composition of calculated fractionated melt after increments of 10% Rayleigh fractionation of an estimated K-feldspar-rich cumulate (see text) from the starting point FS-3018 (star symbol). The calculated composition of residual melts closely follows the trend defined by the most evolved leucogranites (group 2, square symbols) whereas the cumulate rocks plots towards K-feldspar accumulation (group 3, circle symbols).

Concentrations of some trace elements (e.g. Zr, Th, and LREE) incompatible with the major granite-forming minerals decrease with increasing SiO_2 (Fig. 4.10), for example, Zr and P_2O_5. This behavior indicates the magma became saturated in zircon and apatite and crystallised both these phases, which were then subsequently removed. The same is true for U, it generally increases with SiO_2, but in more detail Groups 1 and 2 have higher U contents than Group 3.This is interpreted to reflect that the cumulate rocks forming Group 3 were not saturated in a U-bearing phase, whereas that was the case for the more evolved Group 1 and 2 magmas. This is to be expected considering the high SiO_2 content of the leucogranites from the Opinaca, which are almost all above 70%. Elements that strongly partition into these accessory minerals behave similarly (i.e. La and LREE into the P_2O_5 phases) and also decline as SiO_2 increases. The fact that some trace elements decline with increasing from SiO_2 (or Na_2O) further indicates that the leucogranites from the Opinaca were already strongly evolved when intruded and had already crystallised accessory minerals prior to injection. Trace elements which do not strongly partition into the accessory minerals that were observed, accumulate in the residual melt and increase with SiO_2 until, eventually, the magma becomes saturated and crystallises a suitable accessory phase to host them, as shown for example by the highly evolved Y-rich samples from Group 2 which contain garnet (Fig. 4.10). Even the least evolved leucogranites, those with the lowest SiO_2 content, show a decrease of incompatible trace elements with increase in SiO_2. This indicates that even the cumulate material crystallised from a melt which had

already attained saturation and depletion in certain accessory minerals, and was thus already evolved.

4.7.2 H_2O RELEASED IN THE HOST

Many metasedimentary rocks in the Opinaca Subprovince have been rehydrated at high temperatures and orthopyroxene replaced by anthophyllite + magnesiohornblende, cummingtonite + magnesiohornblende or by biotite (Fig. 4.5b; Morfin et al., 2013). This widespread rehydration requires the addition of H_2O. The common pegmatitic and aplitic texture in leucogranites together and their evolved compositions indicate that these melts reached a high degree of fractionation and consequently elevated contents of volatiles which were released at, or just prior, to solidification. The injected leucogranite magmas are thus, a potential source of aqueous fluids in and around the injection complex.

4.7.2.1 $\Delta^{18}O$ REEQUILIBRATION

Considering that the $\delta^{18}O$ values for the Opinaca metasedimentary units that show rehydration of orthopyroxene to anthophyllite + magnesiohornblende remain near 9‰ (Fig. 4.12) and that leucogranites both from the Opinaca and the Ashuanipi Subprovinces have similar values between 8.5 and 9.3 ‰, reequilibration with the high-temperature fluid released upon crystallisation of the leucogranites ($\delta^{18}O$ ~9‰) is likely. The H_2O cannot be

from sources such as sea water, meteoric waters or fluid derived from the crystallisation of basaltic ($\delta^{18}O$ of 5.3-6.1‰,; Eiler, 2001) or ultramafic rocks ($\delta^{18}O$ of 5.4-5.6‰, Harmon and Hoefs,1995) all of which have lower values and would result in a decrease in whole rock $\delta^{18}O$ during replacement of the orthopyroxene to biotite or amphibole. In addition, samples from mafic and ultramafic units which initially had $\delta^{18}O$ ~6‰, show an increase in $\delta^{18}O$ toward the values typical of the metasedimentary units and leucogranites. Hence, these rocks are interpreted to have interacted with oxygen reservoirs with $\delta^{18}O$ ~ 9‰, possibly their metasedimentary host rocks, or with fluids released by the crystallisation of the leucogranites. Two samples of sedimentary rocks that have experienced retrograde metamorphism at lower temperatures in shear zones have their $\delta^{18}O$ values reduced to 6.5‰; these are interpreted to have reequilibrated with later low $\delta^{18}O$ H_2O fluids. One of these samples had clearly been retrogressed since it contains secondary muscovite.

4.7.2.2 H_2O AVAILABLE

In this section, we address the issue of the amount of H_2O required to rehydrate the high grade metasedimentary assemblages of the Opinaca. Since most of the orthopyroxene contained in the host metasedimentary rocks are partially retrograded, sufficient H_2O had to have percolated throughout the region to accomplish this. As previously inferred from the oxygen isotopes, the metasediments had equilibrated with a fluid released by the leucogranites.

The metasedimentary units account for 40% of the study area and are dominated by psamitic bulk compositions, in these, the maximum modal proportion of orthopyroxene observed is 10%. Assuming that 10% orthopyroxene was present throughout the metasedimentay units, rehydrating all this orthopyroxene would produce ~16.3% biotite (Guernina and Sawyer, 2003) which contains typically 4 wt.% H_2O (in addition to the primary biotite). This requires an addition of 0.65 wt.% of H_2O to the whole rock composition. This figure is voluntarily overestimated since most metagreywackes contained no, or less than 10% orthopyroxene. In addition, only the retrogression of orthopyroxene to biotite is considered, but retrogression to amphibole is commonly observed, since this reaction would require less H_2O, only the retrogression to biotite is considered in order to estimate the maximum H_2O necessary.

Over 60% of the study area is composed of leucogranite. Although the initial H_2O content of the leucogranites is unknown, we assume they typically contain 4 wt.% H_2O initially based on the solubility data of Holtz et al. (2001) and possibly more after crystal fractionation. Thus, the potential contribution of H_2O (2.4 wt. %) from the leucogranites is more by, at least a factor of three, than is needed to rehydrate the orthopyroxene-bearing assemblages (0.65 wt.%). Whether or not all the available H_2O present in the granitic melt was released at the crustal level of the injection complex is not certain. Nevertheless, the large proportion of pegmatitic veins throughout the injection complex indicates that many veins had reached the stage of H_2O saturation and exsolved an H_2O-rich fluid into the host rocks.

Upon release from the crystallising leucogranites the aqueous fluid may have diffused pervasively through the rock along the grain boundaries, or been somewhat more focussed along the foliation planes, or it may have been strongly focussed through cracks, or possibly some combination of all three. The very widespread and almost complete retrogression in the area mapped by Simard and Gosselin (1999) suggests that migration of an H_2O fluid there was pervasive through the rocks. The fact that the injection of leucogranite was pervasive and the veins closely spaced enhanced the potential for retrogression as fluid was also released throughout the metasedimentary host rocks, thus the actual path length for diffusion of H_2O through the rock was short, perhaps only tens of centimeters. Yet, elsewhere in the Opinaca Subprovince some orthopyroxene-bearing assemblages are conserved, possibly due the strong local focussing of the fluids into well-defined channels, such as along foliation planes and the thin pelitic layers, rather than a distributed flow through the more abundant, but less permeable, metagreywacke layers.

4.7.2.3 IMPORTANCE OF WATER FLUXED PARTIAL MELTING

The release of H_2O at mid- to deep crustal depth and temperature has an enormous potential for triggering water-fluxed partial melting. Some secondary, water-fluxed partial melting might have happened in the Opinaca injection complex, but it was not widespread because the lack of K-feldspar in the metagreaywake assemblage would not permit a reaction such as

$Kfs + Qtz + Pl + H_2O = Liq$

which is expected in presence of water at amphibolite facies conditions.

Metapelite in the Opinaca would have suffered this process, but clear evidence for water-fluxed partial melting was not found, since the above reaction produces no peritectic phases any melting-related microstructures produced could be attributed to the dehydration melting event which produced the peritectic garnets and cordierites at granulite facies.

Nevertheless, a process that releases H_2O in the middle crust could produce significant secondary melting given a host with an appropriate mineral assemblage and adequate temperature (Berger et al., 2008; Genier et al., 2008; Sawyer, 2010). It is not observed in the Opinaca injection complex due to its specific composition, but this process is potentially an important mechanism in the continental crust.

4.7.2.4 IMPLICATIONS OF WATER RELEASE

Granulite facies is often described, and sometimes defined (Fyfe, 1973), as being anhydrous. The situation in the Opinaca Subprovince shows that large volumes of water released from injected leucogranite as it crystallisation has the potential to rehydrate large volumes of granulite facies crust at the end of a granulite facies anatectic event. Some granulite terranes could thus be lost, overprinted by hydrous amphibolite facies mineral assemblages, due to subsequent rehydration because of the deep-seated accumulation of

anatectic melt in injection complexes (e.g. Phillips, 1981). Rehydration in the continental crust may be more common and widespread than previously thought, and former granulite facies terranes may have been mapped, or interpreted, as amphibolite or lower facies terranes.

With respect to the process of crustal differentiation, the incomplete transfer of H_2O from the lower granulite crust to its upper levels renders the rehydrated middle crust more fertile, and hence more prone to melting than anticipated during partial melting in a subsequent metamorphic event or crustal reworking during younger orogenic events.

4.8 CONCLUSION

The geochemistry of the leucogranitic veins and dykes injected into the Opinaca Subprovince is characterised by a decrease in K_2O and an increase in Na_2O with increasing SiO_2 and remarkably low (FeO_t + MgO + TiO_2) contents. Geochemical trends in the Opinaca leucogranites are controlled by the crystallisation and removal mainly of K-feldspar from the melt. This indicates that early-crystallising and fractionated phases such as calcic plagioclases, biotite and/or orthopyroxene had already been fractionated from the magmas before they were injected into the Opinaca Subprovince. Opinaca leucogranites crystallised from magmas that were already fractionated. Thus, a diagnostic geochemical feature of injection complexes may be the evolved compositions of the felsic veins and dykes that they contain. Injection complexes are, in effect, magma reservoirs of evolved

anatectic melts formed at a depth close to the solidus. Thus, from a chemical point of view, this study confirms the conceptual model explored by Leitch and Weinberg (2002) in which the pervasive movement of anatectic melt (and the associated processes of melting, fractionation and solidification) may be confined to below, or close to the solidus depth in the crust. A corollary is that since the melts injected to create the injection complex were already evolved, then the early stages of fractionation must be preserved at a still deeper level; that is still closer to, or actually in, the source region of the melt.

Two important consequences arise from this study of the Opinaca injection complex. 1) A better understanding of the distribution of the granitic component in the crust following regional anatexis. We showed that fractionation of anatectic melt can begin in the granulite facies source region and end at the boundary between granulite and amphibolite facies crust. 2) If anatectic melt remains in the lower or middle crust, as in the case of an injection complex, then the middle and lower crust are compositionally less depleted, i.e. more fertile, with a higher H_2O content than previously thought, which can modify its behaviour during subsequent metamorphic events.

4.9 ACKNOWLEDGMENTS

This study represents part of the first author's Ph.D research. This project was possible because of the financial and logistical support through two seasons of field mapping in northern Quebec, we express our gratitude to the Bureau d'exploration géologique du

Quebec for this support and their unwavering encouragement. We wish to thank R. Tartèse and R. Weinberg for their comments which helped improve the manuscript. The cost of oxygen isotopes analyses was met from a Natural Sciences and Engineering Research Council (NSERC) Discovery Grant to Sawyer.

4.10 REFERENCES

Bandyayera, D., Burniaux, P., Morfin, S., 2011. Géologie de la région du lac Brune (33G07) et de la baie Gavaudan (33G10). Ministère des Ressources Naturelles du Québec, p. 25.

Bandyayera, D., Rhéaume, P., Maurice, C., Bédard, É., Morfin, S., Sawyer, E.W., 2010. Synthèse Géologique du Secteur du Réservoir Opinaca, Baie-James. Ministère des Ressources Naturelles du Québec, p. 44.

Berger, A., Burri, T., Alt-Epping, P., Engi, M., 2008. Tectonically controlled fluid flow and water-assisted melting in the middle crust: An example from the Central Alps. Lithos 102, 598–615.

Bons, P.D., Becker, J.K., Elburg, M.A., Urtson, K., 2010. Granite formation: Stepwise accumulation of melt or connected networks? Special Paper of the Geological Society of America, 105-115.

Bowen, N.L., 1928. The evolution of the igneous rocks. Dover, NY.

Brown, M., Korhonen, F.J., Siddoway, C.S., 2011. Organizing Melt Flow through the Crust. Elements 7, 261-266.

Brown, M., Solar, G.S., 1999. The mechanism of ascent and emplacement of granite magma during transpression: a syntectonic granite paradigm. Tectonophysics 312, 1-33.

Card, K.D., 1990. A review of the Superior Province of the Canadian Shield, a product of Archean accretion. Precambrian Research 48, 99-156.

Collins, W.J., Sawyer, E.W., 1996. Pervasive granitoid magma transfer through the lower-middle crust during non-coaxial compressional deformation. Journal of Metamorphic Geology 14, 565-579.

Connolly, J.A.D., Podladchikov, Y.Y., 1998. Compaction-driven fluid flow in viscoelastic rock. Geodinamica Acta 11, 55-84.

Cruden, A.R., 2006. Emplacement and growth of plutons: implications for rates of melting and mass transfer in continental crust, in: Brown M, R.T. (Ed.), Evolution and Differentiation of the Continental Crust. Cambridge University Press, pp. 455-519.

Eiler, J.M., 2001. Oxygen Isotope Variations of Basaltic Lavas and Upper Mantle Rocks. Reviews in Mineralogy and Geochemistry 43, 319-364.

Erdmann, S., Clarke, D.B., MacDonald, M.A., 2004. Origin of chemically zoned and unzoned cordierites from the South Mountain and Musquodoboit Batholiths, Nova Scotia. Earth and Environmental Science Transactions of the Royal Society of Edinburgh 95, 99-110.

Fyfe, W.S., 1973. The granulite facies, partial melting and the archaean crust. Philosophical Transactions of the Royal Society of London. Series A, Mathematical and Physical Sciences 273, 457-461.

Genier, F., Bussy, F., Epard, J.-L., Baumgartner, L., 2008. Water-assisted migmatization of metagraywackes in a Variscan shear zone, Aiguilles-Rouges massif, western Alps. Lithos 102, 575–597.

Goutier, J., Dion, C., David, J., Dion, D.J., 1999. Géologie de la région de la passe Shimusuminu et du lac Vion (33F/11 et 33F/12). Ministère des Ressources Naturelles du Québec.

Goutier, J., Dion, C., Ouellet, M.-C., 2001. Géologie de la région de la colline Bezier (33G/12) et du lac de la Montagne du Pin (33G/13). Ministère des Ressources Naturelles du Québec.

Guernina, S., Sawyer, E.W., 2003. Large-scale melt-depletion in granulite terranes: an example from the Archean Ashuanipi Subprovince of Quebec. Journal of Metamorphic Geology 21, 181-201.

Harmon, R.S., Hoefs, J., 1995. Oxygen-isotope heterogeneity of the mantle deduced from global O-18 sytematics of basalts from different geotectonics settings. Contributions to Mineralogy and Petrology 120, 95-114.

Harris, N., Ayres, M., Massey, J., 1995. Geochemistry of granitic melts produced during the incongruent melting of muscovite: Implications for the extraction of Himalayan leucogranite magmas. Journal of Geophysical Research: Solid Earth 100, 15767-15777.

Hobbs, B.E., Ord, A., 2010. The mechanics of granitoid systems and maximum entropy production rates. Philosophical Transactions of the Royal Society A: Mathematical, Physical and Engineering Sciences 368, 53-93.

Holtz, F., Johannes, W., Tamic, N., Behrens, H., 2001. Maximum and minimum water contents of granitic melts generated in the crust: a reevaluation and implications. Lithos 56, 1-14.

Johnson, T.E., Hudson, N.F.C., Droop, G.T.R., 2003. Evidence for a genetic granite–migmatite link in the Dalradian of NE Scotland. Journal of the Geological Society 160, 447–457

Johnson, T.E., White, R.W., Powell, R., 2008. Partial melting of metagreywacke: a calculated mineral equilibria study. Journal of Metamorphic Geology 26, 837-853.

Koester, E., Pawley, A.R., Fernandes, L.A.D., Porcher, C.C., Soliani, E., 2002. Experimental Melting of Cordierite Gneiss and the Petrogenesis of Syntranscurrent Peraluminous Granites in Southern Brazil. Journal of Petrology 43, 1595-1616.

Lambert, I.B., Heier, K.S., 1968. Geochemical investigations of deep-seated rocks in the Australian shield. Lithos 1, 30-53.

Lapointe, B., 1996. Un exemple de minéralisation aurifère en milieu profond :l'indice d'or du Lac Lilois dans le complexe d'Ashuanipi, Province du Supérieur, Nouveau-Québec. Chicoutimi : Université du Québec à Chicoutimi, 1996.

Lavaure, S., Sawyer, E.W., 2011. Source of biotite in the Wuluma Pluton: Replacement of ferromagnesian phases and disaggregation of enclaves and schlieren. Lithos 125, 757-780.

Le Fort, P., Cuney, M., Deniel, C., France-Lanord, C., Sheppard, S.M.F., Upreti, B.N., Vidal, P., 1987. Crustal generation of the Himalayan leucogranites. Tectonophysics 134, 39-57.

Leitch, A.M., Weinberg, R.F., 2002. Modelling granite migration by mesoscale pervasive flow. Earth and Planetary Science Letters 200, 131-146.

Milord, I., Sawyer, E.W., Brown, M., 2001. Formation of Diatexite Migmatite and Granite Magma during Anatexis of Semi-pelitic Metasedimentary Rocks: an Example from St. Malo, France. Journal of Petrology 42, 487-505.

Montel, J.-M., Vielzeuf, D., 1997. Partial melting of metagreywackes, Part II. Compositions of minerals and melts. Contributions to Mineralogy and Petrology 128, 176-196.

Morfin, S., Sawyer, E.W., Bandyayera, D., 2013. Large volumes of anatectic melt retained in granulite facies migmatites: An injection complex in northern Quebec. Lithos 168–169, 200-218.

Nash, W.P., Creecraft, H.R., 1985. Partition coefficients for trace elements in silicic magmas. Geochim. Cosmochim. Acta 49, 2309-2322.

Pan, Y., E. Fleet, M., Heaman, L., 1998. Thermo-tectonic evolution of an Archean accretionary complex: U–Pb geochronological constraints on granulites from the Quetico Subprovince, Ontario, Canada. Precambrian Research 92, 117-128.

Patiño Douce, A.E., Beard, J.S., 1995. Dehydration-melting of biotite Gneiss and quartz amphibolite from 3 to 15 kbar. Journal of Petrology 36, 707-738.

Patiño Douce, A.E., Beard, J.S., 1996. Effects of P, f(O2) and Mg/Fe ratio on dehydration melting of model metagreywackes. Journal of Petrology 37, 999-1024.

Percival, J., Stern, R., Rayner, N., 2003. Archean adakites from the Ashuanipi complex, eastern Superior Province, Canada: geochemistry, geochronology and tectonic significance. Contributions to Mineralogy and Petrology 145, 265-280.

Percival, J.A., 1991. Orthopyroxene–poikilitic tonalites of the Desliens igneous suite, Ashuanipi granulite complex, Labrador–Quebec, Canada. Canadian Journal Of Earth Sciences 28, 743-753.

Percival, J.A., 1993. Geology, Ashunaipi complex, Schefferville area, Newfoundland-Quebec. Geological Survey of Canada, p. Map 1785A.

Percival, J.A., Mortensen, J.K., Stern, R.A., Card, K.D., Bégin, N.J., 1992. Giant granulite terranes of northeastern Superior Province: the Ashuanipi complex and Minto block. Canadian Journal of Earth Sciences 29, 2287-2308.

Percival, J.A., Sanborn-Barrie, M., Skulski, T., Stott, G.M., Helmstaedt, H., White, D.J., 2006. Tectonic evolution of the western superior province from NATMAP and lithoprobe studies. Canadian Journal of Earth Sciences 43, 1085-1117.

Petford, N., Lister, J.R., Kerr, R.C., 1994. The ascent of felsic magmas in dykes. Lithos 32, 161-168.

Phillips, G.N., 1981. Water activity changes across an amphibolite-granulite facies transition, Broken Hill, Australia. Contributions to Mineralogy and Petrology 75, 377-386.

Rudnick, R.L., Gao, S., 2003. Composition of the continental crust, in: Heinrich, D.H., Karl, K.T. (Eds.), Treatise on Geochemistry. Pergamon, Oxford, pp. 1-64.

Sawyer, E.W., 1986. The influence of source rock type, chemical-weathering and sorting on the geochemistry of clastic sediments from the Quetico meta-sedimentary belt, Superior Province, Canada. Chemical Geology 55, 77-95.

Sawyer, E.W., 1998. Formation and evolution of granite magmas during crustal reworking: the significance of diatexites. Journal of Petrology 39, 1147-1167.

Sawyer, E.W., 2010. Migmatites formed by water-fluxed partial melting of a leucogranodiorite protolith: Microstructures in the residual rocks and source of the fluid. Lithos 116, 273-286.

Sawyer, E.W., Cesare, B., Brown, M., 2011. When the continental crust melts. Elements 7, 229-234.

Simard, M., Gosselin, C., 1999. Géologie de la région du Lac Lichteneger (SNRC 33B). Ministère des Ressources Naturelles du Québec, p. 25.

Simard, M., Gosselin, C., Lafrance, I., 2009a. Géologie de la région de la Riviére Sérigny (24C - 23N). MRNF Québec, p. 40.

Simard, M., Parent, M., Paquette, L., Lafrance, I., 2009b. Géologie de la région du Réservoir de Caniapiscau (SNRC 23K - 23N). MRNF Québec, p. 39.

Solar, G.S., Brown, M., 2001. Petrogenesis of migmatites in Maine, USA: Possible source of peraluminous leucogranite in plutons? Journal of Petrology 42, 789-823.

St. Seymour, K., Turek, A., Doig, R., Kumarapeli, S., Fogal, R., 1989. First U–Pb zircon ages of granitoid plutons from the La Grande greenstone belt, James Bay area, New Quebec. Canadian Journal Of Earth Sciences 26, 1068-1073.

Stevens, G., Villaros, A., Moyen, J.-F., 2007. Selective peritectic garnet entrainment as the origin of geochemical diversity in S-type granites. Geology 35, 9-12.

Tartese, R., Boulvais, P., 2010. Differentiation of peraluminous leucogranites "en route" to the surface. Lithos 114, 353-368.

Taylor, S.R., McLennan, S.M., 1995. The geochemical evolution of the continental crust. Reviews of Geophysics 33, 241-265.

Weinberg, R.F., 1999. Mesoscale pervasive felsic magma migration: alternatives to dyking. Lithos 46, 393-410.

Weinberg, R.F., Searle, M.P., 1998. The Pangong Injection Complex, Indian Karakoram: a case of pervasive granite flow through hot viscous crust. Journal of the Geological Society 155, 883-891.

Weinberg, R.F., Mark, G., and Reichardt, H., 2009, Magma ponding in the Karakoram shear zone, Ladakh, NW India, Geological Society of America Bulletin 121, 278-285

Yamato, P., Tartèse, R., Duretz, T., May, D.A., 2012. Numerical modelling of magma transport in dykes, Tectonophysics 526-529, 97-109.

CHAPITRE 5

SYNTHÈSE ET CONCLUSION

5.1 INTRODUCTION

La présente section est un résumé des apports de la thèse. Elle est divisée en deux parties. La première souligne les contributions qui sont d'ordre descriptif, basé sur les constats permettant une meilleure compréhension de la Sous-province d'Opinaca et de sa région. La seconde partie résume les interprétations et les implications proposées. Cette partie met l'emphase sur les processus pouvant affecter tout terrain semblable au complexe d'injection de l'Opinaca. L'étude de ces processus est d'importance globale dans la compréhension de la croûte continentale.

5.2 SOUS-PROVINCE D'OPINACA

5.2.1 LA SOURCE DES MÉTASÉDIMENTS

Les résultats de datation U/Pb sur zircon par la méthode SHRIMP permettent une meilleure compréhension des événements qu'ont subis les unités métasédimentaires de l'Opinaca. Les âges obtenus sur des zircons détritiques corrèlent avec ceux des unités volcaniques ou plutoniques des terrains adjacents. Certains zircons enregistrent des âges mésoarchéens. Or, contrairement au nord, aucune unité situé au sud de l'Opinaca a des âges équivalents. Cela est interprété comme une évidence d'une sédimentation du nord vers le sud. Les observations pétrographiques des zircons ainsi que de leurs ratios Th/U indiquent une probable transition entre la sédimentation et le métamorphisme de haut grade entre 2670 et

2680 Ma. L'analyse de zircons provenant à la fois des unités métasédimentaires et des veines leucogranitiques du complexe d'injection, permet de conclure que l'épisode de métamorphisme granulitique et la cristallisation des injections de leucogranites furent simultanés. Finalement, les âges discordants indiquent une possible perturbation du système isotopique dans les zircons reliés à des âges grenvilliens, autour de 1000 Ma. Cette observation est interprétée comme une mise en circulation de fluides qui pourraient être associés à la perturbation thermique provoquée par l'orogénie grenvillienne.

5.2.2 PRÉSENCE D'UN COMPLEXE D'INJECTION

L'étude pétrologique révèle que les métagreywackes ont partiellement fondu à des conditions de ~820^{o}C et ~7kbar, ce qui a pu générer un maximum de 10 % de liquide anatectique en formant de l'orthopyroxène et/ou du grenat comme phases péritectiques. Les observations de terrain indiquent que les métagreywackes contiennent des quantités variables de leucogranites présents sous forme de veines et de dykes sub-parallèles à la foliation principale est - ouest. D'après l'étude de plus de 1070 affleurements, un affleurement « typique » contiendrait 63 % de matériel leucogranitique, ce qui est beaucoup plus que les 10 % maximum produits par une fusion partielle *in situ*. Il est donc conclu qu'une forte proportion des leucogranites observés est injectée dans un terrain à haut grade métamorphique. Cela fait de la Sous-province d'Opinaca un complexe d'injection.

5.3 PRINCIPALES IMPLICATIONS GLOBALES

5.3.1 TERRAIN GRANULITIQUE QUI N'EST PAS DÉFICITAIRE EN GRANITE

L'un des apports principaux de cette thèse est que, contrairement à certaines définitions, ou du moins conceptions généralement acceptées, les terrains granulitiques ne sont pas nécessairement déficitaires en liquide granitique. L'exemple du complexe d'injection d'Opinaca montre que des terrains qui ont subi des conditions granulitiques (début du faciès granulitique) peuvent au contraire être excédentaires en magmas anatectiques et donc devenir des réservoirs de magmas situés en profondeur.

5.3.2 RÉSERVOIR DE LEUCOGRANITES ÉVOLUÉS

L'analyse géochimique a révélé que le complexe d'injection d'Opinaca est non seulement un réservoir de magmas, mais que ceux-ci ont atteint un degré avancé de fractionnement. Cette information montre que la cristallisation fractionnée joue un rôle important dès les niveaux profonds de la croûte, proche de la source. La présence de granites aussi évolués dans des niveaux profonds de la croûte est aussi importante pour comprendre la distribution des éléments chimiques dans la croûte continentale en général. Si des granites évolués se mettent en place dans la croûte moyenne, alors le transfert de la composante géochimique

des granites (riches en SiO_2, K_2O, Na_2O) n'est pas aussi efficace que ce qu'un modèle de dykes crustaux prédit.

5.3.3 IMPLICATIONS SUR LE RÉGIME THERMIQUE

La présence d'un large volume de leucogranite dans un complexe d'injection affecte le régime thermique de la croûte continentale. Les leucogranites sont enrichis en éléments radiogéniques producteurs de chaleur (HPE) par rapport à leur source. La mise en place des leucogranites dans un complexe d'injection rend donc le transfert des HPE vers les niveaux supérieurs de la croûte incomplet. Cela a pour effet de conserver la croûte située sous le complexe d'injection à haute température pendant de plus longues périodes, ce qui peut favoriser la fusion partielle en profondeur.

5.3.4 IMPLICATIONS DE LA PRÉSENCE D'EAU DANS LA CROÛTE MOYENNE

Les grands volumes de leucogranites constituant le complexe d'injection représente un volume d'H_2O disponible dans les niveaux profonds de la croûte. Ces fluides sont émis lors de la cristallisation des veines et des dykes. Dans le cas du complexe d'injection de l'Opinaca, l'effet majeur observé a été une réhydratation partielle à totale des assemblages granulitiques (en particulier de l'orthopyroxène).

La présence d'eau dans un environnement soumis à des températures du faciès supérieurs des amphibolites permettrait un assez haut degré de fusion partielle si les conditions minéralogiques sont réunies (présence de quartz, plagioclase et feldspath potassique). Dans ce cas, l'impact sur la croûte serait très important, car la cristallisation des granites formant le complexe d'injection pourrait provoquer une fusion partielle secondaire.

5.3.5 IMPLICATIONS SUR LE PROCESSUS GÉNÉRAL DE DIFFÉRENCIATION CRUSTALE

La présence d'un complexe d'injection dans la croûte profonde a plusieurs implications pour l'ensemble de la croûte continentale. 1) le fluide riche en H_2O libéré lors de la cristallisation des leucogranites peut réhydrater des assemblages anhydres granulitiques, ce qui est observé par le remplacement de l'orthopyroxène en amphibole et en biotite. Ces roches réhydratées sont plus enclines à fondre de nouveau dans le cadre d'un évènement ultérieur de haut grade métamorphique que des assemblages anhydres. 2) La rétention de grands volumes de leucogranites dans le complexe d'injection a des conséquences thermiques sur la croûte. Les granites étant enrichis en éléments producteurs de chaleur (Th, U et K), le complexe d'injection qui contient beaucoup de granite a une production de chaleur radiogénique accrue. De plus, la chaleur latente de cristallisation est libérée dans le complexe d'injection. Ces deux effets thermiques font que la croûte continentale inférieure,

si un complexe d'injection est présent, est maintenue à des températures plus élevées pendant de plus longues périodes.

5.3.6 COMPLEXE D'INJECTION COMME DES PLUTONS DIFFUS

LeBreton et Thompson (1988) ont proposé de voir les migmatites comme des granites avortés ("failed granites"). Dans ce sens, une analogie peut être formulée selon laquelle les complexes d'injections sont des plutons avortés (failed plutons). En effet, la présence d'un complexe d'injection peut empêcher le système d'évoluer vers un stade où l'extraction des magmas d'anatexie serait focalisée et non pas diffuse. En ce sens, les complexes d'injections défavorisent la formation de plutons dans la croûte supérieure.

Les complexes d'injections peuvent être vus comme des réservoirs "diffus" collectant les magmas d'anatexie dans la croûte moyenne. Ils peuvent contenir de grandes quantités de magmas et peuvent avoir une influence majeure sur la croûte continentale.

5.4 APPORTS AUX DÉBATS ACTUELS

Brown (2013) propose une revue récente de la littérature et des concepts concernant les granites depuis leur formation jusqu'à leur mise en place. Dans cette revue, il est proposé un état des lieux de la connaissance ainsi qu'une série de direction de recherche pour ce champ

de la géologie. La présente thèse apporte des exemples, basés sur l'étude de terrain, qui ont permis de valider certains de ces modèles et propose des éléments de réponses à certains débats actuels. Par exemple, le travail théorique de Cruden et al. (1998) prédit l'influence de la rétention de magmas dans la croûte profonde et l'impact sur sa fertilité, ce qui est confirmé par notre étude de terrain, en particulier par l'approche géochimique du chapitre 4. Cette thèse apporte aussi de nouvelles données au débat actuel concernant le contrôle de la signature géochimique des leucogranites par l'entraînement de minéraux péritectiques. Notre étude montre que ce mécanisme n'est pas l'origine principale de la signature géochimique des leucogranites d'Opinaca, ce qui va à l'encontre des propositions récentes telles que décrites dans Stevens et al. (2007).

Il est à noter que des études récentes (i.e. Yakymchuk et al., 2013) observent aussi un surplus de matériel leucogranitique dans des terrains similaires à l'Opinaca. L'étude de Yakymchuk et al. (2013) apporte, en outre, une contribution structurale qui permet d'imaginer les mécanismes de formation des complexes d'injections. L'étude citée confirme en partie l'hypothèse proposée dans le chapitre 3 qui stipule que la fabrique planaire initiale de l'hôte ne favorise pas la focalisation du flux de magmas dans de grands dykes et entraîne alors la formation d'un complexe d'injection.

5.5 INVESTIGATIONS FUTURES

Sur le terrain, une des principales difficultés pour identifier un domaine en tant que complexe d'injection est liée au fait que les liquides produits par la fusion *in situ* et ceux injectés ne sont presque pas distinguables. À l'échelle de l'affleurement, seule une attention particulière au degré de fusion partielle potentiel de l'hôte en comparaison avec la quantité de magma injecté permet d'affirmer si une veine leucocrate est un leucosome ou bien un magma injecté. De plus, il faut répéter cette analyse sur une grande échelle pour pouvoir qualifier la zone de complexe d'injection. Face à cette difficulté du terrain, une attention particulière devrait être portée sur ces points pour éviter de cartographier des grandes unités simplement comme des migmatites.

L'influence de la mise en place de complexe d'injection dans la croûte du point de vue thermique devrait être considérée et modélisée dans plus de détails que l'estimation qui est proposée dans la présente étude. Le transfert incomplet des éléments producteurs de chaleurs vers la surface pourrait en effet augmenter la fertilité de la croûte inférieure. La longévité de structures crustales importantes pour le géodynamisme telles que des "channel flows" peut être améliorée si l'on considère la quantité de chaleur qui peut être conservée en profondeur dans un complexe d'injection.

Finalement, deux grandes interrogations persistent après cette étude. Premièrement, si les leucogranites observés ont quitté leur source, à quoi ressemble cette source et comment la reconnaître? La Sous-province d'Ahsuanipi est un terrain qui peut potentiellement

permettre de répondre à cette question. Dans ce cas, y a-t-il des évidences de fractionnement précoce dans les migmatites comme l'indique la géochimie? Quelle distance ont parcouru les magmas anatectiques avant leur mise en place dans le complexe d'injection?

Deuxièmement, bien que le complexe d'injection agisse comme un réservoir de magmas d'anatexie, quel volume a simplement été transféré à travers celui-ci ? Y-a-t-il eu convergence de certaines veines pour former des dykes crustaux alimentant des batholites dans des niveaux supérieurs de la croûte ?

Bien que de grandes interrogations persistent, au cours de cette thèse, une partie des hypothèses formulées dans la problématique n'ont pas été réfutées. Il apparaît que les complexes d'injection sont des domaines qui ont un grand impact sur l'ensemble de la croûte, car ils participent activement au transfert de magmas d'anatexie. Cette thèse a couvert plusieurs domaines tels que le transfert de chaleur, la présence d'eau ou les aspects structuraux. Chacun d'entre eux mériterait une étude approfondie et spécialisée. Cependant, les impacts identifiés au cours de cette thèse encouragent la poursuite des recherches qui apporteraient une meilleure compréhension des complexes d'injections. Les résultats et interprétations de cette thèse montrent aussi que la croûte moyenne est une zone qui ne doit pas être négligée dans les modèles globaux de la croûte continentale.

5.6 RÉFÉRENCES

Brown, M., 2013. Granite: From genesis to emplacement. Geological Society of America Bulletin 125, 1079-1113.

Brown, M. and Rushmer, T. (eds) 2006. Evolution and Differentiation of the Continental Crust. Cambridge University Press, 553 pp.

Cruden, A.R., 1998. On the emplacement of tabular granites. Journal of the Geological Society of London 155, 853–862.

LeBreton, N., Thompson, A.B., 1988. Fluid-absent (dehydration) melting of biotite in metapelites in the early stages of crustal anatexis. Contributions to Mineralogy and Petrology 99, 226-237.

Stevens, G., Villaros, A., Moyen, J.-F., 2007. Selective peritectic garnet entrainment as the origin of geochemical diversity in S-type granites. Geology 35, 9-12.

Yakymchuk, C., Brown, M., Ivanic, T.J., Korhonen, F.J., 2013. Leucosome distribution in migmatitic paragneisses and orthogneisses: A record of self-organized melt migration and entrapment in a heterogeneous partially-molten crust. Tectonophysics 603, 136-154.

ANNEXES

ANNEXE 1

Exemples de structures de de veines leucogranitiques en affleurement

Subvertical, straight veins, subparallel to schistosity. Most common structure

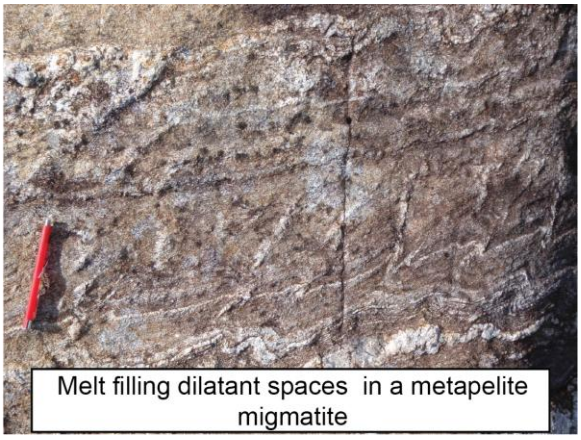

Melt filling dilatant spaces in a metapelite migmatite

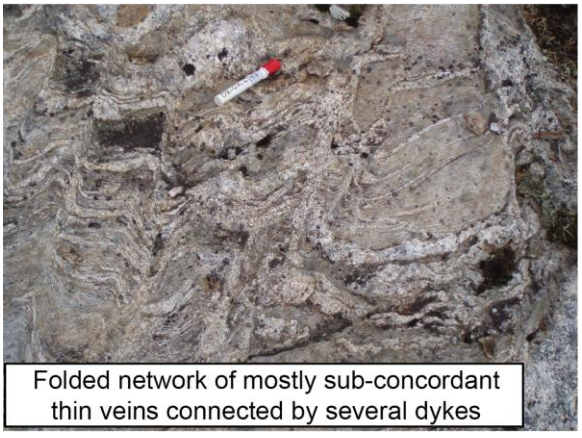

Folded network of mostly sub-concordant thin veins connected by several dykes

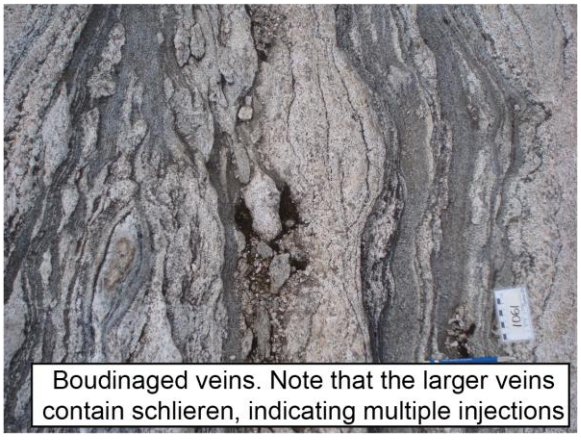

Boudinaged veins. Note that the larger veins contain schlieren, indicating multiple injections

Leucogranitic outcrop composed by numerous injections and containing metasedimentary rafts

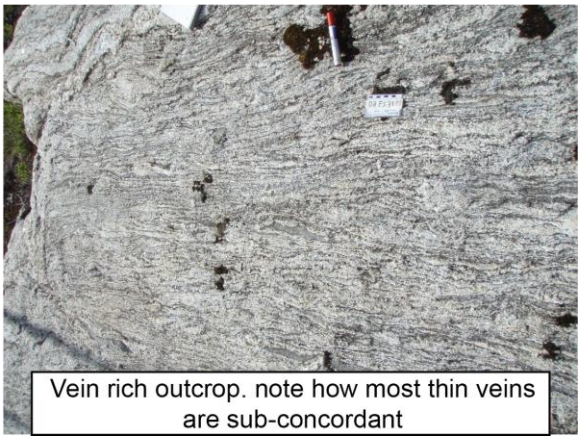

Vein rich outcrop. note how most thin veins are sub-concordant

ANNEXE 2

Whole rock analysis quality control

Analysis Lab	ACME Vancouver via MRNF		MRNF AM072 internal standard	GeoLabs - OGS - Sudbury		E.W. Sawyer EL51 internal standard
Major Oydes Method	$LiBO_2$ fusion + ICP-AES			borate fluxed glass bead + XRF		
	Standard deviation (n= 15)		% Precision	Detection Limits (%)	Standard deviation (n= 5)	% Precision
SiO_2	0.01%	0.2	0.3	0.01	0.4	1
TiO_2	0.01%	-	-	0.01	0.0	3
Al_2O_3	0.01%	0.1	0.8	0.01	0.3	2
FeOt	0.01%	0.2	52.6	0.01	0.1	1
MnO	0.01%			0.01		
MgO	0.01%	0.0	4.4	0.01	0.1	2
CaO	0.01%	0.0	0.5	0.01	0.0	3
Na_2O	0.01%	0.1	1.7	0.01	0.1	4
K_2O	0.01%	0.0	1.8	0.01	0.1	4
P_2O_5	0.01%			0.01		
LOI	0.05%			0.05		
Trace Elem$_2$ fusion + ICP-MS				Closed vessel multiacid disolution + ICP-MS		
Lower Detection Limits (%)						
Cs	0.1	0.03	5.1	0.1	0.08	2
Rb	0.5	0.33	2.8	0.2	6.70	4
Sr	0.5	31.19	3.9	0.6	7.30	3
Ba	0.5	5.80	2.4	0.8	84.00	10
Y	0.1	0.15	6.1	0.05	0.27	5
Zr	0.5	3.14	3.9	6	1.83	2
Hf	0.4	0.16	6.4	0.1	0.05	2
Nb	0.5	0.21	24.8	0.03	0.14	2
Ta	0.1	d.l.		0.02	0.03	5
Th	0.1	0.13	22.5	0.02	0.30	3
U	0.1	0.03	18.8	0.01	0.08	2
REE (ppm)						
La	0.5	0.17	5.3	0.04	0.67	3
Ce	0.5	0.37	5.6	0.12	1.17	3
Pr	0.02	0.05	6.2	0.01	0.13	4
Nd	0.4	0.27	8.0	0.06	0.33	3
Sm	0.1	0.05	8.5	0.01	0.07	3
Eu	0.05	0.01	4.2	0.003	0.04	7
Gd	0.05	0.04	7.0	0.01	0.05	3
Tb	0.01	0.01	10.8	0.002	0.04	7
Dy	0.05	0.04	8.6	0.01	0.05	5
Ho	0.05	0.01	13.0	0.002	0.01	6
Er	0.05	0.02	6.7	0.01	0.02	4
Tm	0.05	0.01	17.3	0.002	0.00	2
Yb	0.05	0.02	6.5	0.01	0.01	3
Lu	0.01	0.01	18.3	0.002	0.00	2

ANNEXE 3

Whole rock analysis detection limits

Sample			SiO2	TiO2	Al2O3	FeOt	MnO	MgO	CaO	Na2O	K2O	P2O5	LOI
06-AF-3007A													
06-AF-3097A													
06-AF-3116A													
06-AF-3145A													
06-AF-3153A													
06-AF-3166A													
06-DB-1081A													
06-MA-4129B2													
06-NT-8012A													
08-CC-8010B													
08-CM-2044B													
08-CM-2045B													
08-DB-1071A													
08-EB-5079A													
08-EB-5107A													
08-EB-5163A													
08-EB-5165A													
08-FS-3018A													
08-FS-3153A													
08-GR-4110A													
08-GR-4119B													
08-PR-6018A													
08-PR-6049A													
09-EB-2108D													
09-SB-5011B													
09-SM-6255A													
09-SM6263C1													
09-SM-6263C2													
98-MB-12													
98-MB-12													
98-SL-3018A													
98-SL-3029A													
CG-1175-3A-97													
JP-5136-3C-97													
MS-125-3A-													
MS-176-3A-97													
MS-71-3A-97													
MS-88-3B-97													
PB-4161-3B-97													
	ACME Vancouver via MRNF												
	$LiBO_2$ fusion + ICP-AES												
	l.d.l. in percent		0.01	0.01	0.01	0.01	0.01	0.01	0.01	0.01	0.01	0.01	0.05
	GeoLabs - OGS - Sudbury												
	borate fluxed glass bead + XRF												
	l.d.l. in percent		0.01	0.01	0.01	0.01	0.01	0.01	0.01	0.01	0.01	0.01	0.05

Sample		Cs	Rb	Sr	Ba	Y	Zr	Hf	Nb	Ta	Th	U	V	Ga	Sn	W
06-AF-3007A	ACME Vancouver via MRNF															
06-AF-3097A	LiBO2 fusion + ICP-MS															
06-AF-3116A	l.d.l. in ppm	0.1	0.5	0.5	0.5	0.1	0.5	0.4	0.5	0.1	0.1	0.1	5	0.5	0.1	0.1
06-AF-3145A																
06-AF-3153A																
06-AF-3166A																
06-DB-1081A																
06-MA-4129B2																
06-NT-8012A																
08-CC-8010B																
08-CM-2044B																
08-CM-2045B																
08-DB-1071A																
08-EB-5079A																
08-EB-5107A																
08-EB-5163A																
08-EB-5165A																
08-FS-3018A																
08-FS-3153A																
08-GR-4110A																
08-GR-4119B																
08-PR-6018A																
08-PR-6049A																
09-EB-2108D																
09-SB-5011B																
09-SM-6255A																
09-SM6263C1																
09-SM-6263C2																
98-MB-12	GeoLabs - OGS - Sudbury															
98-MB-12	Closed vessel multiacid disolution + ICP															
98-SL-3018A	l.d.l. in ppm	0.1	0.2	0.6	0.8	0.1	6	0.1	0	0	0	0	0.8	0	0.2	0.1
98-SL-3029A																
CG-1175-3A-97																
JP-5136-3C-97																
MS-125-3A-97																
MS-176-3A-97																
MS-71-3A-97																
MS-88-3B-97																
PB-4161-3B-97																

Sample			La	Ce	Pr	Nd	Sm	Eu	Gd	Tb	Dy	Ho	Er	Tm	Yb	Lu
06-AF-3007A																
06-AF-3097A																
06-AF-3116A																
06-AF-3145A																
06-AF-3153A																
06-AF-3166A																
06-DB-1081A																
06-MA-4129B2																
06-NT-8012A																
08-CC-8010B																
08-CM-2044B																
08-CM-2045B																
08-DB-1071A																
08-EB-5079A																
08-EB-5107A																
08-EB-5163A																
08-EB-5165A																
08-FS-3018A																
08-FS-3153A																
08-GR-4110A																
08-GR-4119B																
08-PR-6018A																
08-PR-6049A																
09-EB-2108D																
09-SB-5011B																
09-SM-6255A																
09-SM6263C1																
09-SM-6263C2																
98-MB-12																
98-MB-12																
98-SL-3018A																
98-SL-3029A																
CG-1175-3A-97																
JP-5136-3C-97																
MS-125-3A-97																
MS-176-3A-97																
MS-71-3A-97																
MS-88-3B-97																
PB-4161-3B-97																
	GeoLabs - OGS - Sudbury															
	REE (ppm)															
	l.d.l. in ppm		0.04	0.12	0.01	0.06	0.01	0	0.01	0	0.01	0	0.01	0	0.01	0
		ACME Vancouver via MRNF														
		REE (ppm)														
		l.d.l. in ppm	0.5	0.5	0.02	0.4	0.1	0.05	0.05	0.01	0.05	0.05	0.05	0.05	0.05	0.01